THE UNIVERSITY *of* EDINBURGH

The Influence of Lck Abundance on Thymic Selection, Peripheral T Cell Activation and the Formation of T Cell Memory

Kaija Stockner

Degree of Doctor of Philosophy – The University of Edinburgh – 2014

Declaration

I, the undersigned, hereby declare that this thesis has been composed by myself, the work presented within is my own, unless acknowledged otherwise, and it has not been submitted for any other degree or professional qualification except as specified.

Kaija Stockner Date

Acknowledgements

First and foremost, I would like to thank my supervisor, Professor Rose Zamoyska, for the opportunity to undertake this project. I am ever so grateful for the continued trust, guidance, support, and encouragement, particularly in the times when everything seemed to come to a standstill. Thank you for helping me find the 'cabbage patch' and make a story out of it all!

I would also like to thank my second supervisor Dr. Andrew MacDonald, for the support and constructive advice over the years. I am grateful for his lab's generous provision of the IFNγ capture antibody.

To Dr. Stefano Caserta, I owe a massive thank you for all the initial training in all things related to lab and animal work that helped set up the project.

I would like to acknowledge the technical support from Dr. Martin Waterfall, animal staff, Bette the lab fairy, and everyone in IIIR, who helped with reagents or advice along the way - thank you!

Bob, Becky, Thomas, Jess, and Graeme, thank you all for your help and advice with experimental design, scientific discussions, thesis corrections and general lab banter. Collectively, it has helped bring the project together and make sense of the data but, most of all, made it enjoyable. David, thank you for all your help with *Listeria* preparations and dog related chat! I owe a special thank you to Celine, who has helped with many experiments and never failed to bring her energy, even at the early hours. Shinny - my partner in crime, it's been a turbulent time. We've shared tears and laughter, ups and downs, (many cocktails!) and most importantly a mammoth journey - I thank you for all of it!

A massive thank you to all my friends and office buddies, in particular to Beth, Janice G., Gillian H., Dunja, Anna, Kathrine, Maria, Marta, Katie, Gosia, Steph, Martina, Andreas, Calum, Ben, Almu, and Marieke. Whether it was party shenanigans, chitchat, a place to sleep, a veil, nursing concussions, countless coffees, horsing around, white wine spritzers, failed attempts at

camping, Firbush, or the many dog walks, you have all supported me despite differences in distances and time.

This journey would not have been possible without the unyielding support of my parents every step of the way, who have been the councilors, wise men and wedding planners as needed. I'd also like to thank the rest of my family, both old and new, Lucy, and my inspiring sisters. Silvia, thank you for being you; there for me through thick and thin. And my superstar Anita – don't ever stop loving life the way you do!

Finally, I would like to thank my husband Martin for his 'just do it' approach and for patiently providing unfaltering support and encouragement!

Abstract

Selection of the T cell repertoire in the thymus is governed by the need to create a repertoire of peripheral T cells that can respond to any foreign antigen in the context of self-major histocompatibility complex (MHC), while enforcing central tolerance to self-antigens. Perturbations in signalling molecules, that reduce the affinity of thymic selection, can lead to the production of a peripheral repertoire with increased autoimmunity, as has been shown for mutations in the Zap-70 kinase. Upstream of Zap-70 is Lck, the most proximal tyrosine kinase required for T cell receptor (TCR) triggering upon TCR engagement by peptide:MHC.

In order to study how Lck influences T cell activation, a transgenic mouse model (Lck^{VA}), in which Lck is expressed constitutively from a T cell specific transgene and mice have very low expression of Lck (~5% of WT) in both the thymus and periphery, was used.

It has been shown that Lck is critical for successful T cell development, yet the results of this thesis show that even 5% of WT levels of Lck are sufficient for selection of thymic T cells on both polyclonal and F5 TCR transgenic backgrounds.

Previous studies utilising mice expressing an inducible Lck transgene, which also had reduced Lck expression in the periphery, showed Lck to be critical in determining the activation threshold of T cells. In contrast, peripheral T cells in Lck^{VA} mice had similar activation thresholds to wild type T cells, as measured by *in vitro* upregulation of early activation markers. Further analysis of Lck^{VA} peripheral T cells revealed differential influences of low expression of Lck on downstream signalling pathways upon TCR engagement. For example, ERK signalling was impaired, while calcium flux and proliferation were enhanced in Lck^{VA} T cells. Finally, Lck^{VA} T cells were altered in their ability to differentiate, showing enhanced production of cytokines and retaining the capacity to form memory cells.

We assessed how T cells with low Lck expression formed memory cells in response to *in vivo Listeria* infections and whether they might be more robust at resisting a secondary infection. Both, the immunodominant primary and secondary effector responses were poorer in Lck^{VA} mice. However, the overall response to *Listeria* was similar in Lck^{VA} mice to Lck^{WT} mice. Additionally, proportionally more T cells that had incorporated BrdU upon primary infection, survived past the contraction phase in Lck^{VA} mice than in Lck^{WT} mice. These results are consistent with an increased potential to form memory cells and correlated with higher Bcl-2 expression seen both *in vitro* and *in vivo* in Lck^{VA} T cells.

The results presented in this thesis firstly, further our understanding of how manipulation of T cell signalling can impact on T cell effector function and memory formation and secondly, have implications for strategies to optimise vaccination protocols to provide the best memory T cell response in a clinical setting.

Lay Summary

The effector cells of the immune system, T cells, must be able to recognise and respond to any foreign pathogen without attacking self. T cells express a variety of T cell receptors (TCR) of different specificities that recognise pathogenic proteins. When a TCR engages with a pathogen several signalling cascades are initiated within the cell that lead to the expression is effector genes required for pathogen clearance and memory T cell formation, in case the pathogen be encountered again in the future. Many signalling molecules mediate the T cell signalling cascades and of these the most proximal is Lck. Without Lck T cells do not develop properly and there is very little T cell mediated immunity.

In this thesis we studied the role of Lck T cell signalling during T cell development, activation and memory formation by making use of mice that express less than 5% of Lck (Lck^{VA}) compared to control mice. We showed that T cell development in Lck^{VA} mice is comparable to control mice. Although, some TCR signalling cascades were reduced, others were enhanced in Lck^{VA} mice. During bacterial infection, similarly, we found that some responses were reduced as compared to control mice, but others were similar. Finally we showed that the maintenance of a unique population of infection specific T cells into the memory phase was enhanced in Lck^{VA} mice.

The results presented in this thesis firstly, further our understanding of how manipulation of T cell signalling can impact on T cell effector function and memory formation and secondly, have implications for strategies to optimise vaccination protocols to provide the best memory T cell response in a clinical setting.

Abbreviations

ADAP - Adhesion and Degranulation-Promoting Adaptor Molecule

AICD - Activation Induced Cell Death

AP1- Activator Protein 1

APC - Antigen Presenting Cell

ARE - Adenylate/Uridylate-Rich Element

Bcl-2 - B Cell Lymphoma Protein 2

BCR - B Cell Receptor

BM - Bone Marrow

BrdU - Bromodeoxyuridine

Ca2+ - Calcium

CamK - Ca2+ - Calmodulin Dependent Kinase

CARD - Caspase Recruitment Domain

CARMA1 - CARD and MAGUK Containing Scaffold Protein 1

CCL - Chemokine CC Ligand

CCR - C-C Chemokine Receptor

CD - Cluster of Differentiation

CDR – Complementarity Determining Region

CFSE - Carboxyfluorescein Diacetate N-Succinimidyl Ester

CID - Combined Immunodeficiency

CLP - Common Lymphoid Progenitor

CMP - Common Myeloid Progenitors

CMV - Cytomegalovirus

Csk - C-terminal Src Kinase

cTEC - Cortical Thymic Epithelial Cell

CTL - Cytotoxic T Lymphocyte

CTLA4 - Cytotoxic T Lymphocyte Antigen 4

CXCL - Chemokine (C-X-C) Ligand

DAG - Diacylglycerol

DC - Dendritic Cell

Dex - Dextramer

DISC - Death Inducing Signaling Complex

DLL4 - Notch Delta - Like Ligand 4

DN – Double Negative $CD4^-$ $CD8^-$ Thymocyte

DP - Double Positive $CD4^+CD8^+$ Thymocyte

DPC - Distal Pole Complex

DRM - Detergent-Resistant Membrane

ELISA - Enzyme Linked Immunosorbent Assay

EOMES - Eomesodermin

ER - Endoplasmic Reticulum

ERK - Extracellular Signal Regulated Kinase

ERM proteins - Ezrin, Radixin and Moesin

ETP - Early-T Cell Progenitor

ETS - E-Twenty Six Family of Transcription Factors

FACS - Fluorescence Activated Cell Sorting

FADD - Fas Associated Death Domain

FCS - Fetal Calf Serum

Foxp3 - Forkhead Box P3

FRET - Foerster Resonance Energy Transfer

FSC - Forward Scatter

FTOC - Fetal Thymic Organ Culture

Gads - Grb2-Related Adapter Downstream of Shc

Grb2 -Growth Factor Receptor-Bound Protein 2

HKL - Heat Killed Listeria

HPK1 - Hematopoietic Progenitor Kinase 1

huCD2 - Human CD2

i.p. injection - Intraperitoneal Injection

i.v. – Intravenous Injection

ICAM - Intracellular Adhesion Molecule

Id - Inhibitor of DNA-Binding

IFN - Interferon

IFNGR - IFN Gamma - Receptor

Ig - Immunglobulin

IL – Interleukin

IL-2R - IL-2 Receptor

IL-7R - IL-7 Receptor

IMDM - Iscove's Modified Dulbecco's Medium

IP3 - Inositol 1,4,5 – Trisphosphate

IS - Immunological Synapse

iSP - Immature Single Positive Thymocytes

ITAM - Immunoreceptor Tyrosine-Based Activation Motif

Itk - IL-2 Induced Tyrosine Kinase

JNK - c-Jun N-Terminal Kinase

kd - Knockdown

kDA - Kilodalton

KLRG-1 - Killer Cell Lectin-Like Receptor G1

KO - Knockout

LAT - Linker of Activated T Cells

LFA-1 - Leukocyte Function-Associated Antigen 1

LIME - Lck-Interacting Membrane Protein

LN - Lymph Nodes

mAb - Monoclonal Antibody

MAGUK - Membrane-Associated Guanyl Kinase

MALT 1 - Mucosa-Associated Lymphoid Tissue Lymphoma Translocation Protein 1

MAPK - Mitogen-Activated Protein Kinase

MFI - Mean Fluoresccence Intensity

MHC - Major Histocompatibility Complex

MPECs - Memory Precursor Effector Cells

mRNA - Messenger RNA

mTEC - Medullary Thymic Epithelial Cells

mTOR - Mammalian Target of Rapamycin

mTORC1 - mTOR Complex 1

NFAT - Nuclear Translocation of Nuclear Factor of Activated T Cells

NFκB - Nuclear Factor Kappa B

NK – Natural Killer Cell

NKT - Natural Killer T Cell

p:MHC – Peptide MHC Complex

PAG - Phosphoprotein Associated with Glycosphingolipid-Enriched Microdomains

PALS - Periarteriolar Lymphocyte Sheaths

PBMC - Peripheral Blood Mononuclear Cell

PCR - Polymerase Chain Reaction

PD1- Programmed Cell Death 1 Receptor

pHSC - Pluripotent Hematopoietic Stem Cell

PI3K - Phosphoionositide 3-Kinase

PIP2 - Phosphatidylinositol-4,5-Bisphosphate

PKA - Protein Kinase A

PLCγ - Phospholipase C γ

PSGL-1 - P-Selectin Glycoprotein Ligand-1

PTP - Protein Tyrosine Phosphatase

PTPN - Protein Tyrosine Phosphatase, Non Receptor Type

RAG - Recombinase-Activating Gene

RANKL - Receptor Activator of Nuclear Factor Kappa-B Ligand

Rap1- Ras-Related Protein 1

RasGRP - Ras Guanyl Nucleotide-Releasing Protein

RNA - Ribonucleic Acid

rtTA - Tetracycline-Inducible Transactivator Domain

S - Serine

S1P1 - Sphingosine-1-Phosphate Receptor 1

S6K - Ribosomal Protein S6 Kinase

SD - Standard Deviation

SFK - Src-Family Kinase

SH - Src Homology Domain

siRNA - Short Interfering RNA

SLEC - Short-Lived Effector Cell

SLP-76 - SH2 Domain-Containing Leukocyte Phosphoprotein of 76 kDa

SOS - Son of Sevenless

SP – Single Positive Thymocyte

SSC - Side Scatter

STAT5 - Signal Transducer and Activator of Transcription 5

T_{CM} - Central Memory T Cell

TCR – T Cell Receptor

Tdt - Terminal-Deoxynucelotide Transferase

T_{EM} - Effector Memory T Cell

TGFβ - Tumour Growth Factor Beta

TNFα - Tumour Necrosis Factor Alpha

T_{Reg} - Regulatory T Cell

UTR - Untranslated Region

WB - Western Blot

WT - Wild-Type

Y - Tyrosine Residue

Zap-70 - Intracellular Kinase Zeta-Associated Protein of 70 kDa

Contents

List of Figures

List of Tables

Chapter 1: Introduction

1.1 Overview of the Immune System

The mammalian immune system is constantly challenged by infections. A variety of effector cells and molecules of the two overlapping immune components: innate and adaptive immunity, work both independently and in synchrony to protect the host. Successful protection requires fulfilment of four main tasks: recognition of the foreign pathogen, its effective clearance, self-regulation of immunity and formation of immune memory.

1.2 The Innate Immune System

The first line of host defences are protective physical and chemical barriers, although these are not considered part of the immune system proper, their aim is to prevent microbes from entering the host in the first place. These include the skin, the internal epithelium and its mucus lining such as in the respiratory, gastrointestinal and reproductive tracts, as well as chemicals such as lysozyme in tears and saliva. The underlying tissues are rich in innate immune cells and as a pathogen overcomes the protective barriers, the immune system proper is engaged. Important innate cells are cells of the myeloid lineage such as macrophages, neutrophils, eosinophils, basophils, mast cells, dendritic cells (DCs), and some of the cells of the lymphoid lineage such as natural killer (NK) and natural killer (NKT) T cells.

Macrophages are present in almost all tissues and are most often the first cells to respond to invading pathogens. They are able to recognise and ingest pathogens, particularly bacteria, by virtue of the receptors that recognise common constituents of pathogens. Upon recognition of pathogen the macrophages phagocytose it by enclosing it within the phagocytic membrane, which then becomes fused with the cellular destructive machinery forming a phagolysosome, where enzymes, such as lysozyme, mediate destruction of the pathogen.

Internal degradation of pathogens by macrophages leads to secretion of cytokines such as the interleukins (IL) - 1β, -6, -12, tumour necrosis factor alpha (TNFα) and chemokines such as chemokine (C-X-C) ligand 8 (CXCL8). These molecules orchestrate inflammation and recruit other innate cells as well as cells of the adaptive immune system. Activated macrophages also upregulate expression of surface molecules that enable them to act as antigen-presenting cells alongside DCs to T cells (Fearon and Locksley, 1996).

1.3 The Adaptive Immune System

The mammalian bone marrow harbours pluripotent hematopoietic stem cells (pHSC), from which all the different types of blood cells develop. The pHSC give rise to more specialised precursors such as the common lymphoid progenitors (CLP), which develop into B lymphocytes (B cells), T lymphocytes (T cells) or NK cells, and the common myeloid progenitors (CMP), which develop into granulocytes (Prohaska et al., 2002).

The adaptive immune system comprises of B and T cells that are characterised by their unique cell surface antigen receptors (BCR and TCR, respectively). Both BCRs and TCRs develop with an exceptionally wide variability in their antigen-binding regions to recognise any potential foreign invaders. Key difference between B and T cells is that mature B cells (plasma cells) can produce and secrete antibodies of the same antigen specificity as the BCR, whereas the TCR is not secreted (Fearon and Locksley, 1996). Antibodies can interact with pathogens, and their secreted products, in extracellular spaces of the body and recruit immune cells and molecules to destroy them.

1.3.1 The Generation of BCR and TCR Diversity

The BCR is comprised of paired heavy and light polypeptide chains, conventionally termed immunoglobulin (Ig). An Ig of the same specificity as the bound form is secreted as an antibody molecule. An antibody molecule has two identical variable regions made up two antigen-binding sites, each of which is in turn made up of a heavy and a light chain. The heavy and light

chains have variable regions that form hypervariable loops, creating a surface complementary to antigen, hence, these are also known as complementarity-determining regions 1, 2, and 3 (CDR1, CDR2, CDR3). The constant region of an antibody molecule determines its isotype and the functional properties. The constant region is composed of the carboxy-terminal domains of the heavy chains, denoted by Greek letters: δ, μ, γ, α, and ε and determining the five antibody classes IgD, IgM, IgG, IgA, and IgE, respectively. IgM is mainly found in blood and lymph, it can bind bacterial capsular polysaccharides and activate the complement system. IgD is present present at very low levels and is usually co-expressed with IgM. IgA is mainly found in secretions like the epithelium lining of the respiratory tracts. IgG operates mainly in body tissue where it can recruit accessory cells. Finally, IgE, is present at low levels but is bound by mast cells and sensitises them to release chemical reaction inducing mediators causing sneezing, vomiting etc. to expel pathogens.

The TCR is similar to the Ig molecule in that the protein structure also has variable and constant regions. The majority of TCRs express two transmembrane spanning α and β polypeptide chains as a heterodimer. Each polypeptide chain has a variable region and a constant region and the two variable regions together form one antigen-binding site. A minority of TCRs are made of alternative γ and δ chains (Rudolph et al., 2006). The γδ T cells have been shown to carry out specific immune functions in epithelial layers of tissues and they have a much smaller TCR repertoire (Xiong and Raulet, 2007). The core focus of the current thesis is on the αβ T cells and therefore, when referring to TCR henceforth we mean the αβ TCR, unless otherwise specified.

The generation of diversity of lymphocyte receptors is largely similar in T and B cells. The genes for Ig variable regions are inherited as sets of variable (V), joining (J) and diversity (D) gene segments, which are randomly assembled in each cell individually by DNA recombination, mediated by recombinase-activating genes 1 and 2 (RAG1/RAG2), and joined to a number of constant (C) regions creating almost unlimited diversity. In the absence of

RAG genes, in Rag knockout (Rag^{ko}) mice, there is a complete block in lymphocyte development (Mombaerts et al., 1992). The generation of diversity is further enhanced by junctional diversity, where nucleotides are added or subtracted in the joining process of gene segments by Terminal-deoxynucelotide transferase (Tdt) (Cabaniols et al., 2001).

1.3.2 B Cells

B cells undergo a developmental program in the bone marrow from pro-B cells, pre-B cells, to immature B cells that have a membrane-bound immunoglobulin BCR for antigen. Pro-B cells first undergo rearrangement of the immunoglobulin heavy-chain locus with D_H to J_H joining, followed by a second rearrangement of a V_H gene segment to a DJ_H sequence. If this is successful, ~55% of the time, intact μ heavy chains are produced, further rearrangement ceases, and the pro-B cell becomes a pre-B cell. In the pre-B-cell stage the lamda (λ) and kappa (κ) light-chains only undergo gene rearrangements by V to J joining, they lack D segments. Successful light-chain progeny combine with the μ chain and form an immature B cell expressing IgM molecules (Pieper et al., 2013). Immature B cells migrate to the spleen where they can undergo further differentiation into naïve, follicular, or marginal zone B cells (Pieper et al., 2013). Both the heavy chain and the light chain rearrangements are subject to allelic exclusion, ensuring that only one of the two alleles of a gene is expressed. Light chains also display isotypic exclusion ensuring that either the λ or κ chain is expressed by an individual cell, not both (Pieper et al., 2013). Upon stimulation by antigen, B cells can undergo class-switching and express Ig of a different class. Further diversity in the rearranged V regions can be introduced by somatic hypermutation, which occurs at high rates in mature B cells, that have already been activated by their corresponding antigen, and is known as affinity maturation. This ensures clones with the highest affinity are preferentially selected for survival and mature into antibody-producing cells (Pieper et al., 2013).

1.3.3 T Cells

Briefly, T cells also originate from the pHSC in the bone marrow but undergo their development into mature $CD8^+$ or $CD4^+$ T cells in the thymus. The α and β chains of the TCR, like the BCR, also undergo RAG mediated gene rearrangement events to generate receptor diversity. T cells, unlike B cells, function by detecting the presence of intracellular pathogens by peptide presentation on body's own antigen presenting cells (APCs) in the context of the major histocompatibility complex (MHC) class I or class II molecules.

1.3.4 The MHC Molecules

The MHC molecules are encoded as a large cluster of genes, therefore, they are polygenic, but also highly polymorphic, as a single MHC locus can have allelic variants differing by up to 20 amino acids. The majority of differences are found in the peptide-binding groove, which influences diversity. Both class I and class II MHC molecules are heterodimers with two Ig-like domains, an α helix/β sheet superdomain, that forms the peptide-binding site (Rudolph et al., 2006). MHC class I and II molecules bind peptides differently. The MHC class I molecule binds peptides of 8-10 amino acids long and the peptide ends are buried in the peptide-binding groove, whereas, in a class II molecule peptide length is typically 13-17 amino acids, but is not constrained, and the peptide ends are not buried in the peptide-binding groove (Murphy et al., 2008; Rudolph et al., 2006). Therefore the kinds of peptides that the two MHC class molecules bind are also different.

The TCR recognises both the peptide being presented and the MHC molecule that is presenting it on the APC. $CD4^+$ T cells recognise MHC class II and $CD8^+$ T cells recognise MHC class I molecules, meaning that T cell clones are MHC restricted. The CDR1 and 2 loops of the V_α chain of the TCR interact with the peptide MHC complex around the amino terminus of the peptide, conversely the V_β chains CDR 1 and 2 loops interact with the carboxyl terminus of the peptide. In the case of the MHC I molecule, both the V_α and V_β chains interact with its α helices. The CDR3 loops of both V_α and V_β chains of the TCR interact with the central amino acids of the peptide. MHC class I

molecules are found on most nucleated cells, as they can be infected by viruses, and MHC class I restricted $CD8^+$ T cells differentiate into cytotoxic T cells (CTLs) that are specialised to kill infected cells. $CD4^+$ T cells can adopt a variety of immunological functions upon binding peptide presented by MHC class II molecules by differentiating into distinct effector subsets. Depending on the context in which $CD4^+$ T cells are activated they recruit the appropriate effector cells (Murphy et al., 2008; Rudolph et al., 2006).

1.3.5 The Src-Family Kinases

The TCR is associated with its signal transduction unit CD3 (δ chain, γ chain, two ε chains), with two ζ chains and with a cell surface co-receptor either CD4 or CD8. The cytosolic components of the CD3 complex contain immunoreceptor tyrosine-based activation motifs (ITAMs). The TCR itself has no intrinsic enzymatic activity. Upon the binding of peptide:MHC (p:MHC) to the TCR the first molecules activated are Src-family kinases (SFKs) $p56^{lck}$ (Lck) and $p59^{fyn}$ (Fyn) (Zamoyska et al., 2003). The structures of Lck and Fyn are similar. They each have an N-terminal unique domain, Src homology 2 (SH2) and SH3 domains, a tyrosine kinase domain (SH1), and a C-terminal negative regulatory domain (Palacios and Weiss, 2007). The unique domain in Lck contains a di-cysteine motif that enables it to associate with CD4 and CD8 coreceptors (Salmond et al., 2011). The unique domain in Fyn also determines its intracellular localisation such as colocalisation with centrosomal and mitotic structures (Palacios and Weiss, 2004; zur Hausen et al., 1997). In order to target Lck to the plasma membrane and lipid rafts, modifications such as addition of fatty chains of myrisitc and palmityc acid moieties, as well as S-acetylation of the cysteine residues on the N-terminal sites of the Lck molecule are required (Palacios and Weiss, 2004). The SH2 and SH3 domains of Lck and Fyn mediate intra- and inter-molecular protein-protein interaction via recognition of polyproline or phosphotyrosine motifs allowing the SFKs to act as adapter molecules (Palacios and Weiss, 2004).

Genetic evidence, that Lck plays a role in TCR signalling, came from studies on mutant Jurkat subclone cells (JCam1) lacking functional Lck, which failed to transmit TCR signals but transfection of *LCK* cDNA restored TCR

signalling (Straus and Weiss, 1992). Further studies of thymocyte signalling in Lck^{ko} mice found Lck to be critical for ITAM ζ-chain phosphorylation and consequent recruitment and activation of the intracellular kinase ζ-associated protein of 70 kDa (Zap-70) (van Oers et al., 1996a).

The roles of Lck and Fyn in thymocyte development and T cell activation, and their regulation are discussed in turn in the relevant sections below.

1.4 T Cell Development

T cell development occurs in the thymus. The αβ T cells can give rise to $CD4^+$ and $CD8^+$ T cells, NKTs, and regulatory T cells (T_{Regs}) (Rothenberg et al., 2008). The process of development is guided by the thymic microenvironment as well as TCR rearrangements and different stages of development are marked by changes in gene expression and developmental potential (Fig.1.1). The combinatorial expression patterns of various surface markers on developing thymocytes allow us to follow their progression during development.

The thymus is an epithelial-mesenchymal tissue, structurally divided into a cortex and a medullary region with functionally distinct stromal cells known as cortical thymic epithelial cells (cTECs) and medullary thymic epithelial cells (mTECs), respectively (Anderson and Takahama, 2012). At mid-gestation, the CLPs from the bone marrow, that will develop into T cells, are recruited into the thymus by adhesion molecules like P-selectin on thymic endothelial cells (Rossi et al., 2005), and chemokines like chemokine CC ligand (CCL) 21, CCL25, and CXCL 12, which are expressed on the TECs (Liu et al., 2005). The CLPs express selectin-like receptors, such as P-selectin glycoprotein ligand-1 (PSGL-1), in order to be able to respond to these signals (Rossi et al., 2005). The progenitors are exposed to the thymic microenvironment in the thymic cortex containing IL-7, and the Notch Delta-Like Ligand 4 (DLL4), that induce their proliferation and differentiation (Anderson and Takahama, 2012; Schmitt and Zuniga-Pflucker, 2002). IL-7 signals are transduced via the IL-7R receptor (IL-7R), which is comprised of the α-chain (CD127) and the common cytokine-receptor γ-chain (CD132) (Mazzucchelli and Durum, 2007). The early progenitor T cells, as they

migrate through the thymic cortex, are progressing through the $CD4^-$ and $CD8^-$ double negative (DN) stages of development (Rothenberg et al., 2008).

At the DN stage of development, it is crucial for T cells to receive IL-7 signals for maturation and thus CD127 expression is high (Sudo et al., 1993). The DN stages can be further subdivided by CD25 and CD44 expression: DN1 are $CD25^-CD44^+$, DN2 are $CD25^+CD44^+$, DN3 are $CD25^+CD44^-$ and DN4 are $CD25^-CD44^-$. DN1, 2 and 3 are very heterogeneous and do not only consist of early-T cell progenitors (ETPs). ETPs, as opposed to the NKT cells, and γδ T cells can be purified using the high expression of receptor tyrosine kinase, KIT at the DN1 stage. DN2 stage can also be further subdivided into DN2a (KIT^{hi}) and DN2b (KIT^{med}), the latter is characterised by loss of dendritic cell potential. Finally at the DN3 stage cells can be subdivided into DN3a ($CD27^{lo}$) pre-β or γδ- chain selection and DN3b ($CD27^{hi}$) post-selection thymocytes (Rothenberg et al., 2008). During the DN stages thymocytes continually migrate towards the capsule, once committed to the T-cell lineage, at the DN3 stage, cells undergo the first developmental checkpoint of TCR β chain selection and also express an invariant TCR pre-α chain. This pre-TCR- $\alpha\beta$ complex must associate with CD3ζ complex at the cell surface and be able to transmit signals for further maturation (Germain, 2002). A small number cells that achieve this will proliferate through DN4 and differentiate into $CD4^+$ and $CD8^+$ double positive (DP) thymocytes. During the DP stage thymocytes stop proliferating and CD127 expression is downregulated (Sudo et al., 1993; Yu et al., 2006). The *Tcrb* locus, encoding the TCR β protein, becomes inaccessible, and the RAG1 and RAG2 genes are activated to initiate rearrangement at the *Tcra* locus, encoding the TCR α chain, in quiescent DP thymocytes (Hogquist et al., 2005). In polyclonal wild type mice approximately 80-90% of all thymocytes are at the DP stage and have successfully rearranged a TCR α chain (Germain, 2002; van Oers et al., 1996b). DP thymocytes undergo TCRα chain recombination, positive selection and CD4/CD8 lineage divergence, whilst migrating back through the cortex towards the medulla where they started as ETPs (Fig.1.1) (Petrie and Zuniga-Pflucker, 2007; Rothenberg et al., 2008). Positive selection in the cortex is mediated by cTECs that present self-MHC associated antigens to

assess immunocompetence of the newly produced αβ TCR. Only 1-5% of TCRs make appropriate affinity interactions and are induced to survive and differentiate into $CD4^+$ or $CD8^+$ SP thymocytes (Anderson and Takahama, 2012). If thymocytes do not recognise self-MHC complexes they die by neglect (Werlen et al., 2003).

If the pre-TCR is unable to associate with the CD3ζ complex cell development stops at the DN3 stage. Additionally, if there are defects in the *Rag1, Rag2* genes causing failure of β chain rearrangement, or defects in pre-*TCRα, TCRβ,* or *CD3ε* genes that also hinder pre-TCR- αβ signaling complex formation and expression, no signal transduction occurs and cell development is arrested at the DN3 stage (Fehling et al., 1995; Malissen et al., 1995; Mombaerts et al., 1992; Shinkai et al., 1992).

Interactions with cTECs induce the expression of C-C chemokine receptor 7 (CCR7) on T cells and receptor activator of nuclear factor kappa-B ligand (RANKL). The ligands for CCR7 are CCL19 and CCL21 and are highly expressed on mTECS, as is the receptor for RANKL. Together, the effects of these molecules ensure that the positively selected thymocytes migrate into the medulla (Anderson and Takahama, 2012; Petrie and Zuniga-Pflucker, 2007). In the medulla mTECs carry out promiscuous expression of tissue restricted genes, facilitated by nuclear protein Aire, and by means of cross-presentation to DCs enable DCs to cooperate in the fine-tuning of negative selection. Together mTECs and DCs ensure deletion of tissue specific self-reactive thymocytes (Petrie and Zuniga-Pflucker, 2007).

This final checkpoint ensures self-tolerance and also contributes to the production of naturally occurring T_{Regs} (Anderson and Takahama, 2012). Finally, SP thymocytes express sphingosine-1-phosphate receptor 1 (S1P1), the ligand for which is S1P that is ubiquitously expressed in the circulation. This attracts thymocytes to the circulation and facilitates their egress from the thymus (Anderson and Takahama, 2012)

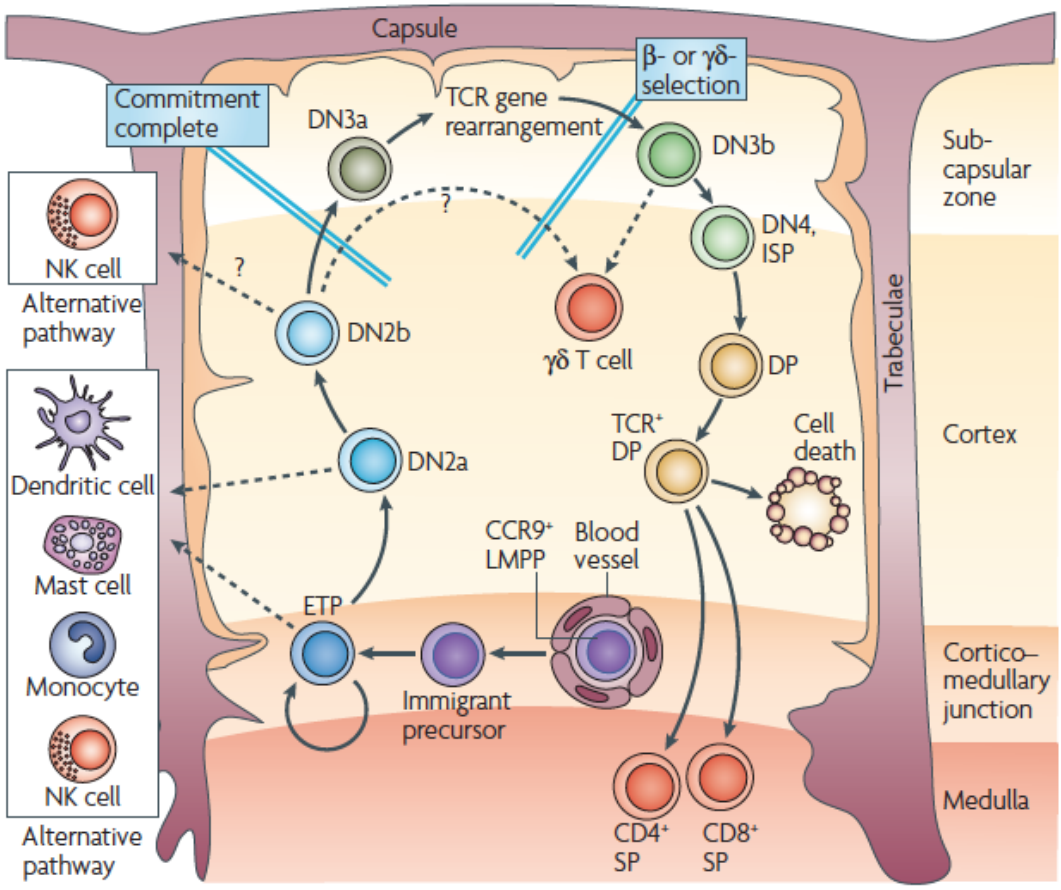

Fig. 1.1 T cell development in the thymus (from Rothenberg *et al* 2008)
Cross-section through a thymus depicting the maturation of thymocytes from ETPs through to CD4$^-$ and CD8$^-$ SP thymocyte stage as they migrate through the thymic environment. Blood vessels near the cortico-medullary junction allow the entry of thymocyte precursors from the bone marrow. At the DN2a and DN2b stages cells can still adopt alternative phenotypes. All non-T cell options are lost by the DN3a stage where TCRβ or γδ gene rearrangement occurs. Positive selection of the αβTCR takes place at the DP stage in the cortex and upon success the final pre-egress maturation of CD4$^-$ and CD8$^-$ SP thymocytes occurs in the medulla.

1.4.1 The Roles of Lck in Thymocyte Development

At both the DN stage (β - chain selection) and the DP stage (positive/negative selection), signalling via the TCR determines whether a cell will survive and progress, or die (Germain, 2002). The first key molecule in TCR signal transduction is Lck. Lck is functionally and physically associated with the CD4 and CD8 co-receptors (Barber et al., 1989; Rudd et al., 1988; Veillette et al., 1988). Both the affinity and the dwell time of the TCR interaction with p:MHC are influenced by the CD4 and CD8 co-receptors, which, facilitate the recruitment of Lck (Artyomov et al., 2010; Palmer and Naeher, 2009). Lck phosphorylates ITAMs in the TCR/CD3ζ complex. Phosphorylated ITAMs create a binding site for the SH2 domains of Zap-70, which is then phosphorylated by active Lck. The cascade continues with active Zap-70 phosphorylating Linker of Activated T cells (LAT) and many other enzymes and adaptors. Ultimately this signaling cascade leads to the increase of intracellular calcium (Ca^{2+}) promoting the nuclear translocation of nuclear factor of activated T cells (NFAT) and subsequent activation of the Mitogen-Activated Protein Kinase (MAPK) pathways (Germain, 2002).

The importance of Lck in thymocyte development was evidenced by studies where both, transgenic overexpression of wild type Lck (Lck^{Y505}) or constitutively active Lck (Lck^{F505}), led to the development of thymic tumours (Abraham et al., 1991). The thymocytes in Lck^{Y505} and Lck^{F505} mice were immature, indicating that Lck activity needs to be maintained under stringent control during development (Abraham et al., 1991). The first Lck^{KO} mouse study, described by Molina and colleagues, showed that the mice manifest with profound thymic atrophy due to an incomplete block at the DN stage of development, which reduces the numbers of thymocytes progressing to the DP stage to one-tenth of wild-type levels (Molina et al., 1992). Very few SP thymocytes, predominantly $CD8^+$, populate the periphery in Lck^{KO} mice, which is in line with the signal-strength model of thymocyte selection (Molina et al., 1992). Lck was shown to have a vital role in thymocytes for sensing appropriate rearrangement of the TCRβ chain, which explains the block at the DN stage of development seen in Lck^{KO} mice (Levin

et al., 1993). Fyn can compensate for Lck during thymic development to some extent as Lck^{ko} mice exhibit an incomplete block and double knockout mice, $Fyn^{ko}Lck^{ko}$, have a complete block in thymocyte development (van Oers et al., 1996b). Lack of Fyn alone did not impact on thymic development suggesting its minor role (Appleby et al., 1992; Stein et al., 1992).

1.4.2 Signalling for Positive and Negative Selection

In the above section I described how thymocyte development occurs in a stepwise manner. Two key questions that have puzzled immunologists for years are, what mechanisms determine that only TCRs with useful ligand specificities are expressed and how do DP thymocytes make a lineage choice.

The T cell repertoire in the thymus is governed by the need to create a repertoire of peripheral T cells that can respond to any foreign antigen in the context of self-MHC, while enforcing central tolerance to self-antigens. The TCR is thus a unique receptor, able to distinguish very fine differences in affinities (analogue input), and translate them into distinct biological outcomes (digital output), such as life or death in positive and negative selection, respectively (Daniels et al., 2006). One proposed signalling pathway involved in positive and negative selection is the ERK/MAPK pathway. TCR ligation leads to the activation of low molecular weight G protein Ras, which mediates MAPK signalling via MEK (MAPK kinase) (Fig.1.2).

In an *in vitro* culture system, where thymocytes could either develop into $CD8^+$ T cells or die by negative selection, Mariathasan et al. showed that low level but sustained extracellular signal related kinase (ERK) signaling downstream of MAPK, promoted positive selection, but strong and transient ERK activation led to negative selection (Mariathasan et al., 2001). The localisation of these signalling molecules within the cell is also influenced by signal strength (Daniels et al., 2006). Positively selecting, low-affinity signals induced less CD3ζ phosphorylation and recruitment of LAT, and had no effect of growth-factor receptor–bound protein 2 (Grb2) and the guanine

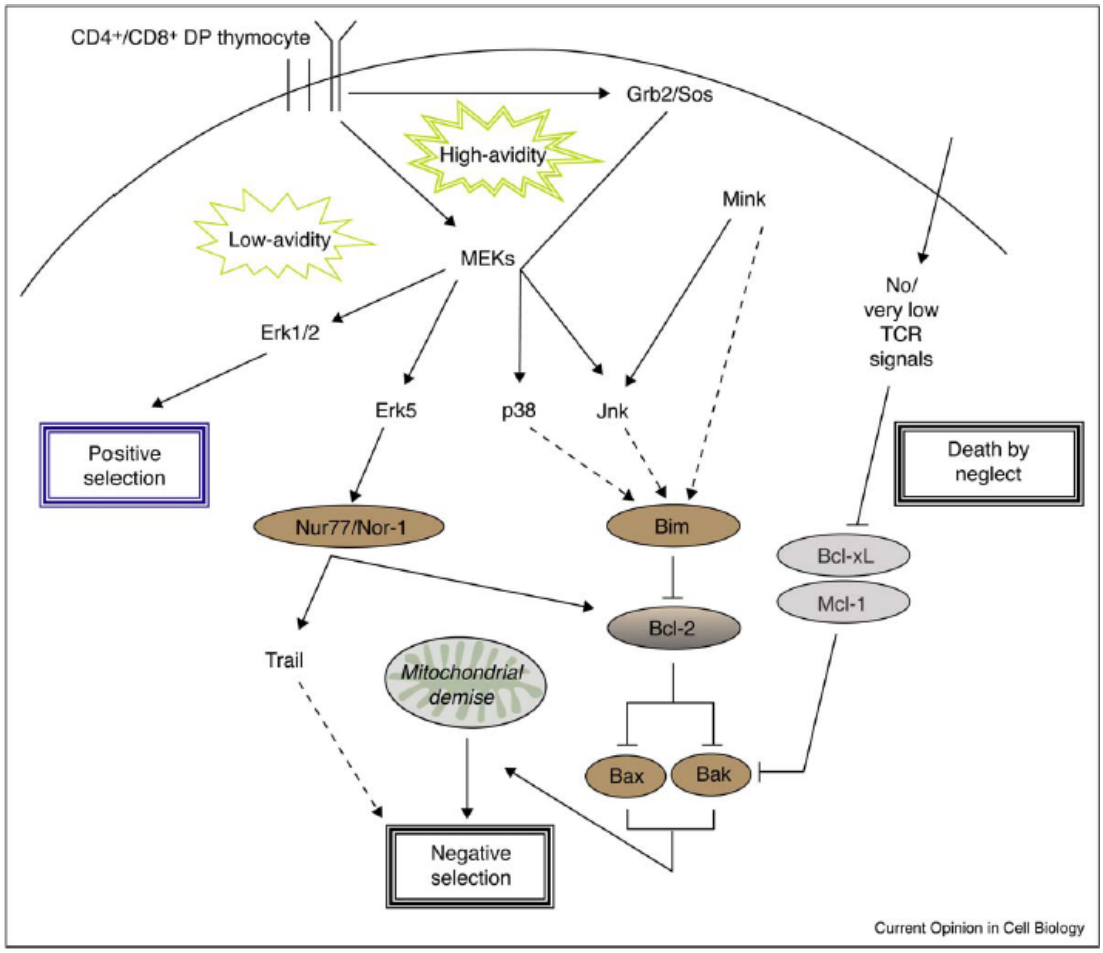

Fig. 1.2 TCR signalling pathways involved in positive vs negative selection of DP thymocytes (from Hernandez *et al* 2010).
TCR signalling in DP thymocytes discriminates very fine differences in affinities (analog input) high vs low, and translate them into distinct biological outcomes (digital output), by differential regulation of signalling pathways downstream of MEK. High-avidity signals lead to Grb2-SOS recruitment to the membrane, activation of JNK and p38, which repress anti-apopotic Bcl2 and up-regulate the pro-apopotic molecule Bim, altogether causing cell death by allowing Bax and Bak to cause mitochondrial dysfunction. Positively selecting, low-affinity signals activate RasGRP-Ras-Raf1 and ERK1/2 at the Golgi. In the absence of appropriate TCR signals, T cells die by neglect mediated by the pro-apoptotic molecules Bax and Bak.

nucleotide exchange factor Son of Sevenless (SOS) recruitment to the membrane, but instead activated the Ras guanyl nucleotide-releasing protein (RasGRP) – Ras - Raf1 and ERK pathway at the Golgi (Daniels et al., 2006). Negatively selecting, high-affinity signals, induced 3 times higher concentrations of Zap-70 at the membrane than positive selecting signals, and enhanced LAT phosphorylation, resulting in recruitment of Grb2-SOS and activation of Ras-Raf1-ERK at the plasma membrane (Daniels et al., 2006; Mallaun et al., 2010). Negatively-selecting signals also activate c-Jun N-terminal kinase (JNK), which represses expression of anti-apopotic Bcl-2 and up-regulates the pro-apopotic molecule Bim (Dong et al., 2002; Morris and Allen, 2012) to induce cell death. The sequestration of ERK to the membrane may be permissive for JNK activation as haplo-insufficiency of Grb2 compromised negative selection and JNK activation, but not ERK activation, suggesting that JNK has a higher activation threshold (Gong et al., 2001).

Additional work, using Foerster resonance energy transfer (FRET) microscopy, has shown that CD8 and TCR interactions induced by negatively selecting signals lead to FRET signals that accumulate faster and are more short-lived than the positively selecting ligands (Mallaun et al., 2008). This is in line with the studies suggesting ERK signalling needs to be sustained for positive selection (Mariathasan et al., 2001).

Perturbations in signalling molecules downstream the TCR, such as in Zap-70, can lead to the production of a peripheral repertoire with increased autoimmunity. The Sakaguchi lab discovered the SKG strain of mice that had a spontaneous mutation in the SH2 domain of Zap-70 causing reduced expression of Zap-70 and spontaneous autoimmune arthritis (Sakaguchi et al., 2003). The mutated Zap-70 molecule is more rapidly degraded and is less efficient at downstream tyrosine phosphorylation (Tanaka et al., 2010). These mice were used to address how changing the abundance of functional Zap-70 could impact on thymic selection. To this end Sakaguchi and colleagues compared wild-type (WT) (+/+), heterozygous (*skg*/+), homozygous (*skg*/*skg*) and hemizygous (*skg*/-) mice and found that autoimmune clones of T cells, normally deleted due to increased TCR affinity, were selected into the

peripheral repertoire in mice with SKG mutations due to reduced Zap-70 signalling and the consequent 'selection shift' (Tanaka et al., 2010). A graded expression of mutated Zap-70, that acts directly downstream of Lck, was therefore shown to result in alterations in positive and negative selection of T cells in the thymus (Tanaka et al., 2010).

1.4.3 Models of Lineage Divergence in DP Thymocytes

Many models have been put forward to explain how the CD4 versus CD8 lineage choice is determined in bipotential DP thymocytes that express both CD4 and CD8 co-receptors. Two classical models of lineage choice are stochastic and instructive, depending on whether termination of co-receptor transcription is thought to be random or instructed (Singer et al., 2008). The stochastic model proposes a two-step mechanism of lineage choice by which termination of co-receptor expression occurs randomly, and a second TCR signal rescues either $CD4^+$ or $CD8^+$ cells (Davis et al., 1993). For example, Davis et al. biased T cell development toward class II specificity by constitutive, transgenic CD4 expression and showed CD4 signals rescued a long-lived $CD8^+$ T cell population with mismatched MHC class II (Davis et al., 1993). The instructive model proposes a one step mechanism of selection dependent on the strength of the TCR signal. It posits that in DP thymocytes with mismatched co-receptors, *Cd8* or *Cd4* gene expression is instructively terminated because co-receptor engagement with MHC is class restricted and the co-receptors transduce qualitatively different signals. It has been shown that the CD8 co-receptor binds Lck with a lower affinity than CD4 (Bramson et al., 1991) thereby transducing weak signals, whereas the CD4 co-receptor can transduce strong signals. Itano et al. made use of a chimeric co-receptor transgene encoding CD8α molecules expressing the cytosolic domain of CD4 (Itano et al., 1996). The expression of the chimeric CD8-CD4 molecule resulted in development of MHC I restricted $CD4^+$ T cells. Experiments with bispecific antibodies that co-ligate TCR/CD3 with either CD4 or CD8 molecules, showed that agonist signals bringing Lck to the signalling complex, both CD3/CD4 or CD3/CD8, direct $CD4^+$ SP maturation, however these experiments were unable to determine how $CD8^+/CD4^+$ SP maturation

was triggered (Bommhardt et al., 1997). Additionally, Hernandez-Hoyos and colleagues bred mice with a catalytically inactive Lck with a class II-restricted transgenic (AND) mice and mice with constitutively active Lck with class I-restricted transgenic (OT-I) mice (Hernandez-Hoyos et al., 2000). They hypothesised, that if Lck being brought to the signalling complex is determinative, then lack of Lck in AND mice would change lineage commitment toward $CD8^+$ SP, and conversely, excessive Lck on an OT-I background will change commitment towards $CD4^+$ SP. Their results showed that regardless of class restriction, amount of Lck was indeed responsible for determining the fate of thymocytes (Hernandez-Hoyos et al., 2000). These studies collectively suggested that DP thymocytes are instructed into the CD4 or CD8 lineage depending on the strength of the signal, defined by the abundance of Lck, that TCR and co-receptor binding to class I or II MHC can transduce intracellularly.

However, several studies have since shown that by altering the signal intensity of the co-receptor molecules themselves it was possible to induce increased thymic selection of MHC class-I restricted T cells as well, without impacting the CD4/CD8-lineage choice. For example, Erman et al. engineered the endogenous *CD8a* gene to encode the cytosolic tail of CD4 and cause strong-signalling via the stronger interaction with Lck. This increased positive selection of MHC class-I restricted thymocytes cells but overall had no impact on CD4/CD8-lineage choice (Erman et al., 2006). Additionally, Bosselut et al. replicated the initial study done by Itano et al. but in CD8α deficient mice with CD8-CD4 chimeric co-receptors (Bosselut et al., 2001). They also found that, the strength-of-signal, mediated by amount of Lck, did not determine the CD4/CD8 lineage choice but influenced the proportions of developing cells (Bosselut et al., 2001). Collectively, these studies showed that the enhanced interaction between the CD4 co-receptor and Lck in the thymus leads to the development of higher proportions of $CD4^+$ SPs than $CD8^+$ SPs.

Attempts to disprove models have led to the development of new models, one of them being the non-classical kinetic signalling model of CD4/CD8

lineage choice. The kinetic signalling model proposes that regardless of MHC restriction in DP thymocytes, TCR signalling can induce arrest of the *Cd8* gene transcription creating an intermediate $CD4^{lo}CD8^{-}$ population, which retain the potential to become either $CD4^{+}$ or $CD8^{+}$ T cells. Lineage choice is based on whether CD8 downregulation induces a 'break' in TCR signalling or not. If it does, then IL-7 signaling, which is reciprocal with TCR signalling (Hong et al., 2012), would induce 'co-receptor' reversal and CD8 re-expression leading to the $CD8^{+}$ SP lineage. If it does not induce a 'break' in TCR signalling the cell would become a $CD4^{+}$ SP thymocyte (Brugnera et al., 2000; Singer et al., 2008).

The kinetic signalling model is supported by the more intricate control, at a transcriptional level, of CD4 and CD8 lineage choice. TCR signalling in DP thymocytes can induce arrest of *Cd8* gene transcription (by suppressing the *Cd8* gene enhancer $E8_{I}$) and upregulate expression of DNA-binding protein TOX, thereby maintaining *Cd4* expression and facilitating the development of the intermediate $CD4^{hi}CD8^{-}$ population (Singer et al., 2008). If TCR signalling does not cease, suggesting that the signal is MHC II restricted, the expression of nuclear factors GATA-3 and ThPOK increase promoting the development of the CD4 lineage by suppressing IL-7 signals and the expression of genes defining the CD8 lineage (Xiong and Bosselut, 2012). If, on the other hand, the TCR signalling ceases, suggesting that it is MHC I restricted, IL-7 signals and enhanced expression of transcription factor Runx3 promote the development of $CD8^{+}$ T cells by suppressing the expression of the *Cd4* gene and *ThPOK* (Woolf et al., 2003; Xiong and Bosselut, 2012). Runx3KO mice are impaired in making the CD4 versus CD8 lineage decision, and peripheral T cells express both co-receptors, supporting the importance of this transcription factor in lineage decisions (Woolf et al., 2003).

A recent study made a case for both signal strength (quantitative) and kinetic signalling models (co-receptor reversal) of development acting in concert during lineage development (Alarcon and van Santen, 2010; Saini et al., 2010). The study by Saini et al. showed that Zap-70 expression is developmentally and temporally regulated in the thymus and it creates

distinct temporal windows for each lineage to be selected at different TCR signaling thresholds (Saini et al., 2010). CD4 development happened earlier and in response to stronger TCR signals ($CD5^{hi}TCR^{med}$) than the CD8 lineage ($CD5^{med}TCR^{hi}$), which was delayed by ~3 days, and CD8 lineage commitment required accumulation of Zap-70 and thus a higher sensitivity to TCR ligation (Saini et al., 2010).

1.5 Peripheral T Cell Signaling

Peripheral T cells are the key mediators of the adaptive immune response. Upon exposure to antigen, T cells differentiate, acquire effector function, proliferate and finally form memory. T cells are selected in the thymus based on their responsiveness to self-p:MHC. Therefore, mature peripheral T cells have the potential to be self-reactive. This is an important feature for T cell survival in a resting state, as they must receive tonic, low-affinity signals from self-p:MHC complexes as well as signals via the IL-7R (Seddon and Zamoyska, 2002). The threshold of activation must be precisely set in T cells in order for them to respond to any foreign antigens, whilst enforcing central tolerance to self-antigens. Fate decisions thus ultimately depend on interpretation of the combined environmental cues by the T cell receptor (TCR) – signal 1, signals from co-stimulatory molecules – signal 2, and cytokine receptors – signal 3 (Salmond et al., 2009b; Zamoyska et al., 2003).

It is convenient to think of the TCR signalling cascades and regulatory modules according to the classifications assigned to the TCR signalosome (the entire TCR signaling machinery) by Acuto *et al.* (2008). The first is the SFK regulation module, including Lck and the associated positive and negative regulators of Lck activity. The second is the signal triggering module consisting of ten ITAMs in the dimeric CD3 chains of the TCR complex, and Zap-70. The third and final module is the signal diversification and regulation module (Acuto et al., 2008). The intricate connectivity, inter-regulation and abundance of the molecules in these different modules give the TCR the unique fine-tuning ability to discriminate between signals. The

following sections will look at each of TCR signal initiation, propagation and ultimately regulation.

1.5.1 Module 1: Kinase Regulation

Lck activity is tightly regulated, independently of TCR engagement, by the phosphorylation states of its two tyrosine (Y) residues - the inhibitory residue Lck^{Y505} in the C-terminal domain and the activatory Lck^{Y394} in the kinase domain (Salmond et al., 2009b). Lck^{Y505} is phosphorylated by C-terminal Src kinase (Csk), permitting the molecule to adopt a closed conformation with the inhibition of kinase activity. Lck^{Y505} is dephosphorylated by CD45, resulting in upregulation of kinase activity. The kinase domain Lck^{Y394} is regulated by autophosphorylation and dephosphorylated by phosphatases CD45, protein tyrosine phosphate non receptor type 6 (PTPN6 also known as Shp1), and PTPN22 (Cloutier and Veillette, 1999).

Mice deficient in Csk show hyperactivity of Lck (Imamoto and Soriano, 1993; Schmedt et al., 1998), and CD45 deficient mice display severe defects in thymic development due to hyperphosphorylation of Lck^{Y505}, which renders Lck inactive and prevents TCR triggering (Byth et al., 1996; Hermiston et al., 2003). The reconstitution of CD45 deficient mice with graded expression levels of CD45, demonstrated that low activity of CD45 led to reduced TCR signalling, and intermediate CD45 activity caused hyperactivation of $CD4^+$ and $CD8^+$ T cells (McNeill et al., 2007). These studies indicated the importance of the dynamic regulation of Lck, and identified CD45 and Csk as gatekeepers of TCR activation.

In naïve cells, 40% of Lck was shown to be constitutively doubly phosphorylated on both the Y505 and Y394 residues, and in an open conformation 'poised' for activation. Tonic signaling in T cells maintains partial phosphorylation of TCR ζ -chains by Lck (Nika et al., 2010; Stefanova et al., 2002).

1.5.2 Module 2: Zap-70

Upon TCR engagement with p:MHC, the negative regulators are thought to be excluded from the synapse, and Lck can phosphorylate the ITAMs without immediate dephosphorylation (Fig.1.3) (Springer, 1990). When two ITAMs in a dimeric CD3 chain (γε, δε and ζζ) of the TCR complex are phosphorylated they bind the SH2 domain of Zap-70 (van Oers et al., 2000). The binding of multiple Zap-70 molecules to ITAMS is thought to 'unlock' Zap-70 from an inactive configuration (Deindl et al., 2007), allowing it to be autophosphorylated and phosphorylated by Lck to subsequently continue the cascade of downstream phosphorylation events (Smith-Garvin et al., 2009). In resting cells some unphosphorylated Zap-70 is associated with partially phosphorylated ITAM ζ-chains due to tonic self-p:MHC signalling, allowing for a quicker signal transduction upon TCR agonist-ligand engagement (van Oers et al., 1994).

The first direct targets of Zap-70 are the transmembrane adapter protein LAT and the cytosolic adapter SH2 domain-containing leukocyte phosphoprotein of 76kDa (SLP-76). The absence of either LAT or SLP-76 results in a loss of T-cell signaling as they are critical for the spatiotemporal arrangements of subsequent effector molecules (Smith-Garvin et al., 2009). Zap-70 is therefore instrumental in controlling the connectivity of the TCR signalosome.

1.5.3 Module 3: Signal Diversification

Phosphorylation of 9 tyrosine residues on LAT upon TCR engagement leads to its binding of phospholipase C gamma (PLC-γ), phosphoionositide 3-kinase (PI3K), the adapters Grb2 and Grb2-related adapter downstream of Shc (Gads) (Patel and Mohan, 2005; Smith-Garvin et al., 2009). It is via the recruitment of Gads, that LAT binds SLP-76. SLP-76 has an N-terminal acidic domain with three tyrosines that when phosphorylated interact with SH2 domains of Vav1, Nck, and IL-2 induced tyrosine kinase (Itk). SLP-76 also has a proline-rich domain that binds Gads and PLC-γ and finally its C-terminal SH2 region facilitates the binding of adhesion and degranulation-promoting adaptor molecule (ADAP) and hematopoietic progenitor kinase 1

(HPK1) (Koretzky et al., 2006). Itk is required for the recruitment of Vav1, whilst Vav1 is itself required for Itk activation and optimal phosphorylation of SLP-76. Similarly, PLC-γ interacts with LAT, Vav1, SLP-76 and Itk, most probably to stabilise the complex.

Downstream of PLC-γ are Ca^{2+}, diacylglycerol (DAG) and Ras (a guanyl nucleotide-binding protein) mediated pathways. PLC-γ hydrolyses phosphatidylinositol-4,5-bisphosphate (PIP_2) producing inositol 1,4,5 – trisphosphate (IP_3) and DAG.

The PLC-γ mediated IP_3 production stimulates Ca^{2+}-permeable ion channel receptors (IP_3R) on the membrane of the endoplasmic reticulum (ER) leading to Ca^{2+} flux into the cytoplasm. When ER Ca^{2+} is depleted, CRAC channels are activated and lead to Ca^{2+} influx by the 'store-operated' mechanisms of Ca^{2+} entry through the plasma membrane (Oh-hora and Rao, 2008). Ca^{2+} is an important second messenger by causing the activation of several transcription factors among which are NFAT, and Ca^{2+}-calmodulin dependent kinase (CamK) (Smith-Garvin et al., 2009). These mediate gene regulation resulting in cell proliferation and cytokine gene expression (Oh-hora and Rao, 2008).

DAG is important for PKC mediated pathways. There are several PKC family enzymes, but the best known is PKCθ. PKCθ mediates phosphorylation of caspase recruitment domain (CARD) and membrane-associated guanyl kinase (MAGUK)-containing scaffold protein (CARMA1) (Hayashi and Altman, 2007). CARMA1 forms a complex with mucosa-associated lymphoid tissue lymphoma translocation gene 1 (MALT1) and Bcl10. This large complex recruits and activates the IKK complex thereby allowing the IKK complex to phosphorylate IκB. IκB is normally bound to the p50-p65 subunits of nuclear factor kappa B (NFκB), but the phosphorylation of IκB degrades it and releases NFκB. Consequently, NFκB translocates to the nucleus and binds specific κB sequences on DNA which control transcription of genes involved in inflammation, cell survival and cell division (Gerondakis et al., 2014).

DAG also recruits Ras guanyl nucleotide-releasing protein (RasGRP), which is phosphorylated by PKCθ to activate Ras (Houtman et al., 2005). Ras mediates MAPK pathway activation via Raf-1 culminating with the activation of ERK1 and ERK2 (Smith-Garvin et al., 2009). MAPK pathways ultimately lead to gene regulation by activating transcription factors such as activator protein 1 (AP1) (Oh-hora and Rao, 2008; Smith-Garvin et al., 2009).

TCR stimulation also impacts on actin reorganisation and inside-out integrin mediated cell adhesion pathways. Upon ligation by p:MHC on an APC, the T cell undergoes morphological changes that lead to cell polarisation and formation of the immunological synapse (IS) as well as the cessation of T cell mobility to facilitate stronger contacts with the APC. For these purposes Vav1 dephosphorylates ezrin, radixin and moesin (ERM) proteins to increase the fluidity of the plasma membrane by unlinking it from the actin cytoskeleton (Smith-Garvin et al., 2009). TCR signal mediated activation of the small GTPase-Ras-proximity 1 (Rap1) enhances T cell binding in an ADAP dependent manner to intracellular adhesion molecule (ICAM) via leukocyte function-associated antigen 1 (LFA-1) (Peterson et al., 2001; Smith-Garvin et al., 2009)

1.5.4 Module 3 Continued: Negative Regulation of TCR Signalling

Dysregulation at any stage of T cell activation can result in immune disorders, including autoimmune diseases, and therefore T cell activation is actively negatively regulated. Negative regulation assures that TCR signalling is controlled appropriately, in terms of the strength and duration of the signal, and makes up the final component of the third module of signal diversification and regulation of the TCR signalosome. Many different negative regulation pathways and molecules that act at different stages of the TCR signalling cascade have been described, including inhibitory membrane-bound receptors such as cytotoxic T lymphocyte antigen 4 (CTLA4), programmed cell death 1 receptor (PD1), and CD5 that recruit protein tyrosine phosphatases (PTPs) (Acuto et al., 2008). An accumulation of activated T cells in $CTLA4^{ko}$ mice (Waterhouse et al., 1995) and lupus like

disease in PD1^{ko} mice (Nishimura et al., 2001) underline their importance in terminating TCR signalling. CD5 deficiency does not cause any immune disorders, although mice display altered T-cell development (Tarakhovsky et al., 1995).

Mice lacking inhibitory membrane-bound scaffold proteins such as phosphoprotein associated with glycosphingolipid-enriched microdomains (PAG) and Lck-interacting membrane protein (LIME), do not show overt phenotypes despite these molecules recruiting protein and lipid kinases and phosphatases as a means of controlling TCR signalling, suggesting there are sufficient compensatory mechanisms (Acuto et al., 2008). However, a mutation in PTPN22, a cytoplasmic negative regulator, that disrupts its binding with Csk is associated with an increased risk for autoimmune disease in humans (Begovich et al., 2004; Bottini et al., 2006; Zhang et al., 2011). It is thought that PTPN22 is associated with Csk and thereby recruited to the plasma membrane to negatively regulate SFKs (Cloutier and Veillette, 1999). Upon TCR ligation Fyn dephosphoryalates PAG, which releases Csk and subsequently allows for Lck to start the TCR signalling cascade, particularly in effector and memory T cells. However, PAG association with Csk is most likely not the only mechanism by which PTPN22 gets to the membrane, as PAG$^{-/-}$ mice do not show an overtly lymphoproliferative phenotype (Smida et al., 2007).

An important TCR-dependent proximal negative feedback mechanism, induced directly in response to TCR signaling, is the cytoplasmic PTPase SHP1. Antagonist-p:MHC signals recruit SHP1 rapidly to the TCR signalling complex, and cause its activation by Lck, which in turn leads to SHP1 downregulating Lck activity (Stefanova et al., 2003). SHP1$^{-/-}$ mice develop autoimmune disease due to dysregulated thymocyte selection and T-cell activation (Lorenz et al., 1996). Negative regulation by SHP1 therefore acts as an additional regulator of TCR signals. More proximal components of the signalosome are negatively regulated by Dok1 and Dok2 adaptor proteins (Yasuda et al., 2007).

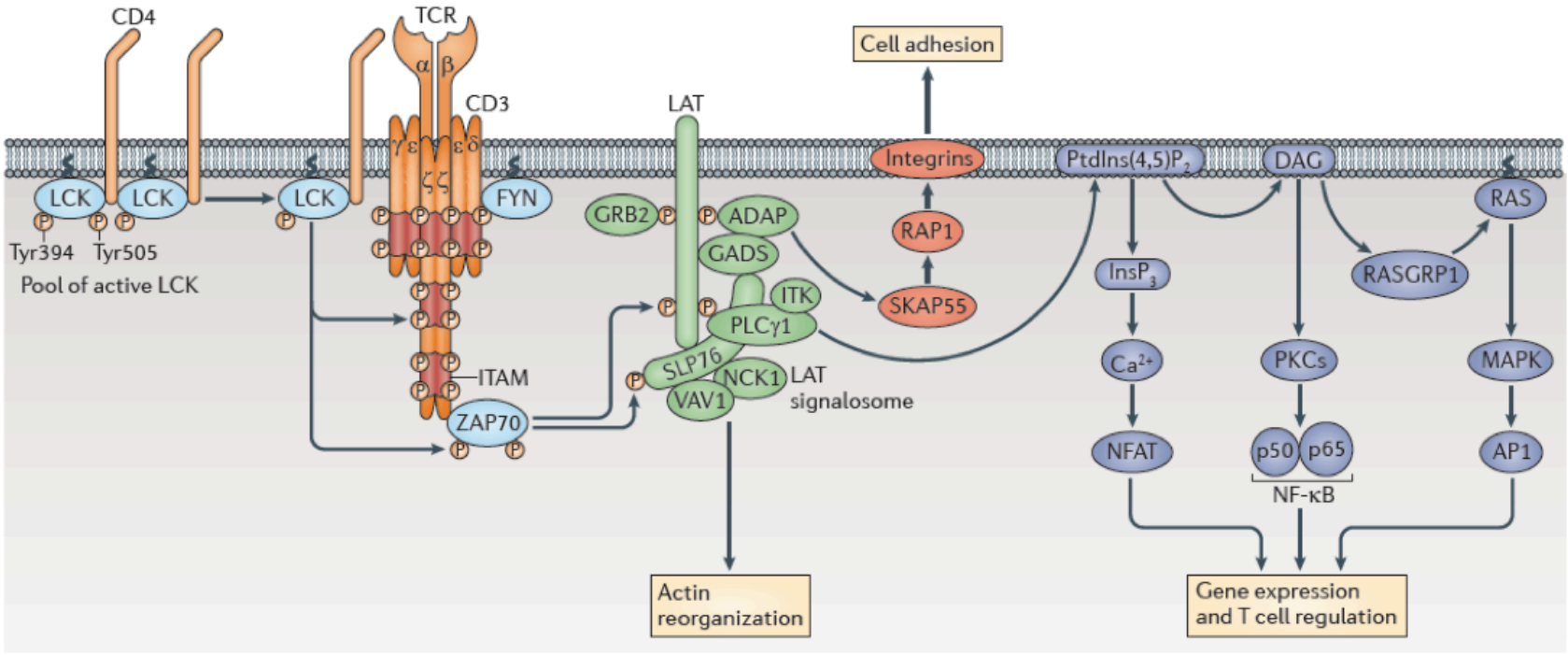

Fig. 1.3 Proximal T cell signalling cascades (from Brownlie *et al* 2013).
TCR engagement with p:MHC leads to co-receptor associated Lck recruitment. Lck is responsible for phosphorylation of the ITAMs, which recruit Zap-70. Zap-70 recruits and phosphorylates LAT and SLP-76, which form the LAT signalosome with PLC-γ, Gads, Itk, Nck1, Vav1, ADAP and Grb2. From the LAT signalosome three major TCR signalling pathways are triggered: the Ca^{2+}, MAPK and NFκB pathways via PtdIns(4,5)P_2, Ras, and DAG, respectively. These lead to gene expression changes influencing actin reorganisation and integrin mediated cell adhesion pathways.

Schoenborn et al. described a potential interaction between Dok1 and Csk that may contribute to negative regulation of Lck activity in response to TCR ligation (Schoenborn et al., 2011). Indeed, $Dok1^{-/-}Dok2^{-/-}$ mice have increased TCR-induced IL2 production, and proliferation correlating with increased phosphorylation of Zap-70, LAT and ERK, suggesting the Dok proteins have an important role in TCR signalling, however, their exact mechanism of action has yet to be determined.

In addition to these early/immediate regulatory mechanisms in response to TCR-signalling, there is a more downstream mechanism: the HPK1-SLP-76-14-3-3 pathway (Di Bartolo et al., 2007) In response to TCR stimulation, Lck phosphorylates HPK1, which then binds and phosphorylates $SLP\text{-}76^{Ser376}$, which in turn associates with 14-3-3 proteins. HPK1 phosphorylation of SLP-76 occurs after 10-15min of TCR stimulation, and lasts up to an hour (Ling et al., 2001). HPK1 deficiency results in increased TCR-dependent tyrosine phosphorylation of SLP-76, PLCγ, LAT, Vav1, and Zap-70, leading to a more severe form of experimental autoimmune encephalomyelitis, again highlighting the importance of negative regulation (Shui et al., 2007).

1.5.5 Initiating TCR signal transduction

The TCR is unique in its ability to discriminate between a high level of self p:MHC molecules (noise) and a lower level of foreign p:MHC ligands (signal) (van der Merwe and Dushek, 2011). It demonstrates extensive versatility and structural diversity when binding multiple ligands with different affinities and producing different biological outcomes (van der Merwe and Dushek, 2011). Several models have been proposed to explain the mechanisms behind TCR triggering. The following section will briefly summarise the three main models of aggregation, conformational change, and segregation.

Aggregation

Two types of aggregation can occur for TCR triggering – co-receptor heterodimerisation or pseudodimer formation. The co-receptor

heterodimerisation model proposes that the co-receptor can bind to the same p:MHC complex as the TCR and recruit Lck into proximity with the CD3 complex and ITAMs, thereby initiating the TCR signaling cascade (van der Merwe and Dushek, 2011). On the other hand the pseudodimer formation model suggests that one TCR complexes with an agonist-p:MHC and a neighbouring TCR complexes with a self-p:MHC thereby enhancing the TCR trigger to low density agonist-p:MHC ligands (van der Merwe and Dushek, 2011).

Conformational Change

Studies have looked at the conformation of TCR in bound and unbound states and found that there may be a conformational change in the TCRα chain constant domain (Kjer-Nielsen et al., 2003). In order for this model to explain how the TCR can transduce different signals to the cell interior it was suggested that there are differences in dimerisation upon conformation change, therefore combining the conformation change model with the aggregation model (Kjer-Nielsen et al., 2003). It has also been suggested that the conformational change occurs at the level of the CD3 residues associated with the TCR. Subtle repositioning of CD3ε cytoplasmic domains may release them from lipid bilayer of the plasma membrane, lead to exposure of the cryptic epitope in CD3ε and make them available as substrates for Lck (Minguet et al., 2007). Indeed, the level of CD3 phosphorylation was shown to be incomplete with low affinity stimulation of TCR ligands (Sloan-Lancaster et al., 1993). Additionally, it has been proposed that the sheer mechanical force of MHC binding to the TCR that is transduced through the CD3$\gamma\varepsilon$ heterodimer causes conformational changes and in that scenario the discrimination between different ligands would be mediated by the duration of ligand binding (Kjer-Nielsen et al., 2003).

Segregation

Models of segregation suggest that the distribution of TCR-CD3 complexes with respect to other cell membrane-associated proteins control TCR triggering. The kinetic segregation model suggests that the TCR is positioned

in Lck rich areas of the lipid membrane, and due to large ectodomains of the negative regulator CD45, upon MHC binding it is excluded from these areas of close-contact (Acuto et al., 2008; Springer, 1990; van der Merwe and Dushek, 2011). Exclusion of negative regulators increases half-lives of phosphorylated ITAMs which then recruit Zap-70 and trigger the downstream signalling cascade (Davis and van der Merwe, 2006). The half-life of the TCR-MHC interaction however influences the extent of ITAM phosphorylation (Davis and van der Merwe, 2006).

In summary it is possible that a combination of different models most accurately describes TCR triggering. Indeed, Van der Merwe and Dushek proposed the following sequence of events: 1. p:MHC binding to TCR tilts the balance of phosphorylation/dephosphorylation of Lck such that its kinase activity is increased, by exclusion of local phosphatase activity. 2. TCR engagement also causes conformational change in the TCR-CD3 complex enhancing the susceptibility to phosphorylation and activation. 3. Given that the ligand enagegement is lasting microclusters of 10-100 TCRs are formed. 4. The large clusters enable discrimination of rare antigenic-p:MHC complexes from abundant self-p:MHC complexes by cooperative interactions (van der Merwe and Dushek, 2011).

1.6 T Cell Effector Function

The $CD8^+$ T cell response has two goals; firstly, to quickly generate enough cytotoxic T lymphocytes (CTLs) to clear the infection and, secondly, to retain a subset of memory cells that can act faster, should the same pathogen be encountered again. A $CD8^+$ T cell requires antigen stimulation, CD28-dependent co-stimulation, and IL-12 or Type I interferons (IFNs) for activation and commitment to clonal expansion and effector cell differentiation (Williams and Bevan, 2007). CTLs are characterised by extensive proliferation, the ability to produce granzymes and perforin to kill target cells, as well as the secretion of antiviral cytokines such as IFNγ and TNFα (Kaech and Cui, 2012; Mescher et al., 2006).

Upon TCR activation in a naïve T-cell, rapid and transient secretion of IL-2 is seen, which induces expression of the IL-2 receptor (IL-2R). IL-2 is a well-known and important cytokine as on one hand it induces T-cell expansion, survival, effector differentiation, and memory cell survival. On the other hand it also controls the contraction of inflammatory responses by promoting growth and survival of T_{Regs} and stimulating activation induced cell death (AICD) (Martins and Calame, 2008). IL-2 signaling leads to activation of the transcription factor Stat5 and its own negative-feedback loop (Malek, 2008). Among other molecules IL-2 also induces expression of Blimp-1 (Martins et al., 2008). The expression of IL-2 and Blimp-1 upon TCR stimulation is inversely correlated. Indeed, it has been shown that Blimp-1 represses the *Fos* gene (Martins et al., 2008). The Fos protein is a component of the IL-2 inducing transcriptional pathway mediated by AP-1. Therefore, the *IL-2* gene is repressed by Blimp-1 via its control of Fos (Martins et al., 2008).

Activated $CD8^+$ T cells produce TNFα that can mediate antiviral effects by binding to TNFα receptors on cells and enhancing the expression of transcription factors NFκB and AP-1, which induce expression of pro-inflammatory and immunomodulatory genes (Herbein and O'Brien, 2000).

Co-stimulation by IL-12 leads to the production of the type II interferon, IFNγ, which binds the IFNγ-receptor (IFNGR) and signals through the Jak-Stat pathway (Schroder et al., 2004). IFNγ enhances MHC class I expression on the cell surface and causes the expression of the 'immunoproteasome' instead of the constitutively expressed proteasome (Schroder et al., 2004). It is thought that the enhanced MHC class I expression increases the abundance and variety of peptides presented on the cell surface, increasing the chances of recognition by CTLs (Schroder et al., 2004). IFNγ can also upregulate the expression of class II MHC molecules, and enhance peptide presentation to and activation of $CD4^+$ T cells (Schroder et al., 2004).

The aim of $CD8^+$ T cells is to eliminate infected target cells by inducing their apoptosis. Cell apoptosis is mediated by caspases, a family of cysteine proteases (Nicholson and Thornberry, 1997). CTLs activate the caspase

pathway in target cells upon making contact and releasing granules of specialised secretory lysosomes containing cytolytic effector proteins, such as perforin, granzymes, FasL as well as lysosomal hydrolases (Jenkins and Griffiths, 2010). In the cleft between the target and the CTL the presence of Ca^{2+} causes polymerisation of perforin, which damages the target cell membrane and can mediate granzyme entry (Russell and Ley, 2002). Granzyme B has many substrates, such as apoptotic nucleases that can induce DNA fragmentation as well as pro-caspases, that lead to the activation of the caspase mediated death pathway, and ultimately also to DNA fragmentation (Russell and Ley, 2002). FasL induces apoptosis of Fas expressing target cells. Fas engagement by FasL causes the assembly of death inducing signaling complex (DISC), which induces activation of caspases. Part of DISC formation is Fas mediated recruitment of Fas associated death domain (FADD) and caspase 8 (Nicholson and Thornberry, 1997).

1.6.1 Co-stimulation and the Role of Cytokines

Ligation of the TCR alone leads to T cell anergy (Schwartz, 2003). For full activation a T cell requires co-stimulation signals in addition to TCR engagement. CD28 on T cells binds CD80 (B7.1) and CD86 (B7.2) on APCs, which are upregulated during activation, and this engagement enhances TCR mediated signaling. CD28 signaling enhances proliferation and survival by promoting production of IL-2 (Sharpe and Freeman, 2002). The importance of the CD28 co-stimulatory pathway is exemplified by CD28 blockade being used clinically to treat autoimmune disease (Kremer et al., 2003). There are also additional co-stimulatory molecules OX40 (CD134), 4-1BB (CD137), and CD27, that are said to aid continued cell division that was initially started by CD28 (Croft, 2003; Williams and Bevan, 2007).

Optimal T cell activation also requires a third signal that can be delivered by IL-12, type I IFNs and TLR ligands (Williams and Bevan, 2007). IL-12 promotes effector function development by enhancing IFNγ and granzyme B production (Croft, 2003; Williams and Bevan, 2007). Type I IFNs have been shown to promote T cell survival during activation in a manner distinct from the functions of IL-2 or CD28 (Marrack et al., 1999).

1.7 Regulatory T Cells (T_{Regs})

T_{Regs} are a subset of $CD4^+$ T cells that are important for maintaining immune tolerance by countering adaptive immune responses (Liston and Gray, 2014; Setoguchi et al., 2005). T_{Regs} are commonly further split into two subsets of natural T_{Regs} that develop in the thymus and peripheral or induced T_{Regs} that develop in the periphery. Natural T_{Regs} are thought to develop in the thymus in response to enhanced sensitivity to self and they commonly express high levels of IL-2Rα and represent ~5-10% of $CD4^+$ T cells (Klein and Jovanovic, 2011; Setoguchi et al., 2005). Indeed, IL-2 has been shown to play an important role in maintenance of natural T_{Reg} populations (Setoguchi et al., 2005). Extrathymic development of induced T_{Regs} from naïve $CD4^+$ T cells was found to be tumour growth factor β (TGFβ) mediated (Apostolou and von Boehmer, 2004). Both subsets of T_{Regs} are characterised by the expression of the X chromosome-encoded member of the winged-helix family of transcription factors (Foxp3) (Williams and Rudensky, 2007). Foxp3 deficiency in humans leads to severe immune dysregulation (Gambineri et al., 2003) and similarly, IL-2 deficiency substantially reduces proportions of natural T_{Regs} causing lymphoproliferative inflammatory disease in mice (Papiernik et al., 1998).

1.8 T Cell Memory

The ability to form immunological memory is the hallmark of the adaptive immune system. Memory cells are characterised by their ability to mount more rapid and enhanced immune responses upon secondary encounters with pathogens, a consequence of their increased sensitivity to antigen, as they can be activated by 10 to 50-fold lower peptide concentrations than naïve T cells (Pihlgren et al., 1996).

Many different mechanisms have been proposed that provide memory cells the higher signalling efficiency than that of naïve cells (Zehn et al., 2012). One potential explanation is that antigen-experienced $CD8^+$ T cells have an altered and more efficient signal transduction cascade, potentially due to the differential spatial reorganisation of negative regulators and TCR signal mediators (Borger et al., 2013). In addition to negative regulators of TCR

signaling being redistributed away from the site of TCR engagement in CD8+ memory T cells, it was shown that Lck was more efficiently recruited to the site of TCR engagement (Borger et al., 2013), possibly because of the reported increased localisation with the CD8 co-receptor (Bachmann et al., 1999). In contrast, however, Tewari et al. have reported that memory CD8+ T cells were Lck-independent with less stringent requirements for antigen-specific TCR signaling to activate them (Tewari et al., 2006). It has also been proposed that memory cells have more lipid rafts with a higher content of important signalling molecules like LAT, ERK and JNK compared to naïve cells, that could account for their more rapid activation (Kersh et al., 2003). Another proposed mechanism, for the enhanced activation of memory cells, is the epigenetic modulation of effector molecule genes, that are 'poised' for rapid polymerase accessibility and transcriptional activation (Youngblood et al., 2013). For example, it has been shown that the IFNγ locus is highly methylated in naïve cells, while the methylation was only partial in memory cells, allowing for a more rapid production of IFNγ upon stimulation (Kersh et al., 2006). The same has been shown to be true for other effector molecules such as perforin and granzyme B (Araki et al., 2008). Epigenetic regulation of pro-survival genes (Araki et al., 2009), and genes encoding molecules that mediate inhibitory signals, have also been shown to play a role in regulating the sensitivity of memory cells to activation (Youngblood et al., 2011).

Approximately 90-95% of the initial heterogenous effector cell pool generated during a primary immune response die and only the remaining small percentage become memory cells. Recent years have seen a great increase in research defining phenotypic markers to discriminate between terminal effector and memory precursor effector cells and characterising the mechanisms behind effector versus memory fate decisions (Kaech and Cui, 2012). Conventionally, CD44 and CD62L surface expression are used to identify central memory T cells (T_{CM}) and effector memory T cells (T_{EM}) as $CD44^{hi}CD62L^{hi}$ and $CD44^{hi}CD62L^{lo}$, respectively (Sallusto et al., 1999). Additionally, a subset of effector cells that develop into memory cells, memory precursor effector cells (MPECs), can be characterised by their $CD127^{hi}$, $CD27^{hi}$, $Bcl\text{-}2^{hi}$ and decreased expression of killer cell lectin-like

receptor G1^{lo} (KLRG-1) phenotype, conversely, a terminally differentiated short-lived effector cell (SLEC) is typically CD127^{lo} and KLRG-1^{hi} (Joshi et al., 2007; Sarkar et al., 2008).

Several models have been proposed to explain what determines whether a cell becomes a terminal effector cell or a memory cell summarized in brief below.

Separate Precursor Model

This model proposed that naïve T cells are 'pre-programmed' in the thymus to adopt either an effector fate or memory cell fate upon activation. However, studies showing that individual naïve CD8^{+} T cells give rise to both effector and memory cells when transferred (Stemberger et al., 2007). Additionally, cellular barcoding experiments, in which cells were retrovirally transduced with a unique semirandom stretch of noncoding DNA and could therefore be identified by a barcode-microarray, demonstrated that a common pool of precursors could give rise to different pools of effector cells (Schepers et al., 2008).

Asymmetric Cell Fate Model

According to this model a single cell could give rise to multiple cell fates by asymmetric division (Chang et al., 2007). The proposition is based on the finding that a daughter cell that inherits the immunological synapse receives stronger signals and the subsequent cells over several division thus become effector cells. The asymmetric cell fate model thus indicates that a lineage decision is made as early as in the first cell division (Jameson and Masopust, 2009).

Decreasing Potential Model

The decreasing potential model is also known as the linear progression model, where all T cells pass through an early effector phase, but those receiving additional signals after priming undergo terminal differentiation and adopt the effector cell fate, and the T cells that do not receive these

signals become memory T cells (Ahmed and Gray, 1996). Indeed, Sarkar et al. showed curtailing antigenic stimulation near the end of an acute infection enhanced memory cell formation (Sarkar et al., 2008). Similarly, studies where antibiotic treatment was used to restrict inflammation, showed that this encouraged memory cell formation (Badovinac et al., 2004).

Signal-Strength Model

This model is similar to the asymmetric cell division model in that the first signals encountered could determine the lineage fate by distinguishing effector cells that develop in response to strong signals, and memory precursor cells that develop in response to weaker signals (Lanzavecchia and Sallusto, 2002). However, the signal-strength model also uniquely maintains that there is plasticity throughout the effector phase. Both effector and memory cells harbour effector cell properties initially and through the development of the immune response memory precursors could still become short-lived effector cells. Studies have shown that high expression of CD127, can distinguish a pool of effector cells at the peak of the primary response that are more likely to become memory cells later (Kaech et al., 2003). Additional studies supporting the signal-strength model have shown, that the amount of inflammation cells are exposed to can modulate the expression of Tbet (Joshi et al., 2007). High levels of Tbet were found to promote effector cell differentiation and conversely low levels to promote memory cell formation. Thus, studies consistent with the decreasing potential model are also consistent with the signal-strength model in that restricted inflammation can promote memory cell formation. Thus, the signal-strength model accounts for the development of effector cell heterogeneity early on but also maintains that the ultimate fate decisions depend on continual integrated interpretation of the environmental cues by the TCR – signal 1, signals from co-stimulatory molecules – signal 2, and cytokine receptors – signal 3 (Kaech and Cui, 2012).

1.8.1 Transcriptional Regulation of Memory Development

How differences in the signals that T cells receive can determine different cell fates was described by Best *et al* (2013), who recently published an extensive profiling of gene-expression signatures throughout infection i.e. the $CD8^+$ T cell transcriptome (Best et al., 2013). They grouped different factors into clusters based on their kinetic patterns of expression and the biological processes associated with them (Best et al., 2013). For example, they showed that cells biased toward memory precursor potential had lower expression of genes of cell cycle and division cluster, and of short-term effector memory cluster, than their short-lived effector memory counterparts (Best et al., 2013). T-bet and eomesodermin (Eomes) are two T-box transcription factors, characterised by their homologous T-box DNA-binding domain, that have important roles in the formation and function of effector and memory $CD8^+$ T cells (Kaech and Cui, 2012). T-bet, encoded by Tbx21, regulates many genes encoding effector molecules such as the expression of IL-2 and IFNγ (Intlekofer et al., 2005), and as such belongs to the memory formation cluster, along with Blimp1 and IL-12R (Best et al., 2013). T-bet expression is governed by IL-12 signaling. Abundance of IL-12 has been shown to enhance $CD8^+$ effector cell formation but decrease memory cell formation (Cui et al., 2009), further highlighting how the 3 signals in T cell effector and memory fate development are intricately linked. Eomes has cooperative and redundant functions to T-bet in regulating effector gene transcription (Intlekofer et al., 2005). Mice with mutations in both Eomes and T-bet expression ($Eomes^{+/-}$ $Tbet^{-/-}$) were shown to have defects in memory $CD8^+$ T cell development and cytotoxic effector programming (Intlekofer et al., 2005).

Another set of transcription factors, implicated in memory $CD8^+$ T cell subset formation, are DNA-binding inhibitors Id2 and Id3 (Yang et al., 2011). A deficiency in both Id2 and Id3 leads to a loss of $CD8^+$ effector and memory populations. Cells expressing high levels of Id3 become long lived memory T cells, and upregulate markers associated with memory potential such as CD127 (Yang et al., 2011). Id3 expression is regulated in response to TCR

signals as well as environmental cues. Interestingly, Blimp-1 has been shown to antagonise Id3 expression (Savitsky et al., 2007).

More recently the T_{CM} and T_{EM} balance was also shown to be influenced by Elf4 an E-twenty-six (ETS) family transcription factor (Mamonkin et al., 2013). Upon *L.monocytogenes* infection *Elf4*$^{-/-}$ formed lower numbers of effector cells despite developing a normal pool of T_{CM} cells.

1.8.2 Role of Cell Metabolism in Memory Cell Formation

The signals that control the transcriptional programme of T cell differentiation have also been shown to coordinate T cell metabolism. In comparison to naïve cells, effector cells have increased cellular nutrient uptake and energy production to sustain the increased proliferation. It has been proposed that upon T cell activation, the subsequent changes to T cell metabolism dictate the memory versus effector T cell fate decision (Finlay and Cantrell, 2011). This view stems from the observation that AKT and mammalian target of rapamycin (mTOR) are potentially at the core of integrating signals from antigens, cytokines and co-receptors (Finlay and Cantrell, 2011). For example experiments where mTOR was inhibited showed increased memory cell production from effector cells (Araki et al., 2009). One potential explanation is that mTOR is able to also influence the migration pattern of T cells by regulating expression patterns of CD62L and CCR7 (Sinclair et al., 2008), or expression patterns of Tbet and Eomes (Rao et al., 2010). Importantly, there are different magnitudes of AKT activity, potentially influenced by strength of TCR triggering. Low levels of AKT activity were sufficient for T cell growth and proliferation but not enough to change the chemokine and adhesion receptor profile of naïve cells to that of CTLs (Waugh et al., 2009).

1.9 Thesis Aims

The overarching aim of this thesis is to characterise the role of Lck in thymocyte development, peripheral T cell activation and memory formation. Lck is the first proximal SFK to be activated upon TCR ligation by p:MHC and it has been shown that Lck is important wherever TCR signaling is required during a T cells life span. Previous studies with transgenic mice with reduced Lck expression have shown that 5% of wild-type (WT) levels of Lck (Lck^{VA} mice) were sufficient to rescue thymic development. We therefore used the Lck^{VA} mice to address the following central aims of this thesis:

- To characterise the positive selection, thymocyte maturation, TCR sensitivity and the resulting naïve peripheral T cell pool in Lck^{VA} mice to better understand what effect abundance of Lck has on T cell development.
- To elucidate the role of Lck abundance in $CD8^+$ T cell activation and the generation of effector functions *in vitro.*
- To assess the impact of Lck abundance on effector to memory cell differentiation during *in vivo* bacterial infection in Lck^{VA} mice.

Chapter 2: Materials and Methods

2.1 Mouse Models

All mouse strains used were maintained and bred under pathogen-free conditions in the University of Edinburgh animal facilities according to Home Office regulations. All mice were bred on the C57BL/6 background, which were therefore also used as controls, henceforth referred to as Lck^{WT}.

2.1.1 Lck^{ind}

To study the time and concentration dependent roles of Lck, the Zamoyska group designed a mouse model with inducible Lck expression (Legname et al., 2000). A tetracycline-inducible transactivator domain (rtTA) was expressed constitutively as a T-cell specific transgene driven by human CD2 (huCD2) regulatory regions together with an Lck transgene under the control of a tetracycline-responsive/minimal cytomegalovirus (CMV) promoter (Fig.1). In the absence of the tetracycline derivative doxycycline there is no Lck expression in animals with the endogenous Lck knocked out (Lck^{ind}OFF), and they lack peripheral T-cells. Upon doxycycline administration Lck expression is switched on (henceforth termed Lck^{ind} mice) and the T-cell development in restored. Lck^{ind} mice express a range of Lck levels in the thymus, but only 15-20% of Lck compared to Lck^{WT} mice in the periphery (Legname et al., 2000; Lovatt et al., 2006).

2.1.2 Lck^{VA}

The Zamoyska group also designed a transgenic Lck mouse model with constitutively low levels of Lck expression (Lck^{VA}) (Salmond et al., 2011). The transgene (LckVA.1) was expressed in Lck^{KO} mice on the C57BL/6 background. LckVA.1 confers constitutive expression of less than 5% of WT Lck levels in both the thymus and the periphery.

2.1.3 F5 TCR Transgenic Mice

The Lck^{VA}, Lck^{ind} and Lck^{WT} mice were crossed with F5TCR transgenic Rag1 – knockout ($Rag1^{KO}$) mice. The F5 $Rag1^{KO}$ mice are transgenic for a class I MHC-restricted T-cell receptor, F5, and only develop $CD8^+$ T cells. The soluble cognate high-affinity peptide antigen is derived from an influenza virus nucleoprotein 68 (NP68) NP68 is a 9-mer peptide (Ala, Ser, Asn, Glu, Asn, Met, Asp, Ala, Met) corresponding to amino-acid residues 366-374 from strain A/NT/60/68 (H3N2) (Mamalaki et al., 1992). The low affinity peptide NP34 is also a 9-mer (Ala, Ser, Asn, Glu, Asn, Met, Glu, Thr, Met) corresponding to amino acid residues 366-374 from strain A/PR/8/34 (Mamalaki, Norton et al. 1992) Both, NP68 and NP34 are presented to T cells in the context of $H2\text{-}D^b$ (Mamalaki et al., 1992; Townsend et al., 1986). The peptides were synthesised by the Division of Protein Structure at the NIMR, Mill Hill, UK.

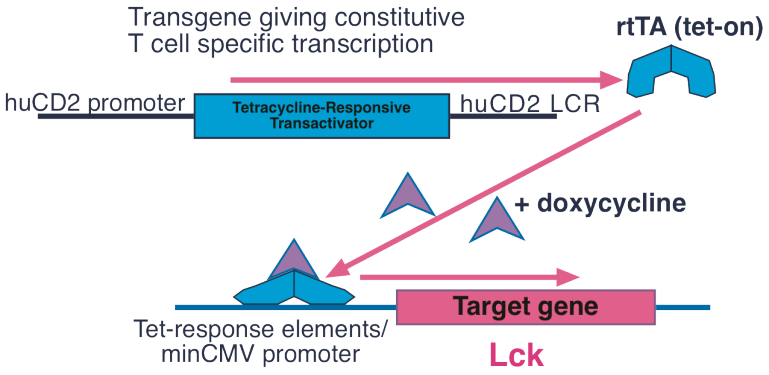

Fig. 2.1 Doxycycline inducible Lck expression in Lck^{ind} mice (from Zamoyska *et al.*, 2003).
Mice transgenic for the rtTA, constitutively expressed under the control of the T-cell specific huCD2 promoter, were crossed to transgenic mice that expressed Lck under inducible control of Tet-response elements upon administration of tetracycline or its derivatives. Both mouse lines were on the LckKO background.

2.2 Mouse Genotyping

2.2.1 Genotyping by Blood

ACK Lysis Buffer

150 mM Ammonium Chloride (Sigma-Aldrich, UK)

10 mM Potassium Bicarbonate (Sigma-Aldrich, UK)

0.1 mM EDTA (Sigma-Aldrich, UK)

50 μL of blood was collected by tail bleed into 50 μL of heparin (1000 U mL^{-1}) (Sigma-Aldrich, UK). After a PBS wash, 3 mL of ACK lysis buffer was added. Blood was thoroughly mixed and incubated for 5 minutes, followed by a PBS wash and subsequent antibody staining for flow cytometry (section 2.7).

2.2.2 Genotyping by PCR

Ear Digestion Buffer

100 mM Tris HCI pH 8.5 (Fisher – Scientific, UK)

5 mM EDTA (Sigma-Aldrich, UK)

0.2 % SDS (Bio-Rad, USA)

200 mM NaCl (Fisher Scientific, UK)

PCR Mastermix

5 μL - 10x Buffer (Invitrogen)

1.5 μL - 50 mM $MgCl_2$ (Sigma-Aldrich, UK)

1 μL - 10 mM dNTP (Promega, USA)

2.5 μL - 20 μM Primer (1OD)

0.4 μL -Taq polymerase (Life Technologies, USA)

dH_2O – make up to 49 μL/sample (depending on number of primers used)

F5 Primers (Product: 435bp) (Life Technologies, USA)

Forward: 5′ - CTCCCTCTTCAAGCCAAAAGGAGCC – 3′

Reverse: 5′ – TGAAAATCAGAAGGAAGCTGGCTACAAA – 3′

VA primers (Product: 265bp) (Life Technologies, USA)

Forward: 5′ – ATAAAAAGCACTGTGGATTTCTGC – 3′

Reverse: 5′ – AGAGGGGACAGGAAATCTCTAAGA – 3′

PCR Program

1. 94.0°C for 3:00
2. 94.0°C for 1:00
3. Annealing temp for 0:30 (57°C for VA, 61°C for F5)
4. 72 for 1:00
5. Go to 2, 29 times
6. 72.0 for 10:00
7. 4.0 for 10:00
8. End

TAE (50x)

242 g Tris Base (Fisher – Scientific, UK)

57.1 mL Acetic Acid (Fisher – Scientific, UK)

100 mL - 0.5 M EDTA pH 8.0 (Sigma- Aldrich UK)

Make to 1 L with dH_2O

Agarose Gel 2% (100 mL)

2 g Agarose (Life Technologies, USA)

100 mL of 1xTAE

2 μL Gel Red (Biotium, USA)

Loading Buffer (50mL)

25 mL of 20% Ficoll (type 400) (Sigma-Aldrich, UK)

12.5 mL of 25% Glycerol (Sigma-Aldrich, UK)

0.5 mL of 1 M Tris pH 7.6 (Fisher – Scientific, UK)

0.1 mL of 0.5 M EDTA pH 8.0 (Sigma- Aldrich UK)

0.125 g of Bromophenol Blue (Sigma-Aldrich UK)

0.125 g of Xylene Cyanol (Sigma-Aldrich UK)

Stock was stored at -20°C and the aliquot in use was stored at 4°C.

General Polymerase Chain Reaction (PCR) Protocol

100 μL of Lysis Buffer and 5 μL mL^{-1} of Proteinase K (New England Biolabs, USA) were added per ear sample, and incubated overnight with agitation at 56°C in a waterbath. The following day samples were vortexed and 1 μL was used for PCR analysis. 49 μL of PCR master mix and 1 μL of sample DNA were aliquoted into PCR tubes (Starlab, USA). The tubes were centrifuged in a desktop microcentrifuge (Spectrafuge, Labnet International, USA) prior to being transferred to the PCR block and run with the appropriate program.

Agarose Gel Electrophoresis

An agarose gel was prepared. 10 μL of PCR product with 1 μL loading buffer was loaded onto the gel and run at 120 V for no more than 30 minutes. The results on the gel were visualised using InGenius gel documentation equipment (Syngene, USA). A 1kb DNA ladder was used to estimate molecular weights of DNA bands (New England Biolabs, UK).

2.3 Cell Culture

Cell Culture Medium

Iscove's Modified Dulbecco's Medium (IMDM) (Sigma-Aldrich, UK)

5% Heat Inactivated Fetal Calf Serum (FCS) (Serotec, UK)

100 U mL^{-1} Penicillin (Sigma-Aldrich, UK)

100 μg mL^{-1} Streptomycin (Sigma-Aldrich, UK)

$2x10^{-3}$ M L-Glutamine (Sigma-Aldrich, UK)

$5x10^{-5}$ M 2β-mercaptoethanol (Sigma-Aldrich, UK)

Isolation of thymocytes and peripheral T cells for in vitro analysis

Mice were dissected for axillary, brachial, superficial cervical, inguinal and mesenteric lymph nodes (LN), which were collected into culture medium on ice. For some experiments thymus and spleen were also collected. Under sterile conditions organs were gently pushed through a sterile 70 μm nylon cell strainer (BD Falcon, USA) with the end of a syringe plunger and cells were suspended in culture medium. Splenocytes were always subjected to ACK lysis (5 mL for 5 minutes), after which they were washed, re-filtered, and used as required. An aliquot of cells was counted using the CASY-1 automated cell counter according to the manufacturer's instructions (Scharfe System, Germany).

2.4 Cell Labelling for Proliferation Analysis

Cell labelling with CFSE

Carboxyfluorescein diacetate N-succinimidyl ester (CFSE) (Sigma-Aldrich, UK) is an intracellular dye used as a marker for cell proliferation. Prior to subjecting cells to conditions inducing proliferation, CFSE was added at a concentration of 1 μM in PBS to cells at a density of $20x10^{6}$ cells mL^{-1} at room temperature for 8 minutes in the dark. The dye was quenched with equal volume of complete medium and 10% v/v FCS for 5 minutes at room temperature. The cells were subsequently washed, re-suspended in culture medium, and recounted.

Cell labelling with Cell Trace

Cell labelling with Cell Trace Violet (Life Technologies, USA) was performed according to the manufacturer's instructions, modified such that the dye was added to lymphocytes at a concentration of 2.5 μM in pre-warmed PBS at a cell density of $3x10^{6}$ cells mL^{-1} at 37°C/5% CO_2 for 20 minutes in the dark. The dye was quenched with an equal volume of complete medium for 5 minutes at room temperature. The cells were subsequently centrifuged to wash off

any excess dye, re-suspended in culture medium, and recounted before downstream application.

2.5 In Vitro T Cell Activation Assays

2.5.1 Phospho-protein Analysis

(pZap^{493}, pShc, pSrc^{416}, pLck^{505}, pERK, pS6, pp38, pFoxo1)

CFSE labelled and 1:1 pooled cells were resuspended in serum-free IMDM medium (containing all additives except FCS) at $4x10^7$ cells mL^{-1}. $1x10^6$ cells were plated in 96 U-well plate (Corning Inc., USA) in triplicate when cell numbers permitted. Depending on the experiment the following control treatments were included: unstimulated, PP2, pervanadate, PdBU, UO126 SB203580, Ly29004, and the required time course of 1 μM NP68 peptide stimulation. When only some samples received a treatment, equal volume of serum-free IMDM was added to all others. At desired time points samples were fixed with 2% v/v PFA (Acros, USA) and incubated for a minimum of 15 minutes at RT prior to downstream application. For intracellular staining samples in PFA were centrifuged at 1700 rpm for 3 minutes, PFA was aspirated and samples were resuspended in 100 μL of prewarmed BD Phosflow Lyse/Fix (Cat. 558049, BD Biosciences, USA). After an incubation of 10 minutes at 37°C/5% CO_2, samples were centrifuged (1700 rpm for 3 minutes) and resuspended in 100 μL of BD Phosflow Permeabilization Buffer I (Cat. 557885, BD Biosciences, USA). Samples were incubated for 20 minutes at RT after which they were centrifuged (1700 rpm for 3 minutes). Samples were subsequently stained with intracellular antibodies for flow cytometry in BD Phosflow Permeabilization Buffer I as described in section 2.7.2.

PP2 Treatment

As a negative control $1x10^6$ cells at a concentration of $40x10^6$ mL^{-1} were treated with 1 μM PP2 (Cat. PHZ1223, Life Technologies, USA) a SFK inhibitor, for 15 minutes at 37°C/5% CO_2 prior to addition of NP68 peptide stimulation.

UO126 Treatment

As a negative control, when assessing ERK phosphorylation, $1x10^6$ cells at a concentration of $40x10^6$ mL^{-1}, were treated with 10 μM UO126 (Calbiochem, UK) a MEK inhibitor, for 15 minutes at 37°C/5% CO_2 prior to addition of NP68 peptide stimulation.

SB203580 Treatment

As a negative control, when assessing p38 phosphorylation, $1x10^6$ cells at a concentration of $40x10^6$ mL^{-1} were treated with 1 μM SB203580 (Cell Signalling, USA) a p38 inhibitor, for 30 minutes prior to addition of NP68 stimulation for 6 hours at 37°C/5% CO_2.

Ly294002 Treatment

As a negative control, when assessing Foxo1 phosphorylation, $1x10^6$ cells at a concentration of $40x10^6$ mL^{-1} were treated with 1 μM Ly29004 (Cell Signalling, USA) that blocks PI3K dependent Akt phosphorylation and Foxo1 phosphorylation, for 30 minutes prior to addition of NP68 stimulation for 6 hours at 37°C/5% CO_2.

Pervanadate Treatment

As a positive control, $1x10^6$ cells at a concentration of $40x10^6$ mL^{-1} were treated with 50 μL pervanadate ($Na_3VO_4H_2O_2$) for 10 minutes at 37°C/5% CO_2.

Two individual stocks were made:

stock 1: 100 μL Na_3VO_4 (Sigma-Aldrich, UK) + 250 μL PBS

stock 2: 10 μL H_2O_2 (30%v/v) (Sigma-Aldrich, UK) + 90 μL PBS

At 15 minutes prior to use: 150 μL of stock 1 + 789 μL PBS + 61 μL of Stock 2 were combined in an eppendorf and incubated in the dark before use.

PdBU Treatment

As a positive control in pERK or pS6 experiments, $1x10^6$ cells at a concentration of $40x10^6$ mL^{-1} were treated with 100 nM Phorbol 12, 13-dibutyrate (PdBU) (Sigma-Aldrich, UK) for 15 minutes at 37°C/5% CO2.

NP68 Stimulation

$1x10^6$ cells at a concentration of $40x10^6$ mL^{-1} were treated with 1 μM NP68 for required lengths of time at 37°C/5% CO_2.

2.5.2 Ca^{2+} - Flux Assay

The entire assay was performed at RT (except for specific incubations), this included pre-warming all reagents and keeping the organs at RT from dissection onwards. The assay required the ability to distinguish two cell populations in the same 5 mL polystyrene round bottom tube (BD Biosciences, USA), so that the start of stimulation was the same. Therefore, cells were first labelled with low (0.01 and 0.1 μM) concentrations of CFSE (Section 2.4). $2x10^7$ of CFSE labelled cells ($10x10^6$ of each genotype) were loaded with 2 μM Indo-1 (Life Technologies, USA) at a concentration of $1x10^7$ cells mL^{-1} of PBS. Sample was incubated at 37°C/5% CO_2 for 40 minutes after which 1% cell culture medium (with 1% v/v FCS) was added in excess and sample was washed by centrifuging. Sample was split into requried groups for antibody staining (e.g. Group 1: TCRbio and CD8bio, Goup 2: TCRbio alone) in 100 μL of 1% cell culture medium 15 minutes at RT. Thereafter samples were resuspended in 600 μL of 1% culture medium for acquisition on a flow cytometer. After 45 seconds of running the sample on the LSR II (BD Biosciences, USA) streptavidin APC was added for crosslinking of biotinylated antibodies. As a positive control after 8 minutes of acquisition 1 μg mL^{-1} of Ionomycin (Sigma-Aldrich, UK) was added.

2.5.3 Overnight T cell Activation for Analysis by Flow Cytometry

$0.1\text{-}0.3x10^6$ total LN cells or thymocytes treated with either CFSE, Cell Trace or left untreated were seeded in a 96-well U-bottom tissue culture plate in

cell culture medium. A titration of specific doses of soluble NP68 or NP34 peptide was then added and plates were incubated at 37°C/5% CO_2. Cell cultures were terminated at desired time points for analysis by centrifuging the plates (1700 rpm for 3 minutes) and aspirating the medium. Samples were then stained for flow cytometry analysis as described in section 2.7.

2.5.4 Overnight T cell Activation for Cytokine Production Analysis

$30x10^6$ total LN cells or ACK purified spleen cells were seeded in T25 flasks (Corning Inc., USA) in 15 mL of complete cell culture medium and 100 nM of NP68. At a desired time point cells were washed, stained with Live/Dead reagent, CD8 and CD44 surface antibodies (section 2.7) and seeded at a density of $0.1\text{-}0.3x10^6$ cells in 100 µL per well in a 96 well U-bottom tissue culture plate. Cells were restimulation with specific concentrations of NP68 in the presence of 5 µg mL^{-1} of Brefeldin-A (Sigma-Aldrich, UK) for 6 hours. Controls in the restimulation included unstimulated samples, 0.05 µg mL^{-1} PdBU and 0.5 µg mL^{-1} Ionomycin combined, and 20 ng mL^{-1} IL-2. After 6 hours plates were centrifuged and samples were stained for intracellular cytokines (section 2.7.2).

Alternatively cells were washed after culture with 100 nM of NP68, a sample taken for analysis by flow cytometry, and $5x10^6$ cells were cultured in T75 flasks (Corning Inc., USA) with 25 mL of cell culture medium and 20 ng mL^{-1} of IL-2 (Peprotech, USA) for a further 2 days. Thereafter cells were collected, washed, recounted and treated as described above for measuring intracellular cytokines after recall.

Note: whenever F5Lck^{ind} cells were cultured, 2 µg mL^{-1} of doxycycline was always added to the wells for all samples (including F5Lck^{WT} and F5Lck^{VA}).

2.6 *In Vivo Listeria monocytogenes* Infection

LmOVA was always kindly prepared by David Wright.

Attenuated recombinant *Listeria monocytogenes (L.monocytogenes)* expressing chicken ovalbumin (*LmOVA*) was kindly provided by Prof. Hao Shen (University of Pennsylvania School of Medicine). A 500 mL stock culture was prepared in Brain Heart Infusion (BHI) Medium containing 5 μg mL^{-1} erythromycin hydrate (Cat. 856193, Sigma-Aldrich, UK) and cultured in shaking incubator (37°C, 120 rpm) until reaching OD600 = 0.43. 50 mL of culture was mixed 1:1 with 80% glycerol solution and frozen at -80°C in 1 mL aliquots. Average aliquot Colony formation unit (CFU) was calculated by thawing 3 aliquots, titrating 100 μL of each in a 10-fold serial dilution, and plating 10^{5} dilution on Brain Heart Infusion Agar (Cat.70138, Sigma-Aldrich, UK) containing 5 μg mL^{-1} erythromycin hydrate. Colony formation was counted 24 hours after incubation at 37°C/5% CO_2 with an average of 7.85 x 10^{8} CFU mL^{-1}. This was used as a basis for dilutions required for injection.

On days of injections, 1 mL aliquots were thawed, centrifuged at 13000 rpm for 2min and resuspended in 1 mL PBS. 900 μL of this was diluted for injection in PBS based on the formula:

$$\frac{\text{CFU x dilution factor x volume plated x volume injected}}{\text{volume of diluent added}}$$

Remaining 100 μL was titrated as before to confirm CFU for injection. CFU remained relatively consistent (±10%) throughout the course of injections.

The primary infection was induced by intravenous (i.v.) tail vein injection of $1x10^{6}$ *LmOVA* in 200 μl of PBS per mouse. The secondary infection was also induced by i.v. injection but with $10x10^{6}$ *LmOVA* in 200 μl of PBS per mouse.

The primary T cell immune response to *LmOVA* was assayed on day 7 post-infection. The memory response was assayed on day 42 post-infection (in

some cases day 39) and a secondary infection was induced, which was assayed 4 days later.

2.6.1 Assessing the CD4 and CD8 Immune Responses to *LmOVA*

Designed based on kind advice from Robert Salmond, Ph.D.

Briefly, spleens were harvested, single cell suspensions were made, red blood cells (RBCs) were lysed, and cells counted using a CASY counter (section 2.3).

To assess the cytokine production in response to the total *LmOVA* infection, *LmOVA* was resuspended at $2x10^7$ bacteria mL^{-1} and heat killed at 90°C for 30 minutes (henceforth referred to as heat killed listeria (HKL)). An overnight stimulation with a titration of HKL in 24 well plates with $4x10^6$ splenocytes per well in 1 mL of complete cell culture medium was performed. At desired time point plates were centrifuged and the culture medium was collected and frozen for ELISAs (section 2.8).

To assay the *ex vivo* phenotype of cells $3x10^6$ splenocytes were seeded in 96-well plates and incubated for 10 minutes at 4°C with Fc block (CD16/32, Biolegend, USA) and Live/Dead Aqua reagent in 50 µL of PBS. Thereafter to assay the number and proportion of OVA-specific CD8 T cells dextramer-PE (Dex) staining (Immudex, Denmark) was used. Excess Fc block and Live/Dead were washed off and cells were incubated in 20 µL flow buffer with 5 µL Dex for 15 minutes at 4°C, thereafter 25 µL of surface staining antibody mix was added directly to Dex staining and samples were incubated another 15 minutes at 4°C.

To assess peptide-specific cytokine production in $CD8^+$ T or $CD4^+$ T cells on day 7 and day 46, $3x10^6$ splenocytes were seeded in 96-well culture plates in 200 µL of cell culture medium alone or with different concentrations of either the N4 peptide for $CD8^+$ T cells, or the listeriolysin O protein ($LLO_{190-201}$) for CD4 T cells in the presence 5 µg mL^{-1} of Brefeldin-A for 4 hours at 37°C/5%

CO_2. Thereafter intracellular staining for TNFα and IFNγ was done as described in section 2.7.2.

2.6.2 BrdU Treatment

Designed based on kind advice from Stefano Caserta, Ph.D.

Bromodeoxyuridine (BrdU) stock (Cat. B5002-5G, Sigma-Aldrich, UK) was dissolved in 500 mL dH2O (Millipore, USA) and filter sterilized with Stericup (Millipore, USA). 50 aliquots of 10 mL (10 mg mL^{-1}) in 15 mL Falcons were prepared and frozen at -20°C until needed. For intraperitoneal (i.p.) injections on day 4, the required amount of BrdU aliquots were defrosted at RT and a mix of 1.2 mg of BrdU in 200 µL of PBS per mouse was prepared. BrdU was given on days 4-10 in drinking water at a concentration of 0.8 mg mL^{-1} in 100 mL per cage.

2.7 Analysis of T Cell Function by Flow Cytometry

Flow Buffer

1x PBS (Gibco BRL, UK)

0.05% Sodium Azide (Sigma-Aldrich, UK)

0.5% Bovine Serum Albumin (Sigma-Aldrich, UK)

2.7.1 Surface Staining

The expressions of cell surface markers in *ex vivo* and *in vitro* activated or treated cells were assessed by flow cytometry. $1x10^6$ cells in 100 µL were pipetted into 96-well plates (Greiner Bio-One, Germany), centrifuged (1700 rpm for 3 minutes), and resuspended in 30 µL PBS with 1/750 dilution of Live/Dead Aqua reagent. Live/Dead Aqua staining was incubated for 10 minutes, 100 µL PBS was then added to wash off excess Live/Dead by centrifugation. Samples were then resuspended in 30 µL flow buffer with antibodies to surface markers of interest in specific dilutions (Table 2.3). In experiments with splenocytes, $3x10^6$ cells were used and stained in a total volume of 50 µL.

Surface staining was incubated for 15 minutes on ice, followed by a flow buffer wash. If required, cells were resuspended in 30 μL with secondary streptavidin conjugated antibodies to reveal biotinylated antibody binding. Samples were again incubated for 15 minutes on ice, followed by a wash. Finally, samples were resuspended in 100-250 μL for flow cytometry acquisition performed either with LSR II (BD Biosciences, USA), Canto (BD Biosciences, USA) or MacsQuant (Miltenyi Biotec, Germany) flow cytometry instruments.

2.7.2 Intracellular Staining

Surface staining was performed as normal and after a final wash, removing excess secondary antibodies, one of the following intracellular staining protocols was used:

Foxp3 Intracellular Staining Kit (Cat. 00-5523-00, eBioscience, USA)

This kit was used in accordance to manufacturers recommendations when staining for: Lck, Foxp3, Tbet, Eomes, IFNγ, TNFα, Granzyme B.

Briefly, cells were resuspended in 100 μL of Fixation/Permeabilization Buffer. Samples were incubated for a minimum of 30 minutes at 4°C in the dark (or left overnight at 4°C if required). Thereafter the samples were centrifuged (1700 rpm for 3 minutes), buffer was aspirated and samples were washed in 100 μL of Permeabilization Buffer. Samples were stained with primary intracellular antibodies for 30 minutes at 4°C in the dark in Permeabilization Buffer. Thereafter, samples were resuspended in appropriate secondary antibody for 30 minutes at 4°C in the dark in 30 μL of Permeabilization Buffer. Finally, cells were washed once in Permeabilization Buffer, once in flow buffer, and resuspended in 100-250 μL flow buffer for acquisition by flow cytometry.

Intracellular Staining for BrdU

Method kindly provided by Dominik Ruckerl, Ph.D.

After staining for Dex and other cell surface markers, samples were resuspended in 100 µL of Fixation/Permeabilization Buffer from the Foxp3 Intracellular Staining Kit described above, and left at 4°C overnight (**note: shorter incubations did not work).** The following day samples were centrifuged and washed twice in Permeabilization Buffer (from the same Foxp3 kit). Cells were resuspended in 100 µL DNase-I solution (300 µL DNase –I Stock at 1 mg mL^{-1} (Cat. D5025-15KU, Sigma-Aldrich, UK), in 700 µL dPBS (Cat. D8537, Sigma-Aldrich, UK) and 0.42 M $MgCl_2$) and incubated at 37°C/5% CO_2 for 30 minutes wrapped in aluminium-foil. Thereafter cells were washed once in Permeabilization Buffer and stained with 5 µL of anti-BrdU FITC antibody (Cat. 556028, BD Biosciences, USA) in 15 µL Permeabilization Buffer and incubated at RT for 30 minutes. Finally cells were washed twice with Permeabilization Buffer and resuspended in 250 µL flow buffer for acquisition on a flow cytometer.

Intracellular Staining for Bcl-2

Method kindly provided by Stefano Caserta, Ph.D.

Cells were washed with 100 µL of 0.03% Saponin Buffer (Stock: 150 µL of 10% Saponin (Sigma-Aldrich, UK) in 50 mL dH_2O diluted in flow Buffer). After centrifugation (1700 rpm for 3 minutes) the buffer was aspirated and samples were resuspended in a mix of 40 µL 0.03% Saponin buffer and 10 µL Bcl-2 per well for 20 minutes at 4°C in the dark. After the incubation samples were washed once in excess 0.03% Saponin Buffer, and thereafter once in flow buffer. Samples were resuspended in 100-250 µL flow buffer for acquisition on a flow instrument. Samples were never fixed for Bcl-2 staining.

Table 2.1 Flow Cytometry Antibodies – Surface Staining

Surface Staining					
Primary Antibodies					
Fig.	**Specificity**	**Clone**	**Host**	**Conjugate**	**Supplier**
3.9	Anti-Mouse CD3	145-2C11	Armenian Hamster	Biotin	eBioscience, USA
3.1; 3.3; 3.11; 3.14; 3.5; 3.6; 3.7; 3.9; 3.10; 3.13; 5.6; 5.7	Anti-Mouse CD4	RM4-5	Rat	Pacific Blue	Biolegend, USA
3.15; 5.1; 5.4	Anti-Mouse CD4	RM4-5	Rat	PerCP-Cy5.5	Biolegend, USA
3.12	Anti-Mouse CD4	RM4-5	Rat	PE	eBioscience, USA
5.10; 5.13	Anti-Mouse CD4	MCD0427	Rat	Alexa Fluor750	Life Technologies, USA
3.8	Anti-Mouse CD4	RM4-5	Rat	PeTxRed	Life Technologies, USA
3.5; 3.7; 3.8; 3.10; 3.11; 4.1	Anti-Mouse CD5	53-7.3	Rat	APC	BD Biosciences, USA
3.13; 3.12	Anti-Mouse CD8b	eBioH35-17.2	Rat	FITC	eBioscience, USA
3.10; 3.11; 4.1; 4.2; 4.4; 4.5; 4.11; 4.14; 4.15; 5.1	Anti-Mouse CD8a	53-6.7	Rat	PerCP	Biolegend, USA

3.14; 3.6; 3.7; 4.2	Anti-Mouse CD8a	MCD0817	Rat	PeTxRed	Life Technologies, USA
3.1; 3.3; 3.5	Anti-Mouse CD8a	53-6.7	Rat	PE	eBioscience, USA
4.3; 4.12; 4.13; 5.2; 5.3; 5.6; 5.7	Anti-Mouse CD8a	53-6.7	Rat	BV421	Biolegend, USA
5.18	Anti-Mouse CD8b	eBioH35-17.2	Rat	PeCy7	eBioscience, USA
5.8; 5.9; 5.10; 5.11; 5.12; 5.14; 5.15; 5.16; 5.17	Anti-Mouse CD8a	53-6.7	Rat	BV650	Biolegend, USA
3.8	Anti-Mouse CD8a	53-6.7	Rat	PE Cy 5.5	eBioscience, USA
3.11	Anti-Mouse CD69	H1.2F3	Armenian Hamster	PE	eBioscience, USA
3.3	Anti-Mouse CD69	H1.2F3	Hamster	Biotin	BD Biosciences, USA
4.1;	Anti-Mouse CD69	H1.2F3	Armenian Hamster	APC	Biolegend, USA
3.3; 3.5; 3.6; 3.10; 3.11; 4.2	Anti-Mouse TCRβ	H57-597	Armenian Hamster	FITC	eBioscience, USA
4.1	Anti-Mouse TCRβ	H57-597	Armenian Hamster	Biotin	eBioscience, USA
3.1; 3.1; 3.10; 3.12; 3.13; 4.1; 4.12; 5.2; 5.3; 5.4	Anti-Human/Mouse CD44	IM7	Rat	APC-eFluor780	eBioscience, USA

5.8; 5.9; 5.10; 5.12; 5.13; 5.15; 5.16; 5.17	Anti-Mouse/HumanCD 44	IM7	Armenian Hamster	BV570	Biolegend, USA
3.13; 3.14;	Anti-Mouse CD45.1	A20	Mouse	APC	eBioscience, USA
3.13; 3.14	Anti-Mouse CD45.2	104	Mouse	PE	Biolegend, USA
5.13; 5.16	Anti-Mouse CD62L	MEL -14	Rat	PE	eBioscience, USA
5.12	Anti-Mouse CD62L	MEL -14	Rat	APC	eBioscience, USA
3.1; 3.10; 4.1; 4.2	Anti-Mouse CD25	PC61.5	Rat	PE	eBioscience, USA
3.5; 3.6; 3.7; 3.11	Anti-Mouse CD24	M1/69	Rat	Pe-Cy7	BD Biosciences, USA
4.13	Mouse CD122	5H4	Rat	FITC	BD Biosciences, USA
4.13; 5.14; 5.15	Anti-Mouse CD127/IL-7Rα	A7R34	Rat	BV421	eBioscience, USA
3.6	Anti-Mouse CD127/IL-7Rα	A7R34	Rat	PE	eBioscience, USA
5.14; 5.15	Anti-Mouse KLRG1	2F1	Golden Syrian Hamster	Biotin	eBioscience, USA
5.16	Anti-Mouse CXCR3/CD183	CXCR3-173	Armenian Hamster	PerCP-Cy5.5	eBioscience, USA
3.9	Anti-Mouse Vα2	B20.1	Rat	PE	eBioscience, USA
3.9	Anti-Mouse Vα8.3	B21.14	Rat	FITC	eBioscience, USA
3.9	Anti-Mouse Vα11	RR8-1	Rat	APC	eBioscience, USA
3.8; 5.18	TCR Vβ panel (Cat.557004)			FITC	BD Biosciences, USA
Secondary Antibodies					

5.14	Streptavidin			PeCy7	Biolegend, USA
4.1	Streptavidin			PE	eBioscience, USA
3.3; 3.9	Streptavidin			PerCP	Biolegend, USA

Table 2.2 Flow Cytometry Antibodies - Intracellular Stainings

Intracellular Primary Staining					
Fig.	**Specificity**	**Clone**	**Species**	**Conjugate**	**Supplier**
4.3	pZap^{Y493}		Rabbit mAb		Cell Signalling, USA
4.3	pSrc^{Y416}		Rabbit mAb		Cell Signalling, USA
4.3	pShc$^{Y239/240}$		Rabbit polyclonaly		Santa Cruz, USA
4.4	Phospho-p44/42 MAPK (pERK)		Rabbit mAb		Cell Signalling, USA
4.5	pS6$^{S235/236}$		Rabbit mAb		Cell Signalling, USA
3.3; 4.1;	Lck	3A5	Mouse mAb		Merck Millipore, USA
4.10; 5.11	Anti-Mouse Bcl-2	A19-3	Hamster	FITC	BD Biosciences, USA
4.11; 4.12 5.6; 5.7	Anti-Mouse IFNγ	XMG1.2	Rat	Alexa Fluor 488	Biolegend, USA
4.12; 5.7	Anti-Mouse TNFα	MP6-XT22	Rat	PerCP-Cy5.5	Biolegend, USA
4.11;	Anti-Mouse TNFα	MP6-XT22	Rat	APC	eBioscience, USA
4.13; 5.17	Anti-Human/Mouse Tbet	eBio4B10	Mouse	PerCP-Cy5.5	eBioscience, USA
4.13; 5.17	Anti-Mouse Eomes	Dan11mag	Rat	Alexa Fluor647	eBioscience, USA
4.13	Anti-Mouse Granzyme B	NGZB	Rat	PE	eBioscience, USA
5.3; 5.4	Anti-Mouse Ki-67	SolA15	Rat	FITC	eBioscience, USA
3.15	Anti-Mouse/Rat Foxp3	FJK-16s	Rat	PacBlu	eBioscience, USA
4.14	Pp38$^{Thr180/Tyr182}$	3D7	Rabbit mAb		Cell Signaling, USA
4.15	pFoxO1$^{Ser\ 256}$		Rabbit mAb		Cell Signaling, USA

Table 2.3 Flow Cytometry Antibodies - Intracellular Stainings Continued.

Intracellular Secondary Staining					
Fig.	Specificity	Clone	Species	Conjugate	Supplier
3.3	Anti-Mouse IgG		Chicken	Alexa Fluor 647	Life Technologies, USA
3.3; 4.1;	Anti-Mouse IgG		Goat	FITC	Jackson ImmunoResearch, USA
4.14; 4.15	Anti-Rabbit IgG		Goat	Alexa Fluor 647	Life Technologies, USA

2.7.3 Flow Cytometry Data Analysis

Flow cytometry data was analysed using FlowJo software v.9.6 (TreeStar Inc.). All samples were first gated on intact lymphocytes, thymocytes or splenocytes using forward scatter (FSC) and side scatter (SSC). Wherever possible cells were then gated as singlets on FSC area (FSC:A) and FSC height (FSC:H). Additionally, when possible, cells were gated as live based on low Live/Dead Aqua incorporation. Subsequent gating was dependent on populations and markers of interest used in each experiment.

2.7.4 Proliferation Data Analysis

To analyse data from CFSE or Cell Tracer Violet labelling assays, the proliferation index parameter in FlowJo was applied. Cells that had undergone division rounds lost fluorescence and several peaks, representing rounds of division, were visualised. The proliferation index is a measure of the total number of cell divisions divided by the number of cells that went into division. This measure only takes into account the cells that underwent at least one division.

2.8 Enzyme Linked Immunosorbent Assay (ELISA)

2.8.1 ELISA Reagents

ELISA Coating Buffer

1 L dH_2O

1.59 g Sodium Carbonate (anhydrous, 15 mM) pH 9.4-9.6 (Sigma-Aldrich, UK)

2.93 g Sodium Bicarbonate (anhydrous, 35 mM) (Sigma-Aldrich, UK)

0.05% Sodium Azide (Sigma-Aldrich, UK)

ELISA Wash Buffer

1x PBS (Gibco BRL, UK)

0.05% Tween-20 (Scientific Laboratory Supplies Ltd)

ELISA Blocking Buffer

1x PBS (Gibco BRL, UK)

10% Heat Inactivated Fetal Calf Serum (FCS) (Biosera, USA)

ELISA Stop Buffer

0.18 M Sulphuric Acid (Carl Roth, Germany)

2.8.2 ELISA General Protocol

Cytokine ELISAs were performed on supernatants that were previously harvested from culture plates and stored at -20°C. IL-2 and TNFα production was measured with the mouse IL-2 Ready-Set-Go Kit (Cat. 88-7024, eBiosciences, UK) and mouse TNFα Ready-Set-Go Kit (Cat.88-7324-88, eBioscience, USA), respectively. Kits were used according to the manufacturer's protocols. For measuring IFNg production, anti-IFNg primary antibody (R46A2) was kindly provided by the MacDonald

Laboratory (The University of Edinburgh) and buffers used are described in section 2.8.1.

Capture antibodies (Table 2.4) were coated onto 96-well plates (NUNC, Maxisorp, Denmark) in 50 μL/well of coating buffer overnight. The following day plates were blocked for 1 hour at room temperature. Supernatants and doubling dilutions of recombinant protein standards were added in 50 μL/well of blocking buffer. Standards were always assayed in duplicate. Plates were incubated for 2 hours RT. Secondary-biotinylated antibodies were added in 50 μL blocking buffer and plates were incubated for 45 minutes at 37°C/5% CO_2. Streptavidin-peroxidase was added in 50 μL of blocking buffer and incubated for 30 minutes at 37°C/5% CO_2, after which 50 μL of TMB (Calbiochem, USA), a colorimetric substrate of peroxidase, was added. When the blue colour change was noted (or maximum 15 minutes later), the stop solution 0.18 M H_2SO_4 was added and plates were read at 450 nm within 30 minutes. Plates were washed 3-8 times between steps with ELISA wash buffer.

Table 2.4 ELISA Antibodies

Specificity	Conjugated	Clone	Host	Usage Conc.	Manufacturer
Standard					
IL-2	Recombinant				eBioscience, USA
TNFα	Recombinant				eBioscience, USA
IFNγ	Recombinant			50 ng mL^{-1}	Biolegend, USA
Capture Antibody (For coating)					
IL-2	Purified				eBioscience, USA
TNFα	Purified				eBioscience, USA
IFNγ	Purified	R46A2		2 μg mL^{-1}	MacDonald Laboratory
Secondary Antibody					
IL-2	Biotinylated				eBioscience, USA
TNFα	Biotinylated				eBioscience, USA
IFNγ	Biotinylated	XMG1.2	Rat	0.2 μg mL^{-1}	eBioscience, USA

2.9 Radiation Bone Marrow Chimaeras

$Rag1^{KO}$ mice were sub-lethally irradiated (800 rads). Femurs and tibia from C57BL/6 (Ly5.1) and Lck^{VA} (Ly5.2) mice were collected into medium and cleaned of as much muscle as possible. In specific experiments Lck^{ind} (Ly5.2) were also used. Under sterile conditions, the ends of the bones were cut off and a syringe was used to flush out the bone marrow (BM) into a clean petri dish. Extracted bone marrow was then filtered into a 50 mL centrifuge tube (Sarstedt, Germany) and resuspended at a concentration of $3x10^{7}$ mL^{-1} in culture medium. Cells were stained with antibodies for CD8 (clone: 3.168) and CD4 (clone: RL172.4) for 15 minutes at 37°C/5% CO_2. 1 mL of Complement (Cedarlane, USA) was added and the samples were incubated for a further 45 minutes at 37°C/5% CO_2. Finally cells were washed and recounted. The efficiency of complement lysis was assessed by flow cytometry, comparing pre-complement and post-complement samples for TCR^{+} populations.

Irradiated $Rag1^{KO}$ mice were injected i.v. with $1x10^{7}$ mixed BM cells from C57BL/6 (Ly5.1) and Lck^{VA} (Ly5.2) mice in a 1:9 or 1:20 ratio. In specific experiments $1x10^{7}$ mixed BM cells from C57BL/6 (Ly5.1) and Lck^{ind} (Ly5.2) mice in a 1:9 or 1:20 ratio were also used. Peripheral reconstitution of mice was assessed by flow cytometry analysis of blood samples taken at 4 weeks and 8 weeks post BM transplantation.

2.10 Western Blot (WB)

2.10.1 General Reagents

Western Blot Lysis Buffer

1% NP-40 (Fluka – Sigma -Aldrich UK)

1% Maltoside (Merck Millipore)

150 mM Sodium Chloride (Sigma- Aldrich UK)

20 mM EDTA pH8.0 (Sigma- Aldrich UK)

10 mM Tris-Cl pH7.5 (Fisher – Scientific, UK)

dH_2O

Inhibitors added immediately before use:

1 mg mL^{-1} Protease Inhibitor Cocktail (Sigma-Aldrich UK)

1 mM Sodium Fluoride (Sigma-Aldrich UK)

1 mM Sodium Orthovanadate (Sigma-Aldrich UK)

Western Blot 4x Reducing Sample Buffer

40% v/v Glycerol (Sigma-Aldrich, UK)

10% v/v SDS (Sigma-Aldrich, UK)

0.05% w/v Bromophenol Blue (Sigma-Aldrich UK)

8% v/v 2β-mercaptoethanol (Sigma-Aldrich, UK)

0.4 M Tris-HCl pH 6.8 (Fisher – Scientific, UK)

12.5 mM EDTA (Sigma- Aldrich UK)

2.10.2 Sample Preparation

Cells were pelleted by centrifugation (1700 rpm for 3 minutes) and supernatant discarded. The pellet was resuspended at $10x10^7$ cells per 1 mL of lysis buffer with protease inhibitors and incubated for 30 minutes on ice. Lysates were subsequently microfuged at 13000 rpm for 10 minutes at 4°C to pellet nuclei. The post-nuclear supernatants were transferred to clean 1.5 mL centrifuge tubes and if not used immediately then stored at -20°C. Samples were defrosted and an 10 μL aliquot of $1x10^6$ cells was mixed with 2 μL dH_2O and 4 μL sample buffer prior to running it on a gel.

2.10.3 Western Blot (pre cast gel)

Western Blot Running Buffer (I)

NuPAGE® MOPS SDS Running Buffer 20x for Bis-Tris Gels only (Life Technologies, USA)

Gel running

NuPage Novex Bis-Tris 4-12% (Life Technologies, USA) was placed in electrophoresis system with running buffer (Novex, Life Technologies, USA). The protein ladder (Precision Plus Protein Standards All Blue, Bio-Rad, US) and samples were loaded. The gel was run at 200 V for 1 hour.

2.10.4 Western Blot (Laemmli gel)

Western Blot Resolving Gel 8% Buffer

27.75 mL dH_2O

16.05 mL 30% Acrylamide/Bis Solution (Bio-Rad, UK)

15 mL 1.5 M Tris-Base (pH 8.8) (Fisher – Scientific, UK)

0.6 mL 10% APS (Sigma-Aldrich, UK)

0.6 mL 10% v/v SDS (Sigma-Aldrich, UK)

0.036 mL TEMED (Sigma-Aldrich, UK)

Western Blot Stacking Buffer

13.6 mL dH_2O

3.4 mL 30% Acrylamide/Bis Solution (Bio-Rad, UK)

2.5 mL 1.0 M Tris-Base (pH 6.8) (Fisher-Scientific, UK)

0.2 mL 10% v/v SDS (Sigma-Aldrich, UK)

0.2 mL 10% APS (Sigma-Aldrich, UK)

0.02 mL TEMED (Sigma-Aldrich, UK)

Western Blot Running Buffer 10x (II)

30.3 g Tris-Base (Fisher – Scientific, UK)

144.2 g Glycine (Fisher – Scientific, UK)

10 g SDS (Fisher-Scientific, UK)

Make up to 1 L with dH_2O

pH 8.3

Gel Preparation & Running

Gel electrophoresis was performed using twin vertical electrophoresis system (Galileo, Bioscience, USA). A resolving gel was poured into glass plates and covered with isopropanol. Once the gel was polymerized the isopropanol was discarded. The stacking gel was laid over the resolving gel with a comb placed inside. Once the stacking gel was polymerized the protein ladder (Precision Plus Protein Standards All Blue, Bio-Rad, US) and samples were loaded. Gel electrophoresis was run at 30V overnight or 100-120 V for 2-3 hours.

2.10.5 Western Blot Transfer

Western Blot Transfer Buffer 10x

30.2 g Tris-Base (Fisher – Scientific, UK)

144 g Glycine (Fisher – Scientific, UK)

Made to 1 L with dH_2O

100 mL of 10x transfer buffer was added to 700 mL dH_2O and 200 mL methanol. This was made fresh prior to each use.

Western Blot Wash Buffer

1x PBS 1 L (Gibco BRL, UK)

0.1% Tween-20 (Scientific Laboratory Supplies, UK)

Transfer Protocol

Resolved proteins were transferred onto PVDF membranes (Millipore, USA) using a wet transfer apparatus (Bio-Rad, UK). First PVDF was soaked in methanol for 30 seconds and then equilibrated in cold transfer buffer. Three pieces of filter paper (Whatman Ltd, UK) and two sponges were immersed in transfer buffer. The gel, PVDF, filter paper, and sponges were packed into the transfer cassette and air bubbles were carefully avoided. Transfer was performed at 100V for 2 hours (Pre-cast gel) or 4 hours (Laemmli gel) at 4°C.

The blotted membrane was blocked for 1h at room temperature in Odyssey blocking buffer (Li-Cor, UK). Incubation with primary antibodies was performed in Odyssey blocking buffer overnight at 4°C. Membrane was washed in wash buffer three times for 5 minutes then it was incubated with the appropriate secondary antibodies in 20 mL wash buffer and 3% BSA for 1 hour RT. Membrane was washed and acquired in PBS using the Odyssey (Li-Cor, UK).

2.10.6 WB Analysis and Quantification

The Odyssey infrared fluorescence imaging system was used to quantify all blots. The benefits of the Odyssey system are that fluorescent signal is directly proportional to the amount of target protein over a wide range of concentrations, and that two different targets can be identified simultaneously with spectrally distinct secondary fluorescent antibodies (Table 2.5).

Following acquisition, relative band intensities were compared by densitometry using the Li-Cor Odyssey software. The background was automatically calculated as median of background of above and below each

rectangle and subtracted. The resulting integrated intensity (counts per mm^2) was recorded.

Table 2.5 Western Blot Antibodies

Specificity	Conjugated	Clone	Host	Manufacturer
Primary Antibody				
Lck		3A5	Mouse	Millipore, USA
β-actin		13E5	Rabbit	Cell Signaling, USA
V5 Probe		E10	Mouse mAb	Santa Cruz Biotech, USA
V5 Probe			Mouse mAb	Life Technologies, USA
α-Tubulin		TU-02	Mouse mAb	Santa Cruz Biotech, USA
Secondary Antibody				
Anti-Rabbit	IRDye800		Donkey	Cat. 611-731-127, Rockland, USA
Anti-Mouse	Alexa Fluor 680		Goat	Cat. A21058, Life Technologies, USA
Anti-Goat	Alexa Fluor 680		Donkey	A21084, Life Technologies, USA
Anti-Rabbit	Alexa Fluor 680		Goat	A21109, Life Technologies, USA

2.11 Statistical Analysis of Results

Statistical analyses were carried out using Prism 6 software (GraphPad Software Inc, USA).

When comparing two samples significance was calculated using the parametric student's t-test, unpaired, and two-tailed. Significance was denoted with the following cutoffs: *P<0.05, **P<0.01, ***P<0.001.

Multiple samples were compared using one-way ANOVA with post-ANOVA Holm-Sidak or Tukey's methods for multiple t-tests with the following cutoffs: * $p \leq 0.05$.

Chapter 3: The Role of Lck Abundance in Thymocyte Development

3.1 Introduction

Thymic development ensures production of a repertoire of mature $CD4^+$ and $CD8^+$ SP thymocytes with clonally expressed, somatically generated TCRs with a huge variety of specificities, that are least likely to induce autoimmunity, but highly capable of responding to a very large array of foreign pathogens (Germain, 2002). At both the DN stage (β - chain selection) and DP stage (positive/negative selection) signalling via the TCR determines whether a cell is directed to survive and progress, or die. Lck is the most proximal kinase activated upon TCR activation and it is critical at all stages of development where TCR signaling is required.

It is thought that weak signals lead to positive selection and strong signals to cell death in the thymus (Hogquist et al., 1994; Jameson and Bevan, 1998). Both the affinity and the dwell time of the TCR interaction with p:MHC are influenced by the CD4 and CD8 co-receptors, which facilitate the recruitment of Lck (Palmer and Naeher, 2009). Signalling differences potentially lead to distinct biological outcomes by inducing differential signaling pathways i.e. negatively-selecting signals induce ERK phosphorylation at the plasma membrane and positively-selecting signals induce ERK phosphorylation at the Golgi (Daniels et al., 2006).

The development of the inducible Lck transgenic mouse (Lck^{ind}) enabled the study of the impact of Lck abundance on TCR signal transduction (Legname et al., 2000). Lck^{ind} mice, bred onto an Lck^{KO} background, have tissue-specific expression of Lck induced upon doxycycline administration (Legname et al., 2000). Legname and colleagues found, that Lck^{ind} mice have restored the expansion of early thymocytes and maturation of $CD4^+$ T cells, both absent in Lck^{KO} mice. Compared to WT thymocytes, Lck^{ind} $CD4^+$ SP cell numbers were fully restored, however, $CD8^+$ SP thymocyte numbers were partially restored, although increased compared to Lck^{KO} mice. These data showed that Lck

expression is important for the development of both CD4+ and CD8+ lineages (Legname et al., 2000). Interestingly, Lck^{ind} mice have a range of Lck expression in DP thymocytes, from one-tenth to 10-times as much as seen in WT thymocytes, but in the peripheral T-cells Lck expression is only 10-20% of WT levels (Legname et al., 2000). The impact of the range in Lck abundance on thymocyte selection was not studied and instead the group focused on consequences on peripheral activation, cell survival and memory formation (Caserta et al., 2010; Legname et al., 2000; Lovatt et al., 2006; Seddon et al., 2000).

Intriguingly, expression of mutated Zap-70, directly downstream of Lck, was shown to result in graded alterations in positive and negative selection of T cells in the thymus (Tanaka et al., 2010). This caused autoimmune clones of T cells, normally deleted due to increased TCR affinity for self, to be selected into the repertoire because of reduced Zap-70 signalling and a 'selection shift' (Tanaka et al., 2010). Complimentary work from the Seddon laboratory has shown, that in addition to controlling TCR sensitivity, the abundance of Zap-70 also distinguishes CD4+ and CD8+ SP thymocyte development in a temporal manner (Saini et al., 2010). Saini and colleagues showed that CD4+ SP T cells emerge from the DP population earlier than CD8+ SP T cells (Saini et al., 2010). Collectively these results showed that the affinity of the selection window in the thymus is very narrow and is influenced by TCR signaling thresholds set by abundance of Zap-70.

If Zap-70 abundance can have such profound effects, what is then the impact of Lck abundance on different stages of thymic development? How does Lck abundance impact on TCR signaling thresholds and positive selection in the thymus? If lack of Lck leads to an incomplete block (Molina et al., 1992) and Lck overexpression leads to thymic tumours (Abraham et al., 1991) then why in Lck^{ind} mice were cells with 10-20% of Lck selected, rather than cells with WT levels? It was part of the aims of the following chapter to address these questions.

Chapter 3: Aims

In addition to the Lck^{ind} mouse, the Zamoyska laboratory have developed the Lck^{VA} transgenic mouse line, in which expression of Lck on an Lck^{KO} background is constitutively low, approximately 5% of WT Lck levels in both thymus and periphery (Salmond et al., 2011). Salmond et al. developed the Lck^{VA} mice as a control for the experiments described in their article, and thymic development was only briefly addressed, but this low level of Lck was also shown to rescue thymocyte development as compared to Lck^{KO} mice (Salmond et al., 2011). However, given that Lck has been shown to influence various stages of thymocyte development (Hernandez-Hoyos et al., 2000; Legname et al., 2000; Nakayama et al., 1989) it was intriguing that only 5% of WT levels of Lck can rescue apparently normal thymic development. The central focus of this chapter was to characterise, in detail, the positive selection, thymocyte maturation, TCR sensitivity and the resulting naïve peripheral T cell pool in Lck^{VA} mice and compare this to the Lck^{ind} mice, to better understand what effect abundance of Lck has on T cell development. Our data showed, as previously published, that reduced Lck expression can rescue thymocyte development, as compared to an Lck^{KO} mouse. Interestingly, variable levels of Lck expression during thymocyte differentiation in Lck^{ind} mice led to increased thymocyte sensitivity to TCR triggering, whereas constitutively low Lck expression in Lck^{VA} mice did not. Additionally we found positive selection proceeded normally in both Lck^{VA} and Lck^{ind} mice, however, SP thymocytes were less mature than in Lck^{WT} cells.

3.2 Results: Thymocyte Development in Lck^{VA} and Lck^{ind} Mice

3.2.1 Thymic development was reconstituted in Lck^{VA} and Lck^{ind} mice

Previous studies have shown that in both the Lck^{ind} mice and Lck^{VA} mice thymic development is rescued and the peripheral T cell compartment restored compared to Lck^{KO} mice (Legname et al., 2000; Lovatt et al., 2006).

Before we assessed the impact of reduced Lck expression in Lck^{VA} mice on thymocyte selection we confirmed levels of Lck expression by WB in thymi of Lck^{WT}, Lck^{VA} and Lck^{ind} mice (Fig.3.1A). Analysis by WB and normalization of band fluorescence showed, that Lck^{VA} had 4% and Lck^{ind} had 152% of Lck expression as compared with Lck^{WT} (100%). These results were in line with previously published data (Legname et al., 2000; Salmond et al., 2011).

To further dissect thymocyte development in the Lck^{VA} and Lck^{ind} mice, CD4 versus CD8 dot plots were studied to assess the proportions of developing $CD4^+$ and $CD8^+$ SP thymocytes (Fig.3.1B). Staining for CD4 and CD8 distinguishes the four developmental stages: DN, DP, $CD4^+$ SP and $CD8^+$ SP. In agreement with previously published data, we showed that Lck^{KO} had very small proportions (5-fold less than Lck^{WT}) of $CD4^+$ SP thymocytes, indicating the importance of Lck for the development of the CD4 compartment (Legname et al., 2000; Molina et al., 1992). Although, $CD8^+$ SP proportions varied little between Lck^{WT} (1.2%±0.11), Lck^{VA} (1.01%±0.05), Lck^{ind} (0.73%±0.06), and Lck^{KO} mice (1.05%±0.11), it was evident from the comparison of total thymocyte numbers (Fig.3.2), that Lck^{KO} have severely compromised thymic development. It is worth noting that CD4 and CD8 co-receptor expression in SP thymocytes is lower in Lck^{VA} and Lck^{ind} mice than in Lck^{WT} thymocytes as has been previously published (Legname et al., 2000; Lovatt et al., 2006; Salmond et al., 2011).

These data showed that Lck^{VA} and Lck^{ind} mice had restored thymic development although the thymi were 2-fold smaller than in Lck^{WT} mice (Fig.3.2). These ratios were approximately maintained at all stages of development except the DN stage. The higher than Lck^{WT} proportions of DN cells in Lck^{VA} and Lck^{ind} mice (Fig.3.1B) indicated a partial DN block as previously published (Lovatt et al., 2006; Salmond et al., 2011). A more detailed investigation of the DN subsets by staining for CD25 and CD44 showed that the proportions of cells in DN3 were increased 2.3-fold in Lck^{KO} (59.6%±4.5), and 1.5-fold in Lck^{ind} (37.4%±17.1) compared to Lck^{WT} (24.5%±1.0). There was a large standard deviation (SD) in Lck^{VA} mice (25.3%±10) but from the total number of DP cells recovered (Fig.3.2) it was

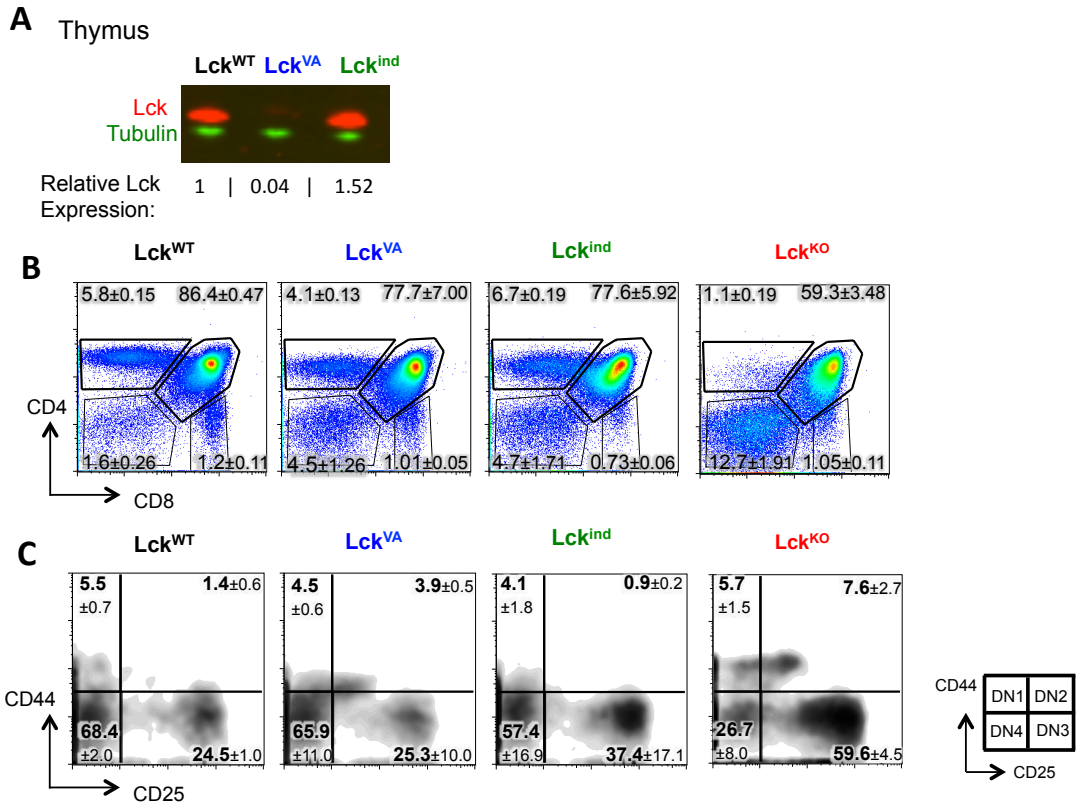

Fig. 3.1 Lck^{VA} and Lck^{ind} mice reconstituted thymic development.
(A) Thymocyte lysates were analysed from age-matched (7-10 weeks) polyclonal Lck^{WT}, Lck^{ind}, and Lck^{VA} mice by western blot (pre-cast gel). The blot was probed with anti-Lck (Upstate) and anti-Tubulin antibodies overnight at 4°C, and then with anti-mouse (for Lck) and anti-rabbit (for Tubulin) fluorescent secondary antibodies for 1 hour. The blot was subsequently scanned using the Li-Cor system. Relative expression of Lck was calculated by normalizing fluorescence of all bands to Lck^{WT} band fluorescence. Data are representative of 3 independent experiments. Full blot is shown in Appendix 7.1. (B) Single-cell suspensions from thymi of age-matched (7-10 weeks) Lck^{WT}, Lck^{ind}, and Lck^{VA} mice were analysed by flow cytometry for CD4 and CD8 expression, determining DN, DP, CD4$^+$ or CD8$^+$ SP thymocyte proportions. (C) The DN cells were gated on TCR and immature TCR cells were further analysed for DN1: CD44$^+$CD25$^-$, DN2: CD44$^+$CD25$^+$, DN3: CD44$^-$CD25$^+$, and DN4: CD44$^-$CD25$^-$ populations. Numbers on dot plots are averages of a minimum of 3 individual animals ± SD. Data are representative of 3 independent experiments with 3 mice per group. Replicate experiments were done with 6 week old mice, and 8-11 week of mice and similar trends were observed.

clear they too had a partial DN developmental block as Lck^{KO}, Lck^{ind} and Lck^{VA} mice had significantly fewer DP cells than Lck^{WT} mice.

Overall, these results confirmed, as previously published, that in Lck^{ind} and Lck^{VA} mice thymic development was restored as compared to Lck^{KO} mice, although total thymocyte numbers and $CD4^+$ and $CD8^+$ SP numbers were significantly lower than in Lck^{WT} mice (Fig.3.2).

3.2.2 Positive selection was efficient despite low Lck expression

Signals via the TCR are critical for determining positive versus negative selection at the DP stage of development, particularly important is the affinity of the selecting TCR signal (Gascoigne and Palmer, 2011). Reduced Lck expression levels in peripheral $CD4^+$ T cells in Lck^{ind} mice were shown to increase TCR signaling thresholds (Lovatt et al., 2006). Meaning, that higher concentrations of peptide are required, for example, to phosphorylate ERK to the same extent as in Lck^{WT} mice. Thymocytes from Lck^{VA} and Lck^{ind} mice may therefore have altered signaling thresholds that will affect how the cells progress through positive selection in the thymus. The following section investigated the impact Lck abundance had on positive selection of thymocytes.

The process of positive selection can be dissected by staining for CD69 and TCR in the total live thymocyte population, as shown in Fig.3.3A (Azzam et al., 1998; Yamashita et al., 1993). The $CD69^-TCR^-$ cells in gate 1 (purple) represented mostly pre-selection $CD4^+CD8^+$ cells. The cells that expressed intermediate levels of CD69 and TCR are $CD4^+CD8^+$ cells initiating positive selection and were in gate 2 (red). In gate 3 were $CD69^{hi}TCR^{hi}$ cells, which corresponded to $CD4^+CD8^+$ cells undergoing positive selection (green) and finally in gate 4 were the mature $CD69^-TCR^{hi}$ $CD4^+$ or $CD8^+$ SP cells (blue) (Fig.3.3A).

It must first be noted, that when comparing Lck^{WT}, Lck^{ind}, Lck^{VA} and Lck^{KO} cells for positive selection, the gates (CD69 versus TCR) for all genotypes were slightly different (Fig.3.3B). In the complete absence of Lck, as in Lck^{KO},

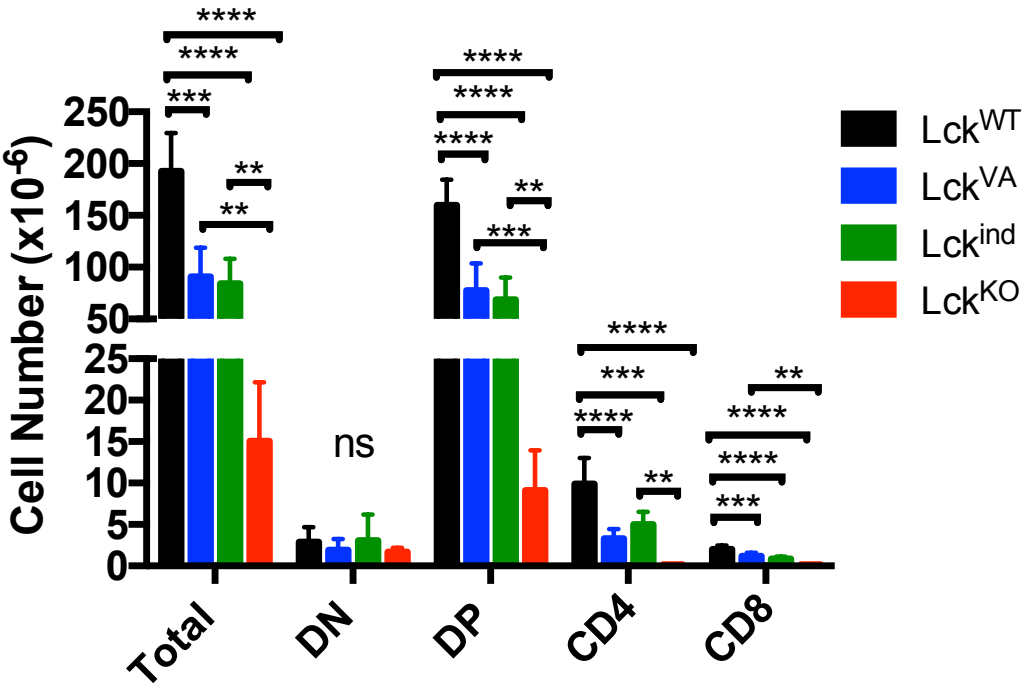

Fig. 3.2 Thymocyte numbers were lower in mice with reduced Lck expression.
The cells numbers were calculated for the different developmental subsets using the percentages from flow cytometry analysis (as shown in Fig.3.1B) and the total thymocyte counts obtained with the CASY counter. Data shown are pooled from 3 independent experiments with n=3 per genotype each time. Bar chart shows averages ± SD. Statistical significance was calculated in Prism with One-Way ANOVA and Tukey's post-ANOVA multiple comparisons test, $p<0.05$.

TCR was higher in pre-selection thymocytes (gate 1), as TCR mediated signaling and thus Lck are required for TCR downregulation (Azzam et al., 1998; D'Oro et al., 1997; Saini et al., 2010; Salmond et al., 2011). Although the gates in Lck^{VA} and Lck^{KO} were therefore shifted to accommodate for this effect, all 4 gates in all genotypes were always back-gated to check that the 4 populations reflect the 4 stages of positive selection as indicated in Fig.3.3A.

The proportions of events in each gate were averaged from 3 individual animals and tabulated in Fig.3.3C. The Lck^{KO} thymus (right most panel in Fig.3.3B) was included in this experiment as a control, to show that lack of Lck caused an incomplete block in the DN to DP progression and consequently positive selection was severely restricted. There were very few cells undergoing positive selection in Lck^{KO} mice, as there were barely any events in gate 2 (0.6%) and none recorded in gates 3, and 4 (Fig.3.3B and C).

Despite the slightly increased TCR expression in Lck^{VA} and the decreased upregulation of CD69 in Lck^{ind} thymocytes the proportions of cells in the different positive selection quadrants were similar to Lck^{WT} thymocytes (Fig.3.3C). This observation suggested, that there potentially was an effect of Lck abundance on thymocyte development, as evidenced by the change in TCR expression, however, it did not affect the progression of thymocytes through the four stages of positive selection.

Cells in each of the 4 gates (CD69 versus TCR) were qualitatively assessed by histogram analysis for Lck expression levels (Fig.3.3D). The filled grey histogram showed Lck staining in gate 1 of Lck^{KO} thymocytes and this was the negative control. Lck expression in Lck^{WT} thymocytes was shown in blue, and it was consistently high at all 4 stages of positive selection. Lck expression in Lck^{VA} thymocytes was shown in purple, and it was consistently lower than in Lck^{WT} but higher than in Lck^{KO} thymocytes. As previously published (Legname et al., 2000), Lck^{ind} thymocytes had variable Lck expression at the DP stage, and this was evident in Fig.3.3D in gates 1 and 2. From Fig.3.3D it was clear that during active positive selection, represented by gate 3, Lck^{ind} thymocytes no longer had bimodal Lck expression, and in

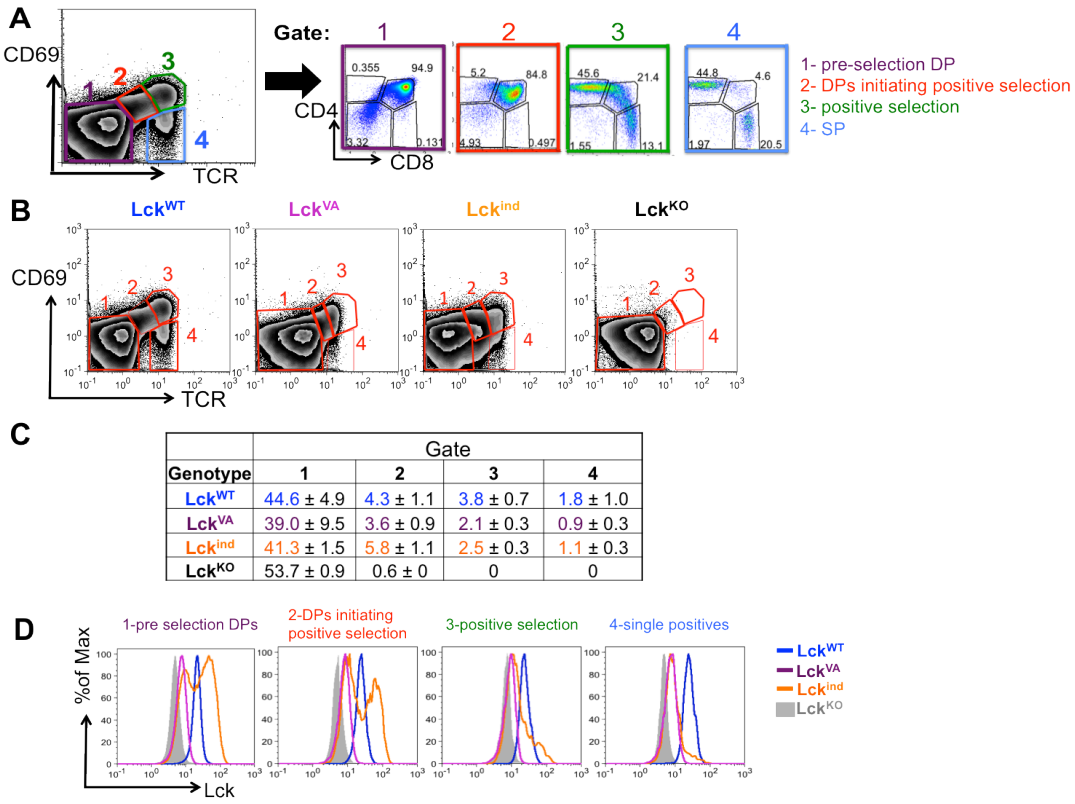

	Gate			
Genotype	**1**	**2**	**3**	**4**
Lck^{WT}	44.6 ± 4.9	4.3 ± 1.1	3.8 ± 0.7	1.8 ± 1.0
Lck^{VA}	39.0 ± 9.5	3.6 ± 0.9	2.1 ± 0.3	0.9 ± 0.3
Lck^{ind}	41.3 ± 1.5	5.8 ± 1.1	2.5 ± 0.3	1.1 ± 0.3
Lck^{KO}	53.7 ± 0.9	0.6 ± 0	0	0

Fig. 3.3 Reduced Lck expression did not impede DP to SP progression of thymocytes. (A) Four stages of positive selection can be followed by flow cytometry when gating live cells for CD69 and TCR staining. Gate 1: CD69^{+}TCR^{-} (pre selection double-positive thymocytes), gate 2: CD69^{+}TCR^{+} (double-positive cells initiating positive selection), gate 3: CD69^{hi}TCR^{hi} (positive selection), and gate 4: CD69^{lo}TCR^{hi} (single positives). (B) Representative contour plots show CD69 and TCR profiles for Lck^{WT}, Lck^{VA}, Lck^{ind}, and Lck^{KO} thymocytes. (C) Table shows average proportions of thymocytes ± SD for the indicated mouse strains in gates 1, 2, 3 and 4. (D) Representative histograms show the Lck expression profile during positive selection in the four gates. Data in B and C are representative of 4 independent experiments, and data in D are representative of 3 independent experiments. In all experiments: Lck^{WT} n=3, Lck^{ind} n=3, Lck^{VA} n=3, Lck^{KO} n=3.

gate 4, the single positive stage, only cells with low Lck expression were found.

There were two possible interpretations of these data. One was that Lck^{ind} cells, through the positive selection process, downregulated Lck expression. An individual cell could not, however, be followed through the positive selection process in this experiment. The second possibility was that Lck^{ind} thymocytes with higher Lck expression than Lck^{WT} thymocytes were negatively selected. As previously published, very high Lck activity is detrimental to thymocyte development (Abraham et al., 1991) and if increased abundance of Lck increases TCR signaling, in a similar manner to increased levels of Zap-70 does (Saini et al., 2010; Tanaka et al., 2010), then it could have led to negative selection. Intriguingly, there were Lck^{ind} cells that had the same Lck expression levels as Lck^{WT} cells, evidenced by overlapping histograms (Fig.3.3D), but by the SP stage, Lck expression in Lck^{ind} thymocytes was more similar to Lck^{VA} cells than to Lck^{WT} cells.

3.2.3 Lck^{VA} mice had normal DP to SP conversion of thymocytes

Lck^{VA} and Lck^{ind} had decreased numbers of SP thymocytes compared to Lck^{WT} mice (Fig.3.2), potentially explained by a defect in DP to SP conversion. Salmond et al. showed that the efficiency of maturation from DP to SP, measured by dividing the number of mature TCR^{+} SP cells by total DP cells, is comparable between Lck^{WT} and Lck^{VA} mice (Salmond et al., 2011). This possibly indicated, that as long as some Lck is expressed, thymocytes can progress efficiently through positive selection. To assess whether the same is true in Lck^{ind} mice the DP to SP conversion was calculated for Lck^{ind} thymocyte numbers (Fig.3.4).

The results in Fig.3.4A and B showed, for $CD4^{+}$ and $CD8^{+}$ SP, respectively, that there were no significant differences in efficiency of maturation from DP between Lck^{WT} and Lck^{VA} T cells as previously published (Salmond et al., 2011). The efficiency of maturation from DP to SP in Lck^{ind} mice was also

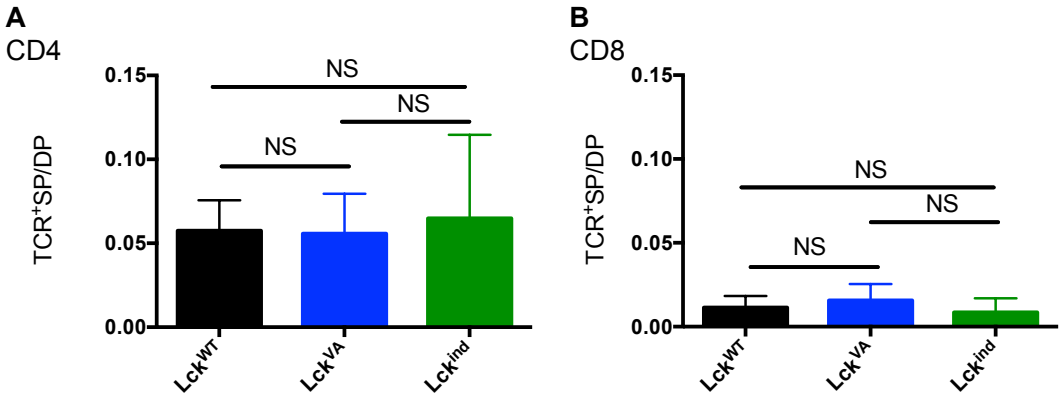

Fig. 3.4 Lck^{VA} had normal DP to SP conversion of thymocytes.
The efficiency of the generation of SP thymocytes from DP thymocytes was calculated by dividing the TCR^{+} mature SP cell count by the total DP cell count. (A) The average proportions ± SD of CD4^{+} and (B) CD8^{+} SP thymocytes relative to DP cells are shown in bar charts. Significance was calculated using One-Way ANOVA with post-ANOVA Holm-Sidak test for multiple comparisons, $p<0.05$. Data are representative of 3 independent experiments with minimum 3 individual animals per group.

similar to Lck^{WT} mice, despite the change in Lck expression from the DP to SP stage of development (Fig.3.3 and 3.4).

3.2.4 The impact of altering Lck expression on $CD4^+$ SP and $CD8^+$ SP maturation

Although we showed that positive selection proceeded unimpeded (Fig.3.3) as did DP to SP conversion (Fig.3.4), in Lck^{ind} and Lck^{VA} mice, we noted that TCR expression was altered in Lck^{VA} and Lck^{ind} thymocytes compared to Lck^{WT} thymocytes (Fig.3.3B). Expression of TCR and also CD5 are developmentally regulated in the thymus (Azzam et al., 1998). Both, TCR and CD5 expression levels increase from DN to DP to SP stages of development, therefore thymocytes at temporally distinct stages of maturation can be distinguished by gating on CD5 versus TCR expression levels (Azzam et al., 1998). We thus assessed, whether abundance of Lck expression impacted on TCR and CD5 expression during thymocyte development.

The DP subset can be divided into three sub-populations by CD5 and TCR staining: DP1 (TCR^{lo} $CD5^{lo}$), DP2 (TCR^{int} $CD5^{hi}$) and DP3 (TCR^{hi} $CD5^{int}$) (Saini et al., 2010). Saini et al. showed that the $CD4^+$ SP population emerged from the DP2 subset at ~48h and that the $CD8^+$ SP population emerged from the DP3 no earlier than day 3 (Saini et al., 2010). To assess the maturation state of cells, expression of heat-stable antigen (CD24) can be used as a marker, because it is highly expressed on immature cells and its expression is lost as cells mature (Wenger et al., 1993; Wilson et al., 1988).

Live thymocytes were divided into three gates based on expression of CD5 and TCR as measured by flow cytometry (Fig.3.5A). As a side note, Saini et al. applied gates for the 3 populations on DP cells only (Saini et al., 2010) but here, for clarity, we gated on total live thymocytes, as that enabled us to show, for each gate, the progression of thymocyte maturation on a CD4 versus CD8 gate and so the gates were labelled 1, 2 and 3 (Fig.3.5A). Complete lack of Lck in Lck^{KO} mice disrupted CD4 and CD8 lineage maturation and there were only very small proportions of events in any of the three gates (Fig.3.5A). Both, Lck^{VA} (**1:** 59.7%±1.0; **2:** 11.0%±1.1; **3:** 9.5%±1.1)

and Lck^{ind} mice (**1:** 54.8%±2.7; **2:** 8.7%±0.9; **3:** 5.8%±0.7) had similar proportions of thymocytes in each of the three gates as compared to Lck^{WT} mice (**1:** 62.6%±0.4; **2:** 7.2%±0.6; **3:** 8.8%±1.5).

Fig.3.5B shows the CD4 versus CD8 profile of each of the 3 CD5 vs. TCR gates. Gate 1 included almost exclusively DP cells in Lck^{WT}, Lck^{VA} and Lck^{ind} mice. Gate 2 revealed a $CD4^{lo}CD8^{-}$ population in Lck^{WT} and Lck^{ind} thymi, but this was almost absent in the Lck^{VA} thymus. This $CD4^{lo}CD8^{-}$ population may represent intermediate thymocytes that initially terminate *Cd8* transcription and if TCR signaling persists they become $CD4^{+}$ SPs, if it ceases the intermediate thymocytes can undergo 'co-receptor reversal' in which *Cd8* transcription will be reinitiated and they become $CD8^{+}$ SP thymocytes (Brugnera et al., 2000). It was curious that Lck^{VA} lacked the intermediate $CD4^{lo}CD8^{-}$ population, yet in gate 3 we found that a majority of DP thymocytes had developed into SP T cells. In gate 3 the distribution of $CD4^{+}$ and $CD8^{+}$ SP cells were similar in all strains of mice.

There are several potential interpretations of these data. Given that $CD4^{+}$ and $CD8^{+}$ T cells develop in normal proportions in Lck^{VA} mice in the absence of the intermediate $CD4^{lo}CD8^{-}$ population, suggests that progression through the $CD4^{lo}CD8^{-}$ stage is not an absolute prerequisite for development. Indeed, in the case of signaling by low-affinity MHC class I-restricted TCRs, intermediate thymocytes have been shown to still appear as $CD4^{+}CD8^{+}$ cells (Lundberg et al., 1995). Alternatively, the development of CD4 and CD8 populations may be delayed because CD4 development requires stronger TCR signals and these may need to accumulate over time in Lck^{VA} cells. In support of this latter view, is the observation that Lck^{ind} cells behaved like Lck^{WT} cells in gate 2 in that they had an intermediate $CD4^{lo}CD8^{-}$ population. Indeed, we showed that a majority of cells in gate 2 are still DP and Lck^{ind} T cells still expressed Lck bimodally at this stage (Fig.3.3D). The cells in Lck^{ind} mice expressing WT levels of Lck may be behaving like Lck^{WT} thymocytes making the proportions of $CD4^{lo}CD8^{-}$ cells similar.

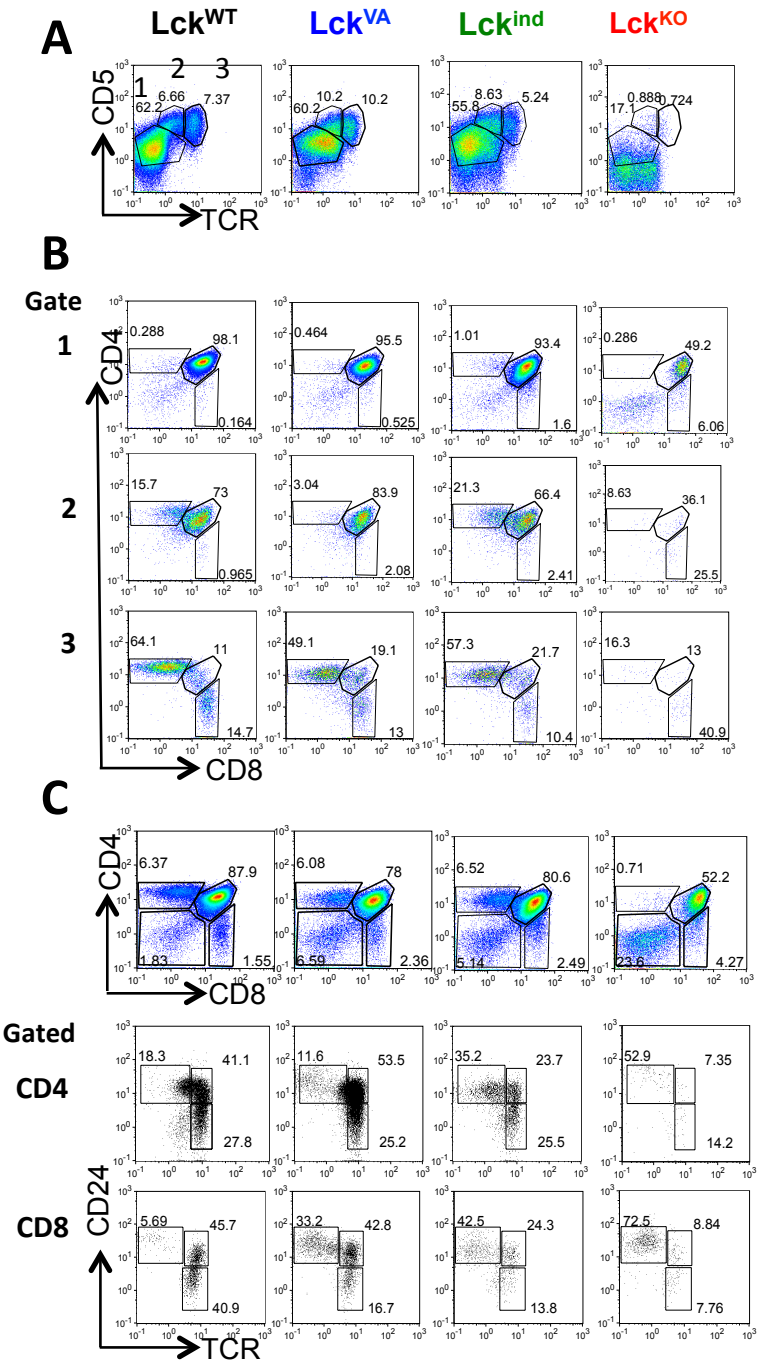

Fig. 3.5 CD4$^+$ SP and CD8$^+$ SP thymocytes were more immature in Lck^{VA} and Lck^{ind} mice.

(A) Representative dot plots show CD5 versus TCR profiles of Lck^{WT}, Lck^{VA}, Lck^{ind}, and Lck^{KO} thymocytes gated on live cells (top row). (B) Representative dot plots show CD4 versus CD8 staining for gates indicated by numbers 1- CD5^{lo}TCR^{lo}, 2 – CD5^{hi}TCR^{+}, 3 – CD5^{hi}TCR^{hi}. (C) Representative dot plots show CD4 versus CD8 gating (top row), with CD4$^+$ SP (middle row) and CD8$^+$ SP cells (bottom row) gated on CD24 versus TCR to assess maturation. Data are representative of 3 independent experiments with n=3 in each group.

The observations made above raised the question whether reducing Lck expression might impact on thymocyte maturity. In order to assess the maturity of the cells in the $CD4^+$ SP and $CD8^+$ SP gates, thymocytes were stained with TCR and CD24 antibodies (Fig.3.5C) (Wenger et al., 1993). Gating on $CD4^+$ SP cells revealed a $CD24^{hi}TCR^{hi}$ population, clearly present in Lck^{WT} and Lck^{ind} thymi, but much reduced in the Lck^{VA} thymus, which is therefore likely to also be the intermediate $CD4^{lo}CD8^-$ population (Brugnera et al., 2000). Amongst the TCR^{hi} cells in the SP gates, all strains had clear $CD24^{hi}$ and $CD24^{lo}$ populations representing, respectively, less mature and fully mature SP thymocytes. The relative proportions of the $CD24^{hi}$ and $CD24^{lo}$ cells in $CD4^+$ SP gates were similar between Lck^{WT} and Lck^{VA} strains (~1.5:1) but in Lck^{ind} the ratio was 1:1.

Curiously, the CD8 gate showed a different pattern between the three strains of mice with a distinct $CD24^{hi}TCR^{lo}$ population present in the Lck^{ind} and Lck^{VA} thymi, which was largely absent from Lck^{WT} mice but very abundant also in Lck^{KO} mice and was therefore, likely to be pre-DP $CD8^+$ immature SP (iSP) population (Xiong et al., 2011).

In summary, these data showed that reduced expression of Lck in $CD4^+$ SP cells in Lck^{ind} mice led to a more immature phenotype. Yet, despite the absence of the intermediate $CD4^{lo}CD8^-$ population in Lck^{VA} mice, constitutively low expression of Lck was sufficient for maturation of $CD4^+$ SP thymocytes. The $CD8^+$ SP population had more immature thymocytes in both Lck^{VA} and Lck^{ind} mice. Finally, it was evident that gating for $CD4^+$ and $CD8^+$ SP cells on the whole thymus is not sufficient to discriminate between different maturation stages during thymocyte development.

The $CD4^{lo}CD8^-$ intermediate thymocytes become $CD4^+$ SPs if TCR signal persists during down regulation of CD8 expression, but if it ceases the intermediate thymocytes can undergo 'co-receptor reversal' in response to IL-7 signaling, which reinitiates *Cd8* transcription and they will become $CD8^+$ SPs (Brugnera et al., 2000). Since our data indicated that Lck^{VA} mice may have delayed maturation of $CD4^+$ SP cells (Fig.3.5B) and both Lck^{VA} and Lck^{ind} SP

thymocytes may be more immature than Lck^{WT} SP thymocytes (Fig.3.5C), we analysed CD127 expression on $TCR^{hi}CD24^{lo}$ and TCR^{hi} $CD24^{hi}$ cells (Fig.3.6).

The results in Fig.3.6 showed, that compared to Lck^{WT}, less mature $TCR^{+}CD24^{hi}$ thymocytes from Lck^{VA} mice expressed ~1.2-fold less CD127 in both $CD4^{+}$ SP and $CD8^{+}$ SP populations and Lck^{ind} thymocytes expressed ~2-fold less CD127. In the more mature $TCR^{+}CD24^{lo}$ thymocytes, a similar pattern of reduced CD127 expression in Lck^{VA} and Lck^{ind} mice relative to Lck^{WT} mice was seen in $CD8^{+}$ SP thymocytes, but in more mature $TCR^{+}CD24^{lo}$ thymocytes $CD4^{+}$ SP thymocytes all strains expressed similar levels of CD127 again (Fig.3.6). Collectively these data suggested that the reduced CD127 expression may have either contributed to the immaturity seen in Lck^{VA} and Lck^{ind} thymocytes due to reduced sensitivity to IL-7 signalling or it might have been reduced because of the more immature phenotype of Lck^{VA} and Lck^{ind} thymocytes compared to Lck^{WT} thymocytes.

Thymocyte development and the CD4 versus CD8 lineage decision is heavily influenced by TCR sensitivity and the expression of signalling molecules such as Lck and Zap-70 (Hernandez-Hoyos et al., 2000; Legname et al., 2000; Saini et al., 2010). CD5 expression can be used as a surrogate marker for TCR sensitivity (Mandl et al., 2013). The observations that TCR expression levels are altered in Lck^{VA} and Lck^{ind} mice (Fig.3.3), together with the changes in CD4 and CD8 maturation (Fig.3.5) and CD127 expression patterns (Fig.3.6) suggested that TCR sensitivity may be affected in Lck^{VA} and Lck^{ind} mice. Therefore we next assessed CD5 expression in $TCR^{hi}CD24^{lo}$ and $TCR^{hi}CD24^{hi}$ SP thymocytes (Fig.3.7).

Fig.3.7 showed that Lck^{ind} and Lck^{VA} $CD4^{+}$ SP thymocytes expressed 1.3 and 1.8-fold less CD5 respectively, than Lck^{WT} thymocytes regardless of maturity. This was in agreement with published data that have shown reduced Lck expression reduced $CD4^{+}$ T cell TCR signaling affinity in the periphery (Lovatt et al., 2006). Interestingly, in mature $TCR^{+}CD24^{lo}$ $CD8^{+}$ SP there were no differences in CD5 expression between the strains.

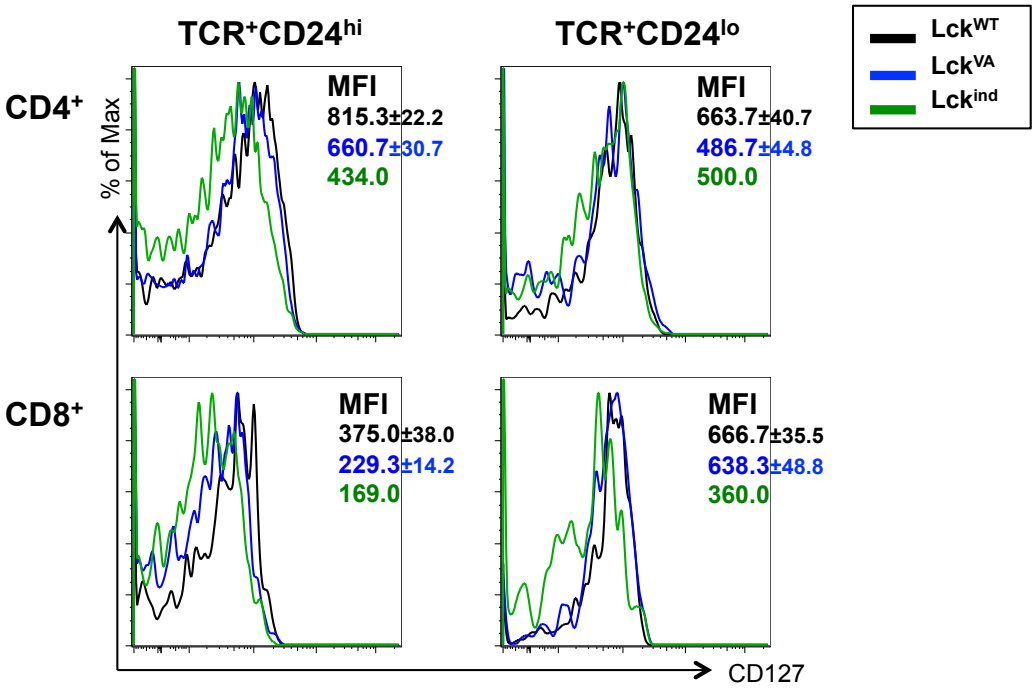

Fig. 3.6 CD127 expression was reduced in Lck^{ind} and Lck^{VA} SP thymocytes.
Histograms show CD127 expression in Lck^{WT}, Lck^{VA}, and Lck^{ind} CD4^{+} SP and CD8^{+} SP thymocytes. SP thymocytes were divided into less mature TCR^{+}CD24^{hi} and more mature TCR^{+}CD24^{lo} populations. Average ± SD of CD127 mean fluorescence intensity (MFI) is shown for indicated gates. Data are representative of 2 independent experiments with n=3 in Lck^{WT} and Lck^{VA} strains, unfortunately only one Lck^{ind} mouse was analysed.

The above data suggested that the bimodal expression of Lck in the DP stage of development in Lck^{ind} mice (Fig.3.3D) did not impede positive selection (Fig.3.3 and 3.4) or CD4/CD8 lineage development (Fig.3.5B). Yet, the SP thymocytes in Lck^{ind} mice expressed low levels of Lck (Fig.3.3), and were more immature (Fig.3.5C) suggesting they may be slower to mature. Additionally, Lck^{lo} $CD24^{lo}TCR^{+}$ SP thymocytes in Lck^{ind} mice had lower CD5 expression (Fig.3.7), which may be compensating for the reduced signalling potential through the TCR . These data suggested that there might have been selection against thymocytes expressing abnormally high quantities of Lck, potentially due to too high a TCR sensitivity, since the cells in Lck^{ind} mice that expressed higher than WT levels of Lck in the DP stage of development were not present in the SP stages (Fig.3.3D).

Our data also showed that constitutively low Lck expression in Lck^{VA} thymocytes allowed positive selection to proceed as it does in Lck^{WT} cells (Fig.3.3 and Fig.3.4). Although, Lck^{VA} mice lacked the intermediate $CD4^{lo}CD8^{+}$ population the development and maturation of $CD4^{+}$ SP cells was unaffected (Fig.3.5), the $CD8^{+}$ SP population that formed in Lck^{VA} thymi had more of the less mature $CD24^{+}TCR^{lo}$ thymocytes than found in Lck^{WT} cells, potentially due to the weaker IL-7 signals they might receive as immature SP thymocytes (Fig.3.6). However, the TCR sensitivity was ultimately similar between mature $CD8^{+}$ SP Lck^{VA} and Lck^{WT} thymocytes, when measured by CD5 expression (Fig.3.7).

3.2.5 The impact of reduced Lck abundance on the Vα and Vβ repertoires

A large variety of TCRs is generated by somatic recombination and random V(D)J gene segment joining. Only a fraction of successful TCR$\alpha\beta$ combinations is selected into the repertoire depending on signal strength (Gascoigne and Palmer, 2011). Our results showed that changes in Lck expression during thymocyte development influenced maturation (Fig.3.5) and TCR sensitivity (Fig.3.7). We therefore next asked whether the TCR repertoire was altered in Lck^{VA} and Lck^{ind} mice.

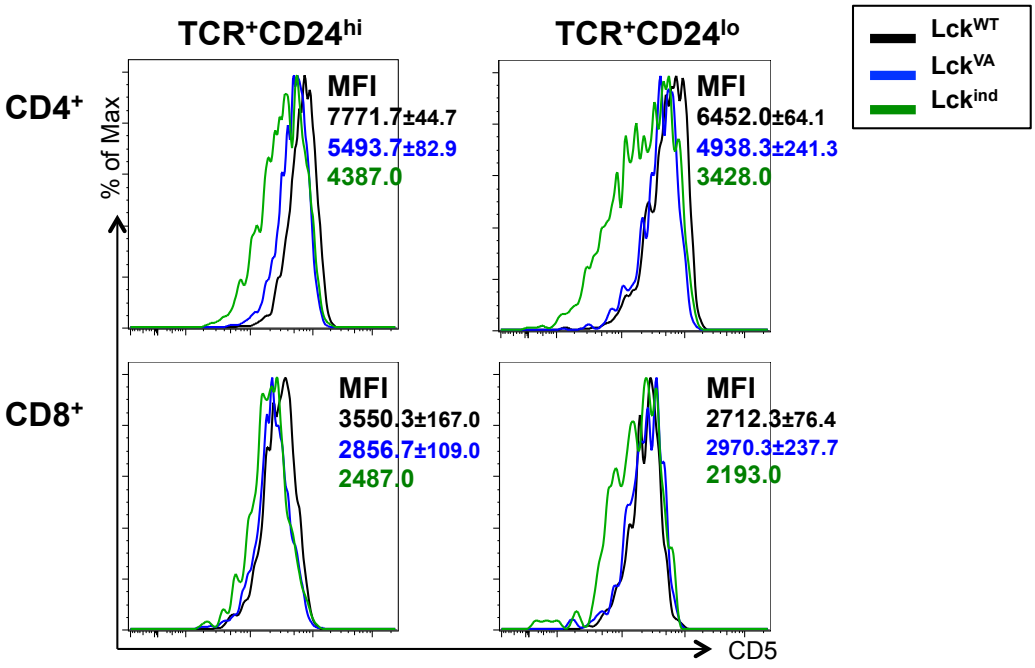

Fig. 3.7 CD5 expression was reduced in CD4^{+} SP thymocytes in Lck^{ind} and Lck^{VA} mice. Histograms show CD5 expression in Lck^{WT}, Lck^{VA} and Lck^{ind} CD4^{+} SP and CD8^{+} SP thymocytes. SP thymocytes were divided by their maturity into less mature TCR^{+}CD24^{hi} and more mature TCR^{+}CD24^{lo} populations. Average ± SD of CD5 MFI is shown for indicated gates. Data are representative of 2 independent experiments with n=3 in Lck^{WT} and Lck^{VA} strains, unfortunately only one Lck^{ind} mouse was analysed.

We assessed the TCRβ repertoire, using a panel of 15 Vβ-specific antibodies, in Lck^{WT}, Lck^{ind} and Lck^{VA} mice. Legname et al. showed that the TCRβ usage repertoire was not different between Lck^{ind} and Lck^{WT} mice (Zamoyska et al., 2003) . The TCRβ repertoire of Lck^{VA} mice has not been assessed before. Two independent experiments were done and the results are shown in Fig. 3.8.

Vβ17 is not expressed in the C57BL/6 strain of mice (Wade et al., 1988) therefore, no staining was expected or observed in all genotypes (Fig.3.8A, B and C) although in one of the experiments a low level of background staining, ~2.5% was identified (Fig.3.8D). Overall it was difficult to make firm conclusions from this study, due to the variability in the two experiments, for example Fig.3.8A suggested that 5% of cells in Lck^{VA} mice expressed Vβ13, however, in the repeat experiment (Fig.3.8B) the expression of Vβ13 was ~1% and similar in all three genotypes. Qualitative observations suggested that there were no consistent and striking differences between the three mouse strains.

Signaling via the TCR in the thymus is critical for allelic exclusion of TCR*α*- and TCRβ-chains (Hogquist et al., 2005; Yamasaki and Saito, 2007). Lck was shown to play an important role at these different developmental stages (Molina et al., 1992), in allelic exclusion of TCRβ-chains (Anderson et al., 1993) and TCR*α*-chains (Niederberger et al., 2003). Failure to properly initiate allelic exclusion can result in the surface expression of two Vα genes on a single T cell. In order to test whether Vα allelic exclusion might be compromised in the presence of low Lck levels, we chose two of the most abundantly expressed Vα alleles and looked for the presence of thymocytes that were positive for both in thymi and lymph nodes of Lck^{WT} and Lck^{VA} mice (Fig.3.9). The results for V*α*2 and V*α*8 expression in $CD8^+$ and $CD4^+$ T cells showed that Lck^{WT} mice expressed either V*α*2 or V*α*8, not both, on $CD8^+$ and $CD4^+$ thymocytes and peripheral T cells (Fig.3.9A). Thus, Lck^{WT} mice were a positive control for successful allelic exclusion of the V*α*-chain.

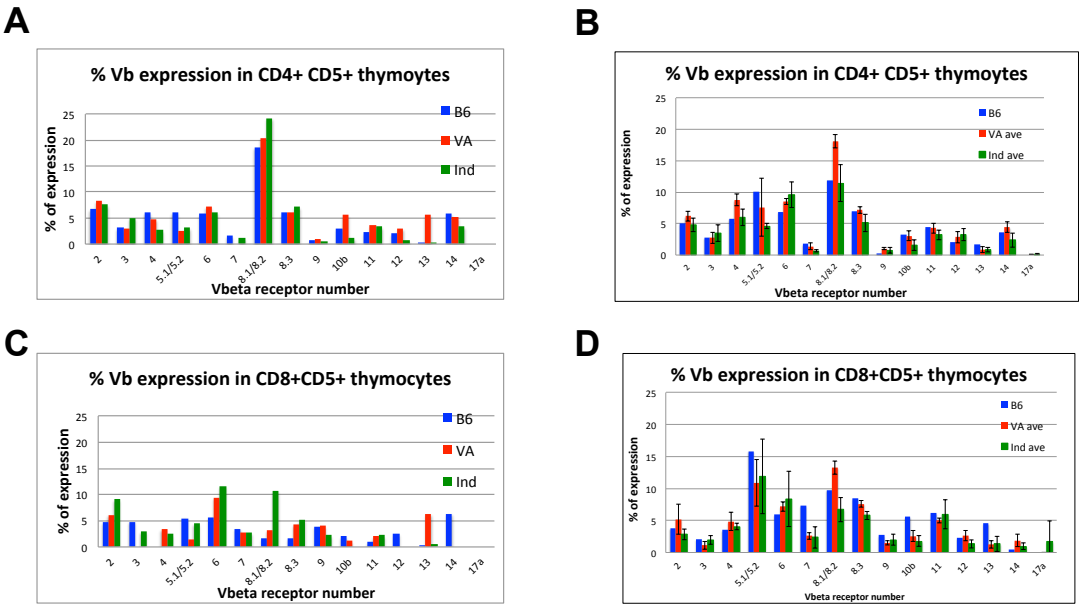

Fig. 3.8 The TCR Vβ repertoire in mature Lck^{VA}, Lck^{ind}, and Lck^{WT} thymocytes.
The bar charts show the percentage of indicated Vβ receptors in mature CD4^{-}CD5^{+} (A and B) and in mature CD8^{-}CD5^{+} (C and D) thymocytes for Lck^{WT} (blue), Lck^{VA} (red), and Lck^{ind} (green). Data in A and C are from one experiment, n=1 for each strain. Data in B and D are from a repeat experiment and shown are averages of n=3 for each strain ± SD.

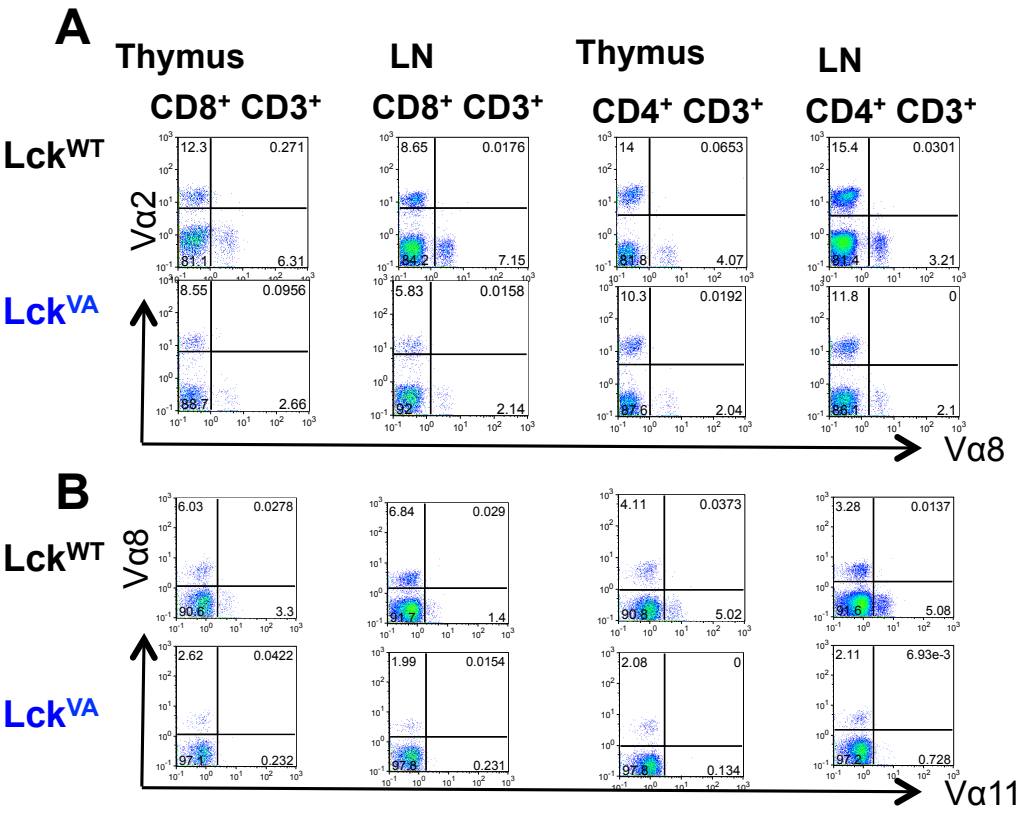

Fig. 3.9 Lck^{VA} mice had normal allelic exclusion of Vα proteins in CD8$^+$ and CD4$^+$ T cells.
Ex vivo expression of Vα 2 versus 8 (A) and Vα 8 versus 11 (B) were assessed in CD8$^+$ and CD4$^+$ mature SP thymocytes and mature lymphocytes in Lck^{WT} and Lck^{VA} mice. Dot plots are representative of 1 experiment where 3 individual animals were pooled per group.

Constitutively reduced Lck expression in $CD8^+$ and $CD4^+$ T cells in Lck^{VA} mice, did not affect the selection of the α-chain as Vα2 and Vα8 expression were also mutually exclusive, despite slightly lower proportions of Vα8 being expressed overall (Fig.3.8A and B). Interestingly, Lck^{WT} T cells expressed some Vα11, however, we did not find any Vα11 expression on thymic or peripheral, $CD4^+$ or $CD8^+$ T cells in Lck^{VA} mice (Fig.3.8B). This could be due to differences in how many times the mice were backcrossed.

Although these experiments need to be repeated to confirm the results, collectively these data suggested that despite very low levels of Lck expression, allelic exclusion of Vα and Vβ chains occurs as normal during thymic development. The ~2 fold reduction in Vα8 expression in both CD8 and CD4 Lck^{VA} T cells and differences in expression levels of some Vβ chains, such as increased Vβ2 in $CD4^+$ T cells and Vβ4 in $CD8^+$ T cells, indicated that there may be differences in the complete TCR repertoire and these may be relevant during immune responses.

3.2.6 Lck abundance influenced TCR sensitivity in thymocytes

During thymic selection TCR signaling thresholds determine positive versus negative selection (Gascoigne and Palmer, 2011). The data presented so far in this chapter indicated that Lck expression levels might affect the TCR signaling thresholds as we observed changes in TCR and CD5 expression levels during maturation (Fig.3.3 and 3.5). We wanted to test whether there were differences in TCR sensitivities in Lck^{VA} and Lck^{ind} thymocytes compared to Lck^{WT} thymocytes. To this end we chose to use F5 TCR transgenic mice.

Crossing mice with F5 TCR transgenic $Rag1^{KO}$ Lck^{KO} mice ensures exclusive differentiation of T cells to the $CD8^+$ lineage (Mamalaki et al., 1992). The F5 TCR utilises Vβ11 and Vα4 chains and we could stimulate the cells with known affinity peptides: a negatively selecting cognate agonist peptide NP68, and a positively selecting antagonist peptide NP34 (Mamalaki et al., 1993; Smyth et al., 1998).

First, we assessed thymic development in F5 TCR transgenic Lck^{WT}, Lck^{VA} and Lck^{ind} mice (Fig.3.10). Our data confirmed that the F5 TCR ensured the development of $CD8^+$ SP thymocytes and only very small proportions <2% of $CD4^+$ SP developed in all strains, which were probably very immature (Fig.3.10A). The $CD8^+$ SP thymocytes were gated for TCR^{hi} cells and the surface expression of TCR and CD5 in these were found to be similar between Lck^{VA} and Lck^{WT} mice. CD5 expression in $F5TCR^{hi}$ $CD8^+$ Lck^{ind} thymocytes was 1.3-fold lower than in Lck^{WT} mice, which was in agreement with our results in polyclonal mice (Fig.3.7). Increased proportions of DN thymocytes, compared to $F5Lck^{WT}$ mice (0.8% ± 0.2), were noted in $F5Lck^{VA}$ and $F5Lck^{ind}$ mice (5.8%±1.5 and 7.6%) (Fig.3.10A). This translated into increased numbers of DN3 and DN4 thymocytes (Fig.3.10D). Despite this the thymus size was significantly reduced in $F5Lck^{VA}$ ($p=0.0002$) and $F5Lck^{ind}$ mice ($72.1\pm11.2x10^6$ and $119.6x10^6$) compared to $F5Lck^{WT}$ mice ($198.8\pm12.2x10^6$).

In order to compare the sensitivity of the thymocytes in the different strains of mice, we cultured thymocytes with different concentrations of NP68 or NP34 overnight and measured CD69 upregulation in DP thymocytes (Fig.3.11). We gated on $CD4^+$ live cells, because this would isolate the DP population in F5TCR transgenic mice. The cells were further gated as $CD5^+CD24^{lo}$ to remove contaminating mature $CD8^+$ T cells. In the media only samples there was <1% CD69 upregulation in all mouse strains, confirming that this acted as a negative control and the CD69 upregulation in the other samples was peptide specific (Fig.3.11A and B). In response to peptide stimulation the percentage upregulation of CD69 was dose-dependent in all mouse strains (Fig.3.11A and B). The upregulation of CD69 was significantly higher in $F5Lck^{ind}$ mice in response to both NP68 and NP34 than in $F5Lck^{VA}$ and $F5Lck^{WT}$ mice (Fig.3.11A and B), suggesting that Lck^{ind} thymocytes were more sensitive, potentially explained by the high Lck expression at this stage of development (Fig.3.3). CD69 upregulation in response to both NP68 and NP34 tended to be lowest in $F5Lck^{VA}$ mice at all concentrations, however it was not significantly different from $F5Lck^{WT}$ thymocytes (except at $1x10^{-3}$ μM NP68) (Fig.3.11A and B).

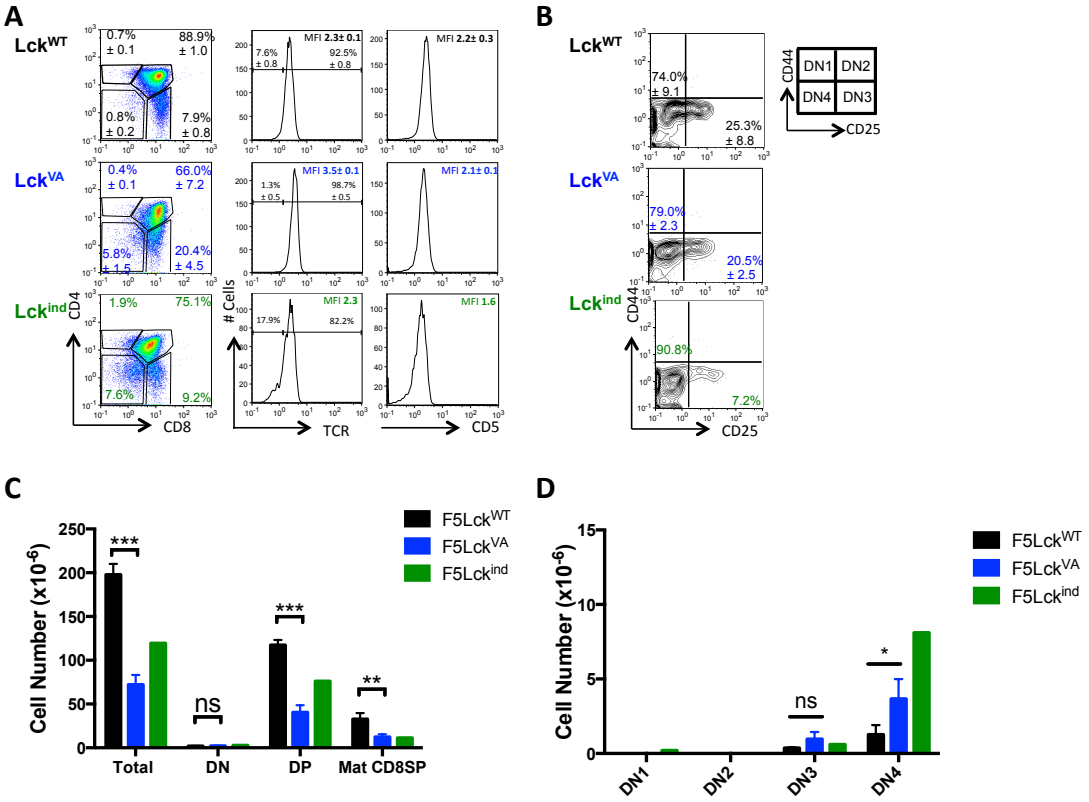

Fig. 3.10 Thymic development in F5 TCR transgenic Lck^{WT}, Lck^{VA}, and Lck^{ind} mice.
Thymi from age matched 6-8 week old F5Lck^{VA} (n=3), F5Lck^{WT} (n=3) and F5Lck^{ind} mice (n=2; no SD) were harvested and thymocyte development was analysed *ex vivo* by flow cytometry. (A) Representative dot plots show frequency of DN, DP and SP T cells with average proportions ± SD. Representative histograms show TCR and CD5 expression in CD8$^+$ SP thymocytes. Numbers on histograms show average proportions ± SD. (B) Representative contour plots show CD44 versus CD25 staining in the DN population and the numbers show average proportions ± SD of cells in quadrants DN3 and DN4. (C) Bar chart shows average numbers ± SD of total thymocytes and cells in each of DN, DP, CD8$^+$ SP compartments. (D) Bar chart shows average numbers ± SD of cells in indicated populations. Statistical analysis on Lck^{WT} and Lck^{VA} samples in parts C and D was done using Prism as follows: parametric, student's t-test, unpaired, two-tailed, *P<0.05, **P<0.01, ***P<0.001. Data are representative of 3 independent experiments.

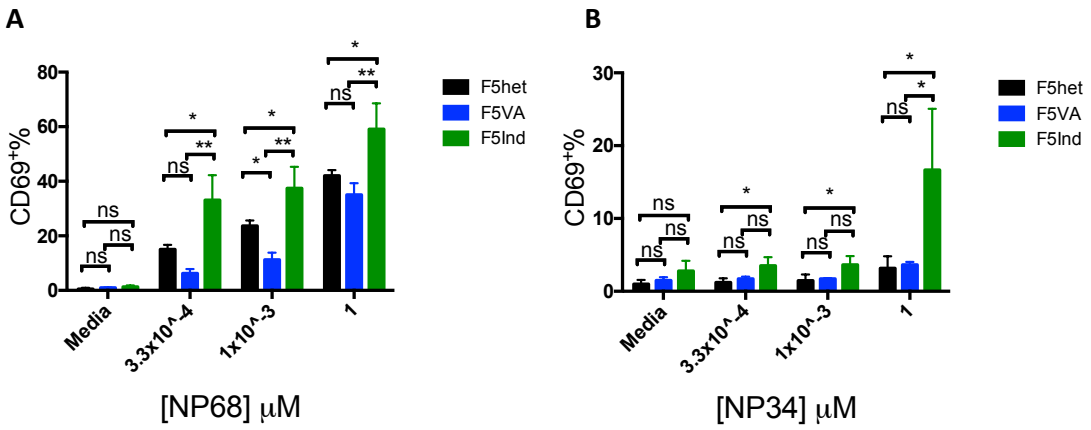

Fig. 3.11 Lck abundance influenced sensitivity of thymocytes to NP68 and NP34 stimulation.
Thymocytes from F5Lck^{WT}, F5Lck^{VA} and F5Lck^{ind} mice were stimulated overnight in the presence of 2 μg mL^{-1} doxycycline, with peptide. Media alone was used as a negative control. Cells were first gated as thymocytes using FSC and SSC, then CD4^{+} Live/Dead Aqua^{-} and finally CD69 upregulation was measured in CD24^{hi}CD5^{+} cells to exclude mature SP cells. Average upregulation of CD69 ± SD is shown in bar charts for (A) NP68 and (B) NP34 stimulation. Data are representative of 2 independent experiments with n=3 individual animals analysed in each group. Statistical significance was calculated using Prism as follows: One-way ANOVA, with post-ANOVA Tukey's test for multiple comparisons, p=0.05.

Although we could not conclude effects on negative versus positive selection of cells in this experiment, the data certainly correlate with the prediction that Lck^{hi} cells in Lck^{ind} mice are negatively selected, because $F5Lck^{ind}$ DP thymocytes were most sensitive to peptide stimulation (Fig.3.11), yet expressed the lowest levels of CD5 in $CD8^+$ SP cells (Fig.3.10A), suggesting that the highly sensitive cells were eliminated.

It would be interesting to increase the concentration of NP34, as in published reports 2 μM was used (Smyth et al., 1998) and to measure apoptosis. This could indicate whether the cells expressing high levels of CD69 are likely to die. It would also be interesting to assess whether the increased CD69 expression in response to NP68 stimulation in $F5Lck^{ind}$ mice was due to the Lck^{hi} cells. The data in Fig3.11 showed that $F5Lck^{VA}$ thymocytes were just as sensitive to NP68 and NP34 stimulation as $F5Lck^{WT}$ thymocytes despite reduced Lck expression.

3.3 Results: Peripheral Phenotype of Lck^{VA} and Lck^{ind} mice

3.3.1 The proportions of $CD44^{hi}$ T cells are increased in naïve mice with reduced Lck abundance

The above sections studied the thymic development in Lck^{VA} and Lck^{ind} mice. We next assessed what the consequences of thymic development with low Lck expression were for the peripheral T cell phenotype on the polyclonal background.

We confirmed low Lck expression in peripheral T cells from Lck^{VA} and Lck^{ind} mice by WB analysis (Fig.3.12A). The results showed that the relative expression of Lck in Lck^{VA} was 9% as compared to 100% in Lck^{WT}. In Lck^{ind} mice it was similarly low: 7% (Fig.3.12A). As one would predict from decreased cell numbers of $CD4^+$ SP and $CD8^+$ SP thymocytes (Fig 3.2), the peripheral $CD4^+$ and $CD8^+$ T cell numbers were significantly reduced in Lck^{VA} and Lck^{ind} mice compared to Lck^{WT} mice. (Fig.3.12B). Reduced T cell numbers can lead to a lymphopenic environment (Salmond et al., 2009a), therefore we assessed the expression of the memory-phenotype and activation marker CD44

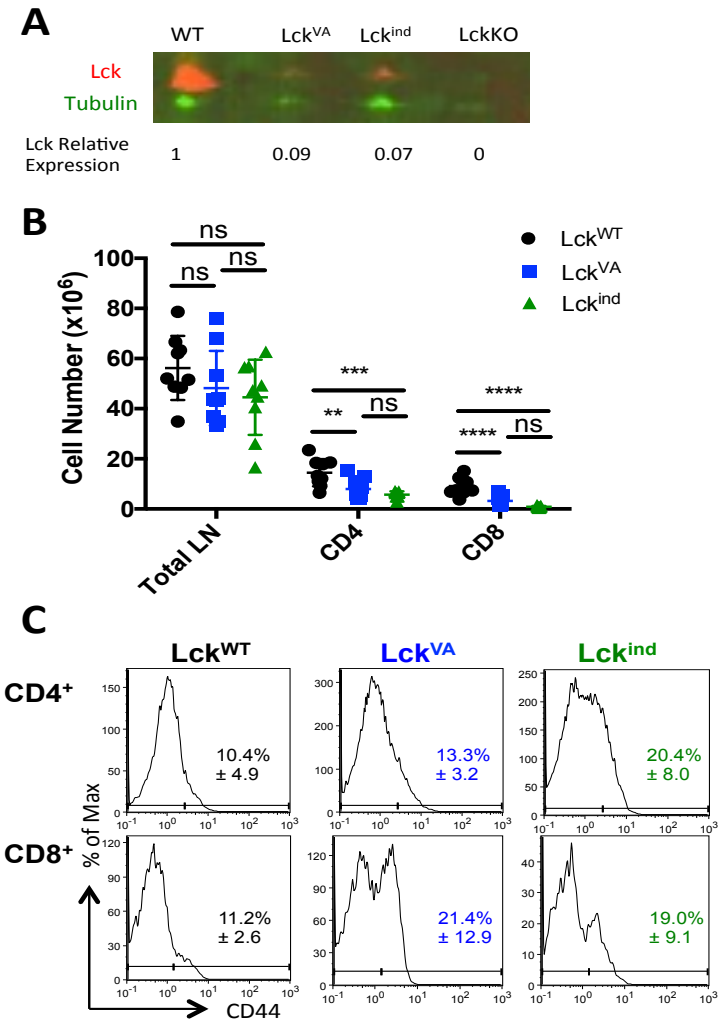

Fig. 3.12 Low Lck expression in peripheral lymphocytes led to increased proportions of memory phenotype cells.
(A) Cell lysates from LN cells from polyclonal Lck^{WT}, Lck^{ind}, and Lck^{VA} mice were analysed by WB (pre-cast gel). The blot was first probed with anti-Lck (Upstate) and anti-Tubulin antibodies overnight at 4°C, and then with anti-mouse (for Lck) and anti-rabbit (for Tubulin) fluorescent secondary antibodies for 1 hour. The blot was subsequently scanned using the Li-Cor system. Data were quantified using the ratio of Lck/Tubulin for each sample and then normalised to Lck^{WT} levels. Full blot is shown in Appendix 7.2. (B) Cell counts on lymphocytes were done using the CASY counter. Data are an average of 3 independent experiments with total n=9 individually analysed mice in each group ± SD. Statistical analysis was done on Prism as follows: One-way ANOVA with post-ANOVA Tukey's multiple comparisons test, p=0.05. (C) CD44 expression was measured for all genotypes, in both $CD4^+$ and $CD8^+$ T cells, as indicated. Percentages on histograms represent averages of a minimum of 3 individual animals ± SD. Data are representative of 3 independent experiments.

(Goldrath et al., 2000) in the three strains (Fig.3.12C). The data showed that in the $CD4^+$ T cell compartment in Lck^{VA} and Lck^{ind} mice (13.3%±3.2 and 20.4%±8.0 respecively) there were increased proportions of $CD44^{hi}$ cells as compared to Lck^{WT} $CD4^+$ T cells (10.4%±4.9). In the $CD8^+$ T cell compartment both Lck^{VA} and Lck^{ind} mice had approximately 2-fold more $CD44^{hi}$ cells than Lck^{WT} mice (11.2%±2.6) (Fig.3.12C). Overall these data correlated with the reduced thymic output in Lck^{VA} and Lck^{ind} mice. A high *ex vivo* CD44 expression can hinder studies of activation as the $CD44^{hi}$ memory phenotype cells are different from naïve cells and may contribute to immune responses (Sprent and Surh, 2011; Su et al., 2013).

3.3.2 Generating Lck^{WT} and Lck^{VA} bone marrow chimaeras.

In order to assess whether the CD44 upregulation in Lck^{VA} mice, seen *ex vivo* (Fig.3.12C), was intrinsic to low Lck expression, or was indeed the result of extrinsic factors such as the lymphopenic environment, we made bone marrow chimeras (Fig3.13). This enabled the study of Lck^{VA} versus Lck^{WT} T cells whilst subjected to the same environmental conditions in the same host. If the degree of CD44 upregulation were more in Lck^{VA} cells compared to Lck^{WT} cells, it would indicate an Lck dependent intrinsic mechanism. If, however, the upregulation of CD44 were the same as seen in Lck^{WT} it would indicate an environment driven lymphopenic response.

Bone marrows of Lck^{VA} and Lck^{WT} donors were depleted of mature T cells by anti-CD4 and CD8 staining and complement lysis (Fig.3.13A). Host $Rag1^{KO}$ mice were reconstituted with mixtures of CD45.2 Lck^{VA} and CD45.1 Lck^{WT} in a 9:1 ratio (Fig.3.13B). This ratio was chosen because previous work with Lck^{ind} chimeras has suggested that the numbers of Lck low cells recovered from chimeras was lower than that of Lck^{WT} cells and our lab has found 9:1 to be the optimal ratio (Caserta et al., 2010). At 4 weeks (Fig.3.13C) and 9 weeks (Fig.3.13D) post-transplantation the chimeras were characterised by flow cytometry. At 4 weeks it was noted that the three animals analysed, had slightly increased proportions of Lck^{WT} lymphocytes ($CD45.1^+$) as compared to Lck^{VA} lymphocytes despite the 9:1 ratio initially favouring the Lck^{VA} cells (Fig.3.13C top panel). This was also reflected in

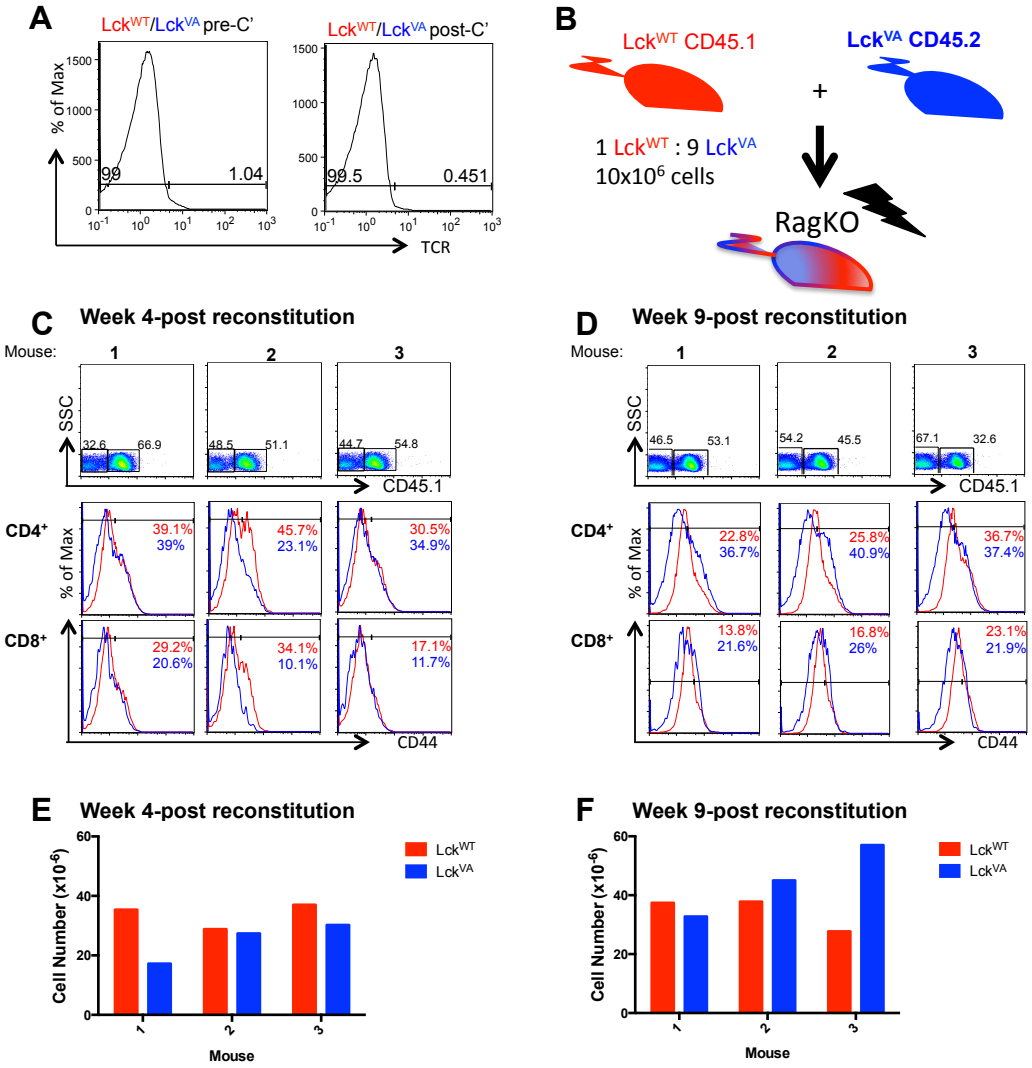

Fig. 3.13 Lck^{VA} and Lck^{WT} cells expressed similar proportions of CD44 in the same lymphopenic environment.
(A) Congenically marked Lck^{VA} (45.2) and Lck^{WT} (45.1) bone marrow cells were pooled in a 9:1 ratio. Mature T cells were depleted with complement lysis and histograms showed decrease in TCR expressing cells after complement treatment. (B) Pooled BM from Lck^{WT} and Lck^{VA} was transplanted into irradiated Rag1^{KO} hosts. At week 4 (C) and week 9 (D) proportions of CD44^{+} expression in CD4^{+} and CD8^{+} T cells in 3 individual mice was assessed by histogram analysis. Lck^{WT} were CD45.1^{+} (red) and Lck^{VA} were CD45.1^{-} (blue). At week 4 (E) and week 9 (F) lymphocyte numbers in the LN of Lck^{WT} cells (red) and Lck^{VA} cells (blue) are shown in bar charts. Data are representative of 2 independent experiments.

total cell numbers (Fig.3.13E). Interestingly the results obtained on week 9 showed that in 2 of the 3 mice analysed Lck^{VA} lymphocytes represented a majority compared to Lck^{WT} lymphocytes (Fig.3.13D and F). However, at both time points histogram analysis of CD44 expression showed that there were no consistent differences between the Lck^{VA} and Lck^{WT} peripheral T cells in CD44 upregulation (Fig.3.13C and D). Suggesting that both Lck^{WT} and Lck^{VA} lymphocytes respond similarly to a lymphopenic environment and that the CD44 upregulation was not an intrinsic feature of the reduced Lck expression in Lck^{VA} mice, but rather a biproduct of the lymphopenic environment caused by the reduced thymic output of cells (this issue is addressed further in chapter 5).

Despite the initial 9:1 ratio of bone marrow cells at transplantation, Lck^{VA} versus Lck^{WT}, this ratio was not reflected in the cell numbers recovered (Fig.3.13E and F). This indicated that Lck^{VA} were less able to compete during thymic development, perhaps due to the partial DN block that led to reduced DP thymocyte numbers (Fig.3.2). To investigate the inability of Lck^{VA} cells to compete with Lck^{WT} cells further, we assessed the proportions of Lck^{WT} and Lck^{VA} cells during different stages of thymic development in the chimaeras by flow cytometry (Fig.3.14).

The data in Fig.3.14 showed that at the DN stage Lck^{VA} cells were in a majority ~72-78% compared to Lck^{WT} cells, which only represented ~3-5%. (The rest of the events, ~20% on the dot plots, were unstained and that was why the proportions did not add to a 100%). At the DP stage, in two of the three mice (no. 1 and 2), Lck^{WT} cells represented ~26 – 35% of the events and a further increase in their predominance was seen in the $CD8^+$ SP population. In contrast, in mouse no.3 the Lck^{WT} cell population remained low (3-6%) at all stages of development.

Overall, these data suggested that reduced Lck expression made T cells less able to compete with Lck^{WT} cells in the DN→DP transition during thymic development in bone marrow chimaeras (Fig.3.14). However, the transition from DP to SP was shown to be comparable between individual Lck^{WT} and

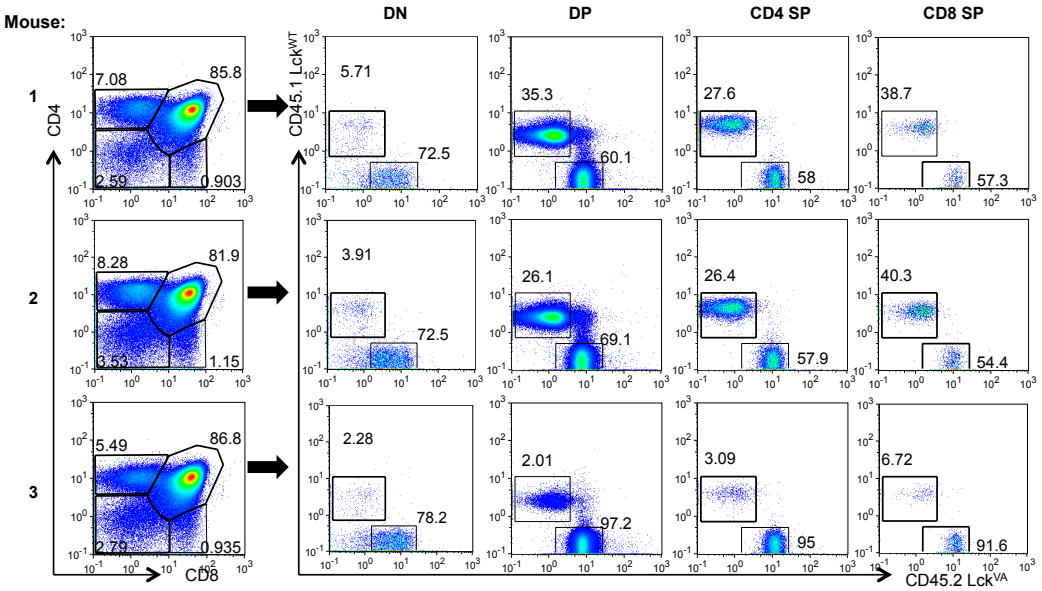

Fig. 3.14 Lck^{VA} cells unable to compete in thymic differentiation in bone marrow chimaeras with Lck^{WT} cells.
Sub-lethally irradiated Rag1^{KO} mice were reconstituted with a 9:1 mixture of congenitally marked Lck^{VA} (CD45.2) and Lck^{WT} (CD45.1) bone marrow cells. At 9 weeks after reconstitution, thymi were analysed by flow cytometry. (A) Representative dot plots show CD4 against CD8 staining for the 4 developmental populations (DN, DP, CD4$^+$ SP, and CD8$^+$ SP) for three individual mice. Each of DN, DP, CD4$^+$ SP, and CD8$^+$ SP populations were gated for relative proportions of Lck^{WT} (CD45.1) and Lck^{VA} (CD45.2) cells. CD4$^+$ and CD8$^+$ SP thymocytes were gated TCR$^+$ cells to exclude immature cells. Data are representative 2 independent experiments.

Lck^{VA} mice (Fig.3.3) and this was also the case in bone marrow chimaeras (Fig.3.14). Transplanting Lck^{VA} cells in a 9:1 ratio with Lck^{WT} cells allowed for some compensation in cell numbers recovered, however, the peripheral pools varied a lot in composition between individual animals.

3.3.3 Lck abundance did not affect peripheral numbers of T_{Reg} cells

Downstream of TCR signalling one of the main targets of Lck is Zap-70. It has been shown that when Zap-70 expression and function are compromised the TCR signaling threshold is changed, which consequentially influences the thymocyte selection threshold such that normally negatively selected clones are positively selected (Tanaka et al., 2010). The negative selection escapees are perpetrators of an autoreactive phenotype in periphery. Importantly, this phenotype is accompanied by an increase in T_{Reg} proportions. Additionally, studies have suggested that natural T_{Regs} are selected in the thymus in response to strong TCR signals (Anderson and Takahama, 2012). Our data indicated that there may be changes in the thymocyte selection thresholds due to changes in Lck abundance (Fig.3.7 and 3.11) and therefore we asked whether this might have led to changes T_{Reg} proportions in the peripheries of Lck^{VA} and Lck^{ind} mice .

Our results of *ex vivo* T cell phenotyping for $CD4^+Foxp3^+$ T cells showed that although Lck^{ind} mice had significantly higher proportions of T_{Regs} than Lck^{WT} or Lck^{VA} mice (Fig.3.15A), the numbers of T_{Regs} were not significantly different (Fig.3.15B) between Lck^{WT}, Lck^{VA} or Lck^{ind} T cells, suggesting that even if there was a change to selection thresholds when Lck abundance was changed, this did not influence T_{Reg} selection.

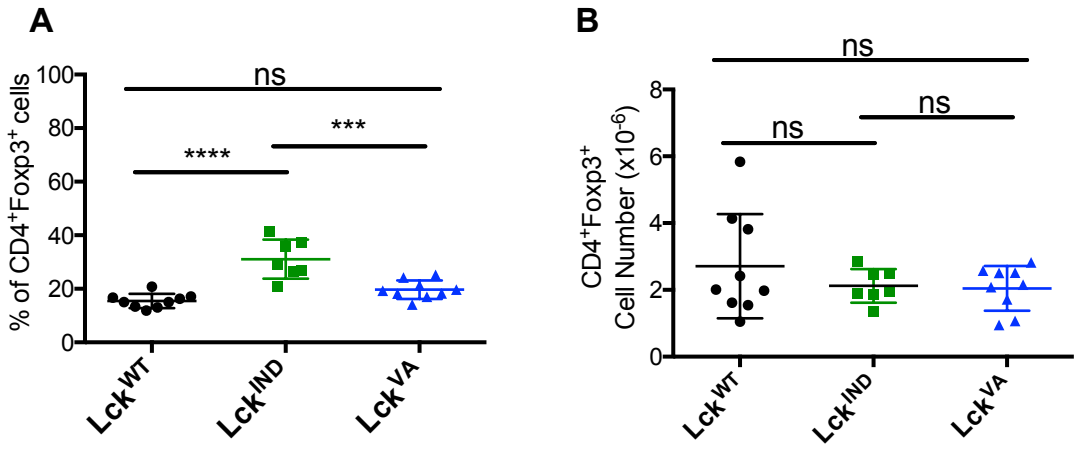

Fig. 3.15 Proportions and numbers of T_{Regs} were comparable to Lck^{WT} in Lck^{VA} and Lck^{ind} mice.
Peripheral lymphocytes from Lck^{WT} (black), Lck^{ind} (purple) and Lck^{VA} (red) mice were analysed by ex vivo intracellular staining for T_{Regs} ($CD4^+Foxp3^+$). The average proportions ± SD (A) and average numbers ± SD (B) of $CD4^+Foxp3^+$ T_{Regs} are shown in bar charts. Data are representative of 3 independent experiments of a minimum of 3 individual animals per group.

3.4 Summary

- Lck^{ind} thymocytes expressed a broad range of Lck in the thymus (Fig.3.3D) while Lck^{VA} mice expressed constitutively low levels of Lck (Fig.3.1 and Fig.3.3D).
- In both Lck^{ind} and Lck^{VA} mice, thymic development was restored as compared to Lck^{KO} mice, although thymocyte numbers were significantly lower than in Lck^{WT} mice (Fig.3.2).
- Neither Lck^{ind} nor Lck^{VA} mice had impediments in thymocyte progression through positive selection (Fig.3.3 and 3.4).
- In Lck^{VA} mice $CD4^{+}$ and $CD8^{+}$ SP thymocytes developed without the formation of the intermediate $CD4^{lo}CD8^{-}$ population (Fig.3.5), although the $CD8^{+}$ SP thymocytes are less mature compared to Lck^{WT} mice.
- Lck^{ind} mice had more immature $CD4^{+}$ and $CD8^{+}$ SP thymocytes than Lck^{WT} SP thymocytes despite the ability to form an intermediate $CD4^{lo}CD8^{-}$ population (Fig.3.5).
- Lck^{WT} DP thymocytes were as sensitive as Lck^{VA} thymocytes, but less sensitive than Lck^{ind} thymocytes, to peptide stimulation (Fig.3.11).
- Any changes to selection thresholds that may have occurred in Lck^{VA} and Lck^{ind} mice, did not affect peripheral T_{Reg} cell numbers (Fig.3.15).
- Reduced Lck expression led to increased proportions of lymphopenia-induced $CD44^{hi}$ memory-phenotype cells in the periphery (Fig.3.13-3.14).

3.5 Discussion

The aim of the work presented in this chapter was to determine the impact Lck abundance has on thymocyte development. To this end we compared the Lck^{ind} mice, which expressed a range of Lck abundance in the thymus (Fig.3.3D) and Lck^{VA} mice, which expressed constitutively low levels of Lck (Fig.3.1. and Fig.3.3D) to Lck^{WT} mice, and where appropriate, Lck^{KO} controls. A number of observations were made, that highlighted Lck dependent differences in thymic development between Lck^{ind} and Lck^{VA} mice, allowing us to better understand the roles of Lck.

The data presented in this chapter confirmed, as reported previously (Legname et al., 2000; Salmond et al., 2011), that both Lck^{ind} and Lck^{VA} mice overcame to some extent, the DN3 block seen in Lck^{KO} mice (Fig.3.1). Despite this reduced DP and SP thymocytes were recovered in Lck^{ind} and Lck^{VA} mice (Fig.3.2). The partial DN3 block found in some cells in the Lck^{ind} thymi, might have been because not all cells expressed the transgene at this stage in development, due to variegated transgene expression previously reported to be a factor in the rtTA x dox genetic system.

Lck has been shown to play a critical role at the first DN checkpoint in thymic development (Molina et al., 1992), as signaling via the TCR is critical for regulating β chain selection. We did not find any striking differences in the TCR Vβ repertoire in Lck^{ind} and Lck^{VA} mice (Fig.3.8). Additionally, TCR signals are critical for α-chain allelic exclusion (Hogquist et al., 2005) yet, interestingly, we showed, that even 5% of WT levels of Lck, in Lck^{VA} mice, were sufficient for allelic exclusion of the TCRα-chains Vα2 and 8 (Fig.3.9). Although, this does not exclude the option that there might be defects in allelic exclusion of other α-chains, we would predict, based on the similar TCR sensitivity in DP thymocytes between Lck^{VA} and Lck^{WT} mice, that this is unlikely, as they appear to signal to the same extent as Lck^{WT} cells (Fig.3.11).

In keeping with previously published data, we showed that at the DP stage of development Lck^{ind} thymocytes expressed variable levels of Lck (Legname et al., 2000), and after the positive selection step they expressed low levels of

Lck (Fig.3.3). Legname et al. predicted that very high Lck expression in DP thymocytes might be unfavourable for thymocyte development (Legname et al., 2000). Indeed, it has been shown that overexpression of WT Lck is detrimental to thymic development as it can lead to development of thymic tumours, therefore there may be selection against high Lck expression (Abraham et al., 1991). When we assessed positive selection using the expression patterns of CD69 and TCR in Lck^{ind}, Lck^{VA} and Lck^{WT} thymocytes (Fig.3.3) we found that in Lck^{WT} mice the TCR expression levels increased during development from DN to DP to SP stages, as would be expected (Azzam et al., 1998). Despite a higher TCR expression in Lck^{VA} and Lck^{ind} DP thymocytes compared to Lck^{WT} thymocytes positive selection proceeded unhindered, as measured by relative proportions of cells at each of the selection stages distinguished by CD69 and TCR expression. The results revealed, however, a change in Lck expression levels in Lck^{ind} mice during positive selection from bimodal to low (Fig.3.3).

Reduced abundance of Lck has been shown to lead to weaker TCR signals (Hernandez-Hoyos et al., 2000), which is also the premise of the signal-strength model of CD4/CD8 lineage development. Therefore, we assessed lineage development in further detail by analysing CD5 versus TCR expression (Fig.3.5). We found that both Lck^{ind} and Lck^{VA} thymocytes, despite reduced Lck expression developed $CD4^+$ and $CD8^+$ SP in approximately the appropriate 4:1 ratio (Sinclair et al., 2013), although in reduced numbers (Fig.3.2).

Interestingly, in contrast to Lck^{WT} and Lck^{ind} thymocytes, Lck^{VA} thymocytes did not develop an intermediate $CD4^{lo}CD8^-$ population (Fig.3.5) (Brugnera et al., 2000) as is considered necessary in the kinetic-signalling model of lineage determination. These data suggested that perhaps the high levels of Lck expression in Lck^{ind} mice at the DP stage of development allow them to behave like Lck^{WT} thymocytes, however, the intermediate $CD4^{lo}CD8^-$ population was not absolutely required for the development of $CD4^+$ and $CD8^+$ SP thymocytes. The reduction in Lck expression in Lck^{ind} mice at the SP stage (Fig.3.3) compromised both $CD4^+$ and $CD8^+$ thymocyte maturation,

whereas in Lck^{VA} mice only $CD8^{+}$ thymocyte maturation was altered (Fig.3.5). Therefore our data challenge the necessity of an intermediate $CD4^{lo}CD8^{-}$ population in thymocyte development and perhaps suggest that Lck abundance is more important for thymocyte maturation.

Signals via the TCR are also critical for determining positive versus negative selection at the DP stage of development, particularly important is the affinity of the TCR for the selecting signal which may be predicted from CD5 expression levels (Gascoigne and Palmer, 2011; Mandl et al., 2013).

Reduced CD5 expression in Lck^{ind} SP thymocytes both on the polyclonal and F5TCR transgenic backgrounds, therefore, suggested that despite the high Lck expression at the DP stage, which potentially explains the increased sensitivity to peptide stimulation (Fig.3.11), the activation threshold is adjusted or the cells expressing high levels of Lck are negatively selected by the SP stage. These predictions are supported by the observation that mature $CD4^{+}$ SP Lck^{ind} thymocytes had lower CD5 expression and peripheral $CD4^{+}$ SP Lck^{ind} T cells have been shown to have an increased activation threshold (Lovatt et al., 2006). However, care must be taken when drawing parallels between transgenic and polyclonal mice. Despite these caveats, these data are in agreement with the notion that Lck expression levels above that found in WT mice, are damaging to the T cell repertoire, which would be in line with published data (Abraham et al., 1991), and that is why after positive selection only cells with low Lck expression in Lck^{ind} mice remain. Additionally, we did not find increased numbers of natural T_{Regs} in the periphery in Lck^{ind}, which might be expected from studies in SKG Zap-70 mutants, further suggesting that the high Lck expression probably leads to death (Tanaka et al., 2010).

These data, however, did not rule out that the change in Lck expression in Lck^{ind} mice could be the result of active downregulation. Indeed, since we found no differences in efficiency of DP to SP conversion in Lck^{VA} and Lck^{ind} mice (Fig.3.4), suggesting that there was no increase in apoptosis in Lck^{ind} mice at the DP stage. Future work dissecting positive and negative selection

in more detail, particularly assessing apoptosis, would be one step towards settling this issue.

Interestingly, we found that CD5 expression was similar in mature Lck^{VA} and Lck^{WT} thymocytes (Fig.3.7), suggesting similar signaling thresholds, which were supported by the observation that there were no significant differences between $F5Lck^{VA}$ and $F5Lck^{WT}$ thymocyte sensitivities to peptide stimulation (Fig.3.11). Unfortunately, it also appeared that the cells respond weakly below the 1 μM concentration to NP34 and it would have been interesting to repeat the experiment with higher concentrations of NP34.

Finally, it is important to bear in mind that the TCR sensitivity to positively and negatively selecting signals were assessed very crudely here, and the results cannot be used to interpret survival or apoptosis after NP68 or NP34 stimulation. The selection window for thymocytes is very narrow and the TCR is highly sensitive and discriminating when responding to p:MHC ligation (Daniels et al., 2006; Naeher et al., 2007). It would be interesting to extend these studies and study the Lck^{VA} mice on an OT-1 transgenic background, to take advantage of the wide range of different affinity peptides, which could elucidate the effect of Lck abundance on signaling thresholds. Furthermore, we could use fetal thymic organ cultures (FTOCs), where culturing a very young thymus, with less than 1% mature SP cells, with a known peptide of a known concentration allows one to calculate the resulting numbers of SP cells to measure efficiency of positive or negative selection (Smyth et al., 1998). Although we are confident that using CD4 staining to mark DP cells was accurate as $CD4^+$ SP proportions in F5 transgenic mice are <2% (Fig.3.10A). As an extension of the flow cytometry assay we could also sort for $CD4^+$ T cells prior to culturing thymocytes overnight, however this would still not directly indicate selection differences.

How different TCR signals indicate positive versus negative selection or CD4 and CD8 lineage choice is still poorly characterised. The combined contributions of strength and duration of TCR signals, unique patterns of gene expression controlled by transcription factors, the expression and

function of which is in turn dependent on spatial and temporal regulation by cytokines and growth factors, can all influence the development of thymocytes (Gascoigne and Palmer, 2011; Mingueneau et al., 2013). Up until the DP stage of development the $CD4^+$ SP cells and $CD8^+$ SP cells develop in unison. At the DP stage a process of selection occurs where the cells with the correct TCR avidity for self-peptides presented on the appropriate MHC molecule class I or II, would differentiate into $CD8^+$ or $CD4^+$ SP, respectively.

If the developmental expression patterns of TCR and CD5 are so determinative in response to TCR signals, why then with <5% Lck expression do we not see more significant disturbances in thymocyte development? Perhaps this is explained by the relative involvement of downstream signaling pathways. For example TCR signaling thresholds have been shown to influence positive versus negative selection via its effects on Ca^{2+} (Freedman et al., 1999; Kane and Hedrick, 1996) and ERK signals (Mariathasan et al., 2001). Strong and transient ERK activation led to negative selection, and sustained low level of activation led to positive selection (Mariathasan et al., 2001). Mechanistically, it has been shown that this is because small changes in signaling strength alters the localization of Ras and MAPK signaling intermediates within the cell: strong signals activate Ras/Raf-1/ERK at the plasma membrane causing negative selection, and weak signals induce their activation at the Golgi, leading to positive selection (Daniels et al., 2006). Similarly sustained Ca^{2+} mobilization in response to strong TCR signals was shown to lead to negative selection (Kane and Hedrick, 1996). Interestingly, however, Salmond et al. did not find any differences in the efficiency of Ca^{2+} flux in Lck^{WT} and Lck^{VA} thymocytes (Salmond et al., 2011), perhaps suggesting that there are no overt differences in the ultimate sensitivity of the TCR with reduced Lck expression levels and therefore we do not see more severe consequences, which is also what our data indicated (Fig.3.11). It would be interesting to assess whether the same is true for ERK signaling in Lck^{VA} mice. Alternatively, assessing Ca^{2+} in response to crosslinking with anti-TCR/CD4 antibodies may be too crude an analysis. In studies with polyclonal *Themis*^{KO} mice Fu et al. were unable to see differences in Ca^{2+} flux in positively selecting thymocytes in response to anti-

CD3/CD4 crosslinking, yet when using the OTI system, with distinct positively and negatively selecting antigen-variant peptides, they showed that Themis deficient thymocytes elicited increased and sustained Ca^{2+} flux with weak agonists, only seen with strong agonists in WT cells (Fu et al., 2013).

Overall, this chapter has highlighted that differences in Lck abundance can influence thymic development on many levels. Interestingly, however, only 5% of WT levels of Lck can rescue thymic development, and appears to be less consequential for development than changes in Lck expression levels during development, as was shown to be the case for Lck^{ind} mice. Perhaps the latter is because Lck is not normally developmentally regulated in the thymus and artificial changes in levels are more difficult to cope with for a cell, whilst setting up thresholds, than constitutively low levels of Lck (Olszowy et al., 1995).

Chapter 4: The Impact of Constitutively Low Lck Expression on Peripheral T cell Signalling

4.1 Introduction

Upon exposure to antigen, peripheral T cells, as key mediators of the adaptive immune response, differentiate, acquire effector function, proliferate, and finally form memory cells. T cells selected in the thymus have the potential to be self-reactive, thus the threshold of activation must be fantigens, whilst enforcing central tolerance to self-antigens. The TCR signalosome can be thought of as consisting of three regulatory units (Acuto et al., 2008). The first is the SFK regulation module, including Lck and the associated positive and negative regulators of Lck activity. The second is the signal triggering module consisting of ITAMs in the dimeric CD3 chains of the TCR complex, and Zap-70. The third and final module is the signal diversification and regulation module (Acuto et al., 2008). The intricate connectivity, inter-regulation and abundance of the molecules in the different modules gives the TCR its unique fine-tuning ability to discriminate between signals. Dysregulation at any stage of this response propagation can result in immune disorders, including autoimmune diseases, and therefore T cells activation is regulated on many levels.

The TCR is devoid of kinase activity itself, and thus it requires Lck to initiate the signaling cascade. Lck phosphorylates TCR-associated ζ-chain and CD3 ITAMs, which allow for recruitment of Zap-70. Zap-70 continues the cascade of phosphorylation events and induces the recruitment of the signal diversification and regulation module (Smith-Garvin et al., 2009). The first direct targets of Zap-70 are the transmembrane adapter protein LAT and SLP-76. The absence of the adapter proteins results in a loss of T-cell signalling, as they are critical for the spatiotemporal arrangements of subsequent effector molecules (Smith-Garvin et al., 2009). Ultimately the downstream signalling cascades lead to gene regulation by activating

transcription factors such AP1, NFκB, and NFAT (Oh-hora and Rao, 2008; Smith-Garvin et al., 2009).

Studies in Lck^{ind} mice, in which lower than WT levels of Lck are expressed in response to doxycycline administration, showed that Lck^{ind} CD4 T cells had an increased activation threshold to anti-TCR stimulation (Lovatt et al., 2006), meaning that higher concentrations of stimulus were required for equal to WT levels of ERK phosphorylation. This suggests that the local abundance of Lck molecules is critical in regulating TCR signalling thresholds. Differences in TCR signal quality and strength can affect which downstream signalling pathways are activated, and thereby determine the biological outcomes for T cells (Daniels et al., 2006; Guy et al., 2013; Inder et al., 2008).

Within the SFK regulation module, Lck activity is tightly regulated, independently of TCR engagement, by the phosphorylation states of its inhibitory residue Lck^{Y505} and activatory Lck^{Y394} in the kinase domain (Brownlie and Zamoyska, 2013; Salmond et al., 2009b).

The TCR signalosome is regulated by negative regulation pathways acting at different stages of TCR signaling, that are triggered by TCR stimulation, assuring that TCR signalling is controlled appropriately, in terms of the strength and duration of the signal. Deficiencies in early negative regulators like CTLA4, PD1, or SHP1 lead to immune disorders (Lorenz et al., 1994; Nishimura et al., 2001; Waterhouse et al., 1995). In the absence of more proximal negative regulation by Dok1 and Dok2 there is increased TCR-induced IL-2 production, and proliferation (Yasuda et al., 2007). Finally, deficiency of the HPK1-SLP-76-14-3-3 negative regulation pathway, which is also activated in response to TCR stimulation by Lck phosphorylating HPK1 can result in increased TCR-dependent tyrosine phosphorylation of SLP-76, PLCγ1, LAT, Vav1, and ZAP-70 (Shui et al., 2007).

Chapter 4: Aims

In chapter 3 our results indicated that changes in Lck abundance has variable effects on thymocyte development. Of particular interest, in light of the

above discussion of Lck being critical in setting up the TCR-signalosome and the consequent negative regulation pathways, is our observation that the activation threshold was similar between F5Lck^{WT} and F5Lck^{VA} thymocytes (Fig.3.11). It has been shown that in F5Lck^{ind} mice the activation threshold of peripheral T cells is increased due to reduced Lck expression, and this effect was shown to proceed linearly down the TCR signalling pathway (Lovatt et al., 2006). Additionally, F5Lck^{ind} thymocytes had a lower activation threshold than F5Lck^{VA} thymocytes (Fig.3.11). Consequently, we hypothesised that F5Lck^{VA} peripheral T cells would behave similarly to F5Lck^{ind} peripheral T cells.

In this chapter, we examined the activation threshold of F5Lck^{VA} CD8^{+} T cells by analysing surface marker expression in response to overnight peptide stimulation. Surprisingly, we found that peripheral T cells in F5Lck^{VA} mice had similar activation to F5Lck^{WT} T cells in terms of the dose of peptide required *in vitro*, to upregulate activation markers.

When assessing activation of downstream pathways such as Ca^{2+} mobilization, ERK phosphorylation, and proliferation, there were variable effects; some pathways were upregulated, some downregulated. Furthermore, cytokine production as a read out of the effector function in F5Lck^{VA} mice was studied and showed that F5Lck^{VA} T cells may have an impaired ability to differentiate into effector cells. Our results therefore are in keeping with published data suggesting that TCR-signals travel via different signalling branches, but not equally (Daniels et al., 2006; Inder et al., 2008).

4.2 Results

4.2.1 F5Lck^{VA} mice had reduced numbers of peripheral T cells

We showed in chapter 3 that naïve polyclonal Lck^{VA} mice had upregulated levels of CD44 expression *ex vivo* due to lymphopenia (Fig.3.12). Studies of peripheral T cell activation using Lck^{VA} mice may be confused by the CD44^{hi} memory-phenotype cells, as these may contribute differently to naïve T cells to the immune response (Sprent and Surh, 2011). In order to study the impact

of reduced levels of Lck on $CD8^+$ T cells, we used F5 TCR transgenic mice. The thymic development of $F5Lck^{VA}$ mice was characterised in chapter 3 (Fig.3.10), and showed a decrease in $CD8^+$ SP thymocyte numbers in $F5Lck^{VA}$ mice as compared to $F5Lck^{WT}$ mice.

Here, we analysed the frequency of peripheral LN F5 $CD8^+$ T cells, and also confirmed their naïve state by measuring expression of activation markers. The results in Fig.4.1A showed that the frequency of the $F5Lck^{VA}$ $CD8^+$ T cell population (96.6% ± 0.1) was equivalent to that in $F5Lck^{WT}$ mice (95.7% ± 1.1). Lck is non-covalently associated with both the CD4 and CD8 co-receptors in T cells (Rudd et al. 1989; Veillette et al 1988). Reduced Lck expression in polyclonal Lck^{ind} mice led to a 3-fold decrease in CD4 expression levels (Lovatt et al., 2006). Therefore, expression levels of CD8 and Lck were assessed (Fig.4.1B). CD8 expression was similar in $F5Lck^{VA}$ (MFI 9.1 ± 0.4) and $F5Lck^{WT}$ mice (MFI 10.0 ± 1.9). As in the thymus, Lck expression was significantly reduced in peripheral $F5Lck^{VA}$ T cells (MFI 11.3 ± 0.9) compared to $F5Lck^{WT}$ T cells (MFI 21.4 ± 0.8). Both $F5Lck^{VA}$ and $F5Lck^{WT}$ T cells expressed higher levels of Lck than $F5Lck^{KO}$ mice (MFI 7.6 ± 0.2). These data, however, did not accurately reflect the expression levels of Lck, as they suggested that Lck expression was only 2-fold lower in $F5Lck^{VA}$ mice compared to $F5Lck^{WT}$, yet in chapter 3 (Fig.3.1) we confirmed the previously published finding (Salmond et al., 2011), that Lck expression driven by the VA-transgene leads to <5% expression of Lck compared to WT levels. This discrepancy may reflect a lack of sensitivity in detecting Lck by flow cytometry compared to WB.

$F5Lck^{VA}$ mice were potentially lymphopenic as the absolute numbers of $CD8^+$ T cells in $F5Lck^{VA}$ mice ($7.76\pm3.4 \times 10^6$) were almost 3-fold lower than in $F5Lck^{WT}$ mice ($22.62\pm11.7 \times 10^6$) (Table.4.1). However, the peripheral $CD8^+$ T cells in both $F5Lck^{WT}$ and $F5Lck^{VA}$ mice were naïve, as *ex vivo* CD44 expression was low and, importantly, similar between mice (Fig.4.1C). Neither $F5Lck^{WT}$ nor $F5Lck^{VA}$ $CD8^+$ T cells were activated, as they did not express activation markers CD69 and CD25 (Fig.4.1C). We also used expression of CD5 as a surrogate marker for measuring TCR sensitivity (Azzam et al., 1998), and

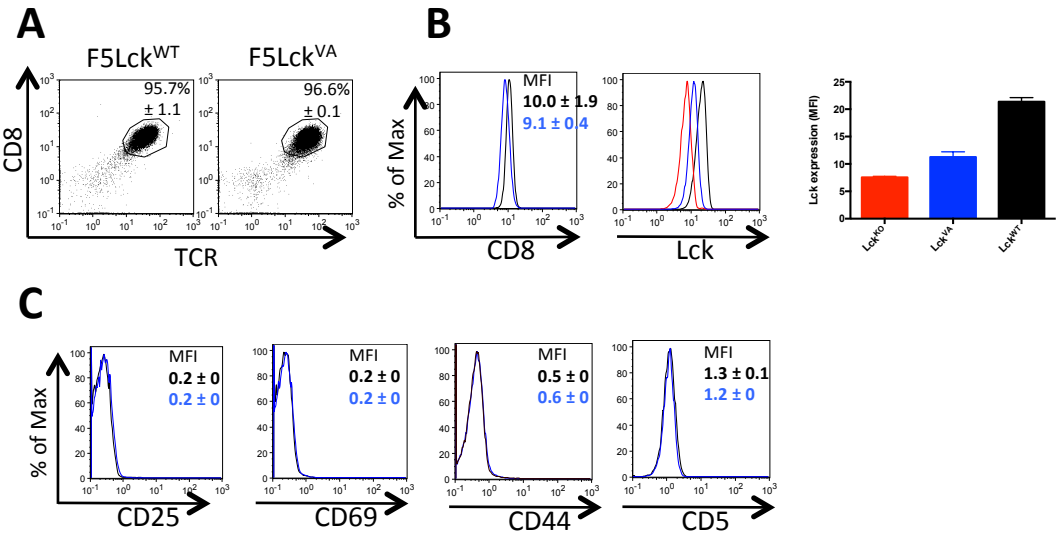

Fig. 4.1 F5Lck^{VA} T cells were of naïve phenotype *ex vivo*.
Peripheral LN cells from F5Lck^{WT} (black), and F5Lck^{VA} (blue) mice were evaluated *ex vivo* for activation markers by flow cytometry. (A) Representative dot plots show the average proportions ± SD of total TCR$^+$CD8$^+$ cells. The values shown are an average of 3 individual mice ± SD. (B) CD8 expression (left histogram) with the average MFI ± SD, and Lck expression (right histogram) were assessed in CD8$^-$TCR$^-$ T cells. The bar chart shows average MFI ± SD for Lck expression where Lck^{KO} (red) is shown as a control. (C) Histograms show the expression of indicated activation markers with average MFIs ± SD shown in the top right corners. The data is representative of 3 independent experiments, n=3 for each genotype.

found that both F5Lck^{WT} and F5Lck^{VA} had equal CD5 surface expression (Fig.4.1C).

Table 4.1 T cell numbers in LN of F5Lck^{WT} and F5Lck^{VA} mice.

Mouse Model	Total LN cell number (x10^{6})	Total CD8^{+}TCR^{+} cell number (x10^{6})
F5Lck^{WT} (n=6)	24.95 ± 12.7	22.62 ± 11.7
F5Lck^{VA} (n=6)	9.29 ± 4.7	7.76 ± 3.4

4.2.2 F5Lck^{VA} T cells were activated as efficiently as F5Lck^{WT} T cells

Reduced Lck expression has been shown to decrease TCR avidity and thereby increase the activation threshold of peripheral CD4^{+} and CD8^{+} T cells (Caserta et al., 2010; Lovatt et al., 2006). We hypothesised that F5Lck^{VA} would behave similarly to F5Lck^{ind} mice, and would have an increased activation threshold compared to F5Lck^{WT} mice.

T cells from LN of F5Lck^{VA}, F5Lck^{ind}, and Lck^{WT} mice were stimulated overnight, *in vitro*, with titrations of the cognate peptide NP68. We measured CD25 upregulation as a read out of activation status. CD25 is the α subunit of the IL-2R, and forms a high affinity complex with the β (CD122) and γ (CD132) subunits, allowing cells to respond to IL-2 (Leonard et al., 1990).

Figure 4.2A showed that, as expected, cells expressing homozygous levels of F5 (F5^{Hom}Lck^{WT}) had 2-fold higher TCR expression (MFI = 978) as compared to TCR expression in heterozygous F5 (F5^{Het}Lck^{WT}) mice (MFI = 487.3). F5^{Hom}Lck^{WT} T cells upregulated CD25 at lower peptide concentrations than F5^{Het}Lck^{WT} T cells, therefore increased TCR expression made them more sensitive to peptide stimulation than F5^{Het}Lck^{WT} cells (i.e. they had a lower activation threshold).

TCR expression levels and activation thresholds were compared between F5^{Hom}Lck^{VA}, F5^{Het}Lck^{VA}, and F5^{Het}Lck^{WT} cells (Fig.4.2B). Surprisingly, F5^{Het}Lck^{VA} (TCR MFI = 578) T cells had 1.6 fold lower TCR expression than F5^{Het}Lck^{WT} (TCR MFI = 942). This was also reflected in sensitivity to peptide as measured by CD25

upregulation at 24h, where F5^{Het}Lck^{VA} T cells required higher concentrations of peptide to upregulate CD25 in 50% of cells than did F5^{Het}Lck^{WT} (Fig.4.2B). On the other hand, F5^{Hom}Lck^{VA} T cells (TCR MFI = 1226) had similar TCR expression to F5^{Het}Lck^{WT} (TCR MFI = 942 ± 44.44), as was seen from the overlapping histograms. The slight difference in TCR MFI's between F5^{Hom}Lck^{VA} and F5^{Het}Lck^{WT} T cells was reproducible (Fig.4.2 B and C), but never reached a two-fold difference as was seen between F5^{Hom}Lck^{WT} and F5^{Het}Lck^{WT}. Whereas, F5^{Hom}Lck^{VA} T cells had two-fold higher TCR expression (TCR MFI = 1226) than F5^{Het}Lck^{VA} T cells (TCR MFI = 578). Surprisingly, induction of CD25 expression by peptide was the same for F5^{Hom}Lck^{VA} and F5^{Het}Lck^{WT} CD8^{+} T cells, indicating that the activation thresholds were equivalent. The reason for why homozygous TCR expression in F5^{Hom}Lck^{VA} mice, was the same as heterozygous surface expression in F5^{Het}Lck^{WT} mice, is unclear.

When we analysed TCR expression in F5^{Het}Lck^{ind}CD8^{+} T cells (TCR MFI = 6.1 ± 0.2), it was equivalent to that in F5^{Het}Lck^{WT} CD8^{+} T cells (TCR MFI = 6.5 ± 0.4), but the activation threshold in F5^{Het}Lck^{ind} CD8^{+} T cells was increased, which was in agreement with previously published data (Lovatt et al., 2006) (Fig.4.2C). Additionally, preliminary experiments in OT1^{VA} mice did not show reduced TCR expression compared to OT1^{WT} mice. One possible explanation is that by driving both the F5 and VA transgenes from the same promoter (hCD2 cassette) there is competition for transcription factors, such that transcription of the TCR is reduced. Since TCR surface expression was shown to have an effect on the activation threshold in wild type mice (Fig.4.2A), we continued our studies with F5^{Hom}Lck^{VA} mice (named for convenience F5Lck^{VA} throughout the thesis) and used the F5^{Het}Lck^{WT} mice as controls (named F5Lck^{WT} throughout the thesis), in order to normalise for TCR expression. In conclusion, contrary to our hypothesis and despite having very low expression of Lck, F5Lck^{VA} mice responded as efficiently as F5Lck^{WT} mice after overnight stimulation with NP68.

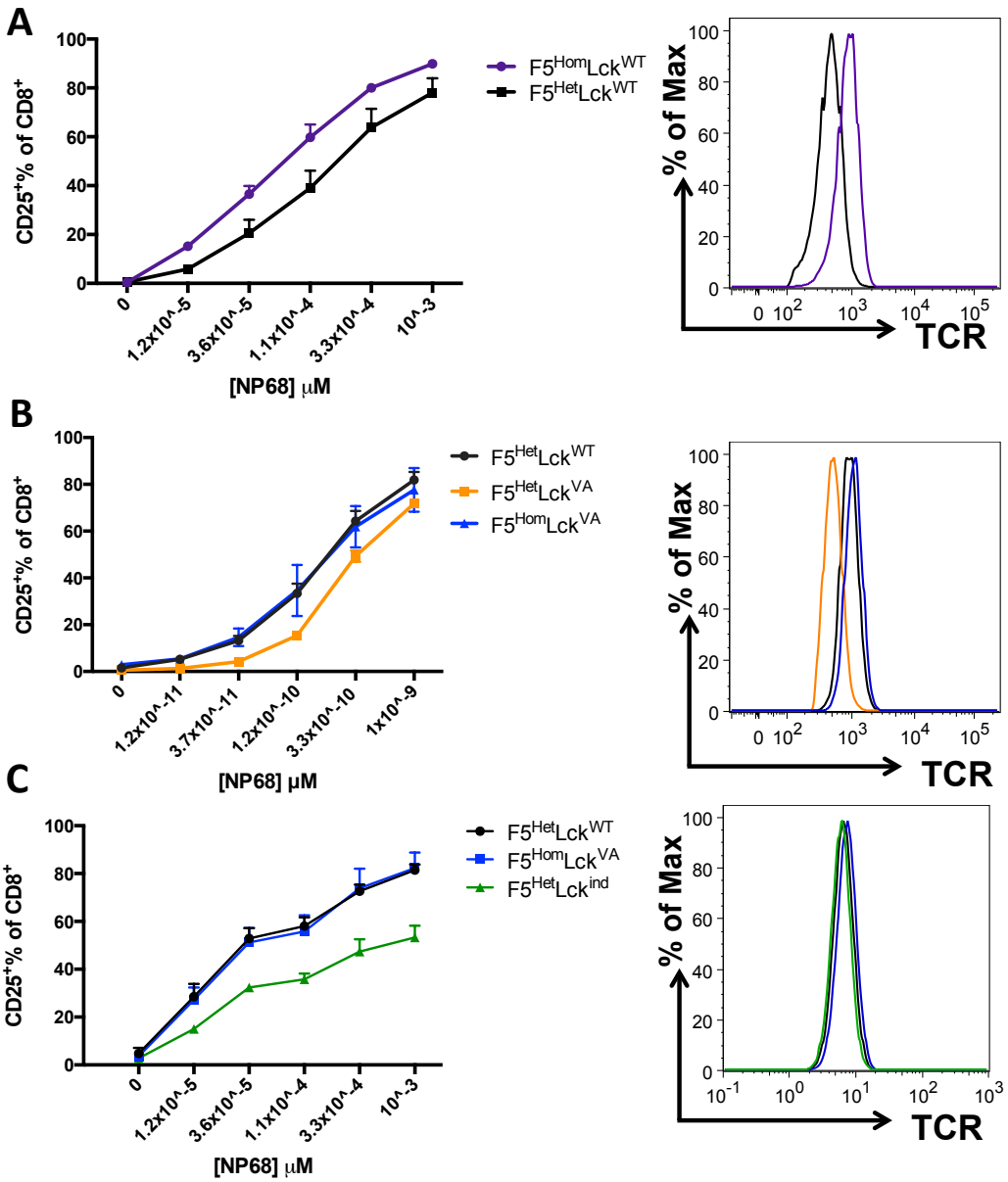

Fig. 4.2 F5Lck^{VA} T cells activated as efficiently as F5Lck^{WT} T cells.
LN cells from F5^{Hom}Lck^{WT}, F5^{Het}Lck^{WT}, F5^{Het}Lck^{ind}, F5^{Hom}Lck^{VA} and F5^{Het}Lck^{VA} were activated with a titration of NP68 overnight. CD25 expression was assessed by flow cytometry, and plotted as percentage of positive cells of total. TCR expression was assessed by histogram analysis as the MFI of expression in *ex vivo* samples. Comparisons were made between (A) F5^{Hom}Lck^{WT} and F5^{Het}Lck^{WT}, (B) F5^{Het}Lck^{WT} and F5^{Hom}Lck^{VA} and F5^{Het}Lck^{VA}, (C) F5^{Het}Lck^{WT}, F5^{Het}Lck^{ind}, and F5^{Hom}Lck^{VA}. Data are representative of: 3 experiments in part A, of 2 experiments in part B and of 2 experiments in part C. Importantly, F5^{Hom}Lck^{VA} versus F5^{Het}Lck^{WT} comparisons have been done in 5 independent experiments. Experiments had an n=2-3 for each genotype.

4.2.3 F5Lck^{VA} T cells had reduced phosphorylation of Lck targets upon TCR signaling

The data in Fig.4.2 raises the question: how can reduced amount of Lck lead to an equal signalling threshold in F5Lck^{VA} mice and not F5Lck^{ind} mice? In order to tackle this issue, we looked at signalling events downstream of Lck upon TCR stimulation, that have been shown to be affected by reduced Lck expression in F5Lck^{ind} mice (Lovatt et al., 2006).

Upon TCR engagement with p:MHC, Lck is recruited to the complex by its association with CD4 and CD8 co-receptors (in the F5 system only CD8). It then undergoes transphosphorylation of its activation loop tyrosine Y394 upon clustering (Palacios and Weiss, 2004). Via this process, Lck becomes proximally positioned to phosphorylate the intracellular ITAMs within the CD3 and TCRζ signalling chains of the TCR receptor, and starts the signalling cascade. The Syk-family kinase Zap-70 is the first to be recruited to the phosphorylated ITAMs via its tandem SH2 domain. Lck phosphorylates and activates Zap-70 on its tyrosine Y319, and for full activation Zap-70 autophosphorylates on residue Y493 (Wang et al., 2010). Zap-70 subsequently phosphorylates T-cell-specific adapter proteins LAT, and SLP-76, that recruit a huge number of different molecules, mediating various signalling pathways with different biological outcomes (Brownlie and Zamoyska, 2013; Palacios and Weiss, 2004; Walk et al., 1998; Wang et al., 2010).

We assessed the extent of phosphorylation of Lck targets in F5Lck^{VA} mice. We labelled naïve LN T cells from F5Lck^{VA} and F5Lck^{WT} mice with different concentrations of CFSE (Fig.4.3A). This enabled them to be identified when pooled in one well to reduce error during stimulation and fixing in the experiment. Cells were stimulated for 2.5, 5, 10 and 20 minutes with 1 μM NP68, and the stimulation was stopped with the addition of 2% PFA. Cells were stained intracellularly for: pZap-70^{Y493}, pSrc^{Y416} (which measures both 416 on Fyn and Lck), pShc and pLck^{505}. The results were acquired by flow cytometry and are shown in Fig.4.3.

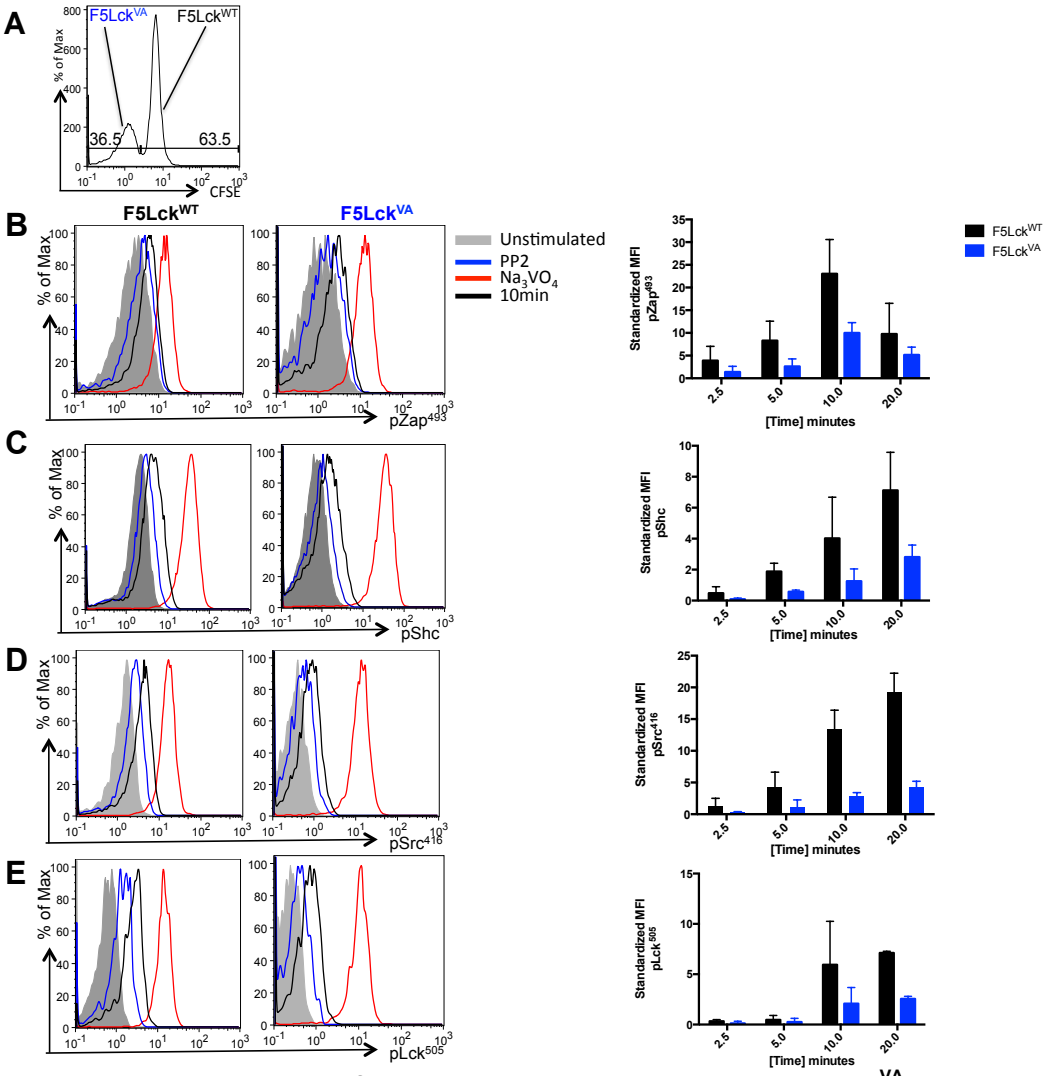

Fig. 4.3 Phosphorylation of Lck targets was decreased in F5Lck^{VA} compared to F5Lck^{WT} T cells.

LN from F5Lck^{WT} and 5 F5Lck^{VA} mice (n=4) were harvested and pooled for each genotype before making single cell suspensions. (A) F5Lck^{WT} cells were labelled with 0.01 μM CFSE. The two genotypes were subsequently pooled and plated in 96-well cell culture plates and cells were stimulated for the indicated times with 1 μM NP68. Phosphorylation of indicated proteins (B-E) was controlled for by comparing to an unstimulated (filled grey), 15min of 1 μM PP2 treatment prior to stimulation with 1 μM NP68 (blue line), or a pervanadate control treated for 10 minutes (red line). The black line on all histograms shows a sample stimulated for 10 minutes. The bar charts on the right show standardised means of MFIs ± SD. These were calculated individually for each of three technical repeats from the formula: (exp – PP2)/(total – PP2) x 100%, where exp is the MFI of the peptide-stimulated sample, PP2 is the MFI of the PP2-treateded sample and total is the MFI of the pervanadate-treated sample. These data are representative of 3 independent experiments.

Histogram analysis was used to study the phosphorylation of indicated molecules (Fig.4.3B-E). Phosphorylation upon pervanadate treatment (red line) and its inhibition when treated with PP2, the SFK inhibitor (blue line), were used as positive and negative controls, respectively. PP2 treatment did not completely inhibit phosphorylation of targets, indicated by its staining at a higher level than the unstimulated control in all cases (Fig.4.3B-E). It is possible that a higher concentration than 1 μM or longer than 15min pre-incubation would be required. Bar charts to the right of each figure show standardised MFIs for each of the different time points for indicated molecules (Fig.4.3B-E). For all targets tested, F5Lck^{VA} showed 2-fold or more reduced phosphorylation at all time points, in keeping with reduced abundance of Lck.

These results suggested that at early time points, reduced Lck expression compromised proximal phosphorylation efficiency, as has been previously shown (Lovatt et al., 2006). There was decreased phosphorylation of pLck^{Y505}, but whether this was a result of changes in the activity of negative regulators of Lck, for example, Csk or CD45, or simply a reflection of the reduced total amount of Lck in not clear. Potentially, reduced pLck^{Y505} expression could explain why F5Lck^{VA} T cells upregulated activation markers as efficiently as F5Lck^{WT} cells (Fig.4.2), as reduced Lck expression could mean reduced induction of negative regulation and consequently a more active Lck molecule.

4.2.4 ERK phosphorylation was reduced in F5Lck^{VA} T cells

Further downstream in the TCR signalling pathway is the MAPK/ERK pathway. The ERK cascade is important for cellular proliferation, differentiation, and survival. Several studies have shown that the ERK pathway can be differentially regulated, depending on the strength of the signal, and this can lead to biologically divergent outcomes (Daniels et al., 2006; Inder et al., 2008). Given that the immediate proximal signalling downstream of Lck was reduced in F5Lck^{VA} T cells (Fig.4.3), yet activation marker upregulation was equivalent to F5Lck^{WT} cells (Fig.4.2), we asked whether F5Lck^{VA} and F5Lck^{WT} mice differed in their activation of ERK.

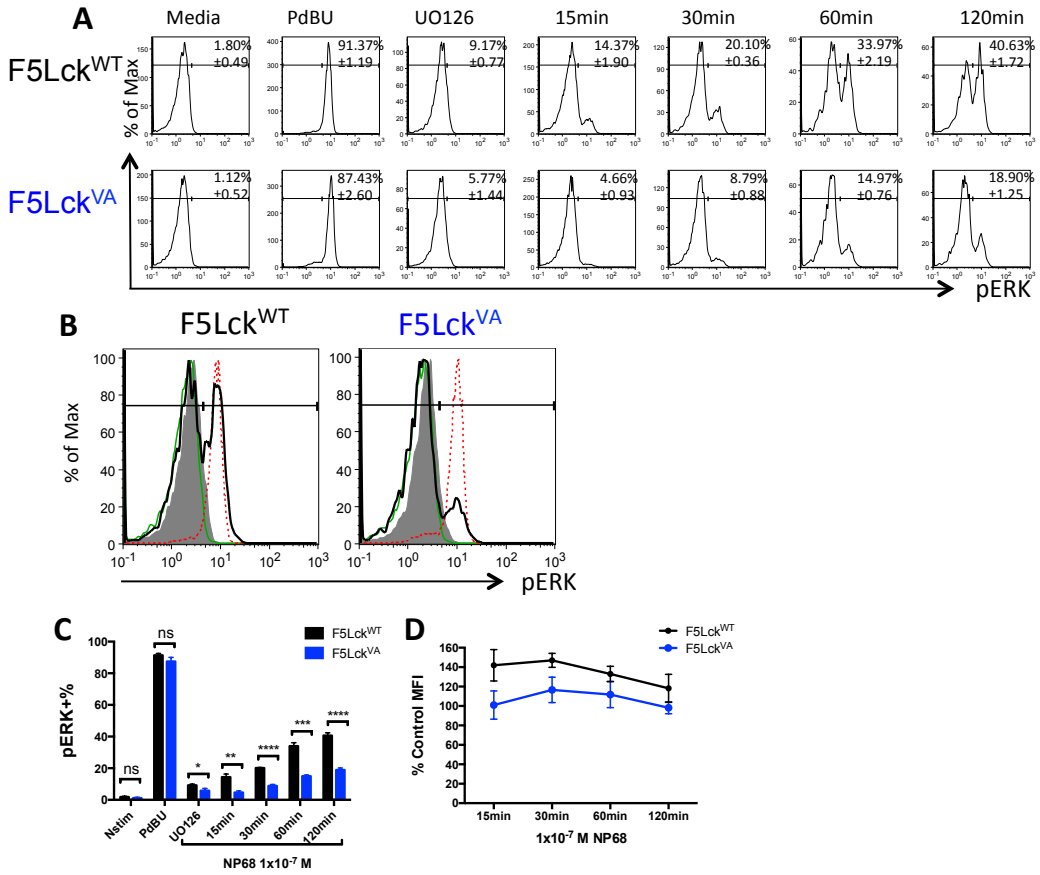

Fig. 4.4 Low levels of Lck expression reduced ERK activation in F5 T cells in response to peptide stimulation.

LN cells from F5Lck^{VA} and F5^{WT} mice were stimulated for indicated times with 1x10^{-7}M NP68. Media only, PdBU, and UO126 treated samples were analysed as controls. (A) Representative histograms show intracellular pERK staining in F5Lck^{WT} (top panel) and F5Lck^{VA} (bottom panel) CD8^{+} T cells. (B) Representative histograms show overlays of intracellular pERK staining in F5 T cells on indicated backgrounds following stimulation for 120 min with media (green) and 1x10^{-7} M NP68 (black line). The controls were treated for 15 min with UO126 and then stimulated for 15min with 1x10^{-7} M NP68 (dark fill), or treated with PdBU alone for 15 min (red dashed line). (C) Bar graph shows average proportions of CD8^{+}pERK^{+} cells ± SD, over the indicated time-course. (D) Mean MFIs ± SD for pERK^{+} cells in response to peptide stimulation were calculated from the formula (exp – UO126)/(total – UO126) x 100%, where exp is the MFI of the pERK^{+} gate from the peptide-stimulated sample, UO126 is the MFI of the UO126-inhibited sample and total is the MFI of the pERK^{+} gate from the PdBU stimulated sample. Data are representative of two independent experiments with 3 mice pooled per genotype. Significance was calculated on Prism: parametric, student's t-test, unpaired, two-tailed *P<0.05, **P<0.01, ***P<0.001.

To assess ERK phosphorylation (pERK) in F5Lck^{WT} and F5Lck^{VA} mice, cells were stimulated *in vitro* with 0.1 μM NP68 for different lengths of time, and pERK was quantified at a single-cell level by flow cytometry (Fig.4.4.). The specificity of the pERK antibody was controlled by using a specific MEK inhibitor UO126 to pre-treat control samples. In F5Lck^{WT} cells, there was some background pERK staining in the UO126 treated cells, as 9% fell into the positive gate which was set on the unstimulated control. This was slightly higher than background levels in untreated F5Lck^{WT} cells (1.8%), but was possibly due to the way the gate was set rather than genuine pERK upregulation, as the clear positive pERK peak present in stimulated samples was inhibited (Fig.4.4A and B). The results in Fig.4.4C showed that the availability of Lck had a direct and significant effect on the proportions of cells that phosphorylated ERK. ERK phosphorylation was always 2-fold higher in F5Lck^{WT} cells at all time points tested, compared to F5Lck^{VA} cells (Fig.4.4C). However, the proportions of cells responding increased with time for both genotypes. The defect in ERK phosphorylation, seen in F5Lck^{VA} cells, was shown to be TCR-signalling dependent as, in response to PdBU stimulation, similar proportions of cells phosphorylated ERK in the two genotypes (Fig.4.4A and B). The MFI of pERK was reduced by ~1.2-1.5 fold in F5Lck^{VA} cells compared to F5Lck^{WT} at all time points tested (Fig.4.4D).

These data were in agreement with results in Fig.4.3, which suggested that reduced Lck abundance in F5Lck^{VA} cells reduced phosphorylation of immediate targets. One of these was adapter molecule Shc (Fig.4.3D), and Shc feeds into the ERK pathway via Grb/SOS (Lovatt et al., 2006; Walk et al., 1998).

These data are also in agreement with published results by Lovatt et al., who showed that despite a more than 95% reduction in the phosphorylation of Zap-70, PLCγ, and LAT in the absence of Lck expression, pERK was still in the order of 10-30% of WT levels (Lovatt et al., 2006). They also showed that Fyn contributes to activation of the ERK pathway via a PLC-γ1/RasGRP1 independent pathway, and influences the magnitude of pERK expression,

whereas Lck controls the threshold of triggering (Lovatt et al., 2006). We did not assess the contribution of Fyn in this experiment.

4.2.5 $S6^{(S235/236)}$ phosphorylation was reduced in $F5Lck^{VA}$ T cells

Upon T cell activation, mRNA translation and protein synthesis are upregulated due to the increased demand in T cells for proteins, lipids, nucleic acids, and ATP for sustaining growth, proliferation, and the acquisition of effector function (Wang and Green, 2012). The mTOR signalling pathway integrates and relays environmental signals to the nucleus, in an effort to regulate growth, metabolism, and survival (Mills and Jameson, 2009). One of the main substrates of the rapamycin-sensitive complex with raptor (mTORC1) is the ribosomal protein S6 kinase (S6K) (Chung et al., 1992). One of the substrates of S6K is the ribosomal protein S6 (rpS6) that is involved in ribosomal biogenesis. It has been shown that TCR stimulation of S6-heterozygous T cells led to normal cell growth, but cell cycle progression was impaired, exemplifying the importance of ribosomal biogenesis in T cells (Sulic et al., 2005). Additionally, it has previously been shown in $F5Lck^{ind}$ mice that phosphorylation of rpS6 is downstream of TCR signalling, and hence, Lck dependent (Salmond et al., 2009a). We measured phosphorylation of rpS6 at residues S235/236 ($pS6^{S235/236}$) in $F5Lck^{VA}$ cells at different times after *in vitro* NP68 stimulation.

The results in Fig.4.5A-C showed that at each time point indicated, proportionally fewer $F5Lck^{VA}$ cells had phosphorylated $pS6^{S235/236}$ compared to $F5Lck^{WT}$ cells. By two hours of peptide stimulation, 47.5% of $F5Lck^{WT}$ CD8 T cells are positive for $pS6^{S235/236}$, but only 29.3% of $F5Lck^{VA}$ had phosphorylated $S6^{S235/236}$. The amount of $pS6^{S235/236}$ expressed per cell at all time points is similar in $F5Lck^{VA}$ cells as compared to $F5Lck^{WT}$ (Fig.4.5D). These data fell in line with a previous study that suggested reduced Lck expression leads to reduced S6 phosphorylation (Salmond et al., 2009a).

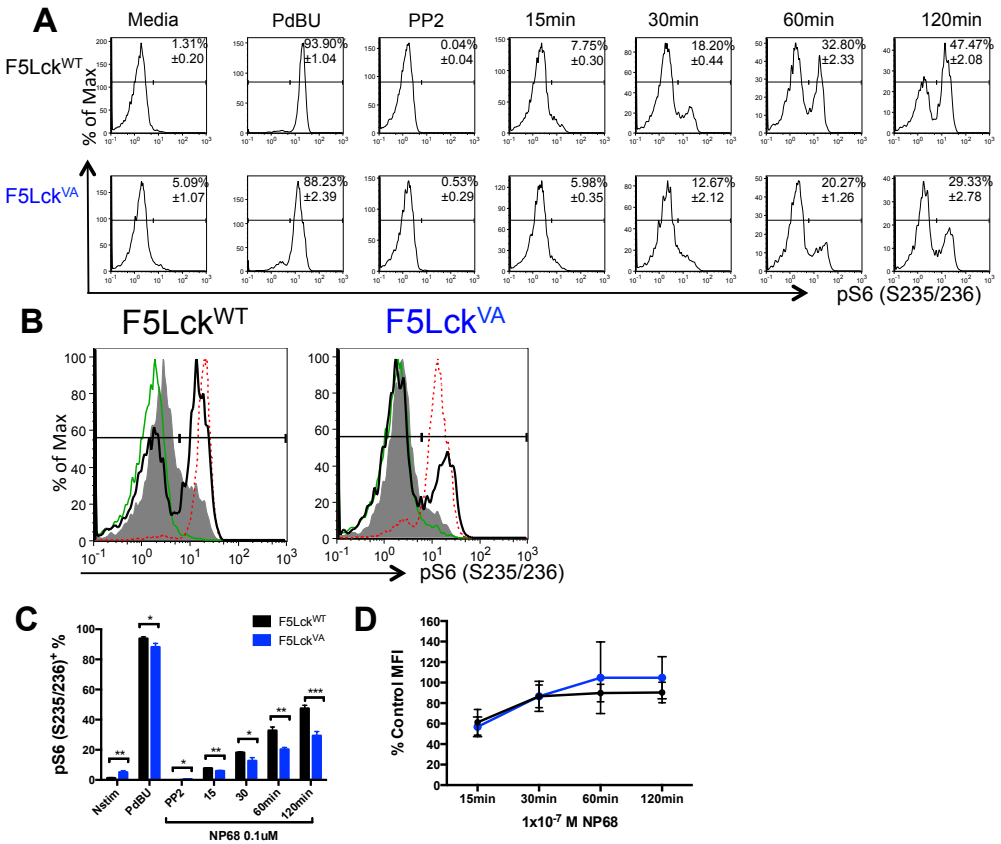

Fig. 4.5 F5Lck^{VA} T cells had reduced S6$^{(S235/236)}$ phosphorylation in response to peptide stimulation compared to F5Lck^{WT} T cells.

LN cells from age matched F5Lck^{VA} and F5Lck^{WT} mice were stimulated for the indicated times with 1x10^{-7} M NP68. Samples treated with media only, 15min PdBU, and UO126 inhibitor were analysed as controls. (A) Representative histograms show intracellular pS6$^{S235/236}$ staining in CD8^{+} F5Lck^{WT} (top panel) and F5Lck^{VA} (bottom panel) cells. Numbers on the graphs are average proportions pS6$^{S235/236}$ cells ± SD. (B) Representative histograms show overlays of intracellular pS6$^{S235/236}$ staining in F5 T cells on indicated backgrounds following stimulation for 120 min with media (green line) and peptide (black line). The controls were treated for 15 min with UO126 and then stimulated for 15min with peptide (dark fill), or treated with PdBU for 15 min (red dashed line). (C) Bar graph shows average proportions of CD8^{+} pS6^{+} T cells for triplicate samples ± SD, in F5Lck^{WT} and F5Lck^{VA} cells. (D) Mean MFIs ± SD for pS6^{+} cells were calculated from the formula (exp – UO126)/(total – UO126) x 100%, where exp is the MFI of the pS6^{+} gate from the peptide-stimulated sample, UO126 is the MFI of the UO126 inhibited sample and total is the MFI of the pS6^{+} gate from the PdBU stimulated sample. Data are representative of two independent experiments with 3 mice pooled per genotype and treated in technical triplicates. Significance was calculated on Prism: parametric, student's t-test, unpaired, two-tailed *P<0.05, **P<0.01, ***P<0.001.

4.2.6 F5Lck^{VA} T cells phosphorylated Lck^{Ser-59} as efficiently as F5Lck^{WT} T cells

It has been shown that ERK can phosphorylate Lck at serine residue 59 (pLck^{Ser-59}) in the N terminus (Watts et al., 1993; Winkler et al., 1993). Initially, Ser-59 phosphorylation was thought to have a negative effect on T cell activation (Watts et al., 1993). However, later research has found that Ser-59 phosphorylation on Lck modified Lck SH2 domain affinity (Joung et al., 1995) for tyrosine phosphorylated SHP1, and thus reduced the interaction of SHP1 with Lck (Stefanova et al., 2003). SHP1 has been identified as a negative regulator of TCR signalling (Pani et al., 1996). Stefanova et al. went on to show that ERK mediated phosphorylation of Lck at Ser-59 interfered with SHP1 binding, thereby allowing for continuation of the activation cascade (Stefanova et al., 2003).

We therefore wished to know whether the reduced ERK activation in F5Lck^{VA} T cells was sufficient to initiate Ser-59 phosphorylation of Lck. Potentially, this would allow F5Lck^{VA} cells to overcome negative regulation by SHP1 and continue signalling. To this end, F5Lck^{WT} and F5Lck^{VA} T cells were stimulated for different times with 1 μM NP68, and the cell lysates were blotted with anti-Lck or anti-V5 tag, respectively. Ser-59 phosphorylation causes retardation of the protein mobility in SDS/PAGE (Winkler et al., 1993), and the specific band can be visualised above the unphosphorylated Lck band.

The data in figure 4.6 showed that over time, the pLck^{Ser-59} band appeared above the total Lck (56 kDa) band in both F5Lck^{WT} and F5Lck^{VA} T cells. The percentage of pLck^{Ser-59} of total Lck was calculated, and both F5Lck^{VA} T cells (44.8%) and F5Lck^{WT} T cells (47.3%) were found to contain equivalent amounts of pLck^{Ser-59} at 60 and 120 minutes, which appeared with indistinguishable kinetics. These results suggested that despite reduced ERK phosphorylation, the threshold for ERK to carry out its effector function and phosphorylate Ser-59 on Lck has been overcome in F5Lck^{VA} T cells by these later time points.

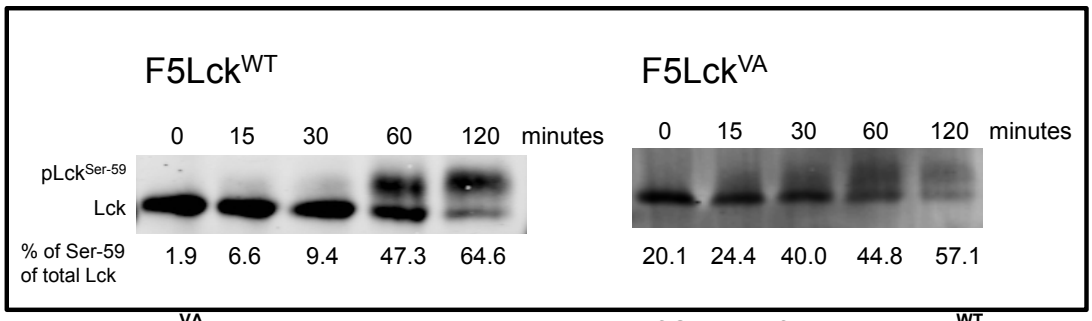

Fig. 4.6 F5Lck^{VA} cells have equal phosphorylation of Ser-59 of Lck to F5Lck^{WT}
LN cells from F5Lck^{WT} and F5Lck^{VA} mice were stimulated with 1 μM NP68 for the indicated times. Lysates were resolved by SDS/PAGE on a big gel overnight (Methods 2.11.4). F5Lck^{WT} and F5Lck^{VA} were probed with anti-Lck and anti-V5 tag, respectively, followed by detection with goat anti-mouse AF680. Blots were analysed using the Li-Cor Odyssey machine. The percentage of Ser-59 phosphorylation of Lck was calculated using the following equation: (pLck^{Ser-59} x 100) / (p56 Lck + pLck^{Ser-59}). Data are representative of three independent experiments. The full blot can be found in Appendix 7.3.

ERK phosphorylation is downstream of PLC-γ, which hydrolyzes PIP_2 to produce IP_3 and DAG. DAG recruits RasGRP1, which leads to the activation of the MAPK cascade. It has recently been shown that bifurcation of signalling into different branches can already occur at the level of ITAM phosphorylation (Guy et al., 2013). Guy et al. modified the number of intact ITAM subunits, and identified that low multiplicity of ITAMs was sufficient for cytokine production, whereas high ITAM multiplicity was required for TCR-driven proliferation (Guy et al., 2013). Seeing that phosphorylation of ERK was reduced (Fig.4.4), but overnight activation of T cells was equal to $F5Lck^{WT}$ cells in $F5Lck^{VA}$ T cells (Fig.4.2), we wondered whether another branch of the TCR signalling cascade was behaving differently. For this reason, Ca^{2+} mobilization was assessed, although it is also downstream of PLC-γ1 it signals via IP_3 as opposed to DAG(Winslow et al., 2003).

4.2.7 Ca^{2+} flux was more efficient in $F5Lck^{VA}$ than $F5Lck^{WT}$ T cells

The regulation of Ca^{2+} in response to TCR engagement and activation of adapter proteins is a critical part of T cell activation. The influx of Ca^{2+} is a mediator for several Ca^{2+} - dependent pathways that lead to differentiation, effector function and gene transcription (Nagaleekar et al., 2008; Oh-hora and Rao, 2008). Ca^{2+} flux has been shown to be defective in cells lacking Lck (Straus and Weiss, 1992; Trobridge and Levin, 2001), as well as in $CD4^+$ T cells in Lck^{ind} mice (Lovatt et al., 2006). Therefore, we wanted to assess Ca^{2+} flux in peripheral T cells in $F5Lck^{VA}$ mice, which have <5% of WT levels of Lck.

$F5Lck^{WT}$ and $F5Lck^{VA}$ LN cells were labelled with different concentrations of CFSE (Fig.4.7A). Cells were subsequently pooled, loaded with Indo-1, and stimulated by crosslinking biotin labelled TCR and CD8 with streptavidin. Indo-1 allows for calcium flux measurement, as it is a ratiometric dye. It changes spectral properties whether it is bound to calcium (emits at 390nm Violet) or unbound (emits at 500nm Blue), and the ratio is used as a measure of calcium flux. Upon crosslinking TCR and CD8, it was seen that $F5Lck^{VA}$ (blue line) responded faster to stimulation by fluxing Ca^{2+} slightly before

F5Lck^{WT} (black line). F5Lck^{VA} T cells also had increased Ca^{2+} compared to F5Lck^{WT} as indicated by the higher ratio of Indo-1 (Blue)/ Indo-1 (Violet), suggesting that there was more unbound Ca^{2+} in F5Lck^{VA} mice (Fig.4.7B). Additional control experiments with crosslinking of TCR or CD3 alone showed similarly faster Ca^{2+} flux in F5Lck^{VA} T cells compared to F5Lck^{WT} T cells, although the results were not as obvious as with crosslinking CD8 and TCR, which would be predicted from Lck being co-receptor associated (Fig.4.7C). Crosslinking with anti-CD8 alone or stimulating with NP68 did not induce Ca^{2+} flux (Fig.4.7C).

The above result of F5Lck^{VA} triggering Ca^{2+} flux more efficiently than F5Lck^{WT} was surprising, because the F5Lck^{VA} cells were found to be less efficient in activation of upstream mediators of the TCR signaling cascade, e.g. phosphorylation of Zap-70^{Y394} and downstream molecules like ERK (Fig.4.4). The MAPK pathway and Ca^{2+} signalling pathways converge at the level of PIP_2, downstream of TCR-signalling, from where IP_3 mediates Ca^{2+} signalling, and DAG via RasGRP1 and Ras mediates the MAPK pathway (Brownlie and Zamoyska, 2013). It is hard to envision how pathways that converge so close to the TCR-trigger can be split in their regulation, but one conceivable explanation is that it occurs at the level of negative feedback loops. The activation of Ca^{2+} signaling is an early event – within 4 minutes of TCR stimulation, whereas ERK phosphorylation occurs later at around 15 min according to our data (Fig.4.4). Perhaps, reduced Lck expression is not sufficient to trigger early negative regulators like Dok1 and 2, adaptor proteins that have been suggested to antagonise Zap-70 binding to ITAMs (Dong et al., 2006; Yasuda et al., 2007), however, at later time points this may not be an issue, as F5Lck^{VA} activating equally efficiently to F5Lck^{WT} at 24h would suggest (Fig.4.2). It should be noted, however, that ERK phosphorylation was assessed in response to peptide stimulation, whereas Ca^{2+} flux was assessed by CD8 and TCR crosslinking and these two stimuli are not exactly equivalent.

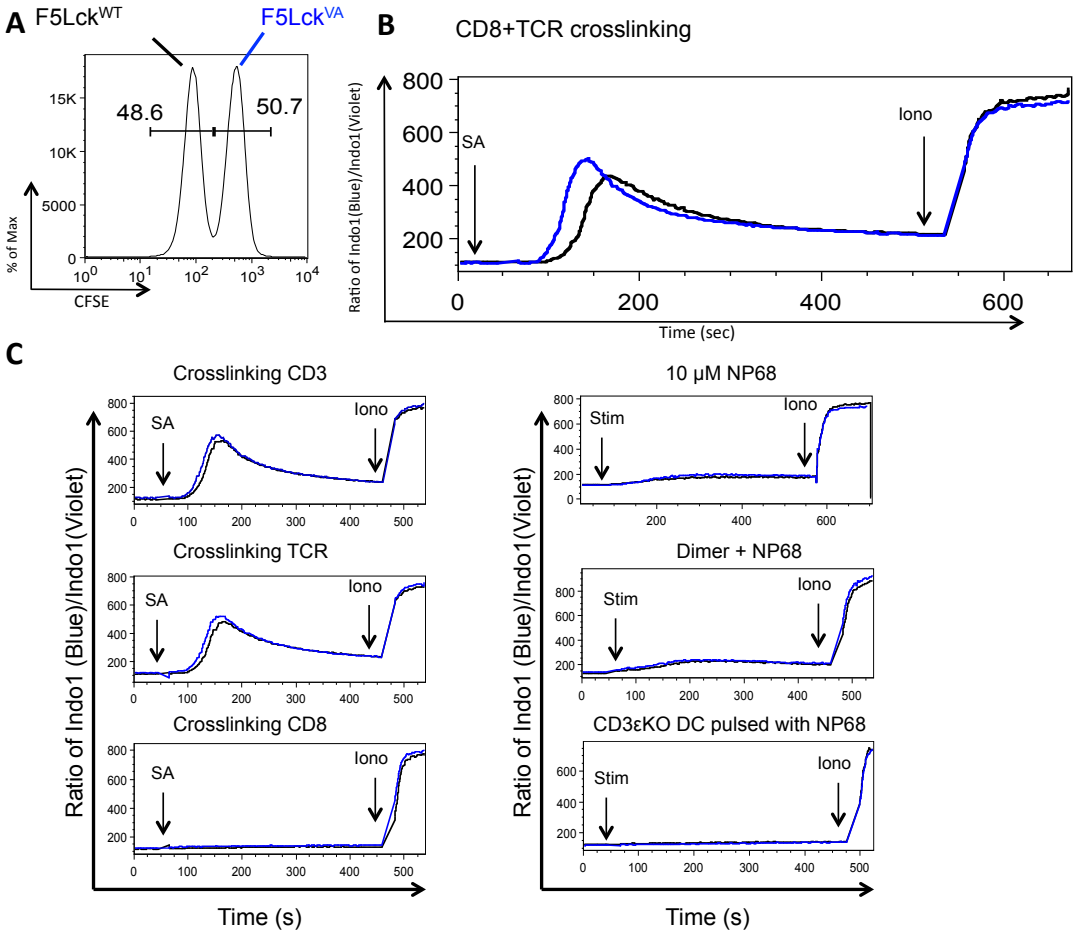

Fig. 4.7 Ca^{2+} was induced faster in F5Lck^{VA} T cells compared to F5Lck^{WT} T cells.
Naïve LN T cells from F5Lck^{WT} and F5Lck^{VA} mice were loaded with 2 µM Indo-1 and examined for Ca^{2+} flux by flow cytometry (A) F5Lck^{WT} and F5Lck^{VA} were labelled with different concentrations of CFSE: 0.1 µM and 0.01 µM respectively, and pooled into one FACS tube in a 1:1 ratio. (B) Arrows indicate induction of Ca^{2+} flux by addition of streptavidin after 45 seconds to crosslink anti-TCR and CD8, and Ionomycin after 8 minutes as a positive control. (C) Additional indicated conditions for inducing Ca^{2+} flux were used as controls. Data are representative of 1-3 independent experiments. The CFSE staining concentrations for the cell types were alternated between each experiment.

4.2.8 IL-2 production was enhanced in F5Lck^{VA} T cells

Ca^{2+} signalling has been shown to be important for IL-2 and IFNγ production in T cells (Nagaleekar et al., 2008), as well as cell metabolism and proliferation (Fracchia et al., 2013). Therefore, the next set of experiments was designed to establish what impact such branching of signalling may have had on downstream pathways such as cytokine production, proliferation and effector function, and how they compared between F5Lck^{WT} and F5Lck^{VA} T cells.

IL-2 is a well-known and important cytokine. On the one hand it induces T-cell expansion, effector differentiation, and memory cell survival. On the other hand, it controls the contraction of inflammatory responses by promoting growth and survival of T_{Regs} and stimulating AICD (Martins et al., 2008).

CD25 expression in response to TCR derived signals was equivalent between F5Lck^{VA} and F5Lck^{WT} T cells (Fig.4.2). IL-2 binds the high affinity receptor CD25, creating a positive feedback loop via STAT5 leading to further CD25 expression (Kim 2001, Smith and Cantrell 1985). We assessed the capacity of F5Lck^{VA} T cells to produce IL-2. To this end, F5Lck^{WT} and F5Lck^{VA} T cells were simulated with a titration of NP68 for 24h and 48h, after which IL-2 production was measured by ELISA.

The results in Fig.4.8A showed that IL-2 production at 24h in F5Lck^{WT} cells reached a plateau after stimulation with $1.1x10^{-4}$μM NP68, whereas in F5Lck^{VA} there was a dose dependent increase until they produced significantly ($p=0.0011$) more than F5Lck^{WT} at the highest concentration of stimulation. Overall, at 48h the IL-2 production in both F5Lck^{WT} and F5Lck^{VA} cells was lower than at 24h, as can be seen from the smaller y-axis scale. Yet, at all concentrations of NP68 stimulation at 48h, F5Lck^{VA} cells produced significantly higher levels of IL-2 than F5Lck^{WT} cells, except at the lowest concentration. Care should be taken in the interpretation of these data as only one experiment has been done, and at 48h the data may reflect

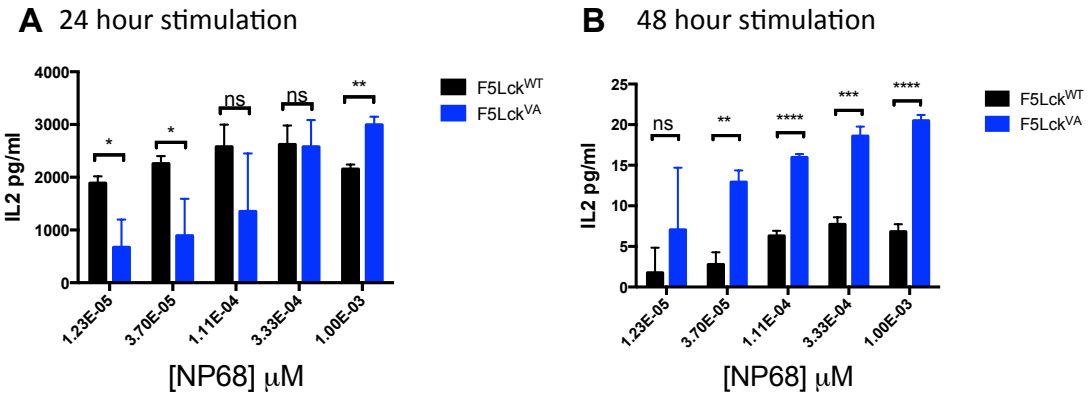

Fig. 4.8 F5Lck^{VA} T cells activated with NP68 produced more IL-2 than F5Lck^{WT} T cells. LN cells from F5Lck^{WT} and F5Lck^{VA} mice (n=5-7) were activated in triplicate with indicated concentrations of NP68 for (A) 24h and (B) 48h. IL-2 production was assessed by ELISA and plotted as average pg mL^{-1} ± SD. Data are representative of one experiment. Significance was calculated on Prism: parametric, student's t-test, unpaired, two-tailed *P<0.05, **P<0.01, ***P<0.001.

differences in consumption as well as be hampered by the sensitivity of an ELISA at such low pg ml^{-1} levels.

Intriguingly, however, Joanna Klezckowska (unpublished data) showed that the IL-2 mRNA expression in F5Lck^{ind} T cells peaked later than in F5Lck^{WT} T cells and remained up for a more prolonged period of time. However, on a protein level, Lovatt et al. showed that in polyclonal Lck^{ind} $CD4^+$ T cells IL-2 production was less than in Lck^{WT} cells after 24h in culture with anti-CD3 and anti-CD28 stimulation (Lovatt et al., 2006). These differences may also reflect differences between $CD4^+$ and $CD8^+$ T cells.

The role of IL-2 in T cell function is multifaceted (Malek, 2008), including roles in sustaining cell division by increasing cell cycling or cell survival - functions that led to its initial identification (Gillis and Smith, 1977; Morgan et al., 1976; Taniguchi et al., 1983). Therefore, in light of the results in Fig.4.8 suggesting that F5Lck^{VA} T cells produce more IL-2, the next section looks at their proliferation and survival potential.

4.2.9 F5Lck^{VA} T cells had enhanced proliferation

Upon antigen recognition, T cells become activated and follow a very typical response pattern of expansion, differentiation, contraction, and memory formation. In order to address if the increased IL-2 production in F5Lck^{VA} T cells correlated with proliferative capacity, both F5Lck^{VA} and F5Lck^{WT} T cells were labelled with Cell Tracer Violet, and stimulated with different concentrations of NP68 for different times. Proliferation was measured as dilution of Cell Tracer and assessed by FACS.

The results in Fig.4.9A showed that both F5Lck^{WT} and F5Lck^{VA} T cells had divided at 24h as seen from the dilution of Cell Trace. Qualitative analysis revealed that already on day 2 at a concentration of $1.2x10^{-10}$M peptide, F5Lck^{VA} (purple line) had diluted Cell Tracer more. This trend was also evident at lower concentrations of peptide on days 3 and 4. Quantitative analysis was done using the proliferation index parameter calculated by FlowJo software as shown in Fig.4.9B. The proliferation index is a measure of

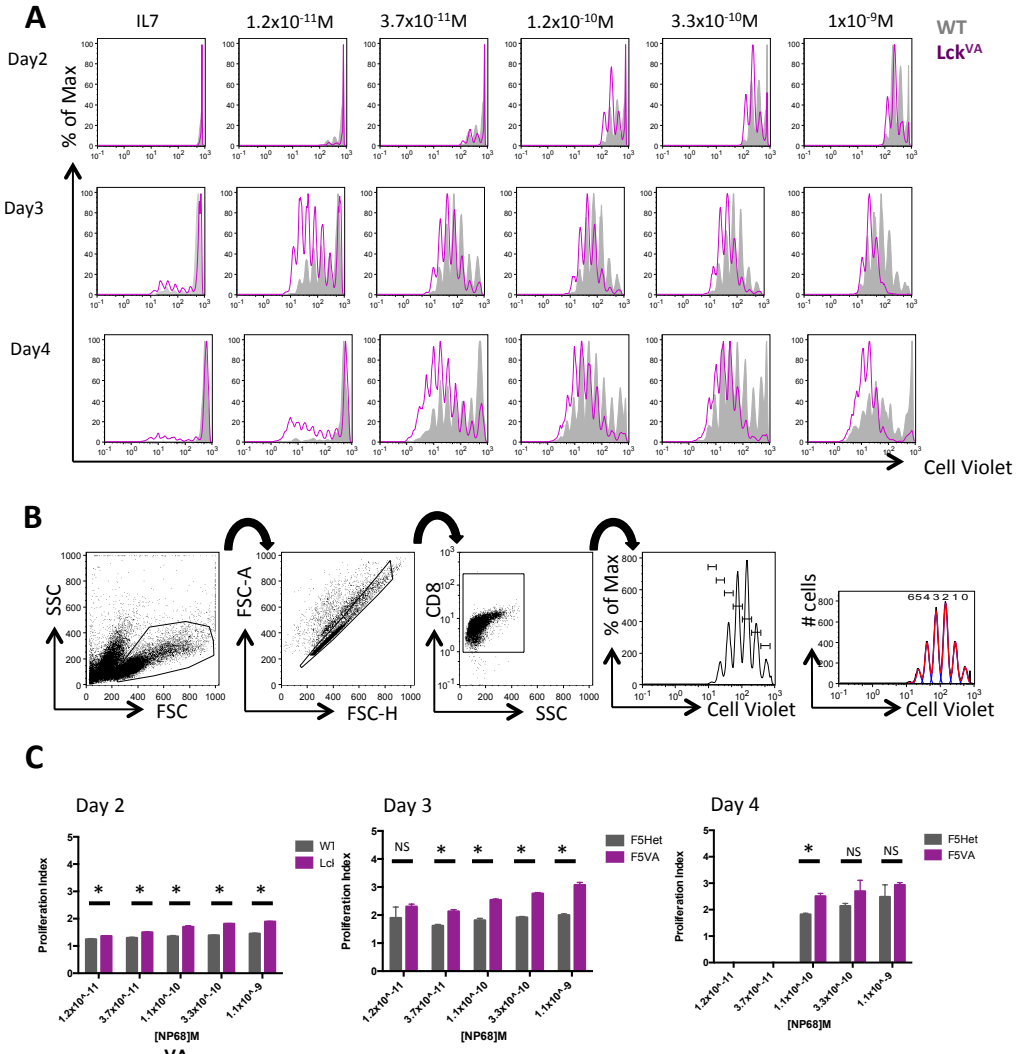

Fig. 4.9 F5Lck^{VA} T cells proliferated more upon stimulation with NP68.
LN cells were pooled from 10 F5Lck^{WT} and 12 F5Lck^{VA} mice and stained with Cell Violet and stimulated for 4 consecutive days in triplicate in 96-well plates with indicated concentrations of NP68. (A) Representative overlays of FACS histograms show Cell Violet staining on days 2, 3 and 4 in CD8$^+$ F5Lck^{WT} (grey) and F5Lck^{VA} (pink). T cells were cultured in either media alone or with IL-7 as controls. On day 4 a Cell Violet high peak has reappeared on most histograms, which is probably autofluoresence of dead cells as it is unlikely that unproliferated cells would reappear. (B) Shown is the gating strategy for calculating proliferation index on FlowJo. First cells were gated as live based on SSC and FSC then the doublets are excluded using FSC-A and FSC-H, finally only CD8$^+$ cells were gated for Cell Violet histograms. FlowJo was used to calculate the proliferation index. (C) Bar charts show the average proliferation index calculated for days 2, 3 and 4 in F5Lck^{WT} (grey) and F5Lck^{VA} (pink) T cells at indicated concentrations of NP68 stimulation. Data are representative of 3 independent experiments. Statistical significance was calculated on Prism: multiple t-tests with Holm-Sidak method * $p \leq 0.05$.

the total number of cell divisions divided by the number of cells that went into division. This measure only takes into account the cells that underwent at least one division. The results of the evaluation shown in Fig.4.9C confirmed what was seen qualitatively in Fig.4.9A, that F5Lck^{VA} proliferated significantly more rounds of division than F5Lck^{WT} on all days and at almost all concentrations of peptide stimulation.

From the above result, that F5Lck^{VA} proliferated more (Fig.4.9), it was not possible to discern whether this was the result of increased IL-2 production – especially since CD8 T cells have been shown to proliferate also in the absence of IL-2 (Kramer et al., 1994). Our results suggested that F5Lck^{VA} T cells had more efficient Ca^{2+} flux (Fig.4.7) and increased Il-2 production (Fig.4.8), that in combination with the increased proliferative capacity (Fig.4.9) suggest a potential correlation between these pathways. In addition to its effects on proliferation, IL-2 has been shown to potentiate T cell survival by up-regulating the anti-apoptotic molecule Bcl-2 (Lord et al., 1998). The next experiment was therefore designed to compare Bcl-2 expression between F5Lck^{WT} and F5Lck^{VA} T cells.

4.2.10 F5Lck^{VA} T cells had increased Bcl-2 expression

The 12 core Bcl2 family proteins are characterised by homologous domains that allow for interactions between the family members, and can either promote or inhibit cell apoptosis (Youle and Strasser, 2008). Bcl-2 and Bcl-XL are pro-survival molecules and possess four domains, BH1, 2 and 4, which are defined by a hydrophobic groove within the molecule to allow the binding of the fourth BH3 domain. Others, such as Bax and Bak, are pro-apoptotic members and possess the domains BH1-3, which can create large pores in membranes in the cell, e.g. the mitochondrial membrane to release cytochrome *c* (Wyllie, 2010). The pro-survival family members, such as Bcl-2 and Bcl-XL, inhibit Bax and Bak, thereby preventing their pro-apoptotic actions (Youle and Strasser, 2008).

Data by Joanna Klezckowska showed that F5Lck^{ind} cells express higher levels of Bcl-2 than WT cells after a 48 hour peptide NP68 stimulation (unpublished

data). In addition, although Caserta et al. did not find differences in Bcl-2 expression in Lck^{ind} cells, they did find the expression of other exhaustion markers, such as KLRG1 and PD1 to be reduced in the T_{CM} pool, suggesting that decreased Lck levels are beneficial for T_{CM} population survival and expansion (Caserta et al., 2010).

In order to assess whether Bcl-2 expression was upregulated in $F5Lck^{VA}$ T cells, as may be predicted from increased IL-2 production (Fig.4.8) and increased proliferation (Fig.4.9), the MFI of Bcl-2 expression was measured *ex vivo* (Fig.4.10A) and upon activation (Fig.4.10B and C).

The results indicated that *ex vivo* expression of Bcl-2 was significantly higher in $F5Lck^{VA}$ T cells (MFI = 5.2±0.17) as compared to $F5Lck^{WT}$ cells (MFI = 3.9±0.02) (Fig.4.10A). In addition, Bcl-2 expression was also higher in $F5Lck^{VA}$ cells throughout a 48-hour peptide stimulation, as was seen from the histogram overlays in Fig.4.10B at different concentrations of NP68. In both $F5Lck^{WT}$ and $F5Lck^{VA}$ T cells, the expression of Bcl-2 was maintained throughout cell division when plotted against Cell Trace in Fig.4.10C. However, at each dividing peak Bcl-2 expression was higher in $F5Lck^{VA}$ cells (blue) than in $F5Lck^{WT}$ (black) T cells. These results suggested that there was a correlation between the increased IL-2 production, increased proliferation, and increased Bcl-2 expression seen in $F5Lck^{VA}$ T cells.

4.2.11 Effector T cells in $F5Lck^{VA}$ produced more IFNγ and TNFα than $F5Lck^{WT}$ T cells

As a naïve $CD8^+$ T cell differentiates into an effector $CD8^+$ T cell, it acquires a different gene expression pattern that allows it to carry out cytotoxic functions and to produce antiviral cytokines (Joshi and Kaech, 2008) – a process that is potentially linked to the proliferative programme (Oehen and Brduscha-Riem, 1998). Our results showed that reduced Lck expression increased the proliferative capacity of $CD8^+$ T cells in $F5Lck^{VA}$ mice, potentially by increased IL-2 production and Bcl-2 production. We wished to assess whether and how reduced Lck expression affected the generation of CTL function *in vitro*.

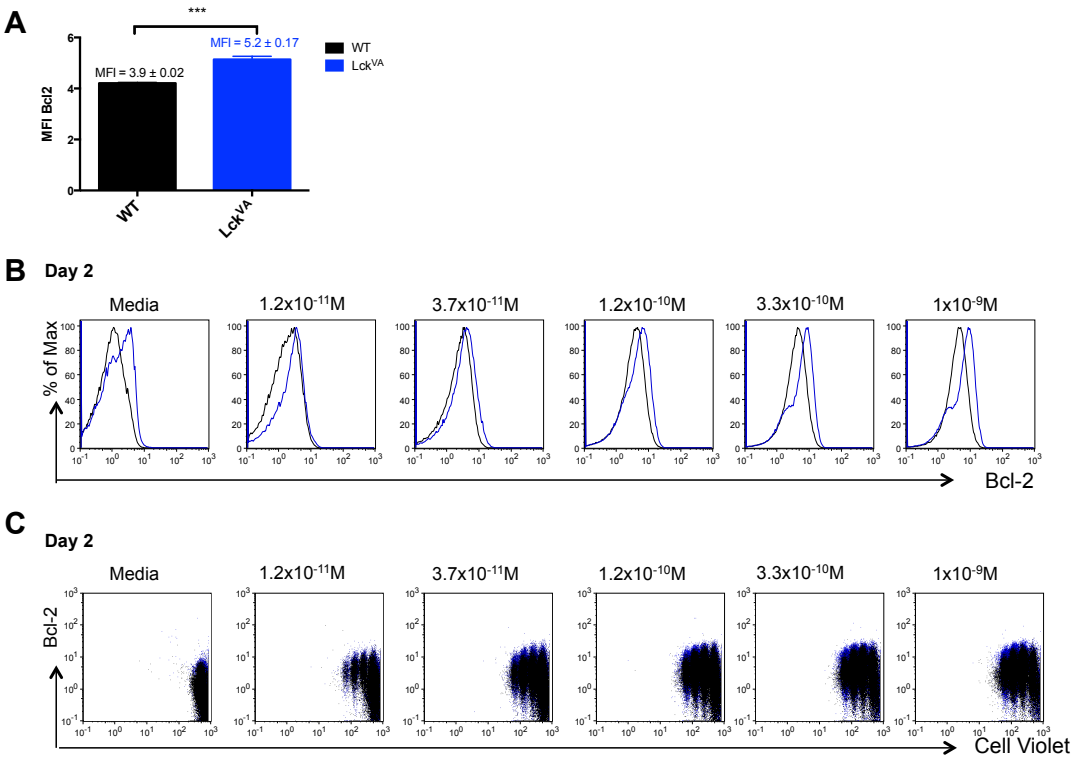

Fig. 4.10 Bcl-2 expression was enhanced in F5Lck^{VA} CD8^{+} T Cells
LN cells were pooled from 10 F5Lck^{WT} and 12 F5Lck^{VA} mice, and stimulated for 4 consecutive days in a 96-well plate in triplicate with a titration of NP68. Bcl-2 expression was measured by intracellular staining. (A) Bar graph shows average MFI in CD8^{+} T cells of technical triplicates ± SD of Bcl-2 expression measured *ex vivo*. Significance was tested with an unpaired, two-tailed, students t-test, ***p=0.0002. (B) FACS histograms show Bcl-2 expression on Day 2 in F5Lck^{WT} (black) and F5Lck^{VA} (blue) cells at different concentrations of NP68 stimulation. Bcl-2 expression was measured by intracellular staining after triplicate wells were pooled. (C) Dot plots show Bcl-2 expression (Y-axis) versus Cell Violet staining (X-axis) on Day 2 in CD8^{+} F5Lck^{WT} (black) and F5Lck^{VA} (blue) cells. Similar results were observed on Day 3 and day 4. Data shown are representative 2 independent experiments.

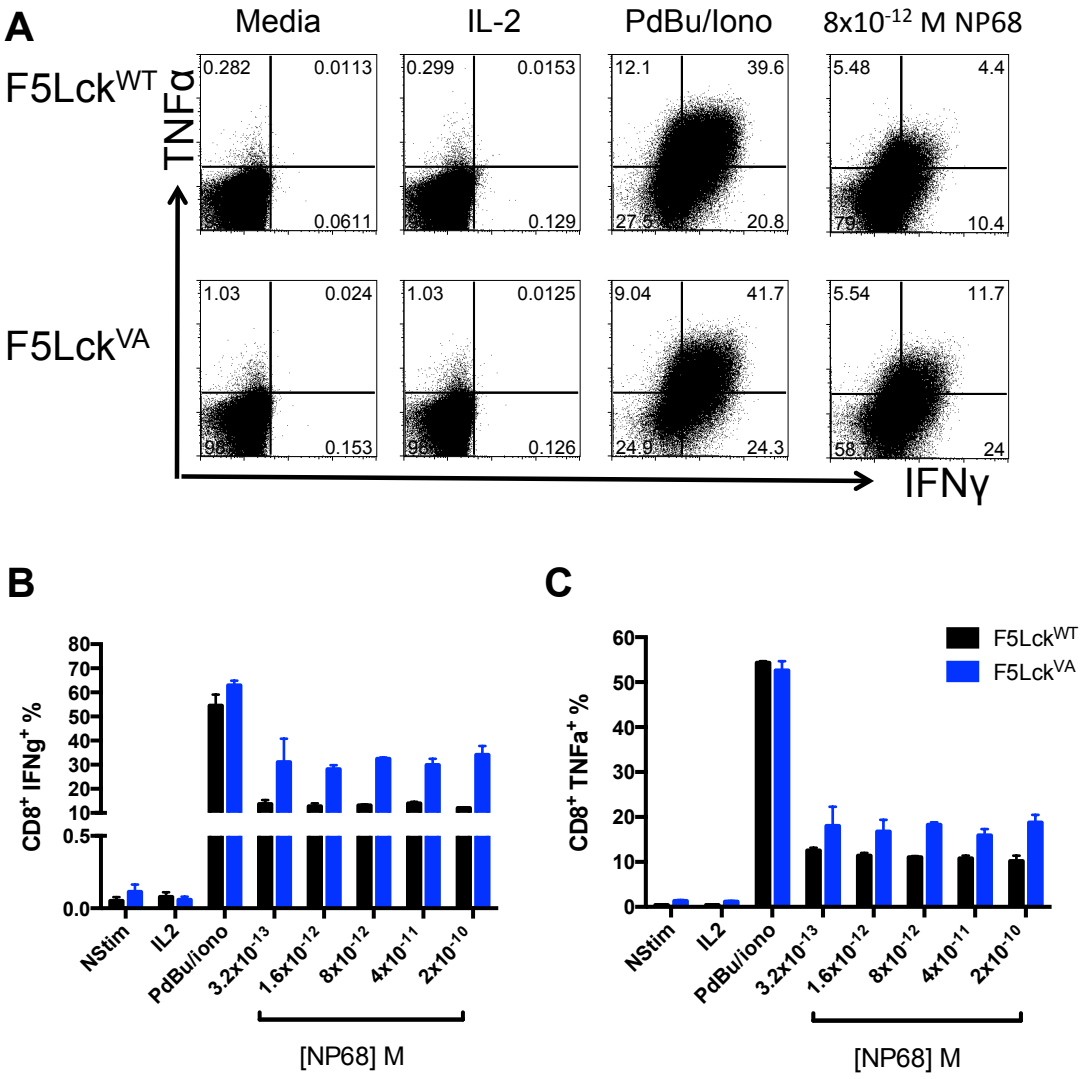

Fig. 4.11 F5Lck^{VA} T cells produced more IFNγ and TNFα than F5Lck^{WT} T cells after activation.
30x10^6 LN cells from F5Lck^{WT} and F5Lck^{VA} mice were cultured in cell culture medium with 100 nM NP68 for 72 hours. Cells were restimulated in triplicate for 6 hours with different concentrations of NP68 in a 96-well plate with Brefeldin-A. (A) Representative dot plots show TNFα and IFNγ production as measured by intracellular staining. Controls used were media only, PdBU/Ionomycin treatment, and IL-2 treatment. (B) The bar charts show the mean ± SD proportions of CD8$^+$ T cells producing IFNγ or (C) TNFα. Data are representative of 2 independent experiments.

Since the activation of effector function is downstream of TCR engagement, we assessed the production of IFNγ and TNF*α*, two effector cytokines, in response to NP68 stimulation in F5Lck^{WT} and F5Lck^{VA} T cells. We cultured cells with 100 nM NP68 for 3 days and then restimulated them with different concentrations of NP68 for 6h in the presence of Brefeldin-A. Figure 4.11A showed that both F5Lck^{WT} and F5Lck^{VA} T cells had the potential to produce IFNγ and TNF*α* upon restimulation in a peptide specific manner, as the level of detected cytokine was above that of media only samples (negative control). In response to PdBU/Iono stimulation, approximately 60% of T cells in both F5Lck^{WT} and F5Lck^{VA} mice produced IFNγ and approximately 55% produced TNF*α*. The titrations of NP68 did not cover enough of a range to produce a dose response curve, but despite this it was noted that F5Lck^{VA} consistently produced more IFNγ and TNF*α* at each concentration of NP68 stimulation than F5Lck^{WT} cells.

4.2.12 F5Lck^{VA} T cells produced less cytokine upon restimulation after culture in IL-2

The CD8$^+$ T cell response has two goals, firstly, to quickly generate enough CTLs to clear the infection and, secondly, to retain a subset of memory cells that would act faster, should the same pathogen be encountered again. Antigen-experienced T cells are activated by 10 to 50-fold lower peptide concentration than naïve T cells (Pihlgren et al., 1996). One theory is that antigen-experienced CD8$^+$T cells have an altered and more efficient signal transduction cascade, potentially due to the differential spatial reorganization of negative regulators of TCR signal mediators (Borger et al., 2013).

In an attempt to mimic an antigen re-encounter *in vitro*, antigen-experienced cells from F5Lck^{WT} and F5Lck^{VA} T cells were produced as shown in Fig.4.12A. Cells were cultured with 100 nM of NP68 for 2 days and then grown in 20 ng mL^{-1} of IL-2 for a further 2 days. On the 4th day, cells were recalled with different concentrations of NP68 over 6 hours (Fig.4.12A). The production of IFNγ and TNF*α* was determined using intracellular staining. Figure 4.12B showed that both F5Lck^{WT} and F5Lck^{VA} produced IFNγ and TNF*α* in a

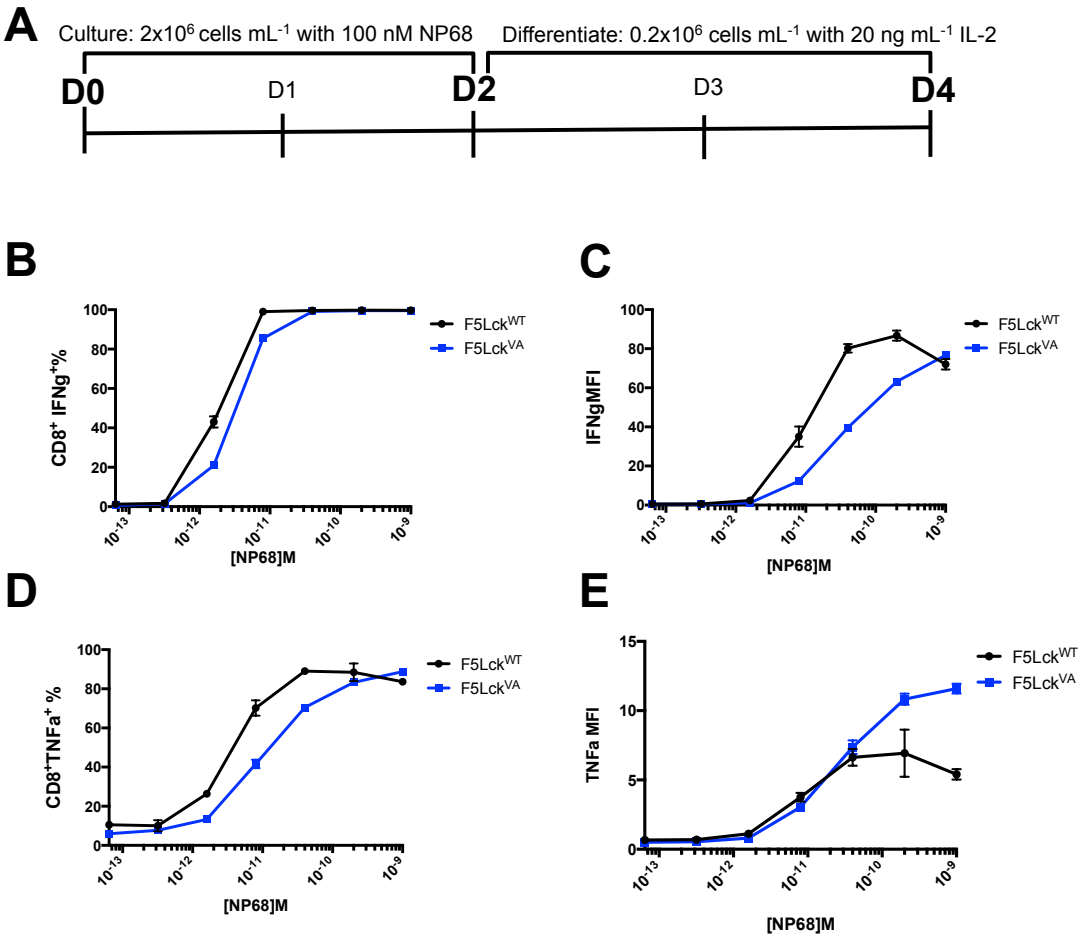

Fig. 4.12 Antigen-experienced F5Lck^{VA} T cells had increased threshold for IFNγ and TNFα production.
(A) F5Lck^{WT} (pool of n=3) and F5Lck^{VA} (pool of n=3) LN T cells were cultured for 2 days with 100 nM NP68 followed by 2 days with 20 ng mL^{-1} of IL-2 to produce antigen-experienced cells. On day 4 cells were restimulated in triplicate with different concentrations of NP68 for 6 hours in the presence of Brefeldin-A. Line graphs show (B) the average proportions ± SD and (C) the average MFIs ± SD of CD8$^+$IFNγ$^+$ F5Lck^{WT} and F5Lck^{VA} T cells at different concentrations of peptide. Similarly, line graphs show (D) the average proportions ± SD and (E) the MFIs ± SD of CD8$^+$TNFα$^+$ F5Lck^{WT} and F5Lck^{VA} T cells at different concentrations of peptide. These data are representative of 4 independent experiments.

dose-dependent manner in response to NP68 restimulation. F5Lck^{VA} T cells had an increased threshold for IFNγ (Fig.4.12B) and TNFα (Fig.4.12D) production compared to F5Lck^{WT} T cells, meaning a higher peptide concentration was required to reach similar proportions of cytokine producing cells. This observation was in agreement with published data, that reduced Lck expression increased the activation threshold (Caserta et al., 2010; Lovatt et al., 2006). We showed that in naïve F5Lck^{VA} T cells the activation threshold was the same as in F5Lck^{WT} T cells (Fig.4.2), and that cytokine production upon naïve cell stimulation was increased in F5Lck^{VA} T cells as compared to F5Lck^{WT} T cells (Fig.4.11). Thus, the current result potentially suggested that the provision of IL-2 has changed the activation threshold in F5Lck^{VA} T cells. At the highest concentration of NP68 stimulation tested (1x10^{-9}M), proportions of F5Lck^{VA} (99.7%) and F5Lck^{WT} (99.6%) cells producing IFNγ (Fig.4.12B) were the same. For TNFα production, the proportions of cells were also very similar; F5Lck^{VA} (67%) and F5Lck^{WT} (77%) (Fig.4.12D).

The MFI of IFNγ or TNFα expression can give an indication of the amount of cytokine produced per cell. Data in the line graph in figure 4.12C showed, that F5Lck^{WT} T cells produced more IFNγ per cell than F5Lck^{VA} T cells, up until the highest concentration of stimulation 1x10^{-9}M. Contrastingly, figure 4.12E showed that in the case of TNFα, reduced Lck expression posed no limitation for the amount of cytokine produced per cell, despite the proportions of F5Lck^{VA} T cells being lower than F5Lck^{WT} (Fig.4.12D). The MFI of TNFα at lower concentrations of NP68 stimulation was the same, and at higher concentrations even higher, in F5Lck^{VA} than F5Lck^{WT} T cells (Fig.4.12E). Overall, the data showed that similar proportions of antigen-experienced F5Lck^{VA} T cells were able to produce similar amounts of cytokine as F5Lck^{VA} T cells, once the activation threshold was overcome.

Two key molecules in effector and memory potential development are T-bet and Eomes (Kaech and Cui, 2012). T-bet and Eomes are transcription factors upregulated upon TCR engagement (Intlekofer et al., 2005; Sullivan et al., 2003). They are partially redundant in their roles of inducing genes necessary

for CTLs such as IFNγ, granzyme B, perforin, CXCR3, and CXCR4 (Intlekofer et al., 2005; Kaech and Cui, 2012).

The results in Fig.4.11 and 4.12 indicated differences between F5Lck^{WT} and F5Lck^{VA} cells in the initial production of IFNγ and TNFα. Therefore, we asked whether there were also differences in the expression patterns of T-bet and Eomes. Fig.4.13A showed that both F5Lck^{WT} and F5Lck^{VA} cells upregulated Tbet and Eomes in response to TCR stimulation by day 2. An overlay of F5Lck^{WT} and F5Lck^{VA} suggested that F5Lck^{VA} expressed slightly higher levels of both T-bet and Eomes on day 2. By day 4, T-bet expression was equal between F5Lck^{WT} and F5Lck^{VA} T cells, and F5Lck^{WT} seemed to express slightly more Eomes than F5Lck^{VA}.

T-bet and Eomes are known to cooperate to sustain memory T cell homeostasis by expression of IL-2Rβ (CD122), which allows for IL-15-mediated signalling and the homeostatic proliferation of memory cells (Kaech and Cui, 2012). Therefore, expression of CD122 was assessed as a further read out of the cooperative functions of T-bet and Eomes. In both F5Lck^{WT} and F5Lck^{VA} T cells, CD122 expression was upregulated after two days of activation (Fig.4.13B), and there was no difference between the two cell types as evidenced by overlayed histograms.

As mentioned above, both T-bet and Eomes are important for controlling the expression of effector molecule genes such as granzyme B (Intlekofer et al., 2005). Granzymes are serine endopeptidases expressed by CTLs, and are released to the intercellular space to eliminate infected cells (Odake et al., 1991; Poe et al., 1991). Eomes has been shown to bind directly to the granzyme B promoter (Sullivan et al., 2003). Therefore, granzyme B expression was assessed as a further read out of the effector capacity on day 2 of activation. Figure 4.13B showed that F5Lck^{VA} and F5Lck^{WT} T cells both upregulated granzyme B expression upon activation by day 2. However, F5Lck^{VA} T cells expressed higher levels of granzyme B, as determined by histogram analysis. On the 4th day, granzyme B expression was still slightly

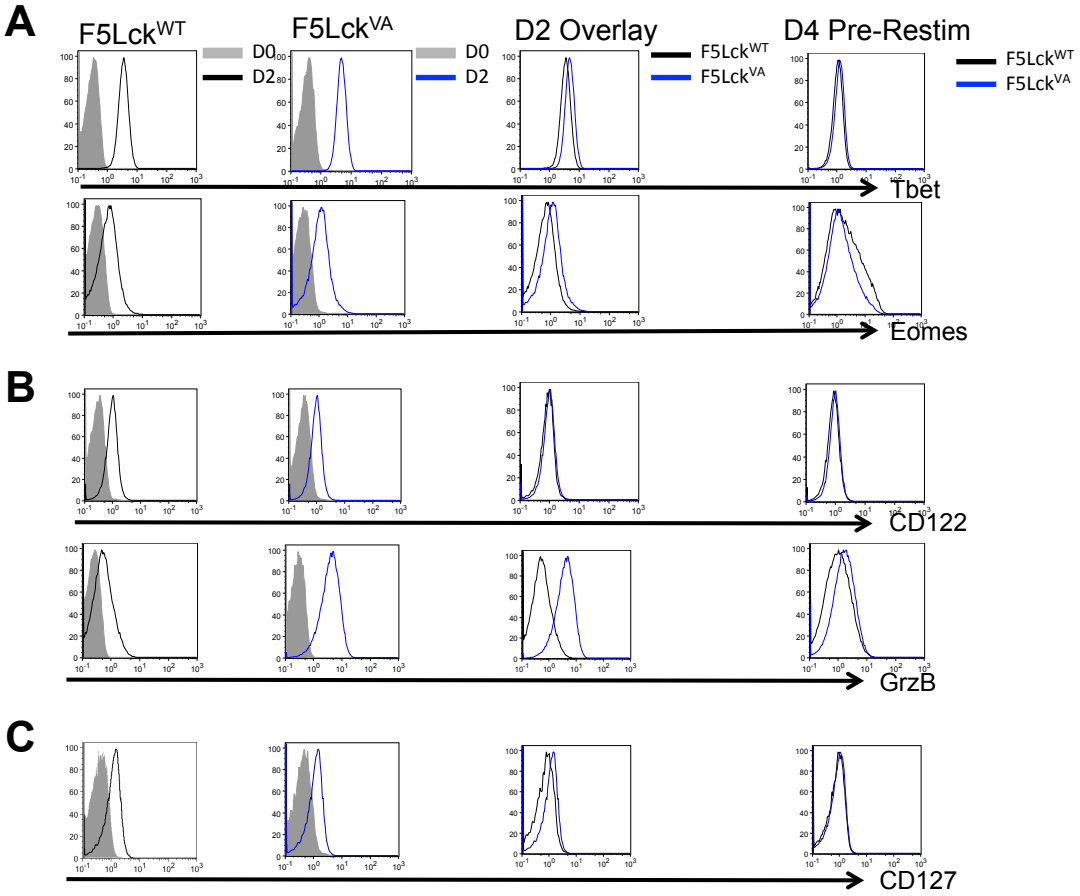

Fig. 4.13 Expression patterns of T-bet and Eomes at different times of antigen-experienced cell generation.
F5Lck^{WT} (black line) and F5Lck^{VA} (blue line) LN T cells from 3 animals of each genotype were cultured for 2 days with 100 nM NP68 and a further 2 days with 20 ng mL^{-1} IL-2. The cells were stained and analysed by flow cytometry at indicated time points for the indicated molecules (A, B and C). Day 0 samples (filled grey) were fixed until day 2 samples were obtained and also fixed in order to stain and acquire them simultaneously. These data are representative of 3 independent but consistent experiments.

higher in F5Lck^{VA} T cells, but the difference between expression in F5Lck^{WT} and F5Lck^{VA} cells decreased.

Naive T cells depend on IL-7 signals via CD127 for survival (Tan et al., 2001). It has been shown that CD127 expression is downregulated in T cell activation by *in vivo* infection, and is upregulated again in memory cells (Best et al., 2013). Indeed, memory cell generation and maintenance have been shown to be IL-7 dependent, potentially by upregulating Bcl-2 (Schluns et al., 2000). Interestingly, our results showed that CD127 expression was low on day 0 and upregulated on day 2 of *in vitro* stimulation in both F5Lck^{WT} and F5Lck^{VA} T cells (Fig.4.13C). CD127 expression was modestly higher in F5Lck^{VA} T cells, which was in correlation with our findings in Fig.4.10, showing increased Bcl-2 expression in F5Lck^{VA} T cells.

These results suggested that although initially F5Lck^{VA} T cells had an increased activation threshold in upregulating IFNγ and TNFα as antigen-experienced cells (Fig.4.12), they reached proportionally the same levels of expression as F5Lck^{WT} T cells at higher concentrations. This suggested that reduced Lck expression increased the threshold of activation required for cytokine production in the presence of IL-2. There appeared to be no defects in the transcriptional regulation of cytokine production as a result of increased threshold of cytokine production in F5Lck^{VA} T cells, since T-bet and Eomes expression were similar to F5Lck^{WT} T cells (Fig.4.13A). Finally, granzyme B expression was enhanced in F5Lck^{VA} T cells as compared to F5Lck^{WT} T cells after 2 days of activation, perhaps a reflection of their more proliferative state (Fig.4.9), and increased cytokine production upon stimulation of naïve cells also seen after 2 days of activation (Fig.4.11).

4.2.13 Phosphorylation of p38 was enhanced in F5Lck^{VA} T cells

The data in this chapter have so far been highly indicative of differential branching of signalling pathways post-TCR stimulation, as some of the read-outs of functional consequences were upregulated when compared to F5Lck^{WT} (proliferation, Ca^{2+} flux) and others were downregulated (pERK, cytokine

production in the presence of IL-2), when Lck expression was reduced. In an effort to identify which upstream pathway could be responsible for the increased proliferation, we assessed the phosphorylation of the MAPK p38.

TCR ligation has been shown to lead to p38 mediated proliferation and cytokine production by its role in phosphorylating adenylate/uridylate-rich element (ARE)-binding proteins (Ashwell, 2006). ARE-binding proteins stabilise and increase translation of mRNAs containing 3' UTR AREs. Additionally, pharmacological inhibition of p38 in humans reduces pro-inflammatory cytokine secretion from *ex vivo* LPS-stimulated peripheral blood mononuclear cells (PBMCs) (Parasrampuria et al., 2003), suggesting that this pathway plays an important role in immune function.

Upon TCR activation by p:MHC, Lck phosphorylates Zap-70, which in turn phosphorylates LAT. LAT activates the GTP exchange factor Vav1, which activates Rac1, a MAPKKK, thus leading to the activation of MKK3 and MKK6. MKK3 and 6 directly phosphorylate p38 on residues Thr-180 and Tyr-182 – the canonical pathway. The activation of p38 and ERK activation are both Lck dependent, however, only p38 activation was shown to be LAT independent (Mittelstadt et al., 2005). Interestingly, it has been found that Zap-70 directly activates p38 on an alternative Tyr-323 residue (Mittelstadt et al., 2005). The proposed reason for MAPK independent activation of p38 is that it may be involved in anergy, as it is active in the absence of co-stimulation by CD28 (Mittelstadt et al., 2005). In addition, the importance of the alternative p38 pathways in T cells was established when mice deficient for the growth-arrest gene *Gadd45a*, that inhibits p38 phosphorylation, were found to harbour hyperproliferative T cells and suffer from autoimmunity (Salvador et al., 2005).

Perhaps F5Lck^{VA} T cells 'preferentially' signalled via the p38 pathway as opposed to the ERK pathway. We did not have access to the antibody specific for the Tyr-323 residue of p38. Therefore, the phosphorylation on residues Thr-180 and Tyr-182, which are part of the canonical p38 activation

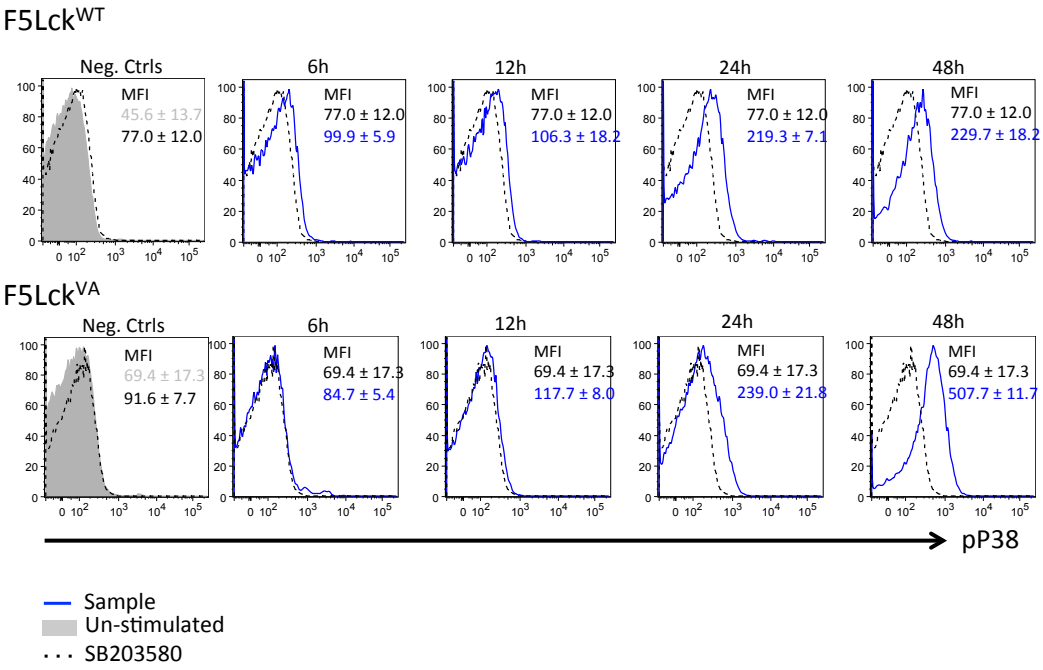

Fig. 4.14 F5Lck^{VA} T cells had enhanced p38 phosphorylation.
F5 Lck^{WT} and F5Lck^{VA} LN T cells (n=2/genotype) were stimulated with 1 μM NP68 for the indicated time points. Specificity of p38 phospho-Thr180/Tyr182 antibody was controlled by inhibitor SB203580 treatment for 30 minutes at 37°C prior to stimulation for 6h. Since inhibitor and unstimulated sample (grey fill) histograms overlapped, the inhibitor sample (black dotted line) was used to overlay with experimental samples (blue line). The numbers on the graphs represent average MFIs of technical replicates ± SD. This experiment has only been done once.

pathway, were assessed instead in an experiment where naïve F5 Lck^{WT} and F5Lck^{VA} LN T cells were stimulated for different times with 1 μM NP68.

The results in Fig.4.14 showed that p38 phosphorylation at Thr-180/Tyr-182 (pp38) was comparable at 6h and 12h time points between F5Lck^{WT} and F5Lck^{VA} T cells. At 24h, the F5Lck^{VA} pp38 MFI was already higher (239 ± 21.8) than in F5Lck^{WT} (219.3 ± 7.1). At 48h, in F5Lck^{VA} T cells pp38 MFI was upregulated by 2 fold from 24h (507.6 ± 11.7), whereas in F5Lck^{WT} T cells it was only upregulated slightly (229.7 ± 18.2). This result suggested that indeed F5Lck^{VA} T cells 'preferentially' signalled via p38 as opposed to ERK. However, it has to be noted the time courses for measuring the two MAPK were very different: ERK was measured for up to 2h, pp38 measurements, however, start from 6h, as there was no p38 phosphorylation at early times in preliminary experiments.

4.2.14 Foxo1 phosphorylation was similar between F5Lck^{VA} and F5Lck^{WT} T cells

Another level of regulation of cellular responses is provided by Foxo transcription factors, which regulate many facets of lymphocyte homeostasis, including differentiation, turnover, and homing (Hedrick et al., 2012). Phosphorylation of Foxo1 at residues T24, S256, S319, S329 (Burgering and Kops, 2002) by Akt, downstream of PI3K, leads to its translocation from the nucleus and therefore degradation and consequent repression of its transcriptional activity (Hedrick, 2009). PI3K activation, and subsequent Akt activation, can occur via TCR ligation or IL-7 mediated signalling. The latter of these can lead to increased expression of Bcl-2 and decreased expression of $p27^{Kip1}$ (a cell cycle inhibitor) (Hedrick, 2009). In the case of Foxo1 deficiency, CD127 expression is hindered because an *Il7r* enhancer is no longer bound (Fabre et al., 2008; Kerdiles et al., 2009). Furthermore, Rao et al. made use of the reductionist and *in vivo* approach to identify Foxo1 as a critical regulator of T-bet and Eomes activity in $CD8^+$ T cells (Rao et al., 2012). This further emphasises the role of Foxo1 in homeostasis and life span of naïve T cells as a means of sensing growth factor availability and fate decisions.

We showed that after 24h of activation, T cells with reduced Lck expression activated as efficiently as F5Lck^{WT} T cells (Fig.4.2). Additionally, at 48 and 72h, F5Lck^{VA} T cells had enhanced proliferation (Fig.4.9), Bcl-2 expression (Fig.4.10), and after 48 hours of activation CD127 expression was also enhanced (Fig.4.13C).

In light of these results, we assessed Foxo1 phosphorylation upon activation of naïve LN T cells from F5Lck^{WT} and F5Lck^{VA} mice for different times with 1 μM NP68. Foxo1 activation was measured by flow cytometry using a phospho-Foxo1 antibody (pFoxo1$^{Ser-256}$), and its specificity was confirmed by using an Akt inhibitor - Ly29004. The results in figure 4.15 showed that until 24h there was no marked increase in pFoxo1$^{Ser-256}$, in either F5Lck^{WT} or F5Lck^{VA} T cells, as measured by MFI of expression, in comparison to the inhibitor treated sample. However, by 48h there was a distinct increase in pFoxo1$^{Ser-256}$ expression in both genotypes, and dividing the MFI at 48h by the MFI for the inhibited sample per each genotype, suggested that in F5Lck^{WT} there was a 9-fold increase and in F5Lck^{VA} there was a 7.5 fold increase in pFoxo1$^{Ser-256}$. The proportions of pFoxo1^{+} cells at the 48h time point were 45%±2.8 in F5Lck^{WT} and 54%±1.3 in F5Lck^{VA} T cells. These results implied that there was a modest increase in Foxo1 phosphorylation in F5Lck^{VA} T cells compared to F5Lck^{WT} cells. It must, however, be noted that this experiment has only been done once and the results are therefore preliminary.

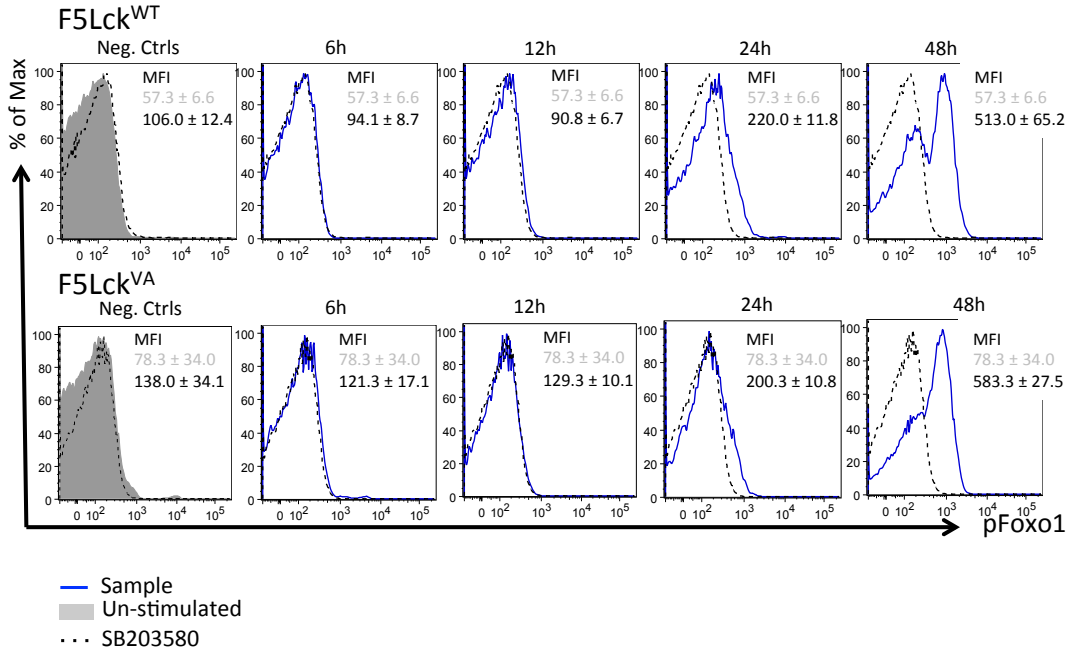

Fig. 4.15 Foxo1 phosphorylation was similar between F5Lck^{WT} and F5Lck^{VA} T cells
F5 Lck^{WT} and F5Lck^{VA} LN T cells (n=2/genotype) were stimulated with 1μM NP68 for the indicated time points. Specificity of the pFoxo1$^{Ser-256}$antibody was controlled by treatment with 1 μM Ly29004 (Akt inhibitor) for 30 minutes at 37°C prior to stimulation with 1 μM NP68 for 6h. Since inhibitor (dotted black line) and unstimulated sample (grey fill) histograms overlapped, the inhibitor sample was used to overlay with experimental samples (blue line). The numbers on the graphs represent average MFI of technical replicates ± SD. This experiment has only been done once.

4.3 Summary

- Phosphorylation of immediate targets of Lck: Zap-70 and Shc was reduced in F5Lck^{VA} mice (Fig.4.3), as was ERK phosphorylation (Fig.4.4).
- T cell activation after 24h of stimulation was equivalent between F5Lck^{WT} T cells and F5Lck^{VA} T cells (Fig.4.2).
- F5Lck^{VA} T cells also had enhanced Ca^{2+} flux (Fig.4.7), produced elevated levels of IL-2 after 24 and 48h of stimulation (Fig.4.8) and had a higher proliferative capacity (Fig.4.9) correlating with higher Bcl-2 expression (Fig.4.10).
- F5Lck^{VA} T cells produced more IFNγ and TNFα than F5Lck^{WT} T cells after 72h of activation and subsequent recall (Fig.4.11) but when cultured in IL-2, prior to recall, F5Lck^{VA} T cells produced proportionally less IFNγ and TNFα (Fig.4.12).

4.4 Discussion

The aim of the work presented in this chapter was to establish the role of reduced Lck expression in the activation of peripheral $CD8^+$ T cells. Data presented in this chapter showed that pathways downstream of TCR-stimulation were differentially regulated when Lck abundance was reduced, meaning that some downstream pathways were downregulated, as might be expected from previously published data (Lovatt et al., 2006), however, others were upregulated.

The data showed that despite reduced Lck expression, T cell activation efficiency, as measured by upregulation of an early activation marker such as CD25 after 24h of stimulation, was equivalent between $F5Lck^{WT}$ T cells and $F5Lck^{VA}$ T cells (Fig.4.2). This was in striking contrast to previously published data that showed $F5Lck^{ind}$ T cells, expressing 20% of WT levels of Lck, had an increased activation threshold compared to WT controls (Lovatt et al., 2006), which we also confirmed in this chapter (Fig.4.2). We investigated several TCR-mediated Lck dependent signalling pathways and their biological outcomes. In correlation with previously published findings, our data showed that phosphorylation of immediate targets of Lck, for example Zap-70 and Shc (Fig.4.3), and a later target ERK (Fig.4.4) were reduced in T cells with reduced Lck expression (Lovatt et al., 2006). On the other hand, we also showed that $F5Lck^{VA}$ T cells had enhanced Ca^{2+} flux (Fig.4.7), produced elevated levels of IL-2 after 24 and 48h of stimulation (Fig.4.8), and had a higher proliferative capacity (Fig.4.9) than $F5Lck^{WT}$ T cells. When we looked at cytokine production upon stimulation of naïve cells (Fig.4.11), we found that $F5Lck^{VA}$ produced increased levels of IFNγ and TNFα. In contrast, when we looked at cytokine production in antigen-experienced cells, we found that growing them in IL-2 had affected the responsiveness of $F5Lck^{VA}$ T cells, and they produced proportionally less IFNγ and TNFα (Fig.4.12). Finally, we showed that $F5Lck^{VA}$ T cells expressed increased levels of p38 (Fig.4.14) and modestly increased levels of pFoxo1 (Fig.4.15).

The following discussion will look at potential explanations for these observations from the perspective of regulation of Lck, its role in T cell signalling, as well as in negative regulation.

Lck is crucial for TCR signalling and its activity is dynamically regulated, negatively by Csk, which phosphorylates its inhibitory tyrosine Y505, and by PTPN22, which dephosphorylates the activatory tyrosine Y394. Lck is both positively and negatively regulated by CD45 that dephosphorylates Y505 as well as phosphorylates Y394. The latter is also phosphorylated by trans-autophosphorylation by Lck. Nika et al. showed that in naïve cells, 40% of Lck was constitutively doubly phosphorylated on Y394 and Y505, potentially keeping T cells poised for activation (Nika et al., 2010). Upon TCR ligation, one potential adapter molecule PAG, which keeps Csk in close proximity to Lck in the plasma membrane, is dephosphorylated and Csk is released. This tips the equilibrium towards CD45 dephosphorylation of Y505 on Lck, and leads to activation and phosphorylation of ITAMs by Lck. The absence negative regulation of Lck leads to sustained TCR signalling even without a peptide ligation (Schoenborn et al., 2011). To show this, Schoenborn et al. modified Csk such that it did not inhibit Lck. They found that inactivating Csk even without TCR ligation, activated the TCR signaling cascade, with Zap-70 phoshorylated on Y319 and also on Y493 (which is a site for both Lck and Zap-70 itself). They found that the signaling cascade was sustained, including the initiation of Ca^{2+} flux and the phosphorylation of ERK (Schoenborn et al., 2011). We showed that reduced Lck abundance led to increased Ca^{2+} flux, and since Schoenborn et al. suggest that more active Lck could lead to a similar result (Schoenborn et al., 2011), it would be interesting to assess whether the reduced Lck levels also led to a more active Lck. The pool of pre-existing Lck may be slightly more activated in F5Lck^{YA} to carry out equivalent functions to wild type Lck – although, extrapolating from our data, this may be unlikely, as immediate phosphorylation events downstream of Lck were reduced (Fig.4.3). Additionally, increased Lck activation without TCR ligation would also lead to increased phosphorylation of ERK (Schoenborn et al., 2011). A helpful determinant of Lck activity is the onset of CD3ζ phosphorylation in response to TCR

ligation, as with a 90% reduction of activated Lck, CD3ζ phosphorylation was strongly delayed (Nika et al., 2010). Thus analysing CD3ζ phosphorylation might be a more accurate reflection of Lck activity.

An interesting study showed that by changing the number of CD3 ITAMs that were phosphorylated (multiplicity) and able to mediate downstream signalling, one could change the biological outcome for the cell (Guy et al., 2013). Low ITAM multiplicity was able to facilitate Zap-70 and ERK phosphorylation equally to wild type controls, as well as to direct secretion of IL-2, IFNγ and TNFα, but it did not lead to proliferation, because of defects in c-Myc activation. High ITAM multiplicity was required for efficient proliferation (Guy et al., 2013). Guy et al. used AND TCR transgenic mice and showed that strong and weak agonist stimulation, correlated with high and low ITAM multiplicity, respectively (Guy et al., 2013). Overall, this study showed that by altering the TCR signalling pathway from one of the most proximal locations, downstream signalling outcomes are changed. The observations that $Ca2^{+}$ signalling and expression of CD25 were intact with low multiplicity ITAMs are in keeping with our data (Guy et al., 2013), the lack of proliferation with low ITAM multiplicity, however, is in significant contrast to our results, as we showed that decreased Lck abundance led to increased proliferation (Fig.4.9). The results presented in this chapter, supported by published data (Guy et al., 2013), suggested that there are differential effects on downstream signalling thresholds when components of the TCR signalling cascade are changed.

This may be a situation where spatiotemporal patterning is relevant and is mediating such contrasting differences as suggested by Singleton and colleagues (Singleton et al., 2009). They propose that the level of intricate control and adaptability of the pathways involved in TCR signalling is dependent on the spatiotemporal patterning of signalling molecules during T cell activation (Singleton et al., 2009). Marking receptor-ligand pairs with sensors such as green fluorescent protein (GFP) allowed them to study the distribution of the entire receptor population and its ligand. They described T cell activation having highly diverse spatiotemporal patterning of

signalling molecules, which is influenced by the strength and context of TCR signalling with physiologically distinct outcomes. The diversity in spatiotemporal patterning would affect the probabilities at which signalling molecules would interact with each other. They went on to suggest, however, that changes to patterning of proximal signalling molecules may be of little consequence to distal signalling events. This was evidenced by their studies comparing T cells from two different transgenic systems with distinct spatiotemporal signalling patterns in proximal signalling molecules. They proposed that if TCR signalling is above a certain threshold, then proximal spatiotemporal patterning is inconsequential (Singleton et al., 2009).

Guy and colleagues proposed that high ITAM multiplicity was required for recruitment of Vav1 and subsequent cytoskeletal remodelling (Guy et al., 2013). Although they did not study the spatiotemporal aspect of TCR signalling, changes in Vav1 expression could correlate with the spatiotemporal patterning of signalling molecules (Schoenborn et al., 2011). It would be interesting to assess the expression of Vav1 and the organization of molecules in the immune synapse by confocal microscopy in F5Lck^{VA} mice to see whether there are any differences compared to F5Lck^{WT} mice.

Ca^{2+} flux and IL-2 production are two critical pathways in T cell signalling. The influx of Ca^{2+} is a mediator for several Ca^{2+} - dependent pathways including differentiation, effector function and gene transcription (Nagaleekar et al., 2008; Oh-hora and Rao, 2008). Engagement of the TCR mediates two independent mechanisms that increase the calcium ion concentration in the cell: IP_3 binding to IP_3 receptors depletes Ca^{2+} stores from the ER, and facilitates 'store operated' entry of Ca^{2+} through Ca^{2+} channels in the plasma membrane (Oh-hora and Rao, 2008). The first effect of increased Ca^{2+} in lymphocytes is to stop their movement, allowing them to form stable interactions with APCs. It has been shown that differences in affinities of antigenic peptides can influence the abundance of calcium fluxed and the frequency of Ca^{2+} spikes, with high-affinity TCR engagement mediating more substantial Ca^{2+} flux and leading to prolonged engagement with APCs (Wei et al., 2007). Ca^{2+} flux has been shown to be defective in cells lacking Lck

(Straus and Weiss, 1992; Trobridge and Levin, 2001), as well as in $CD4^+$ T cells in Lck^{ind} mice (Lovatt et al., 2006). However, in the case of the Lck^{VA} mice, Ca^{2+} flux was shown to be comparable to Lck^{WT} mice upon TCR and CD4 cross linking in DP thymocytes (Salmond et al., 2011). It is therefore interesting that we found faster and increased Ca^{2+} flux in peripheral $F5Lck^{VA}$ T cells (Fig.4.7) upon CD8 and TCR crosslinking. Additionally, we stimulated the T cells in different ways to measure Ca^{2+} flux: CD3 crosslinking and TCR crosslinking seperately, and observed the same results, confirming that it is a TCR-mediated Lck dependent difference (Fig.4.7). Increased Ca^{2+} flux may explain the increased proliferation we see in $F5Lck^{VA}$ T cells, but it is difficult to explain why this particular pathway is upregulated as opposed to ERK, for example. However, the two results cannot be directly compared as Ca^{2+} flux was not measured with peptide stimulation and perhaps ERK phosphorylation in $F5Lck^{VA}$ T cell had not peaked yet and we should do a longer time course. Thus, the ideal control experiment here would be to measure ERK phosphorylation in response to CD8 and TCR crosslinking over a longer time course.

TCR-signal dependent increase of AP1, NFAT, and NFκB, and the translocation of these transcription factors to the nucleus, mediates the binding of the *Il2* promoter (Malek, 2008). In concert with Ca^{2+} signals, the increased IL-2 production may also support the increased proliferative capacity in $F5Lck^{VA}$ T cells (Fig.4.9). IL-2 signalling also induces expression of B lymphocyte maturation protein 1 (Blimp-1) after 2-3 days of stimulation, a key repressor of IL-2 production (Martins and Calame, 2008). Given more time, it would have been interesting to study whether the increased proliferative capacity was truly due to IL-2 expression, by doing IL-2 blocking experiments. It would also be interesting to address Blimp-1 expression in $F5Lck^{VA}$ T cells. Perhaps it is not induced as efficiently as in $F5Lck^{WT}$ T cells, explaining the increased IL-2 production at 48h in $F5Lck^{VA}$ T cells. Additionally, it is possible that $F5Lck^{VA}$ T cells would succumb to AICD more than $F5Lck^{WT}$ T cells, due to sustained IL-2 signalling (Malek, 2008). To assess this, we could analyse the surface expression of PD1 - a molecule associated with T cell exhaustion (Francisco et al., 2010). Therefore, it may be

possible that increasing Ca^{2+} signals and IL-2 production ensures a successful development of effector functions in the cells, to counterbalance the weaker TCR-mediated signalling caused by reduced Lck abundance.

From our study, it also appeared that IL-2 had a significant impact on the behaviour of F5Lck^{VA} cells when it came to effector cytokine production. When studying cytokine production following stimulation of naïve cells (Fig.4.11), we found that F5Lck^{VA} T cells produced increased levels of IFNγ and TNFα, an observation that is potentially in line with increased Ca^{2+} flux and IL-2 production. In contrast, when we looked at cytokine production after growing the cells in IL-2, we found the activation threshold of F5Lck^{VA} T cells was increased and they produced proportionally less IFNγ and TNFα (Fig.4.12). To distinguish whether this effect was really due to the exogenous IL-2, or perhaps differentiation differences between F5Lck^{WT} and F5Lck^{VA} T cells, or indeed the TCR sensitivity, it would be interesting to repeat the experiments by initially activating T cells with a titration of peptide, growing them in IL-2, and recalling them with the same titration of peptide. This would allow us to see whether it is an activation threshold difference. Alternatively, we could activate T cells with a titration of peptide, then grow them in IL-2, and then recall them with an optimal concentration of peptide. This would hopefully indicate whether there is a differentiation difference.

Signalling via the TCR activates intracellular phosphorylation dependent cascades that lead to the appropriate fate decisions. It is yet to be determined how stimulation of the TCR can direct discrete subsets of signalling pathways in order to achieve particular outcomes. Explanations for this 'decision making' range from signal strength to scaffold protein mediated signalosomes (Round et al., 2007). Furthermore, signal strength and duration during the initial immune response have been found to distinguish between full activation and tolerance of responding $CD8^+$ T cells (Williams and Bevan, 2007). Negative regulation is an important mechanism in assuring TCR signalling is controlled appropriately, in terms of the strength and duration of the signal. For example, a mutation in the negative regulator PTPN22 leads to increased TCR signalling and a predisposition to autoimmune

disease, as it interrupts the interaction between PTPN22 and Csk (Brownlie et al., 2012). PTPN22 normally binds Csk and dephosphorylates activating residue Tyr^{394} on Lck, particularly in effector and memory T cells. It would be interesting to assess the expression of PTPN22 in $F5Lck^{VA}$ T cells, as it is possible that their enhanced proliferation is indicative of increased TCR signalling due to reduced PTPN22 expression.

Another TCR-dependent proximal negative feedback mechanism activated by Lck in response to TCR signalling is the cytoplasmic PTP SHP1 (Acuto et al., 2008). $SHP1^{KO}$ mice develop autoimmune disease due to increased positive and negative thymocyte selection and T-cell activation (Charest et al., 1997). When SHP1 is phosprylated by Lck at Y564 it also interacts with Lck (Lorenz et al., 1994). Phosphorylation of Ser-59 on Lck by ERK disrupts the interaction between Lck and SHP1, preventing activation of SHP1 (Acuto et al., 2008; Stefanova et al., 2003). The data in this chapter suggest that Ser-59 phosphorylation of Lck is equal in $F5Lck^{WT}$ and $F5Lck^{VA}$ T cells (Fig.4.6). Such a mechanism of preventing negative regulation is another potential explanation as to why $F5Lck^{VA}$ CD8 T cells activate with equal efficiency to $F5Lck^{WT}$ T cells (Fig.4.2).

A potential interaction between Dok1 and Csk, which may contribute to negative regulation of Lck activity in response to TCR ligation, has been described (Schoenborn et al., 2011). The $Dok1^{-/-}Dok2^{-/-}$ phenotype with increased TCR-induced IL2 production, and proliferation correlating with increased phosphorylation of Zap-70, LAT and ERK, is somewhat similar to what we describe in this chapter, suggesting the reduced Lck expression seems to mimic a negative feedback deficiency. Our data in figure 4.6 suggested Ser-59 phosphorylation is intact in $F5Lck^{VA}$ mice, indicating that reduced Lck abundance is enough to prevent negative regulation. The question is whether it is also sufficient for activating it. It would be interesting to study the expression and activation of Dok1 and Dok2 proteins in $F5Lck^{VA}$ mice to see whether reduced Lck expression is sufficient to overcome their activation threshold.

In response to TCR stimulation, Lck phosphorylates HPK1 of the HPK1-SLP-76-14-3-3 negative regulation pathway, and HPK1 deficiency can result in increased TCR-dependent tyrosine phosphorylation of SLP-76, PLCγ1, LAT, Vav1, and ZAP-70 (Acuto et al., 2008). It is important to note that ERK activation is increased, and not JNK or p38, in HPK1 deficiency. This axis is an example of an additional level of TCR-signalosome control that acts later, potentially regulating the duration of TCR signals and the subsequent biological outcome (Acuto et al., 2008). In this chapter, we show, however, that F5Lck^{VA} mice have increased p38 phosphorylation (Fig.4.14). This and the decreased Zap-70 phosphorylation shown (Fig.4.2), may indicate that there is no HPK deficiency in F5Lck^{VA} cells, but it would be interesting to study the HPK-SLP-76-14-3-3 pathway in F5Lck^{VA} cells to assess whether it is differentially regulated.

Several studies in the past have suggested that the absence of Lck or its reduced expression, compromise TCR signalling. The current study showed that with reduced Lck expression, some signalling pathways were downregulated while others were enhanced. It is possible that differential signalling occurs because regulation of TCR signalling has been altered on multiple levels, such as in the forward signal, but also in different negatively regulating signals that would normally be triggered at different times in the cascade during T cell development with constitutively low Lck expression. In the future it would thus be interesting to assess the gene expression patterns in F5Lck^{VA} T cells compared to F5Lck^{WT} T cells to determine what fundamental changes might be mediating the observations made in this study.

Chapter 5: The Role of Lck in the Formation and Maintenance of Memory T Cells During *Listeria monocytogenes* Infection *in vivo*

5.1 Introduction

In order to successfully eradicate intracellular pathogens, $CD8^+$ T cells must develop potent effector functions as CTLs, such as secretion of IFNγ and target cell lysis through production of granzymes. Upon resolution of the effector response, a memory population remains, that can mount a rapid response should exposure to the pathogen recur.

Our understanding of the factors that determine fate decisions of effector cells and their differentiation into memory cells is still incomplete. CTL formation and subsequent memory development are affected by the strength and duration of the initial trigger between naïve T cells and p:MHC complexes (signal 1), co-stimulation (signal 2) and inflammatory stimuli (signal 3) (Williams and Bevan, 2007). The stages of $CD8^+$ T cell differentiation to generate mature CTLs involve clonal expansion, proliferation and differentiation of effector functions (Williams and Bevan, 2007). In the previous chapter we described the role Lck abundance plays in effector function development *in vitro*. We found that cells with reduced Lck expression had a higher proliferative capacity (Fig.4.9) as well as increased Bcl-2 expression (Fig.4.10) and they are capable of producing effector cytokines, albeit with an increased activation threshold in the presence of IL-2 (Fig.4.12). Consequently, we wished to address the impact of altered signal strength on effector to memory T cell differentiation *in vivo*.

Reduced Lck expression has previously been shown to reduce the functional avidity of TCR interactions and to increase the activation threshold of T cells (Caserta et al., 2010; Lovatt et al., 2006). Therefore, changing Lck expression affects the initial trigger between naïve T cells and p:MHC complexes and this has also been shown to impact on CTL formation and subsequent

memory function (Caserta et al., 2010). Caserta et al. showed that CD4+ T cells with reduced Lck expression had increased effector-effector memory responses and an improved generation of memory populations (Caserta et al., 2010). Additionally, reduced Lck expression prolonged IL-2 expression, increased pro-survival marker expression and reduced exhaustion marker expression (Caserta et al., 2010). Zehn et al. have shown, that the extent of initial proliferation is directly proportional to the affinity of peptide, but very low affinity peptides (low functional avidity interactions) are sufficient for promoting T cell effector and memory T cell development (Zehn et al., 2009).

Studies have shown that both CD4+ (Farber et al., 1997) and CD8+ (Borger et al., 2013) memory T cells demonstrate increased responsiveness to antigen recall associated with changes in proximal TCR signaling. In addition to negative regulators of TCR signaling being redistributed away from the site of TCR engagement in CD8+ memory T cells, Lck was more efficiently recruited to the site of TCR engagement (Borger et al., 2013), possibly because of the reported increased localization with the CD8 co-receptor (Bachmann et al., 1999). Additionally, Tewari et al. have reported that memory CD8+ T cells were Lck-independent with less stringent requirements for antigen-specific TCR signaling to activate them (Tewari et al., 2006).

Collectively, these studies led us to hypothesise that Lck^{VA} T cells, due to reduced effector cytokine production but increased Bcl2 expression and high proliferative capacity, may have compromised primary responses but develop normal memory T cell populations. To determine the effects of reduced Lck expression in the Lck^{VA} mice on the initial response to pathogen and the subsequent formation of memory *in vivo* we employed a *L. monocytogenes* infection model.

L. monocytogenes infection is a useful tool to study the cellular immune responses in mice (Foulds et al., 2002). Intravenous injection induces systemic infection and triggers the innate responses critical for host survival. Macrophages that ingest the bacteria from the bloodstream migrate to the splenic T cell zone, the spleen therefore being the major site of immune

defence, thereby triggering the adaptive immune response that is responsible for the clearance of *L. monocytogenes* (Pamer, 2004). The infection is characterised by rapid expansion of activated $CD8^+$ T cells (Foulds et al., 2002). This initial phase of proliferation peaks around day 5-7 and is followed by a contraction of pathogen specific cells once the bacteria are eliminated (Mannering et al., 2002; Pamer, 2004). Only approximately 5-10% of bacteria specific cells remain and account for the memory pool (Kaech and Cui, 2012; Pamer, 2004). Rechallenging mice with *L. monocytogenes* enables the study of the memory response (Pamer, 2004). We used an attenuated and OVA-recombinant strain of *L. monocytogens* (*LmOVA*), which is actin-assembly inducing protein (Act-A) deficient. Act-A is required for nucleating actin and allowing the bacteria to create actin polymers, which enable it to move within the cytosols of cells as well as move into neighbouring cells (Pamer, 2004). Act-A deficiency thus highly attenuates *L.monocytogenes* virulence but still initiates innate immune responses and induces protective T-cell responses (Pamer, 2004). The beneficial feature of *LmOVA* is that the pathogen expresses OVA and OVA-specific $CD8^+$ T cells can be followed with H2-K^b dimers or dextramers loaded with the immunodominant N4 peptide (Pamer, 2004; Zehn et al., 2009).

It has been shown that in *L. monocytogenes* infection, following T cell priming, the amount of antigen and the duration of its presentation are irrelevant in determining the magnitude of the response (Mercado et al., 2000). Thus, the T cell response is programmed within the first 24h of antigen encounter leading to T cell fate decisions and thus the heterogeneity among the effector and memory pools of $CD8^+$ T cells (Kaech and Cui, 2012; Mercado et al., 2000; Williams and Bevan, 2007).

In order to be able to label T cells that responded to *LmOVA* in the primary infection thereby allowing their detection at later time points, we used 5-bromo-2'-deoxyuridine (BrdU). BrdU is a thymidine analog and is incorporated into the DNA of proliferating cells. The cells that have incorporated BrdU can be tracked up to 70 days later with a specific monoclonal antibody (Mannering et al., 2002). Approximately 90-95% of

effector cells generated during a primary immune response die and only the remaining small percentage go on to become memory cells. Thus the initial effector pool is very heterogenous and recent years have seen a great increase in research defining phenotypic markers to differentiate cells into terminal effectors and memory precursor cells (Kaech and Cui, 2012). Conventionally, CD44 and CD62L surface expression are used to identify T_{CM} and T_{EM} populations, $CD44^{hi}CD62L^{hi}$ and $CD44^{hi}CD62L^{lo}$ respectively (Sallusto et al., 1999). Additionally, subsets of effector cells that develop into memory cells, MPECs can be characterised as $CD127^{+}KLRG\text{-}1^{-}$ and terminally differentiated SLECs are typically $CD127^{-}KLRG\text{-}1^{hi}$ (Joshi et al., 2007; Sarkar et al., 2008).

Chapter 5: Aims

Combining the staining strategies for the characterisation of memory cells by labelling for several key markers with BrdU labelling, allowed us to compare effector to memory cell differentiation in Lck^{WT} and Lck^{VA} T cells during *LmOVA* infection. In this chapter we distinguished between the Ova-specific, immunodominant response, and the total response to *Listeria*. We showed, that Lck^{VA} mice produced fewer Ova-specific $CD8^{+}$ T cells during primary and secondary infections, and in agreement with *in vitro* data from chapter 4, Lck^{VA} T cells produced less effector cytokines and expressed increased levels of Bcl-2. However, we also showed that Lck^{VA} T cells survived better through the contraction phase of the effector response and developed a distinct *Listeria* – specific memory population compared to Lck^{WT} mice.

5.2 Results

5.2.1 Lck^{VA} mice make fewer OVA-specific T cells

In order to assess whether reduced abundance of Lck compromises the primary or secondary responses to infection, Lck^{VA} and Lck^{WT} mice were infected with *LmOVA* using the protocol described in Fig.5.1A. *Listeria* infection leads to an increase in overall splenic cellularity and $CD8^{+}$ and $CD4^{+}$ T cell populations, which are thus a relevant measure of the overall response to infection (Foulds et al., 2002). Therefore, the cell proportions and numbers

were determined in Lck^{VA} and Lck^{WT} mice (Fig.5.1). Henceforth, the terms naïve and uninfected mice are used interchangeably. As shown in Fig.5.1B it was evident that Lck^{VA} mice and Lck^{WT} responded similarly to *LmOVA* infection. Lck^{WT} spleen cell numbers increased significantly (p=0.0047) from $156.5x10^6$±21.5 in naïve mice to $219.4x10^6$±4.9 in infected mice on day 7. Similarly in Lck^{VA} mice, a significant (p=0.0040) increase in spleen cell numbers from $116.5x10^6$±19.5 in naïve mice to $217.3x10^6$±22.0 in infected mice was seen on day 7. There was no significant difference between Lck^{WT} or Lck^{VA} cell numbers on either day 0 or day 7. A contraction at day 42 was seen in both genotypes, cell numbers in Lck^{WT} mice returned to naïve levels ($157x10^6$±32.1) and were also reduced in Lck^{VA} mice ($141.5x10^6$±40.7). The secondary response was measured on day 46, 4 days after re-infection. A significant increase over day 42 cell numbers was seen in Lck^{WT} ($516.8x10^6$±98.6, p=0.0004) and Lck^{VA} mice ($362.3x10^6$±81.6, p=0.0018). There was a significant difference (p=0.037) between Lck^{WT} and Lck^{VA} cell numbers on day 46. The expansion on day 46 over day 42 was 3.3-fold in Lck^{WT} and 2.6-fold in Lck^{VA} mice.

Fig.5.1C showed that the proportions of $CD8^+$ T cells were reduced in Lck^{VA} compared to Lck^{WT} mice at all time points. This translated to significant decreases in $CD8^+$ cell numbers in naïve (p=0.0016), day 42 (p=0.0068), and day 46 (p= 0.0095) groups as shown in Fig.5.1D.

The $CD4^+$ compartment was considerably smaller in Lck^{VA} mice as compared to Lck^{WT} mice as illustrated in Fig.5.1 (E and F). This is in line with published data showing that reduced Lck expression limits $CD4^+$ T cell positive selection more than that of $CD8^+$ T cells (Molina et al., 1992). It is likely that neutrophils and macrophages, the principal mediators of the killing of *L.monocytogenes* (Pamer, 2004), made up for the cell numbers seen in Fig.5.1B.

In chapter 3 we showed that Lck^{VA} had increased proportions of $CD44^{hi}$ cells *ex vivo* potentially partly due to lymphopenic expansion (Fig.3.12), but CD44 is also upregulated in response to infection (Sprent and Surh, 2011). Henceforth, for simplicity we will refer to $CD44^{hi}$ cells found in naïve mice as

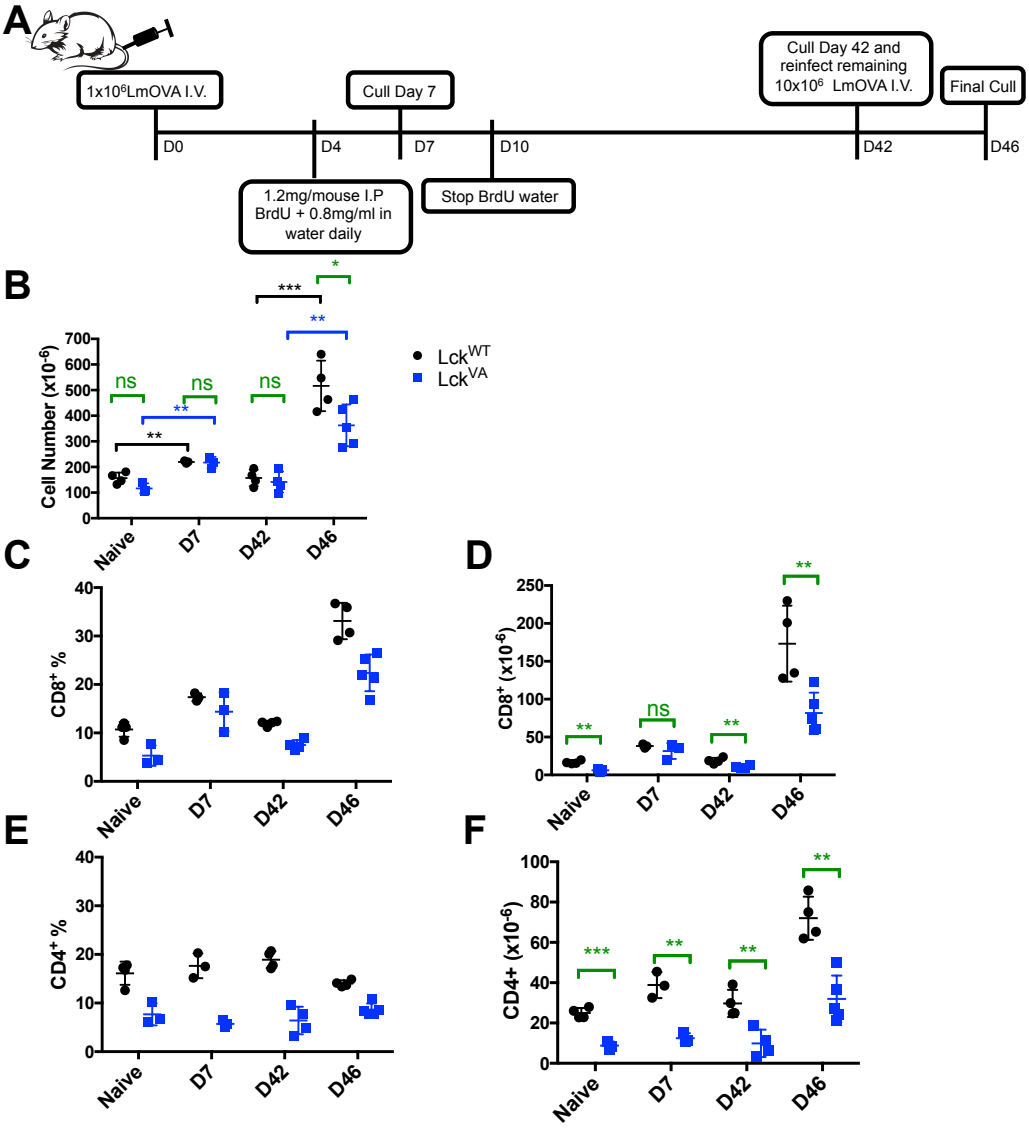

Fig. 5.1 Mice with reduced Lck expression had fewer CD8$^+$ and CD4$^+$ T cells in *LmOVA* infection.

(A) Lck^{VA} and Lck^{WT} mice were infected with *LmOVA* as shown. (B) The absolute number of splenocytes was recorded using the CASY counter throughout the course of *LmOVA* infection. Proportions (C) and absolute numbers (D) of CD8$^+$ T cells and proportions (E) and absolute numbers (F) of CD4$^+$ T cells are shown. Each symbol represents an individual mouse, together with means ± SD of a minimum of 3 mice per group. Significance was calculated on Prism: parametric, unpaired, two-tailed, student's t-test *P<0.05, **P<0.01, ***P<0.001. Data shown is representative of 2 experiments (details of each are outlined in Appendix 7.4).

memory-phenotype cells. Fig.5.2A shows the proportions of $CD44^{hi}$ cells were always higher in naïve Lck^{VA} mice compared to Lck^{WT} mice due to the memory-phenotype cells. The advantage of the *LmOVA* infection model is that specific p:MHC tetramer or dextramer staining can be used to trace responses to the immunodominant OVA epitope, therefore the extent of OVA-specific responses in Lck^{VA} and Lck^{WT} mice were assessed (Fig.5.2). Dot plots showed $CD44^{+}Dex^{+}$ proportions were reduced in Lck^{VA} mice at all time points recorded. Although, there was slightly higher background staining in Lck^{VA} mice in naïve cells (1.7%±0.6 $CD44^{+}Dex^{+}$) compared to Lck^{WT} (0.9%±0.2 $CD44^{+}Dex^{+}$), the proportions of $CD8^{+}CD44^{+}Dex^{+}$ T cells in Lck^{VA} mice were reduced as compared to Lck^{WT} on day 7 and day 46 (Fig.5.2B), and this translated to significant decreases in cell numbers as shown in Fig.5.2C.

Overall, our results showed that OVA-specific primary and secondary T cell responses were significantly reduced in Lck^{VA} mice, despite high CD44 expression at all time points (Fig.5.2).

5.2.2 Total proliferative response to *Listeria* is comparable in Lck^{VA} and Lck^{WT} mice

Listeria infection causes T cell activation, proliferation and significant expansion (Fig.5.1B) (Foulds et al., 2002; Mannering et al., 2002). We showed in chapter 4 that F5Lck^{VA} $CD8^{+}$ T cells proliferated more in response to challenge with cognate peptide *in vitro* (Fig.4.9). Therefore it was of interest to determine the total extent of proliferation *in vivo* during *Listeria* infection, despite lower proportions of OVA-specific cells in Lck^{VA} mice.

One way of measuring extent of proliferation is by staining for the nuclear protein Ki-67 by FACS without distinguishing OVA-specific cells with dextramer. Ki-67 was first identified by Gerdes et al. in a Hodgkins Lymphoma-derived cell line (Gerdes et al., 1983). Ki-67 is specific for cells in all stages of cell cycle except G0, quiescent cells, or those undergoing DNA repair (Soares et al., 2010). As shown in Fig.5.3A and B, proportions of $CD8^{+}Ki\text{-}67^{+}CD44^{+}$ T cells were low in both Lck^{VA} (14.2±1.1%) and Lck^{WT} (9.9±1.4%) mice, although significantly higher in Lck^{VA} mice ($p=0.0062$).

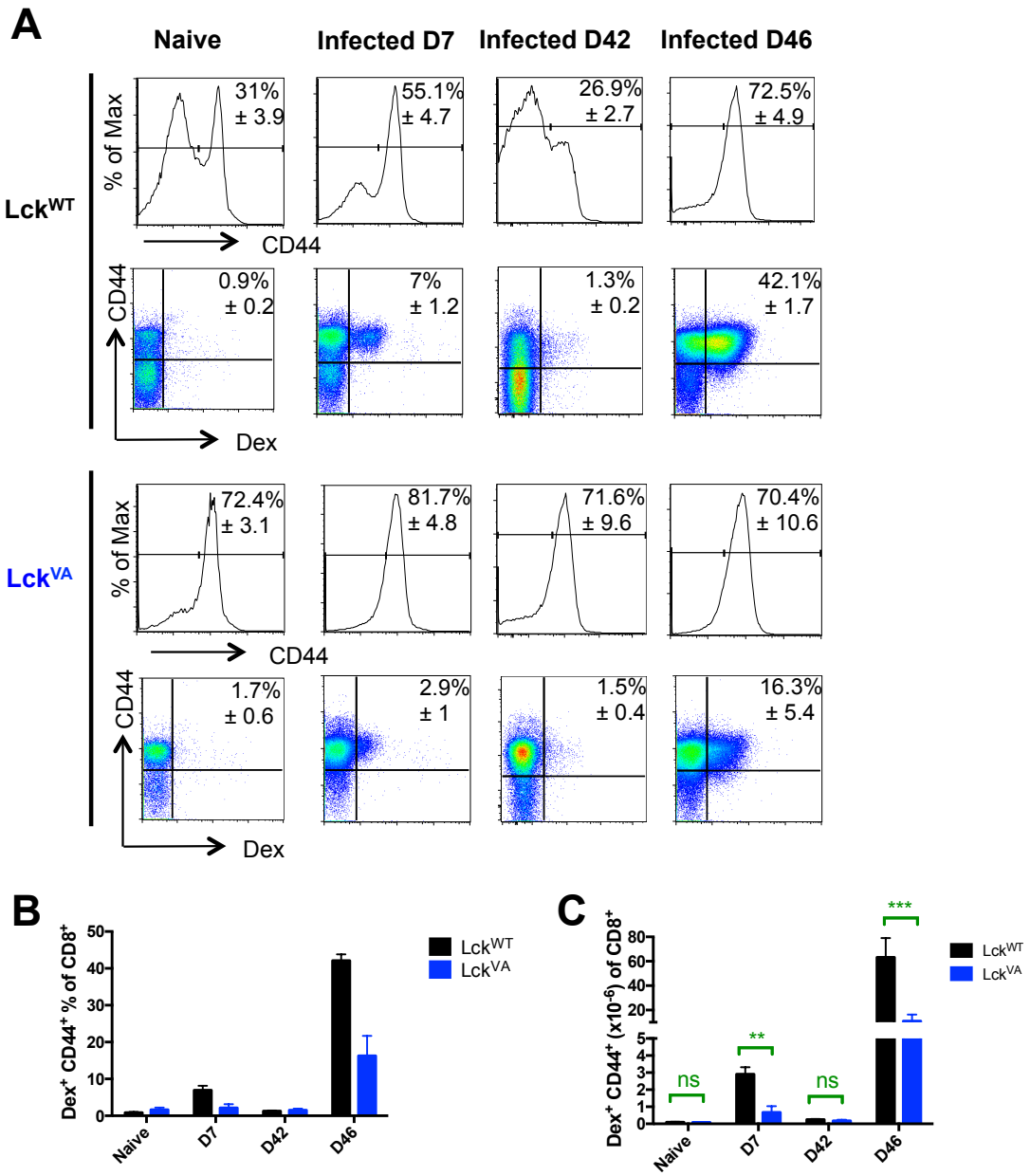

Fig. 5.2 Lck^{VA} mice generated fewer OVA-specific T cells in both the primary and the secondary responses.
CD8$^+$ splenocytes in naïve (uninfected) and infected Lck^{WT} and Lck^{VA} mice were analysed at indicated time points for CD44 and Dex expression. (A) Representative histograms show average percentages ± SD of CD44$^+$ cells (top row). Representative dot plots show CD44 versus Dex staining with proportions of *LmOVA* specific CD44$^+$Dex$^+$ indicated in top right as averages ± SD (bottom row). The average proportions (B) and numbers (C) of CD8$^+$CD44$^+$Dex$^+$ cells are shown in bar charts. All values are plotted as means of 3-5 mice per group ± SD. Data are representative of 2 experiments per time point. Significance was calculated on Prism: parametric, unpaired, two-tailed, student's t-test *P<0.05, **P<0.01, ***P<0.001.

Conceivably, this reflects the increased proportions of memory-phenotype cells in Lck^{VA} mice (Fig.5.2A) that are known to have a continuous slow turnover (Benigni et al., 2005). On day 7 of infection a clear proliferative response to *Listeria* was recorded in both Lck^{VA} (60.4±6.2%) and Lck^{WT} (40.6±2.6%) T cells, again, this was significantly higher in Lck^{VA} mice ($p=0.0071$). By day 42 the pathogen is long cleared, and a contraction of the effector response has occurred (Mannering et al., 2002). The T cells were largely in a resting state, as reflected in the reduced $CD8^+Ki\text{-}67^+CD44^+$ T cell proportions in both Lck^{VA} (8.3±1.1%) and Lck^{WT} mice (5.2±0.2%). Once again, however, the proportions of $CD8^+Ki\text{-}67^+CD44^+$ T cells were significantly higher in Lck^{VA} mice ($p=0.0012$). Upon secondary infection, on day 46, an enhanced recall response was measured with $CD8^+Ki\text{-}67^+CD44^+$ T cell proportions in both Lck^{VA} (75±2.5%) and Lck^{WT} mice (79.3±2.4%), above that seen on day 7. This was significantly higher in Lck^{WT} mice ($p=0.04$).

The $CD8^+Ki\text{-}67^+CD44^+$ T cell numbers were also calculated for each time point (Fig.5.3C). In naïve Lck^{VA} mice, although the proportions of $CD8^+Ki\text{-}67^+CD44^+$ T cells were significantly higher, the actual cell number was significantly lower ($p=0.025$), reflecting the lower total $CD8^+$ T cell numbers calculated in Fig.5.1D. On days 7 and 42, there was no significant difference between Lck^{VA} and Lck^{WT} mice in terms of $CD8^+Ki\text{-}67^+CD44^+$ T cell numbers. On day 46, the $CD8^+Ki\text{-}67^+CD44^+$ T cell numbers were significantly lower in Lck^{VA} mice ($p=0.0083$) compared to Lck^{WT} mice.

Overall, the data here showed that the total proliferation to *Listeria* during the primary response in Lck^{VA} mice was similar to Lck^{WT} mice when comparing $CD8^+Ki\text{-}67^+CD44^+$ T cell numbers, which was in agreement with the equal $CD8^+$ T cell numbers on day 7 (Fig.5.1D). The overall proliferative response in secondary *Listeria* infection, as measured by cell number, was significantly reduced in Lck^{VA} mice as compared to Lck^{WT} mice on day 46, which is also in agreement with the significantly decreased $CD8^+$ T cell numbers on day 46 (Fig.5.1D). However, the observation that both Lck^{WT} and Lck^{VA} T cells had similar proportions of $CD8^+Ki\text{-}67^+CD44^+$ cells, but fewer cells in total, may

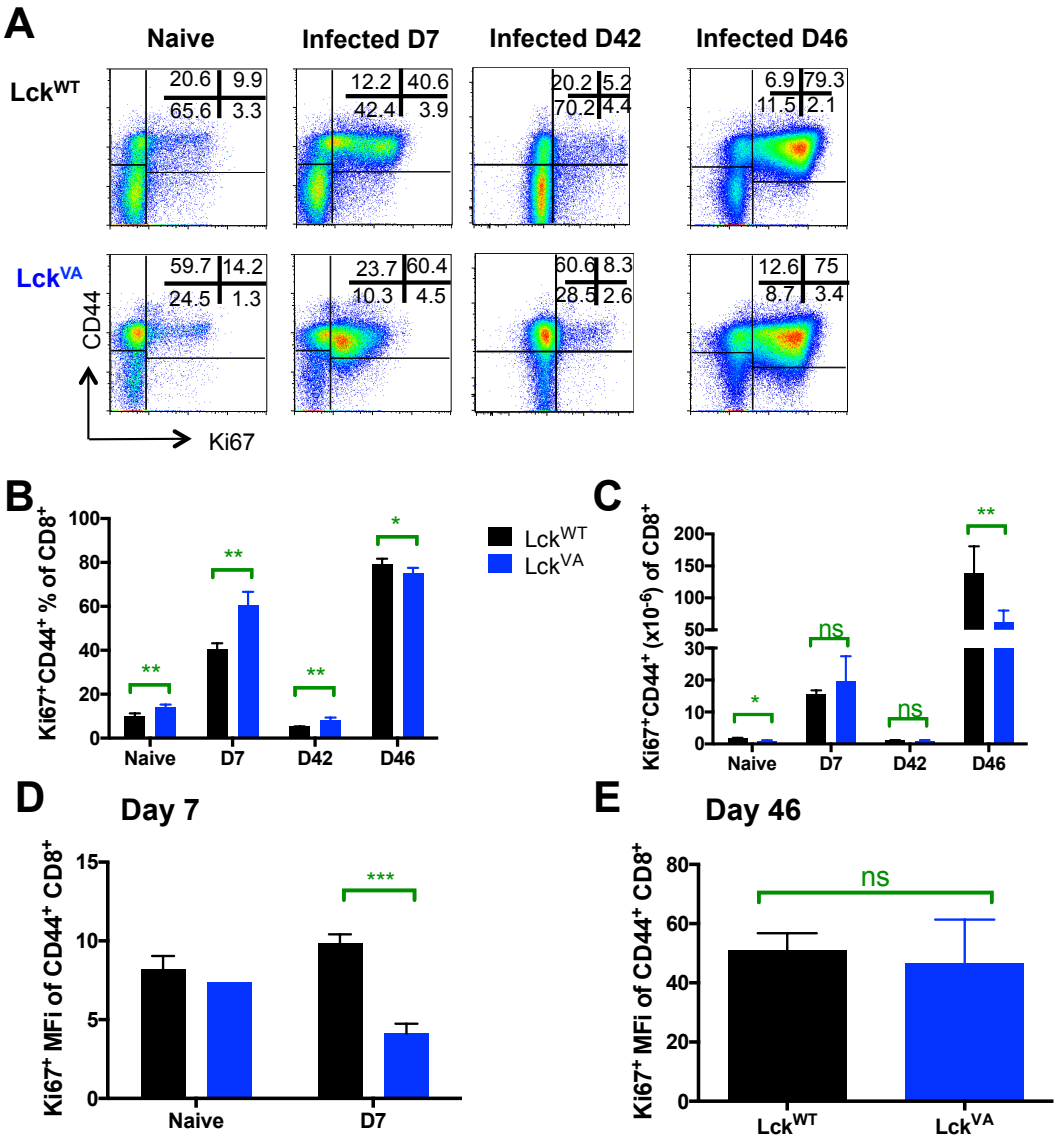

Fig. 5.3 The proliferative response to *Listeria* infection was characterised by Ki-67 expression in Lck^{VA} and Lck^{WT} CD8$^+$ T cells.
Ki-67 expression was measured by intracellular staining in Lck^{WT} and Lck^{VA} mice at indicated time points. (A) Representative dot plots show CD44 versus Ki-67 staining. Quadrants show average percentages of a group of 3-5 animals. Bar charts show average percentages (B) and numbers (C) of CD8$^-$CD44$^-$Ki-67$^-$ cells. The error bars show SD. The average MFI ± SD is shown for CD8$^-$CD44$^-$Ki-67$^-$ gates in naïve and day 7 infected mice (D) and day 46 mice (E). Results are representative of 2 independent experiments. Note that the data for proportions of Ki-67$^-$ cells was pooled between experiments, but for MFI's this was not possible and so no significance test was done on MFI of naïve CD8$^-$CD44$^-$Ki-67$^-$ samples due to n=2. Significance was calculated on Prism: parametric, unpaired, two-tailed, student's t-test *P<0.05, **P<0.01, ***P<0.001.

indicate that Lck^{VA} cells were undergoing more cell death. Both Lck^{WT} and Lck^{VA} T cells had reduced Ki-67 expression on day 42, which indicated that both had undergone a contraction in the immune response and T cells were largely quiescent.

L. monocytogenes infection induces a similar clonal expansion in $CD4^+$ T cells to that seen in $CD8^+$ T cells (Pamer, 2004). $CD4^+$ T cells have also been shown to be important for inducing the long-term memory potential of $CD8^+$ T cells (Sun et al., 2004). Therefore, we also measured Ki-67 expression in $CD4^+$ T cells (Fig.5.4). Basal proliferation in naïve $CD4^+$ cells was proportionally slightly higher than in $CD8^+$ T cells, but there was no significant difference between Lck^{VA} (17.3±3.7%) and Lck^{WT} (12.4±2.3%) $CD4^+Ki\text{-}67^+CD44^+$ T cells. On day 7 $CD4^+Ki\text{-}67^+CD44^+$ increased proportionally in both Lck^{VA} and Lck^{WT} mice. However, there was again no significant difference between Lck^{VA} (30.1±1.6%) and Lck^{WT} mice (25±3.0%). As with $CD8^+$ T cells, an improved recall response was identified in $CD4^+Ki\text{-}67^+CD44^+$ T cells on day 46 in both Lck^{VA} and Lck^{WT} mice, and it was significantly higher ($p=0.0175$) in Lck^{VA} (54.7±4.2%) than Lck^{WT} (44.5±2.7%) mice.

The $CD4^+Ki\text{-}67^+CD44^+$ T cell numbers, shown in Fig.5.4C, were calculated for each time point. The proportions of $CD4^+Ki\text{-}67^+CD44^+$ T cells in naïve Lck^{VA} mice were not significantly different from Lck^{WT}, and neither were the actual cell numbers, but there was a trend for them to be lower in Lck^{VA} mice. During the primary response on day 7, $CD4^+Ki\text{-}67^+CD44^+$ T cell numbers were significantly lower ($p=0.017$) in Lck^{VA} mice compared to Lck^{WT} mice. On day 46 Lck^{VA} had significantly higher proportions of $CD4^+Ki\text{-}67^+CD44^+$ T cells, but the $CD4^+Ki\text{-}67^+CD44^+$ T cell numbers were significantly reduced ($p=0.0064$) in Lck^{VA} compared to Lck^{WT} mice. These results reflected the lower $CD4^+$ T cell proportions and numbers calculated in Fig.5.1E and F. Overall, the data regarding proliferation in $CD4^+$ T cells, suggested two things. Firstly, that the $CD4^+$ T cell primary and secondary proliferative responses were similar in Lck^{VA} and Lck^{WT} mice as measured by the proportions of cells in the cell cycle expressing Ki-67. Secondly, the reduced overall numbers of $CD4^+Ki\text{-}67^+CD44^+$

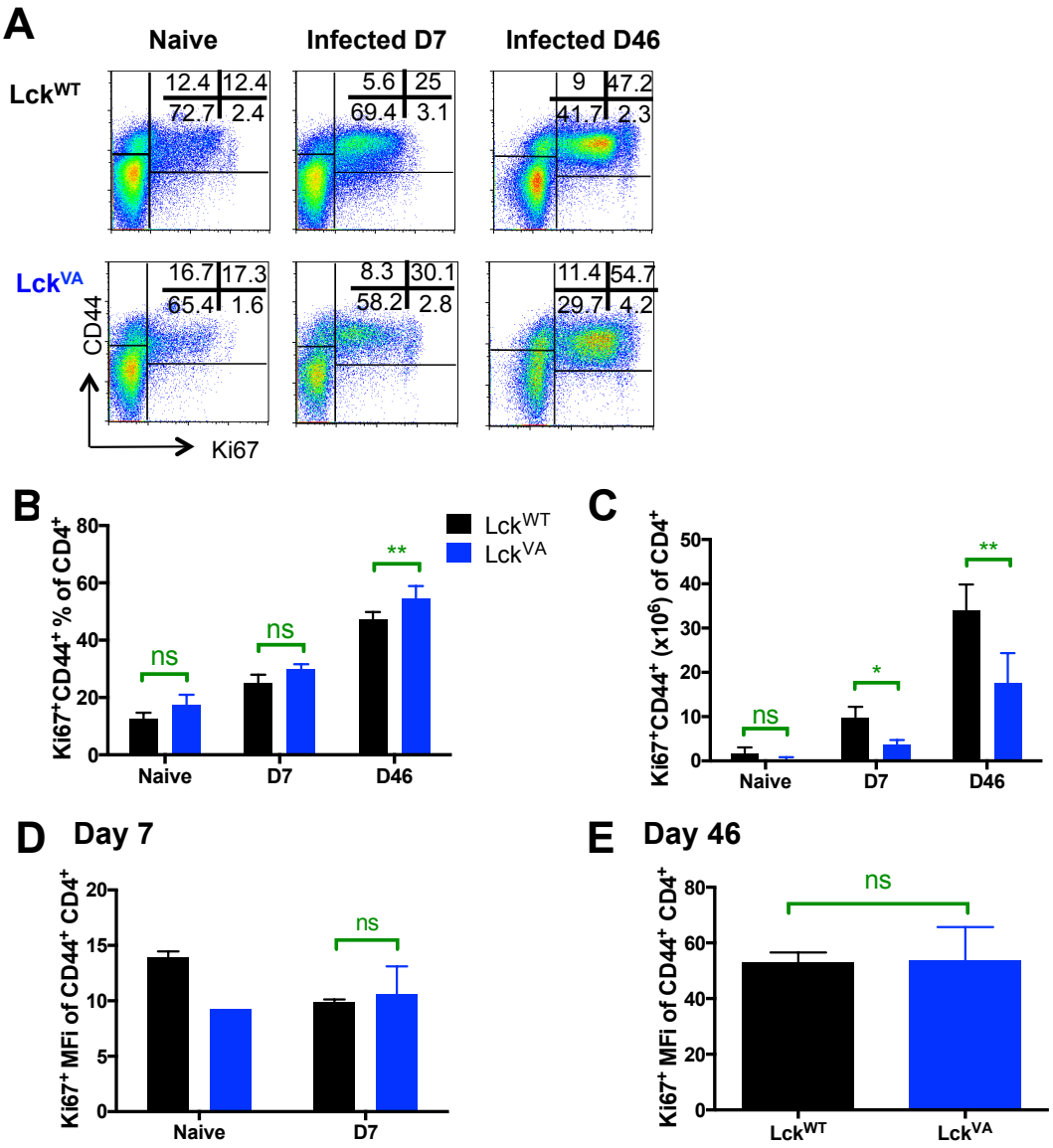

Fig. 5.4 The numbers of CD4$^+$ proliferating cells in *Listeria* infection were reduced in Lck^{VA} mice.

Ki-67 expression was measured by intracellular staining in Lck^{WT} and Lck^{VA} mice at indicated time points. (A) Representative dot plots show CD44 versus Ki-67 expression in CD4$^+$ T cells. Quadrants show average percentages of a group of 3-5 animals. Bar charts of average of proportions (B) and numbers (C) of CD4$^+$CD44$^+$Ki-67$^+$ cells are shown. Error bars denote the SD. The MFI was calculated for CD4$^+$CD44$^+$Ki-67$^+$ cells and the averages ± SD from indicated days are represented in bar charts (D and E). Results are representative of 2 independent experiments. Note that the data on proportions was pooled between experiments but for MFI's this was not possible and so no significance test was done on naïve CD4$^+$CD44$^+$Ki-67$^+$ cell MFIs due to n=2. Error bars represent standard deviations. Significance was calculated on Prism: parametric, unpaired, two-tailed, student's t-test *P<0.05, **P<0.01, ***P<0.001.

T cells in Lck^{VA} mice, although reflecting the lower $CD4^+$ T cell numbers (Fig.5.1E and F), suggested that they too may be undergoing more cell death. There is some evidence that the MFI of Ki-67 staining indicates different cell-cycle stages and differential localization of the Ki-67 protein within cells (Danova et al., 1988; Starborg et al., 1996). Although we did not study the cell-cycle progression in these experiments, we found that on all days, except day 7, there were no differences in MFI of Ki-67 expression in $CD8^+$Ki-67^+CD44^+ T cells between Lck^{WT} and Lck^{VA} mice (Fig.5.3D and E). On day 7, however in Lck^{VA} mice Ki-67 MFI was significantly lower ($p=0.0003$) than in Lck^{WT} T cells (Fig.5.3D). This may suggest an accumulation of cells in the final, M phase (Mitosis - cell is ready to split into two daughter cells) in Lck^{VA} cells, perhaps indicating that they went faster through the cell cycle or that they had delayed mitosis. If they went faster through the cell cycle, we would expect to see increased proliferation in $CD8^+$ T cells on day 7, but this was not the case (Fig.5.1D and Fig.5.3C). Thus it was more likely that Lck^{VA} mice have delayed mitosis or that they went through the cell cycle faster and also died faster. More detailed experiments addressing the cell cycle would need to be done to confirm such conclusions, especially since Ki-67 MFI was not significantly different on day 46 in $CD8^+$ T cells.

There were no differences in Ki-67 MFIs in $CD4^+$Ki-67^+CD44^+ T cells between Lck^{WT} and Lck^{VA}mice (Fig.5.4D and E).

5.2.3 Effector cytokine production from Ova-specific cells was reduced in Lck^{VA} mice in *LmOVA* infection

Production of IFNγ and TNFα by multiple cell types, is a critical component of both innate and adaptive immunity to *L.monocytogenes* infection (Pamer, 2004). Inflammatory cytokine production early in infection is important for naïve cell differentiation into IFNγ producing effector cells (Pape et al., 1997). Furthermore, IFNγ-gene knockout mice readily succumb to *L.monocytogenes* infection (Harty and Bevan, 1995). In chapter 4 we showed differential effects on effector cytokine production in response to *in vitro* stimulation of $F5Lck^{VA}$ T cells. When $F5Lck^{VA}$ T cells cultured with IL-2 and cognate peptide the

cytokine production was reduced, however, culturing them without the IL-2 step the cytokine production was enhanced, as compared to F5Lck^{WT} T cells.

We first assessed the cytokine production in Lck^{VA} and Lck^{WT} mice during *Listeria* infection. To this end splenocytes were harvested from both naïve and infected animals on days 7 and 46 of *LmOVA* infection - the primary and secondary responses, respectively. The cells were cultured overnight with a titration of HKL, made from the same batch of *LmOVA* used in the initial i.v. injections, in an effort to stimulate IFNγ and TNFα cytokine production that we could measure by ELISA.

Although we could not distinguish which cells produced cytokine by this assay, they were specific for prior infection with *Listeria* as no IFNγ was produced in response to HKL by cells from naïve Lck^{VA} or Lck^{WT} cells *in vitro* (Fig.5.5A and B). The amount of IFNγ produced in both Lck^{VA} and Lck^{WT} cell cultures increased in an HKL concentration dependent manner on both days 7 and 46 (Fig.5.5A and B). There was a trend for less IFNγ to be produced by Lck^{VA} cells than by Lck^{WT} cells at all concentrations of HKL stimulation on both days 7 and 46, however, no statistical significance was found (Fig.5.5 A and B). On day 46, IFNγ production was seen already at the lowest 0.1x10^{6} HKL concentration in both Lck^{VA} and Lck^{WT} mice (Fig.5.5B), which is in agreement with the notion that a recall response is stronger than the primary response. There was a large variation between biological replicates, probably highlighting the variability of infection between mice.

TNFα production was only measured on day 7 (Fig.5.5C). The amount of TNFα produced in both Lck^{VA} and Lck^{WT} cultures increased in an HKL concentration dependent manner (Fig.5.5C). Some TNFα production was induced even in naïve mice, indicating that the bacteria could induce some production of TNFα directly in vitro. This may be due to other cells, such as macrophages, producing TNFα during an innate immune response to HKL *in vitro* (Pamer, 2004). Furthermore, at the highest concentration of HKL (10x10^{6}) naïve Lck^{WT} mice produced the same amount of TNFα as infected Lck^{WT} mice *in vitro* (Fig.5.5C). At all concentrations of HKL stimulation Lck^{VA}

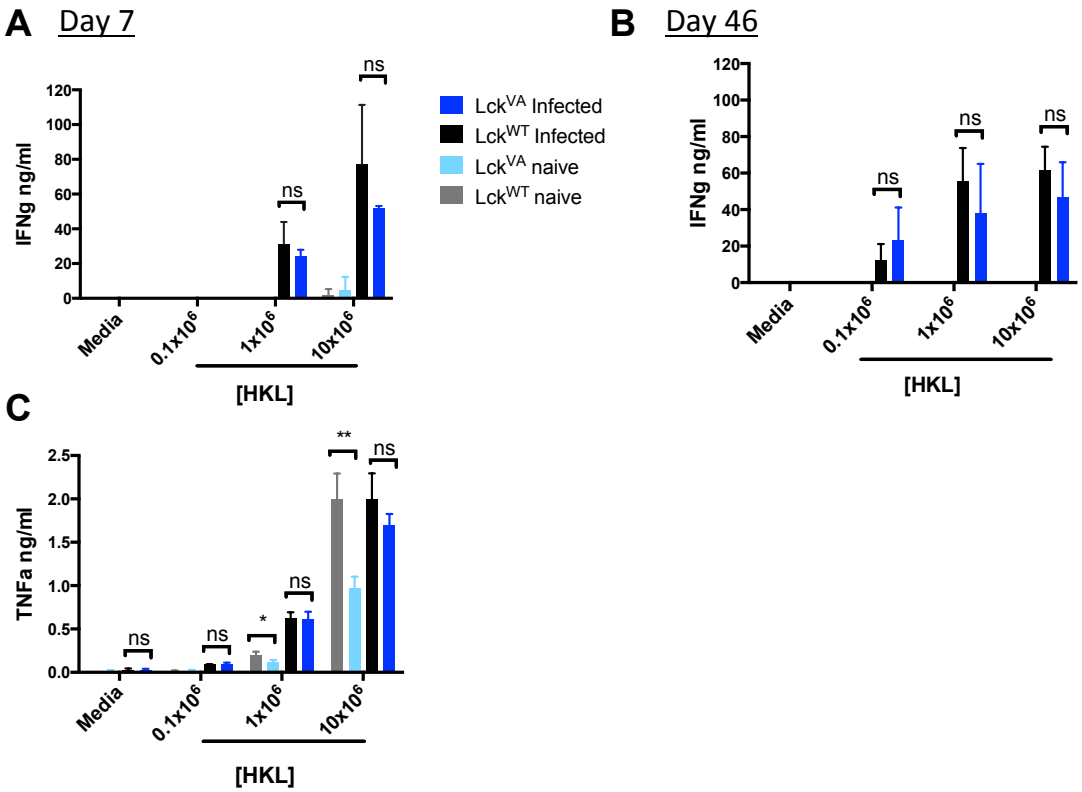

Fig. 5.5 IFNγ and TNFα production upon recall with HKL was similar between Lck^{WT} and Lck^{VA} mice.

Splenocytes from 3 individual Lck^{WT} and Lck^{VA} mice culled at indicated times were cultured overnight with the indicated titrations of HKL. Production of IFNγ on day 7 (A) and day 46 (B), and TNFα on day 7 (B) were measured by ELISA. Data in bar charts represent means ± SD. Significance was calculated on Prism: parametric, unpaired, two-tailed, student's t-test *P<0.05, **P<0.01, ***P<0.001.

cells produced same amounts of TNFα as Lck^{WT} cells, except at the highest concentration of HKL, where both naïve and infected Lck^{VA} cells produced less TNFα than Lck^{WT} cells (Fig.5.5 C).

A caveat with these data is that HKL stimulation has only been done once for each time point of *LmOVA* infection. Overall, the data indicated that there were no differences in TNFα and IFNγ production in response to HKL stimulation in Lck^{VA} and Lck^{WT} cells.

LmOVA infection induces a $CD8^+$ T cell response specific for the H-$2K^b$-restricted SIINFEKL (N4) peptide. IFNγ and TNFα production in response to N4 can thus be used as a measure of TCR sensitivity to antigen stimulation (Joshi et al., 2007). Therefore, we asked whether there was a difference in the production of IFNγ or TNFα from antigen-experienced cells between Lck^{VA} and Lck^{WT} mice infected with *LmOVA* by re-stimulating splenocytes with the N4 peptide *in vitro* 7 days post-infection (Fig.5.6A). When cells from naïve mice were cultured in media only a very small proportion of cells made IFNγ in both Lck^{VA} (0.4±0.05%) and Lck^{WT} mice (0.3±0.12%). The same was true for cells from Lck^{VA} (0.6±0.4%) and Lck^{WT} infected mice (0.4±0.3%) after being cultured in media alone and there were no significant differences between these populations (Fig.5.6A). The low proportions of IFNγ producing cells, found in naïve Lck^{VA} (light blue fill) and Lck^{WT} (grey fill) mice, stayed constant at all concentrations of N4 tested. Overall this confirmed that the increase in proportions of cells producing IFNγ, seen in cells from infected animals, was N4-peptide specific (Fig.5.6A). A concentration dependent increase in the proportions of IFNγ producing cells, in both Lck^{WT} (black line) and Lck^{VA} (dark blue line) infected mice was seen (Fig.5.6A). There were significantly reduced proportions of IFNγ producing Lck^{VA} $CD8^+$ T cells, as compared to Lck^{WT}, at all concentrations of N4-peptide stimulation (Fig.5.6A), which was in line with our data in Fig.5.2B and C that showed Lck^{VA} mice had significantly lower numbers of $CD8^+Dex^+CD44^+$ Ova-specific cells.

In C57BL/6 mice, in addition to a strong $CD8^+$ mediated OVA-antigen specific T cell responses, *LmOVA* also stimulates a strong $CD4^+$ T cell

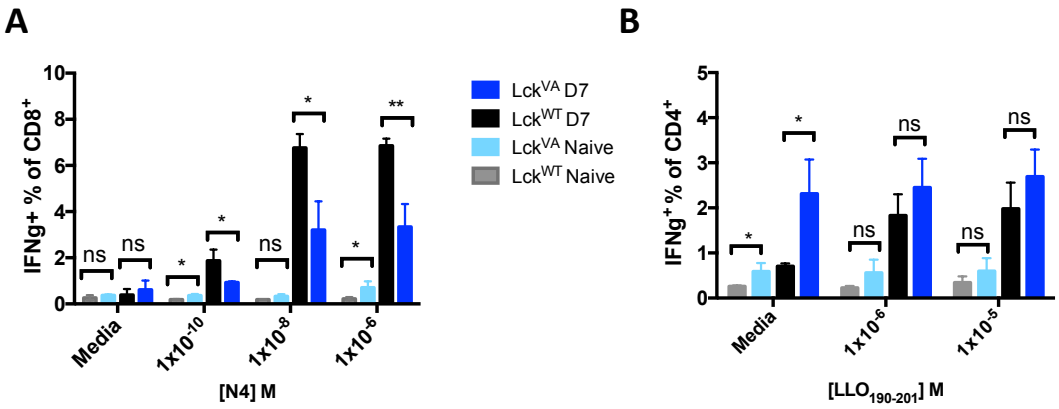

Fig. 5.6 Lck^{VA} mice had reduced proportions of Ova-specific CD8^{+} IFNγ^{+} T Cells upon *in vitro* re-stimulation 7 days post-infection.

Lck^{WT} and Lck^{VA} mice were challenged with *LmOVA* for 7 days. Thereafter splenocytes were restimulated for 4h in the presence of Brefeldin-A with a titration of N4-peptide (A) or LLO$_{190-201}$ peptide (B) for IFNγ producing CD8^{+} or CD4^{+} T cells, respectively. Intracellular staining for cytokines was performed and the results were acquired by flow cytomtery. This experiment was done once with n=3 mice per group. Data represent the mean ± SD. Significance was calculated on Prism: parametric, unpaired, two-tailed, student's t-test *P<0.05, **P<0.01, ***P<0.001.

response to $LLO_{190-201}$ (Geginat et al., 2001; Haring and Harty, 2006). We, therefore re-stimulated splenocytes 7 days post-infection with a titration of $LLO_{190-201}$ and measured the proportions of IFNγ producing $CD4^+$ T cells (Fig.5.6B). Very low proportions, <1% of IFNγ producing cells were found in naïve Lck^{VA} (light blue fill) and Lck^{WT} (grey fill) mice and this stayed constant at all concentrations of $LLO_{190-201}$ stimulation. A concentration dependent increase in the proportions of IFNγ producing cells, from Lck^{WT} (black fill) but not Lck^{VA} (dark blue fill) infected mice was seen (Fig.5.6B). Cells from infected Lck^{VA} mice had significantly higher (p=0.02) proportions of IFNγ producing $CD4^+$ T cells cultured in media alone. The proportions IFNγ producing $CD4^+$ T cells were similar in Lck^{VA} mice compared to Lck^{WT} mice at all concentrations of $LLO_{190-201}$ tested (Fig.5.6B). Unfortunately, this experiment has only been done once on day 7 and would require repeating to confirm the conclusions. However, because the total IFNγ production in response to HKL was similar in Lck^{VA} mice on day 7 but the OVA-specific IFNγ production was significantly reduced (Fig.5.5A and Fig.5.6A) it is possible that Lck^{VA} would have more IFNγ producing $CD4^+$ T cells than Lck^{WT} mice.

We next measured the proportions of peptide specific $CD8^+$ and $CD4^+$ IFNγ and TNFα-producing T cells after a secondary infection on day 46 (Fig.5.7). Very low proportions, <2% of TNFα or IFNγ producing cells were found in naïve Lck^{VA} (light blue fill) and Lck^{WT} (grey fill) mice and this stayed constant at all concentrations of N4 and $LLO_{190-201}$ stimulations (Fig.5.7A-D). A concentration dependent increase in the proportions of IFNγ and TNFα producing $CD8^+$ and $CD4^+$ T cells, in both Lck^{WT} (black fill) and Lck^{VA} (dark blue fill) infected mice, was seen (Fig.5.7A-D). In agreement with data acquired on day 7 (Fig.5.6A), Lck^{VA} mice had significantly reduced proportions of IFNγ producing $CD8^+$ T cells as compared to Lck^{WT} at all concentrations of N4-peptide stimulation (Fig.5.7A) as well as significantly reduced proportions of TNFα producing $CD8^+$ T cells (Fig.5.7B). These data correlate with the results in Fig.5.2 that showed the total numbers of Ova-specific cells were significantly lower in Lck^{VA} mice on day 46. It should be noted that although we saw 80% of $CD8^+$ cells in Lck^{WT} mice were producing IFNγ on day 46 (Fig.5.7A) yet we only recorded 42.1% of $CD8^+$ T cells as being Ova-specific at

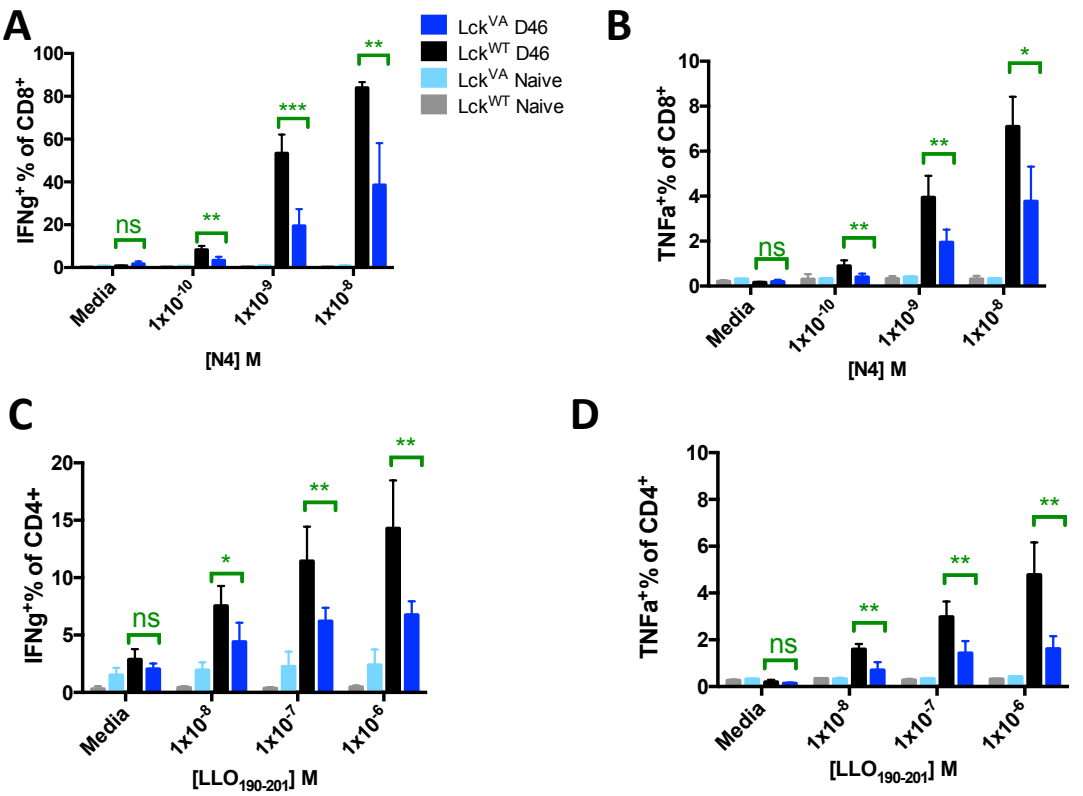

Fig. 5.7 Lck^{VA} mice had reduced proportions of antigen-specific IFNγ and TNFα producing cells after secondary infection.
Lck^{VA} and Lck^{WT} mice were challenged with a secondary *LmOVA* infection on day 42 and results were acquired on day 46. Splenocytes were restimulated for 4h in the presence of Brefeldin-A with indicated concentrations of N4-peptide for proportions of IFNγ (A) and TNFα (B) producing CD8$^+$ T cells, or LLO$_{190-201}$ for proportions of IFNγ (C) and TNFα (D) producing CD4$^+$ T cells. The cytokines were stained for intracellularly and the results were acquired by flow cytometry. Data are representative of 2 independent experiments with n=2 in naïve groups (does not allow for statistical analysis) and n=5 in infected groups. Data represent the mean ± SD. Significance was calculated on Prism: parametric, unpaired, two-tailed, student's t-test *P<0.05, **P<0.01, ***P<0.001.

the same time point (Fig.5.2). Dextramer binding might therefore be underestimating the proportions of antigen-specific T cells. The data also showed that Lck^{VA} mice had significantly reduced proportions of IFNγ producing $CD4^+$ T cells, at all concentrations of $LLO_{190-201}$ stimulation after secondary infection (Fig.5.7 C), as well as significantly reduced proportions of TNFα producing $CD4^+$ T cells at all concentrations of $LLO_{190-201}$ stimulation, as compared to Lck^{WT} cells (Fig.5.7D).

Collectively, these data suggested that Lck^{VA} have similar effector cytokine production in response to primary and secondary *Listeria* infections when measured by HKL recall, however, the antigen-specific effector responses in $CD8^+$ and $CD4^+$ T cells were reduced.

5.2.4 Maintenance of *Listeria* specific T cells through the contraction phase of the immune response was enhanced in Lck^{VA} mice

Although, Lck^{VA} mice had decreased proportions and numbers of *Listeria* specific cells (Fig.5.2) and they made a reduced Ova-specific effector response (Fig.5.6 and 5.7), the data in Chapter 4 indicated that Lck^{VA} T cells expressed increased levels of Bcl-2 (Fig.4.10), an important anti-apoptotic molecule and marker of long-term memory cells (Kaech and Cui, 2012). The questions we wished to address were, whether the survival of Lck^{VA} T cells was altered through the contraction phase following infection, and how this would impact upon the generation of memory cells.

Similarly to Ki-67 staining, BrdU staining can be used as a measure of cell proliferation. BrdU is a thymidine analogue and thus is incorporated into the DNA of proliferating cells (Tough and Sprent, 1994). The advantage of BrdU staining over Ki-67 is that once a cell has proliferated and incorporated BrdU it will remain $BrdU^+$, even when it later becomes quiescent.

We injected mice with BrdU on day 4 after primary *LmOVA* infection and BrdU was also given in drinking water during the peak of the infection days 4 – 10, thereby ensuring that all cells proliferating to *Listeria* could

incorporate BrdU. The BrdU incorporation was measured by analysis of intracellular staining on flow cytometry on days 7, 42 and 46.

Staining for BrdU requires a harsh DNase treatment of the cells. This caused an artefact of staining, the appearance of a very bright Dex^+ population of cells, which was excluded as shown in Fig.5.8A. This population is clearly visible on CD44 versus Dex dot plots in the double positive quadrant (Fig.5.8A top row). The population consistently represented 1-3% of Dex^+ cells, even in naïve mice, where we know the frequency is generally <1% in samples not subject to the BrdU staining protocol, and we therefore gated it out using histogram analysis (Fig.5.8A middle row). The removal of this artefact did not interfere with the real Dex staining (Fig.5.8A bottom row). We continued all further flow cytometry analysis on the gated populations. We used several controls to confirm real BrdU staining (Fig.5.8B). We compared cells without DNAse treatment and without BrdU staining to cells that were DNAse treated, but without BrdU staining. It was clear that the treatment severely affected cell morphology and the live gate on forward and side scatter had to be adjusted. The treatment itself did not create false positive events in the BrdU gate. When we stained DNase treated cells for BrdU we saw a clear population appear in the BrdU gate (Fig.5.8B).

Our results showed that, like Ki-67 staining, BrdU staining reliably measured cell proliferation as there was little BrdU incorporation in $CD8^+$ T cells in naïve Lck^{WT} mice (2.8±1%), but this increased significantly (p=0.0093) with infection (17±6.3%) on day 7. The background staining for BrdU was higher in naïve Lck^{VA} mice (11.4±0.9%) but the proportions of $CD8^+BrdU^+$ T cells still increased significantly (p=0.0079) with infection on day 7 (18±2.8%) (Fig.5.9A). The proportion of $BrdU^+$ cells was significantly higher (p=0.0003) in naïve Lck^{VA} mice than Lck^{WT} mice but there was no significant difference between them on day 7. The higher background staining in Lck^{VA} mice may have been due to the high proportions of $CD44^+$ cells present in naïve mice as shown in Fig.5.2A.

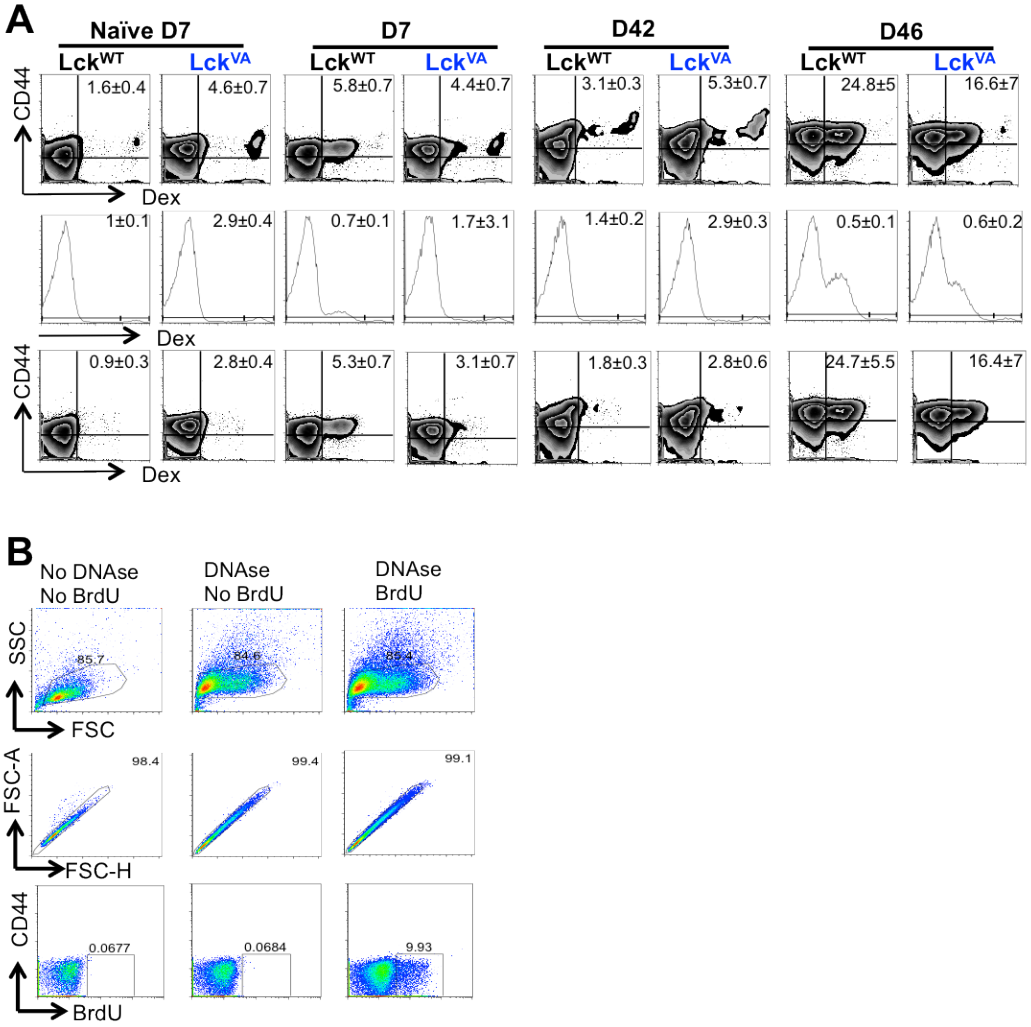

Fig. 5.8 Exclusion of artefacts and the gating strategy for BrdU staining.
Lck^{VA} and Lck^{WT} mice were injected BrdU i.p on day 4 post-infection with *LmOVA*. BrdU was also fed in drinking water on days 4-10 post-infection. (A) Top row shows zebra plots of CD44 vs Dex staining. The middle row shows on a histogram the gating for excluding the $CD44^{-}Dex^{hi}$ artefact. The third row shows new zebra plots of CD44 vs Dex gating without the artefact. Numbers on dot plots show average proportions ± SD. (B) Representative plots of BrdU staining controls with representative values. BrdU was gated for as shown by FSC vs SSC, and doublets were excluded by gating for FSC-H vs FSC-A.

By day 42, the infection has been cleared and the majority of effector cells have died in the contraction of infection, as can be seen in the reduction of cell numbers in Fig.5.1B. The cells that remain represent the memory pool. The proportions of $CD8^+BrdU^+$ cells decreased in infected mice on day 42 in both Lck^{WT} (2.1±0.4%) and Lck^{VA} (8.6±2.2%) mice (Fig.5.9A). Yet, the proportion of $CD8^+BrdU^+$ memory T cells was significantly higher ($p=0.0018$) in Lck^{VA} mice as compared to Lck^{WT} mice on day 42. The background staining for naïve mice culled on day 42 as controls, was low in both Lck^{WT} (1.1%) and Lck^{VA} (2.4%) mice (Fig.5.9A). These results indicated several things, firstly that Lck^{VA} mice maintain increased proportions of cells during the contraction phase that initially proliferated in the primary response, compared to Lck^{WT} mice, suggesting these were true *Listeria* specific memory cells. Secondly, the reduced proportions of $CD8^+BrdU^+$ T cells in naïve mice on day 42 as compared to day 7 suggested that the increased $CD44^+$ pool of cells in Lck^{VA} mice turns over enough to dilute out BrdU incorporation. Finally, not all BrdU incorporation was Dex specific on day 7 (Fig. 5.9B), which suggested the response to *Listeria* involved a broad T cell repertoire.

Ideally, one would also expect to see some Dex^+BrdU^+ cells on day 42, representing the Ova-specific memory response. However, this typically occurs in less than 10% of cells thus the sensitivities of Dex and BrdU may not be sufficient (Pamer, 2004).

To estimate the incorporation of $BrdU^+$ above background levels we subtracted the background BrdU incorporation in Dex^+ and Dex^- cells, as seen in uninfected mice on each day, from the incorporation seen in infected mice (Fig.5.9B). The results of this calculation, shown in Fig.5.9C, indicated that Lck^{VA} mice (5.5%) had 6.8-fold higher proportions of Dex^-BrdU^+ cells on day 42 than Lck^{WT} (0.8%) mice.

On day 46 the proportions of $CD8^+BrdU^+$ T cells were very low in both Lck^{WT} (0.7±0.1%) and Lck^{VA} mice (2.3±1.2%), which suggested that vigorous proliferation in secondary response led to the dilution of BrdU to undetectable levels, confirming that the labelled cells at day 42 from infected

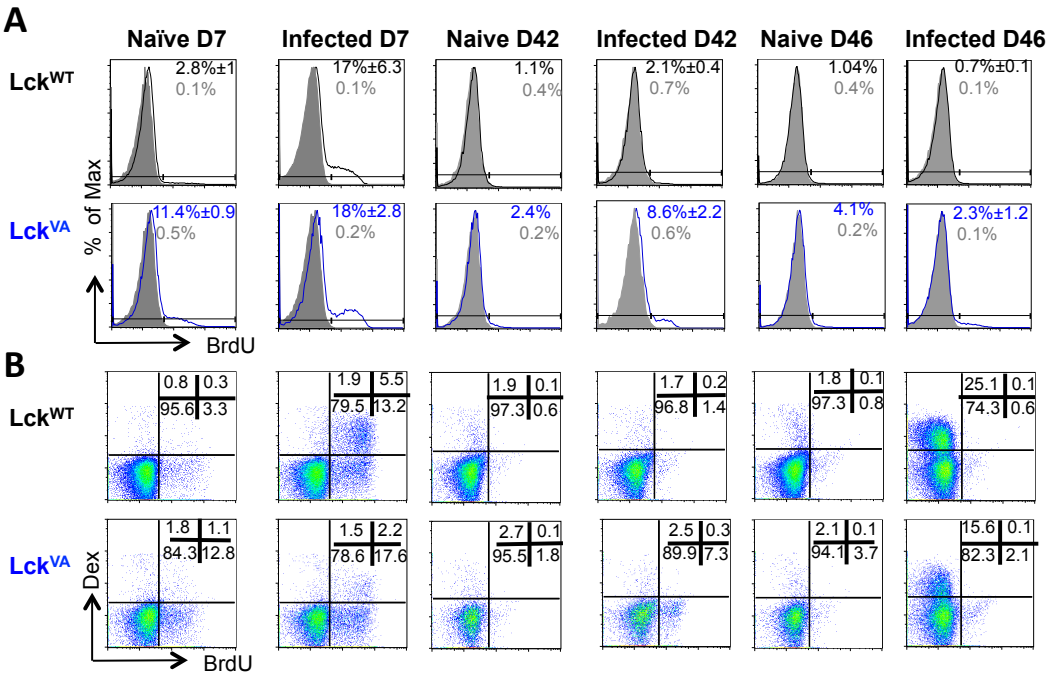

C

Subtraction of naïve background	Day 7		Day 42		Day 46	
	Lck^{WT}	Lck^{VA}	Lck^{WT}	Lck^{VA}	Lck^{WT}	Lck^{VA}
Dex$^+$BrdU$^+$	5.2	1.1	0.1	0.2	0	0
Dex$^-$BrdU$^+$	9.9	4.8	0.8	5.5	0.2	0

Fig. 5.9 Maintenance of *Listeria* specific CD8$^+$BrdU$^+$ T cells was enhanced in Lck^{VA} mice.
Lck^{VA} and Lck^{WT} mice (n=2-5) were injected with BrdU i.p on day 4 post-infection with *LmOVA*. BrdU was also fed in drinking water on days 4-10 post-infection. (A) Representative histogram overlays show isotype control antibody (grey filled histogram) and BrdU staining in Lck^{WT} (black) and Lck^{VA} (blue) mice, gated on CD8$^+$ T cells. (B) Representative dot plots show Dex vs BrdU staining in CD8$^+$ T cells. All numbers in part A and B show average proportions ± SD. (For n=2 the SD was not calculated). (C) The table shows the results of the calculation: Dex$^-$BrdU$^+$% or Dex$^+$BrdU$^+$% in naïve mice minus the result in infected mice on indicated days. Values used are those in part B. Data are representative of 2 independent experiments for Naïve and day 42, and 1 experiment for day 7 and day 46. Significance was calculated on Prism: parametric, unpaired, two-tailed, student's t-test *P<0.05, **P<0.01, ***P<0.001.

mice were indeed *Listeria* specific. This was supported by the observation that Dex and BrdU staining were mutually exclusive on day 46 (Fig.5.9B).

We also assessed BrdU incorporation in $CD4^+$ T cells. The data were similar to that in $CD8^+$ T cells in that naïve Lck^{WT} $CD4^+CD44^+$ T cells had small proportions (3.7±1.3%) of BrdU incorporation initially and this increased on day 7 (11.5±3.1%). However, the background was again higher in naïve Lck^{VA} $CD4^+CD44^+$ T cells (15.6±1.7%) but still increased on day 7 (35.4±3.2%) (Fig.5.10A).

The proportions of $CD4^+BrdU^+CD44^+$ cells were low on day 42 in infected Lck^{WT} (0.8%±0.2) and Lck^{VA} mice (2.1%±0.6), respectively, but not much higher than the proportions of cells in naïve mice on day 42 in Lck^{WT} (0.5%) and Lck^{VA} mice (1.4%). Unfortunately, we could not test for significant differences in naïve mice on day 42 because only 2 mice were culled per group. These results, however, indicated that in contrast to $CD8^+$ T cells there is limited maintenance of $CD4^+$ T cell memory in either mouse strain. On day 46 the proportions of $CD4^+BrdU^+CD44^+$ T cells stayed very low in both Lck^{WT} (0.5±0.1%) and Lck^{VA} (0.7±0.2%) mice.

Collectively, these data suggested that both Lck^{VA} and Lck^{WT} $CD8^+$ T cells maintained a pool of *Listeria* specific $BrdU^+$ memory T cells on day 42 but not $CD4^+$ T cells. The proportions of *Listeria* specific memory $CD8^+$ T cells maintained was significantly greater in Lck^{VA} mice (Fig.5.9).

Expression of the anti-apoptotic molecule Bcl-2 has been implicated in T cell memory formation, particularly in T cell survival during the contraction phase post-primary response (Dunkle et al., 2013). We showed in chapter 4 that F5Lck^{VA} express more Bcl-2 *ex vivo* as well as upon *in vitro* activation (Fig.4.10). Therefore, we next investigated whether Lck^{VA} T cells also express more Bcl-2 during *in vivo* infection, particularly on day 42. To this end we measured Bcl-2 expression in $CD8^+$ T cells from naïve Lck^{WT} and Lck^{VA} mice on days 7, 42 and 46 post-*LmOVA* infection.

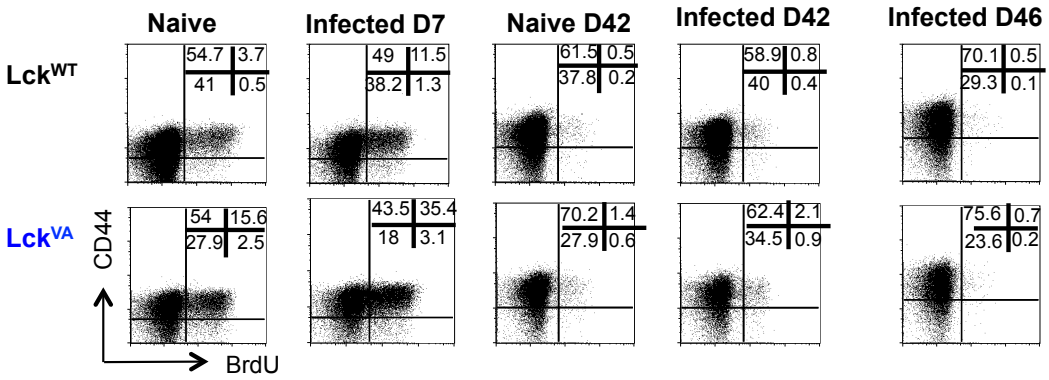

Fig. 5.10 CD4$^+$ T cells did not maintain a *Listeria* specific BrdU$^+$ T cell pool.
Lck^{VA} and Lck^{WT} mice (n=2-5) were injected with BrdU i.p on day 4 post-infection with *LmOVA*. BrdU was also fed in drinking water on days 4-10 post-infection. At indicated time points during the course of *LmOVA* infection splenocytes from Lck^{WT} and Lck^{VA} were intracellularly stained for BrdU. (A) Representative dot plots of CD44 vs BrdU staining are shown for CD4$^+$ T cells, numbers show averages of a minimum of 2 mice in each naïve group and a minimum of 3 in each infected group. Data are representative of 2 independent experiments for naïve and day 42, and 1 experiment for day 7 and day 46.

The data in Fig.5.11 showed that in naïve and infected day 7 cells, stained with the Bcl-2 isotype antibody as a negative control, non-specific staining was minimal in either Lck^{WT} or Lck^{VA} $CD8^+$ T cells. At all time points Bcl-2 and Dex staining were mutually exclusive. The proportions of $CD8^+Dex^-Bcl\text{-}2^+$ T cells were similar at all time points between Lck^{VA} and Lck^{WT} mice. Only on day 46, Lck^{VA} mice had significantly higher proportions (5.5±0.5%, p=0.0028) of $CD8^+Dex^-Bcl\text{-}2^+$ T cells compared to Lck^{WT} mice (3.9±0.4%). On day 42, the proportions of $CD8^+Dex^-Bcl\text{-}2^+$ T cells were ~2-fold higher in Lck^{VA} (8.5±6.8%) mice than in Lck^{WT} mice (3.6±0.9%), however the large SD in Lck^{VA} mice suggests this was not consistent between animals.

We also measured the MFI of Bcl-2 expression in the Dex^-Bcl2^+ gate, which indicated the relative abundance of Bcl-2 expressed per cell (Fig.5.11B-C). A significant decrease in $Bcl\text{-}2^+$ MFI was seen in Lck^{VA} T cells upon infection on day 7 but not in Lck^{WT} T cells (Fig.5.11B) At all time points, except day 46, $Bcl\text{-}2^+$ MFI was higher in Lck^{VA} T cells than in Lck^{WT} T cells and in most cases this was significant (Fig.5.11B and C).

Overall, these data showed that Lck^{VA} $CD8^+$ T cells had a significantly higher MFI of Bcl-2 expression in naïve mice than Lck^{WT}, at the peak of the primary infection on day 7, as well as on day 42 (Fig.5.11B and C). On day 46 the trend for increased Bcl-2 MFI in Lck^{VA} mice was not significant compared to Lck^{WT} mice (Fig.5.11C). Significance could not be tested naïve mice on day 42 because only two animals for each genotype were used, but the trend is the same as in day 7 mice with Lck^{VA} T cells having higher Bcl-2 MFI. The data in Fig.5.11 are thus in agreement with data presented in chapter 4, suggesting that proportionally more Lck^{VA} $CD8^+$ T cells express higher levels of Bcl-2, which might contribute to the enhanced maintenance of $CD8^+BrdU^+$ T cells on day 42.

5.2.5 Role of Lck in the development of distinct memory T cell populations

The effector population of $CD8^+$ T cells that arises in an infection is a very heterogenous pool of cells that can be subdivided into groups with distinct

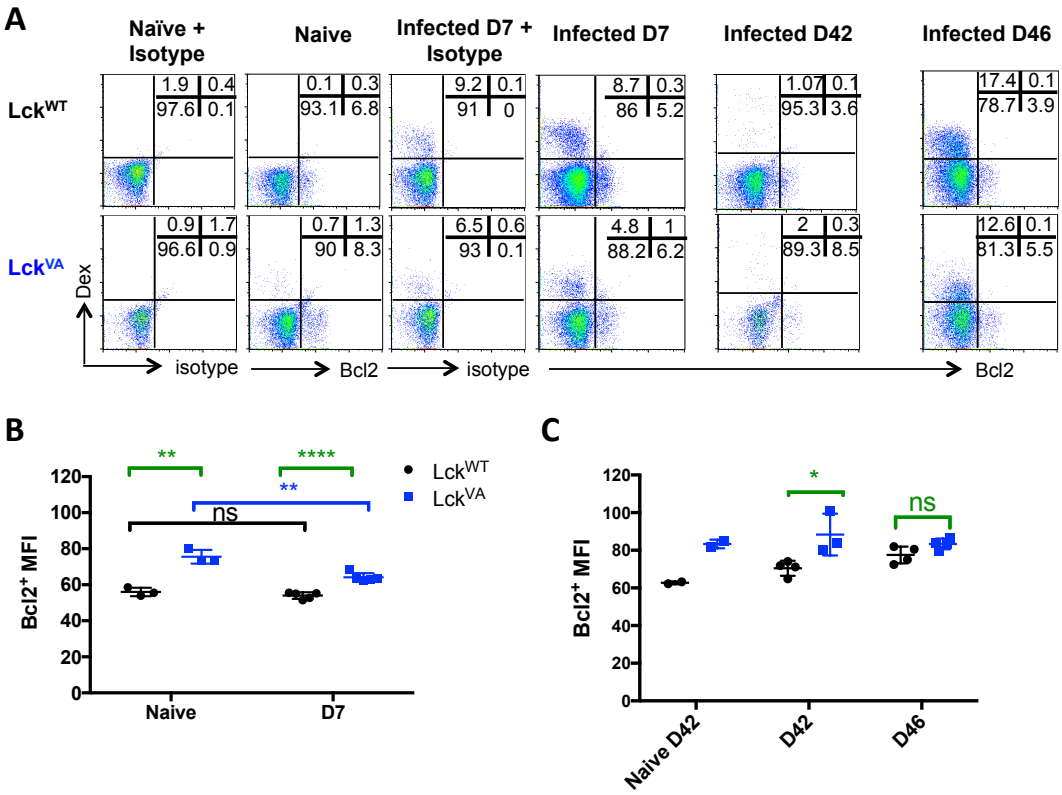

Fig. 5.11 Lck^{VA} CD8^{+} T cells expressed more Bcl-2 than Lck^{WT} CD8^{+} T cells.
Splenocytes from naïve and infected Lck^{WT} and Lck^{VA} mice were stained for expression of Dex, CD8 and Bcl-2 on indicated days. (A) Representative dot plots show Dex versus Bcl-2 staining in CD8 splenocytes. Values shown on the dot plots are means of 2-5 mice per group. Bcl-2 staining was controlled for by isotype staining done on a pool of all samples in each group on indicated days. Graphs of average Dex Bcl-2 MFI ± SD in CD8 T cells on day 7 (B) and days 42 and 46 (C) are shown. Data are from one experiment. Significance was calculated on Prism: parametric, unpaired, two-tailed, student's t-test *P<0.05, **P<0.01, ***P<0.001.

functional properties. Only a small proportion (~5-10%) of responding T cells survives to form a memory population. The expression patterns of CD44, CD62L and CCR7 can be used to broadly characterise T_{EM} and T_{CM} populations (Sallusto et al., 1999). T_{EM} cells typically produce cytotoxic proteins, home to inflamed peripheral tissues. T_{CM} cells typically home to secondary lymphoid organs and mount robust recall responses. CD127 and KLRG1 can be used to subdivide the effector phenotypes into MPECs ($CD127^{hi}KLRG1^{lo}$), and SLECs ($CD127^{lo}KLRG1^{hi}$) (Joshi et al., 2007). Although both MPEC and SLEC populations arise from the effector pool, these populations are functionally distinct. MPECs are destined to survive and become long-lived memory $CD8^{+}$ T cells, whereas SLECs are short-lived. SLECs have enhanced CTL functions, such as enhanced migration, expression of IFNγ and granzyme B (Kaech and Cui, 2012). MPECs on the other hand express increased Bcl-6, which enhances their survival (Kaech and Cui, 2012). However, not all $CD127^{hi}$ cells become memory cells and some $KLRG\text{-}1^{hi}CD127^{lo}$ cells can persist for some time after infection, thus other markers are needed (such as CD27) to further discriminate these populations (Joshi et al., 2007; Kaech et al., 2003).

Additionally, it has been shown that Bcl-2 expressing T cell populations have higher memory potential than $Bcl\text{-}2^{lo}$ cells (Dunkle et al., 2013). Dunkle et al. performed cell transfer experiments, where they transferred cells with different Bcl-2 expression levels and challenged the recipient mice with *LmOVA* (Dunkle et al., 2013). They found that cells expressing the highest Bcl-2 levels yielded the highest numbers of memory cells defined as $KLRG1^{lo}$ $CD127^{hi}$ (Dunkle et al., 2013). KLRG1 versus CD127 staining and CD44 versus CD62L are therefore not exclusive criteria for distinguishing memory cell populations after a primary response, however, in our study we used these markers to broadly characterise the memory potential of Lck^{VA} and Lck^{WT} mice.

We first looked at the proportions of cells in T_{EM} and T_{CM} compartments as characterised by CD44 and CD62L expression in $CD8^{+}$ and $CD4^{+}$ T cells in both Lck^{VA} and Lck^{WT} mice post-*LmOVA* infection (Fig.5.12). In our experiments, unfortunately, CCR7 staining did not work.

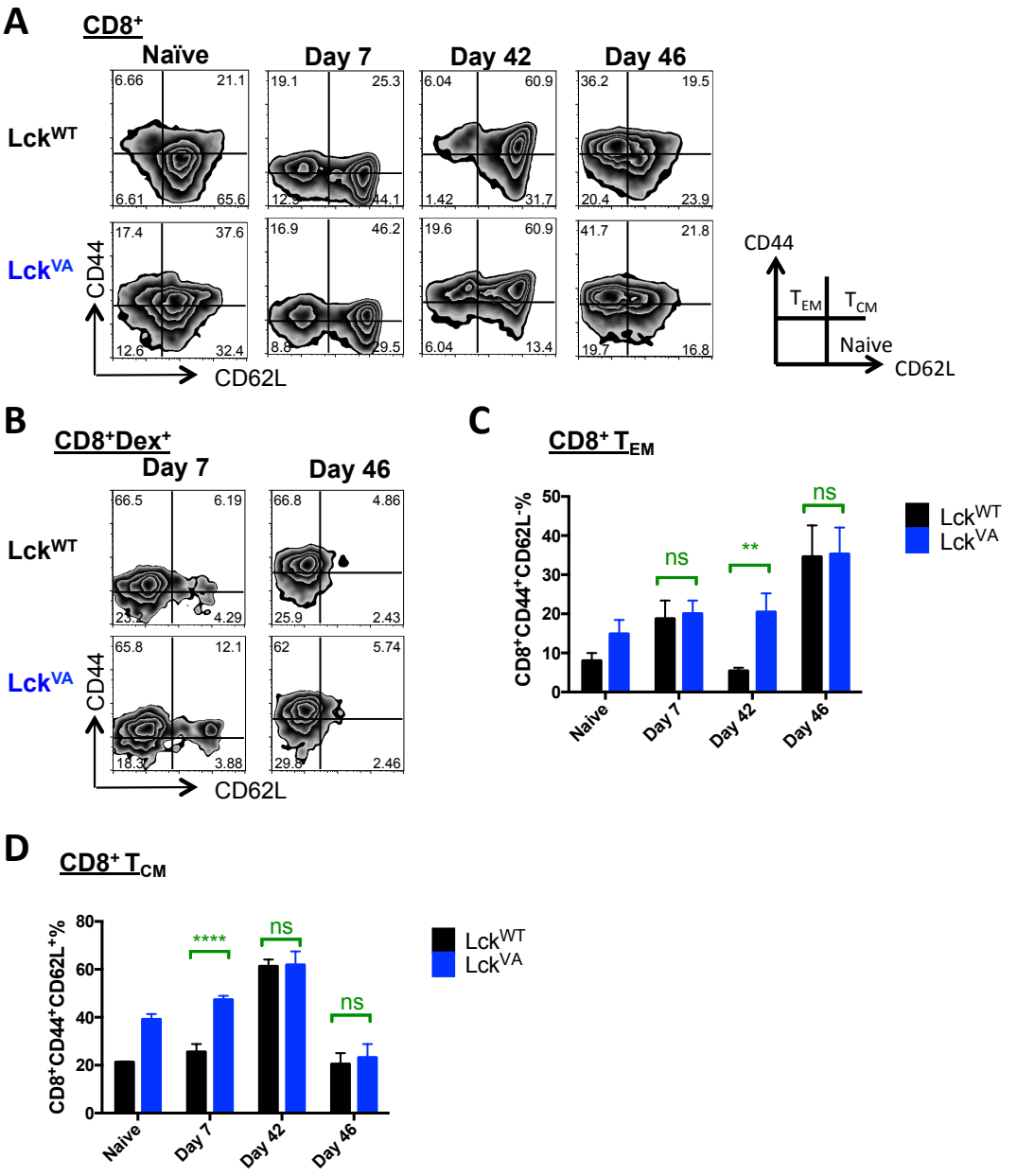

Fig. 5.12 Distribution of T_{EM} and T_{CM} CD8$^+$ T cells in Lck^{WT} and Lck^{VA} mice.
Splenocytes from naïve and *LmOVA* infected Lck^{WT} and Lck^{VA} mice were stained for expression of CD44, CD62L, and Dex on indicated days. (A) Representative dot plots with percentages show distribution of T_{EM} (CD44$^+$CD62L$^-$) and T_{CM} (CD44$^+$CD62L$^+$) populations in CD8$^+$ T cells. Gating was adjusted as necessary on individual days. (B) Representative dot plots with percentages show distribution of T_{EM} and T_{CM} populations in CD8$^+$Dex$^+$ T cells. Bar charts show average proportions (n=2-5) of CD8$^+$ T_{EM} ± SD (C) and CD8$^+$ T_{CM} ± SD. Significance was only calculated for groups where n≥3. Significance was calculated on Prism: parametric, unpaired, two-tailed, student's t-test *P<0.05, **P<0.01, ***P<0.001.

Lck^{VA} naïve mice were found to harbour increased proportions of T_{EM} (14.9 %) cells as compared to Lck^{WT} mice (8.0%), however because n=2 in this group we could not test for significance (Fig.5.12C). The increase in T_{EM} populations was probably due to increased CD44 expression *ex vivo* in Lck^{VA} mice (Fig.5.2). At the peak of primary *LmOVA* infection on day 7 T_{EM} cell proportions increased in both Lck^{WT} (18.8±4.6%) and Lck^{VA} mice (20.1±3.3%) above naïve levels, however, there was no significant difference between the two genotypes (Fig.5.12C). On day 42, Lck^{VA} mice had 4-fold higher proportions of $CD8^+$ T_{EM} cells than Lck^{WT} mice. This reflected the increased proportions seen in naïve mice but also correlated with the increased proportions of *Listeria* specific $CD8^+BrdU^+$ T cells maintained in Lck^{VA} mice as shown in Fig.5.9. On day 46, in both Lck^{VA} and Lck^{WT} mice ~40% of $CD8^+$ T cells were of T_{EM} phenotype, which correlated with the notion that a secondary immune response has a more efficient effector response than the primary.

Significantly higher proportions of $CD8^+$ T_{CM} cells were found in Lck^{VA} mice on day 7 ($p<0.0001$). However, there were no significant differences between $CD8^+$ T_{CM} proportions on days 42 and 46 in Lck^{VA} and Lck^{WT} mice (Fig.5.12D). We also showed that Dex specific $CD8^+$ T cells were ~62-67% of T_{EM} phenotype in both Lck^{VA} and Lck^{WT} mice (Fig.5.12B).

Naïve Lck^{VA} mice had more $CD4^+$ T_{EM} cells (45.1%) than Lck^{WT} mice (15.7%). Again, because n=2 in this group we could not test for significance (Fig.5.13B). On day 7, both Lck^{VA} (51.9%±5.2) and Lck^{WT} mice (25.4%±4.9) had an increase in $CD4^+$ T_{EM} cells in response to infection. On day 42 a contraction in the effector response was seen in both Lck^{VA} and Lck^{WT} $CD4^+$ T cells, but Lck^{VA} maintained significantly ($p=0.0018$) more $CD4^+$ T_{EM} cells than Lck^{WT} mice (Fig.5.13B). Both mouse strains also had a similar increase in T_{CM} populations on day 42, correlating with the formation of a memory pool, although this was smaller than in $CD8^+$ T cells. This is in line with published data that have shown $CD8^+$ T cells form the more prominent memory pool in *Listeria* infection (Ladel et al., 1994; Pamer, 2004). On day 46, proportions of

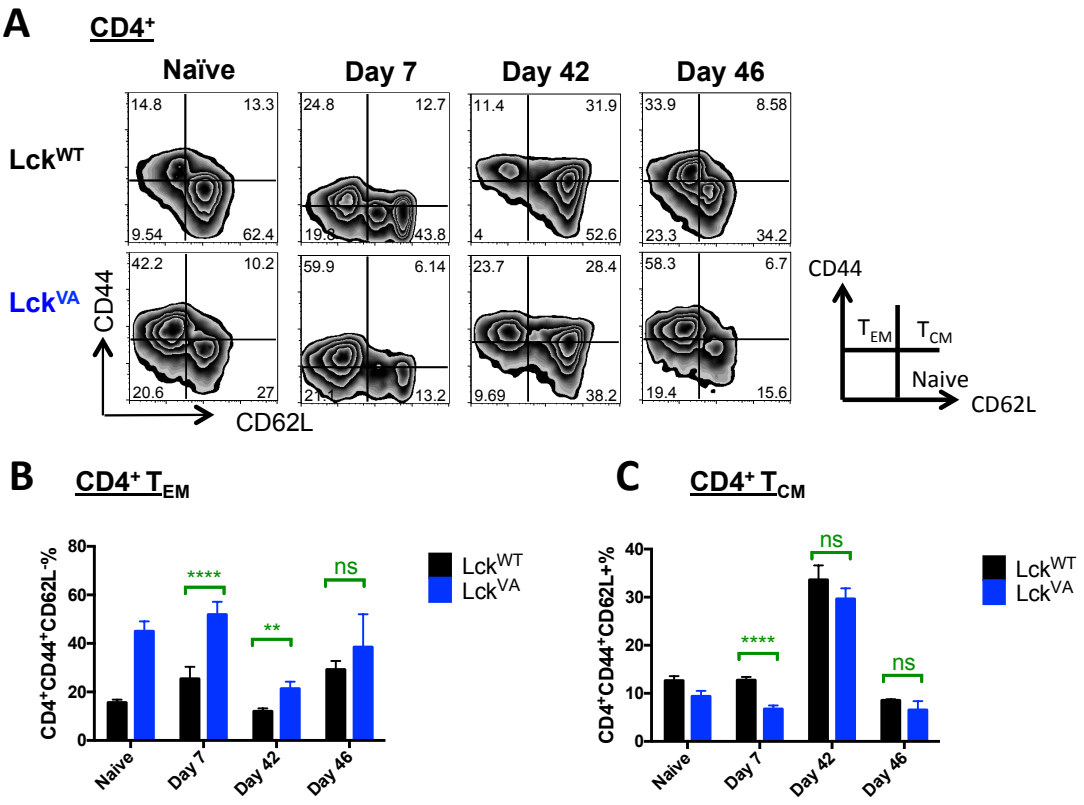

Fig. 5.13 Distribution of T_{EM} and T_{CM} CD4$^+$ T cells in Lck^{WT} and Lck^{VA} mice.
Splenocytes from naïve and *LmOVA* infected Lck^{WT} and Lck^{VA} mice were stained for expression of CD44 and CD62L on indicated days. (A) Representative dot plots with percentages show distribution of T_{EM} (CD44$^+$CD62L$^-$) and T_{CM} (CD44$^+$CD62L$^+$) populations in CD4$^+$ T cells. Gates were adjusted on individual days. Bar charts show average proportions (n=3-5) of CD4$^+$ T_{EM} ± SD (B) and CD4$^+$ T_{CM} ± SD. Significance was calculated on Prism: parametric, unpaired, two-tailed, student's t-test *P<0.05, **P<0.01, ***P<0.001. Data are from one experiment.

T_{EM} and T_{CM} populations were similar in Lck^{WT} and Lck^{VA} $CD4^+$ T cells (Fig.5.13C).

Overall these data showed that there were increased proportions of *Listeria* specific $CD8^+$ and $CD4^+$ T_{EM} populations in Lck^{VA} mice following the contraction phase of the immune response, as assessed on day 42. These cells were unlikely to be the $CD44^{hi}$ cells found in naïve mice because we showed in the BrdU incorporation experiments that $CD8^+CD44^{hi}BrdU^+$ cells were no longer present in uninfected mice on day 42 (Fig.5.9).

We also assessed the relative proportions of MPECs and SLECs in $CD8^+CD44^+$ T cells (Fig.5.14). Both Lck^{WT} and Lck^{VA} naïve (uninfected) mice had a population of $CD8^+$ T cells that were $CD44^{hi}$ and approximately 70% of these were also $CD127^{hi}$, most probably representing a pre-existing memory cell pool (Fig.5.15A and C). During the primary infection on day 7, equal proportions of KLRG-1^+ SLECs appeared in both Lck^{WT} (11.8±4.4%) and Lck^{VA} (10.0±2.6%) mice in response to the primary infection, and a reciprocal decline in the proportions of MPECs was seen (Fig.5.15B and C). Interestingly, our data showed that in both Lck^{WT} and Lck^{VA} mice there was also a $CD8^+CD127^+KLRG1^-$ $CD44^+$ T cell population (DPECS) (Fig.5.14). On day 7 the size of this population was similar in Lck^{WT} (10.48±3.7%) and in Lck^{VA} mice (9.4±3.1%).

The contraction of the effector response was assessed on day 42 and a decline in SLECs was noted in Lck^{WT} mice (2.6±0.4%) and Lck^{VA} mice (9.3±1.3%) compared to day 7 (Fig.5.15B), a pattern that is in agreement with previous reports (Joshi et al., 2007). In Lck^{VA} mice the proportions of SLECs on day 42 were significantly higher ($p=0.0002$) compared to Lck^{WT} mice. Strikingly, on day 42 the proportions of DPECs were also significantly higher ($p=0.0027$) in Lck^{VA} (36.3±11.7%) than in Lck^{WT} mice (5.2±0.5%), a 7-fold difference. Such a double positive effector cell population ($CD127^+KLRG1^+$) emerging after *LmOVA* infection has previously been described (Obar et al., 2011). Obar and colleagues showed that in secondary responses this population had a greater ability than SLECs to undergo expansion but less than that of MPECs and

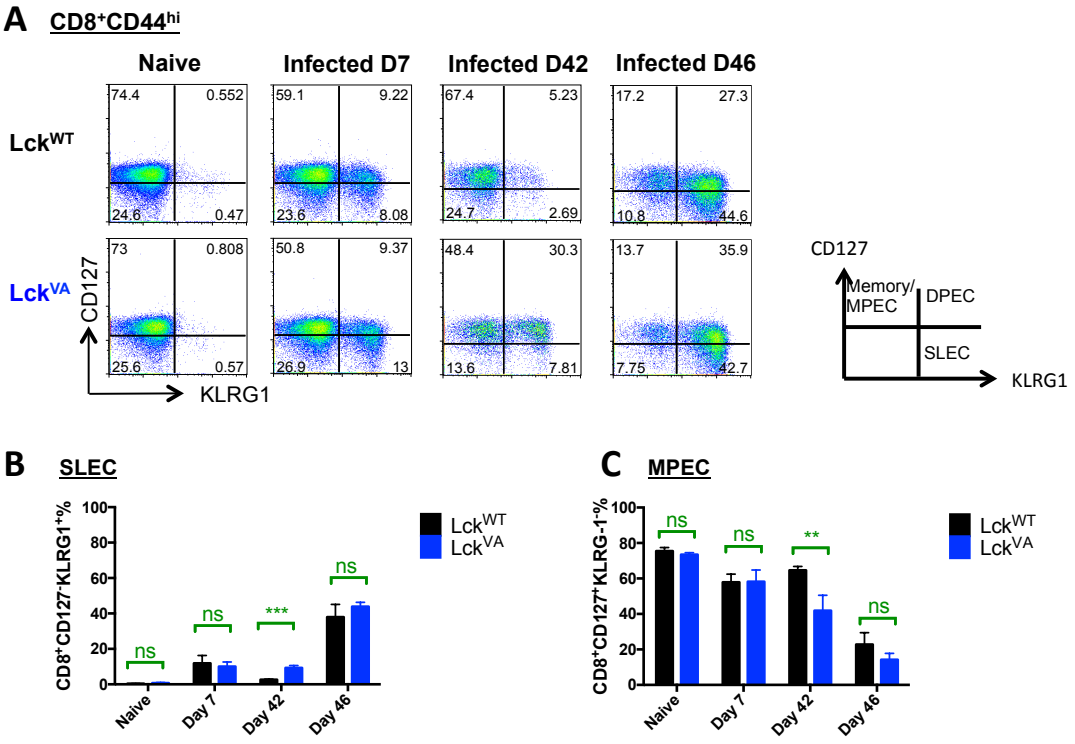

Fig. 5.14 Impact of reduced Lck expression on MPEC and SLEC populations during *LmOVA* infection

Splenocytes from naïve and infected Lck^{WT} and Lck^{VA} mice were stained for expression of CD127, KLRG1, CD44 and Dex on indicated days. (A) Samples were gated on total $CD8^+CD44^-$ T cells and subsequent CD127 versus KLRG1 staining shows distribution of MPEC, SLEC and DPEC populations. Values shown in the top right are means of 3-5 mice per group. Average proportions ± SD on indicated days are summarised in bar charts for SLECs (B) and MPECs (C). Data shown are representative of two independent experiments. Significance was calculated on Prism: parametric, unpaired, two-tailed, student's t-test *P<0.05, **P<0.01, ***P<0.001. Data are representative of two independent experiments.

they therefore suggested that the population can contribute to the effector responses but will not give rise to true MPECs (Obar et al., 2011).

In Lck^{WT} mice we found a modest increase in MPECs from day 7 (57.8±4.6%) to day 42 (64.6±2.1%) but a decrease in Lck^{VA} mice from day 7 (58.2±6.5%) to day 42 (41.9±8.7%). The proportions of MPECs were significantly lower ($p=0.0035$) in Lck^{VA} mice than in Lck^{WT} mice on day 42, most likely because a large proportion of the cells in Lck^{VA} mice were DPECs. There were no significant differences between Lck^{VA} and Lck^{WT} mice in proportions of SLECs or MPECs on day 46 (Fig.5.14) but DPEC proportions remained significantly higher ($p=0.0086$) on day 46 in Lck^{VA} mice (35.3±3.2%) compared to Lck^{WT} mice (25.1±4.2%).

We next asked whether the DPEC population maintained on day 42 in Lck^{VA} mice represented the $CD8^{+}BrdU^{+}$ T cell population described in Lck^{VA} mice on day 42 in Fig.5.9. To this end we gated for CD127 and KLRG-1 on the $CD8^{+}BrdU^{+}$ population. Indeed, the results shown in Fig.5.15 indicated that there were three-fold more DPECs in Lck^{VA} mice (39.9%) than there were in Lck^{WT} mice (13.1%).

5.2.6 Analysis of SLECs and MPECs

For a $CD8^{+}$ T cell to make a commitment decision whether to become a SLEC or an MPEC, several cues have to be integrated, including strength and duration of antigenic stimulation, costimulation, $CD4^{+}$ T cell help and amount of inflammation they are exposed to (e.g. cytokine IL-12 and its modulation of transcription factor T-bet) (Mescher et al., 2006). SLECs and MPECs also differ in functional, proliferative, trafficking and survival characteristics (Olson et al., 2013). One classical marker of localization is CD62L, T_{CM} cells are $CD62L^{+}$ and localise to lymphoid tissues and T_{EM} cells are $CD62L^{-}$ and localise to peripheral sites (Sallusto et al., 1999). We showed in Fig.5.12 that Lck^{VA} mice had increased proportions of $CD8^{+}$ T_{EM} cells and also that they had increased proportions of SLECs during the contraction phase in Fig.5.14. Fully mature T_{CM} $CD8^{+}$ T cells are $CD62L^{hi}$, KLRG-1^{lo}, $CD127^{hi}$, $CD27^{hi}$, $CD44^{hi}$ and their development is associated with low expression of Tbet

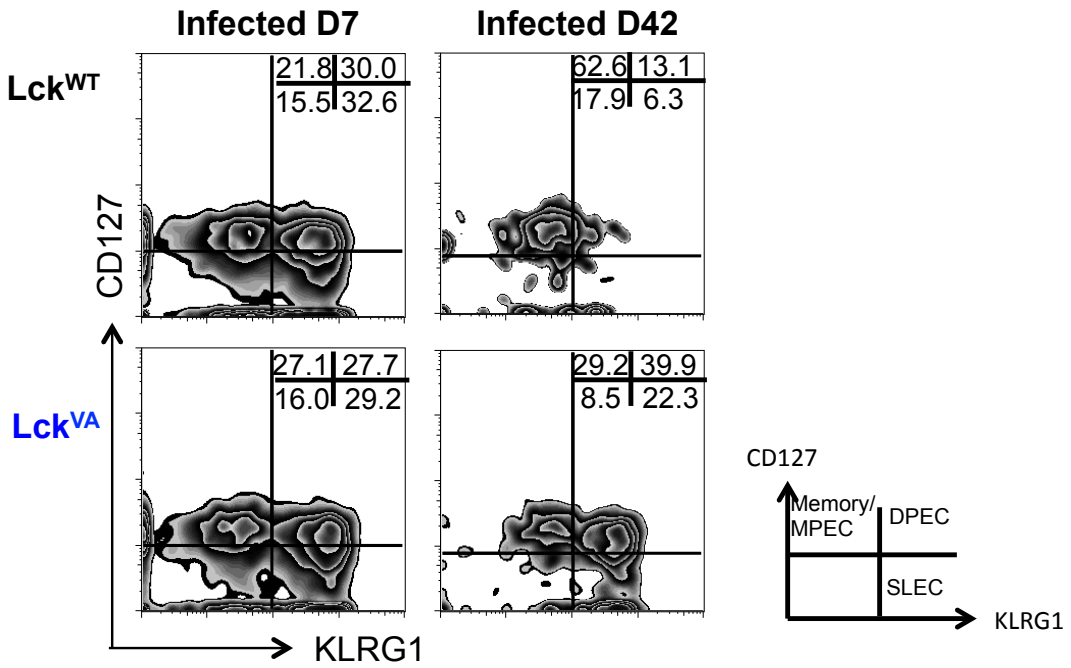

Fig. 5.15 The CD8$^+$BrdU$^+$CD44$^+$ maintained in Lck^{VA} mice after the contraction phase in *LmOVA* infection were KLRG1$^+$CD127$^+$ effector cells.
CD8$^+$BrdU$^+$CD44$^+$ T cells in Lck^{WT} and Lck^{VA} mice were analysed for KLRG-1 and CD127 staining on indicated days post *LmOVA* infection. Zebra plots are representative of n=3-5 individual mice, and the numbers show average proportions in each quadrant. Data are representative of one experiment.

(Joshi et al., 2007; Olson et al., 2013). Expression of the transcription factor Eomes has been shown to induce effector gene expression in activated $CD8^+$ T cells in cooperation with Tbet (Intlekofer et al., 2005). Additionally, a report by Hu et al. shows that the migratory pattern of activated T cells also impacts on the commitment of cell fate (Hu et al., 2011). Expression of CXCR3 in effector $CD8^+$ T cells enables trafficking to virus-infected cells in the periphery. CXCR3 expression peaked with the peak of LCMV infection, however, it was downregulated on $KLRG1^{hi}$ SLECs, terminally differentiated effector cells, but not $KLRG1^{lo}$ MPECs (Hu et al., 2011).

We therefore assessed the expression levels of CD62L and CXCR3, shown in Fig.5.16, as well as Tbet and Eomes, shown in Fig.5.17 in $CD8^+CD44^+$ SLEC and MPEC populations in Lck^{WT} and Lck^{VA} mice during different days of *LmOVA* infection. We wanted to investigate whether there were any Lck mediated differences in expression patterns of these markers that may explain the differences in relative proportions of effector and memory cells.

In naïve Lck^{WT} and Lck^{VA} mice there were very few SLECs (Fig.5.14) and therefore the histograms were quite uneven (Fig.5.16A and B). In naïve mice the MPEC population that was present, represented pre-existing memory cells and there was no difference in proportions of $CD8^+CD62L^+$ T cells between Lck^{WT} and Lck^{VA} mice (Fig.5.16A). The proportions of $CD8^+CD62L^+$ T cells were higher in SLECs than in MPECs on the same day in both Lck^{WT} and Lck^{VA} mice. Lck^{VA} mice had slightly higher proportions, than Lck^{WT} mice, of $CD8^+CD62L^+CD44^+$ T cells in SLECs on days 42 but the difference was not statistically significant. Similarly, on 46, the difference between CD62L expression in SLECs in Lck^{VA} and Lck^{WT} mice was not statistically significant suggesting the two genotypes are similar in their capacity to migrate to secondary lymphoid organs (Sallusto et al., 1999).

In MPECs, there was a bimodal expression of CXCR3 in both Lck^{WT} and Lck^{VA} mice (Fig.5.16B). The proportions of $CD8^+CXCR3^+CD44^+$ T cells were similar in MPECs of Lck^{VA} and Lck^{WT} mice on day 7. On day 42, Lck^{VA} mice had significantly higher proportions ($p<0.0001$) of $CD8^+CXCR3^+CD44^+$ T cells

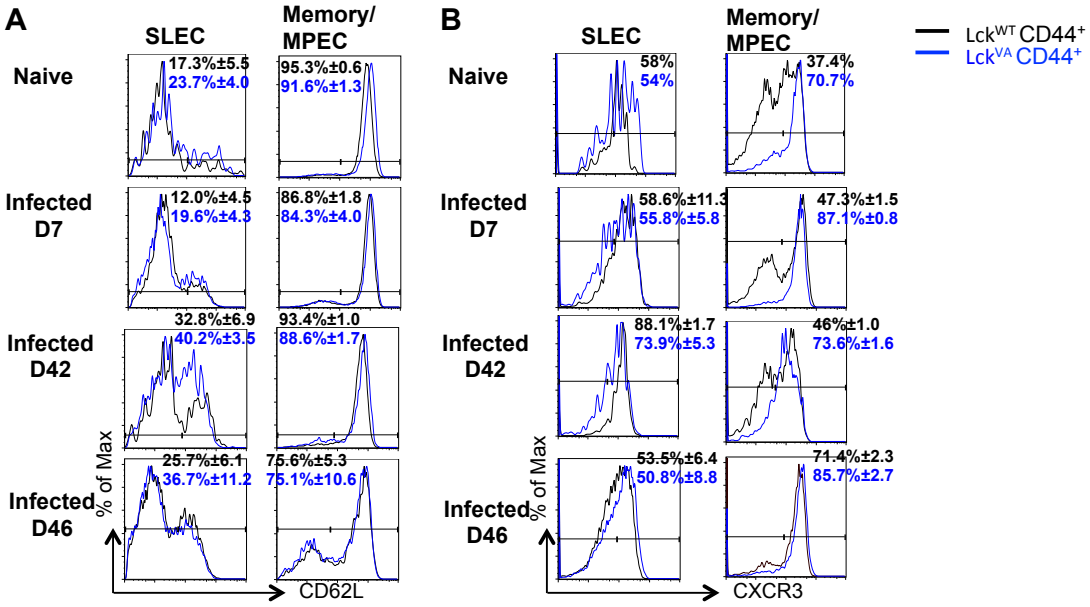

Fig. 5.16 Lck^{VA} CD8^{+} T cells had similar expression of CD62L in SLECs and increased CXCR3 in MPECs, compared to Lck^{WT} mice.
Splenocytes from Lck^{WT} (black line) and Lck^{VA} (blue mice) were stained for (A) CD62L and (B) CXCR3 expression in CD8^{+}CD44^{+} SLEC and MPEC populations in on indicated days post *LmOVA* infection. Histograms are representative of n=3-5 individual mice, and the numbers show average proportions ± SD of either CD62L^{-} or CXCR3^{-} cells. Significance was only calculated for groups where n≥3. Significance was calculated on Prism: parametric, unpaired, two-tailed, student's t-test *P<0.05, **P<0.01, ***P<0.001. Data are representative of one experiment.

and the same was true on day 46 (p=0.0002) (Fig.5.16B). High CXCR3 expression is a characteristic of MPECs (Kaech and Cui, 2012).

Overall, these data showed that CD62L expression is not significantly affected by Lck abundance, however, CXCR3 expression is constitutively higher in MPECs in Lck^{VA} mice than in Lck^{WT} mice although this population was proportionally smaller in Lck^{VA} mice (Fig.5.14 and 5.16).

To assess differences between Tbet and Eomes expression in SLECs and MPECs in Lck^{VA} and Lck^{WT} mice we analysed the MFI of the $CD44^{-}$ population and $CD44^{+}$ populations in infected Lck^{WT} and Lck^{VA} mice at indicated timepoints (Fig.5.17). Tbet expression is crucial for effector cell formation and decreases as the cells form memory populations (Kaech and Cui, 2012). Indeed, in both Lck^{VA} and Lck^{WT} $CD8^{+}$ T cells Tbet expression was higher in $CD44^{+}$ population on day 7 SLECs than in the $CD44^{-}$ population and higher in SLECs than in MPECs in each strain (Fig.5.17A). T-bet expression was higher in $CD44^{+}$ day 42 SLECs in both Lck^{VA} and Lck^{WT} mice compared to $CD44^{-}$ T cells, and the respective $CD44^{+}$ MPECs (Fig.5.16A).

On day 46, interestingly, Lck^{VA} SLECs, both $CD44^{-}$ and $CD44^{+}$ populations had lower Tbet expression than Lck^{WT} cells. This may have indicated that the SLEC population was perhaps not the main effector population on day 46 in Lck^{VA} mice. The proportions of DPECs, were significantly higher in Lck^{VA} than in Lck^{WT} mice on day 46 and may have contributed more to the effector response.

Eomes expression is reciprocal to that of Tbet and is higher in memory populations than in effector populations (Kaech and Cui, 2012). Our data showed that Eomes expression in $CD8^{+}$ T cells, on day 7 in Lck^{WT} MPECs was not higher than in SLECs, but it increased ~2-fold in Lck^{VA} MPECs compared to Lck^{VA} SLECs. Similar patterns were observed on days 42 and 46. Eomes expression was consistently lower in Lck^{VA} SLECs as compared to Lck^{WT} SLECs but there were no consistent differences in Eomes expression between Lck^{VA} or Lck^{WT} MPECs. These data showed by qualitative analysis of histograms, that collectively there were no striking Lck mediated differences

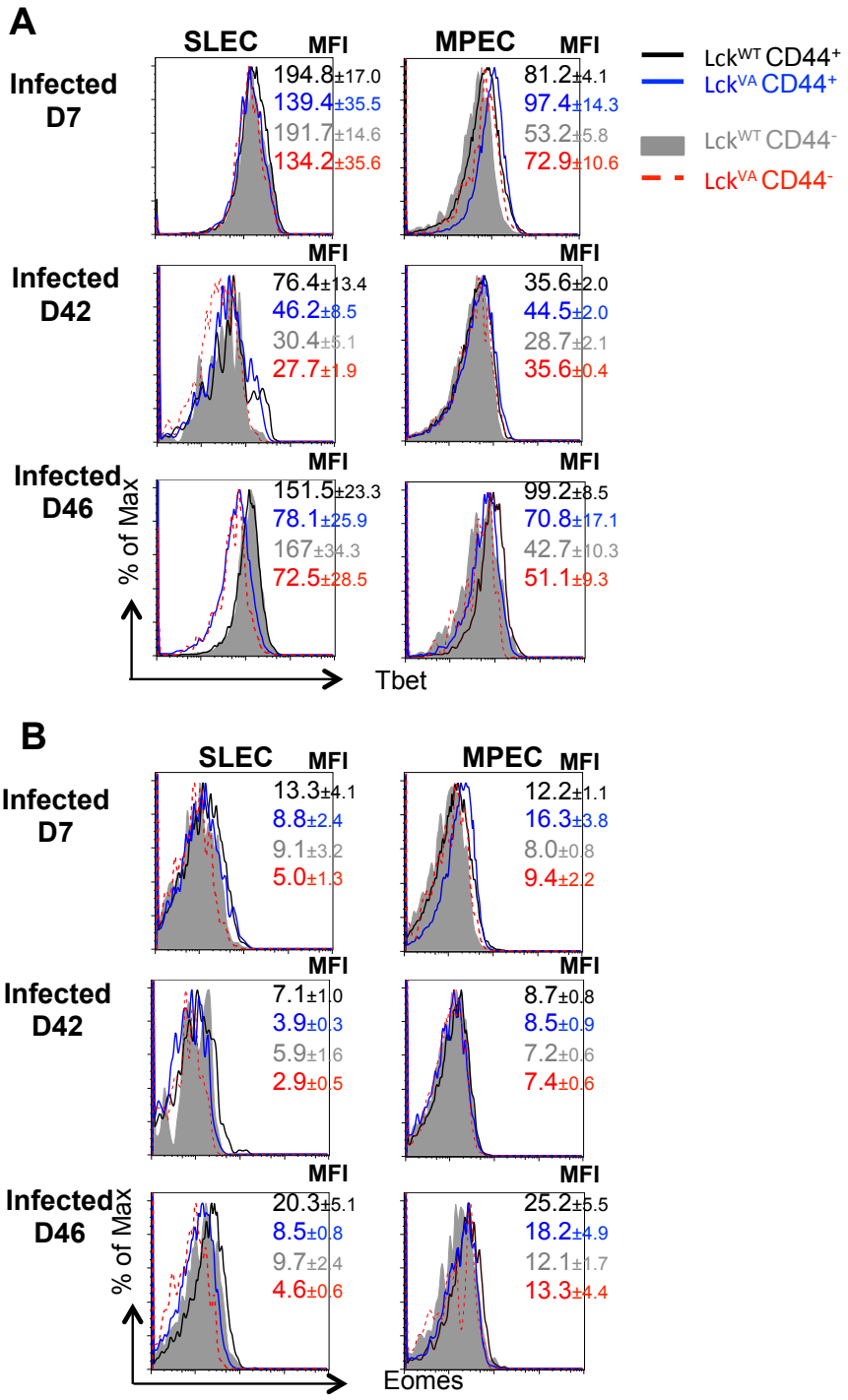

Fig. 5.17 Expression of Tbet and Eomes was similar in Lck^{WT} and Lck^{VA} mice.
Splenocytes from infected Lck^{WT} and Lck^{VA} mice were gated CD8^{-}CD44^{-} Lck^{WT} (black line) and Lck^{VA} (blue line), and CD8^{-}CD44^{+} Lck^{WT} (filled grey histogram) and Lck^{VA} (dashed red line). Histograms show, the expression of (A) Tbet and (B) Eomes in SLEC and MPEC populations on indicated days of *LmOVA* infection. Histograms are representative of n=2-5 individual mice, and the numbers show average MFIs ± SD. SD and significance were only calculated for groups where n≥3. Significance were calculated on Prism: parametric, unpaired, two-tailed, student's t-test *P<0.05, **P<0.01, ***P<0.001. Data are representative of one experiment.

in expression levels of Tbet and Eomes and therefore the expression patterns of these markers do not account for the observed differences in MPEC, SLEC and DPEC proportions during *LmOVA* infection.

5.2.7 TCRβ chain usage during *LmOVA* infection

The data presented in this chapter indicated that although Lck^{VA} T cells made a reduced $CD8^+$ T cells response to the Ova-specific immunodominant peptide (Fig.5.2 and Fig.5.7), the overall response to *Listeria* measured by Ki-67 expression (Fig.5.3) and cytokine production in response to HKL recall, (Fig.5.5) were relatively similar. This indicated that Lck^{VA} might recruit a broader T cell response to other *Listeria* peptides as compared to Lck^{WT} mice. Since T cells expressing TCR Vβ 5.1/5.2 chain are often the highest affinity clones for OVA-peptide we wanted to assess the TCR Vβ usage to identify any obvious differences between Lck^{VA} and Lck^{WT} mice.

Zehn et al. compared the *LmOVA* specific responses of OT-1 transgenic cells (monoclonal repertoire specific for OVA peptide) to endogenous Ova-specific $CD8^+$ T cells in polyclonal mice (Zehn et al., 2009). Four days after *LmOVA* infection, both the transferred OT-1 T cells and the endogenous Ova-specific $CD8^+$ T cells were present in equal proportions, however by day 7 the OT-1 T cells outnumbered the endogenous Ova-specific $CD8^+$ cells 30-fold (Zehn et al., 2009). Additionally they showed that in a C57BL/6 mouse early in the *LmOVA* response (day 4) several different TCR Vβ specificities can be identified, including TCR Vβ 4, 5.1/2, 6, 7, and 8.1/2, however by day 7 TCR Vβ 5.1/5.2 is the most dominant. They concluded that both low and high-functional avidity T cells initially respond to *LmOVA* infection, but the high-affinity T cells expand more and the T cell response undergoes a maturation where weak affinity clones present initially are replaced by high affinity clones (Zehn et al., 2009). However, they did not assess TCR Vβ expression at time points later than day 7.

We showed in chapter 3, that Lck abundance may have some bearing on the TCR repertoire (Fig.3.8 and 3.9) and therefore we assessed the TCR Vβ usage during secondary *LmOVA* infection in Lck^{VA} and Lck^{WT} mice.

Fig.5.18A showed that in uninfected Lck^{WT} mice of the $CD8^+$ $CD44^-$ T cells the expression of each of TCR Vβ 6, 7, 8.1/8.2, and 11 were similarly ~8-10%. The expression of TCR Vβ4 was <1%. The same pattern was observed in $CD8^+$ $CD44^+$ T cells in uninfected Lck^{WT} mice. The selection of TCR Vβs covered in this experiment added up to about 50% of the repertoire. There was no difference between Lck^{WT} and Lck^{VA} uninfected mice for TCR Vβ expression in $CD8^+CD44^-$ T cells. However, in Lck^{VA} uninfected mice higher proportions of Vβ5.1/5.2 and lower proportions of Vβ 7 were found in $CD8^+CD44^+$ T cells compared to Lck^{WT} suggesting a slight bias in the starting Lck^{VA} TCR repertoire.

In secondary infection, an increase in the proportions of Vβ5.1/2-expressing $CD8^+CD44^+$ T cells was seen in Lck^{WT} mice (compare proportions of $CD44^-$ (light grey) to $CD44^+$ (black) cells in Figs 5.18A and B), as would be expected from published data (Zehn et al., 2009). A concomitant decrease in expression of TCR Vβ 6, 7, 8.1/8.2, and 11 was seen to <5% in Lck^{WT} mice. The expression patterns of all TCR Vβs tested in Lck^{WT} $CD8^+CD44^-$ populations did not change with infection. In Lck^{VA} mice the expression of Vβ5.1/5.2 increased by ~5% in $CD44^-$ populations upon infection (compare light blue bars between Fig.5.18A and B) but the proportion of the other TCR Vβs changed little. In Lck^{VA} $CD44^+$ populations the proportion of all TCR Vβs tested did not change upon infection. One explanation for these data is that because uninfected Lck^{VA} mice already have a bias towards $Vb5.1/5.2^+$ cells in the $CD44^+$ compared to the $CD44^-$ T cell populations, they may have fewer naïve $Vb5.1/5.2^+$ T cells able to be activated in response to *Listeria* infection.

Overall these data confirmed in both Lck^{VA} and Lck^{WT} polyclonal repertoires many different TCR Vβ clones are recruited to the response but the predominant TCR expressed was Vβ 5.1/2, as would be expected from a response to *LmOVA* infection (Zehn et al., 2009). There did not appear to be any significant differences between Lck^{WT} and Lck^{VA} mice in TCR Vβ use during secondary infection. These results indicated that the reduced Ova-specific response in Lck^{VA} mice could not be due to absence of TCR Vβ5.1/2 expression, however, we may have missed other differences due to testing a

limited range of Vβ chains that only covered about 50% of the repertoire. Secondly, we did not verify whether any of the individual T cells express more than one TCR Vβ chain.

A caveat of this study is that we only looked at day 46 when the immune response is predicted to be relatively mature, meaning high affinity clones have replaced the low affinity clones, as Zehn et al. showed that the immune response matured already by day 7 (Zehn et al., 2009). Finally, the experiment shown in Fig.5.18 has only been performed once, although on several individual animals, despite this the experiment should be repeated before many firm conclusions are made.

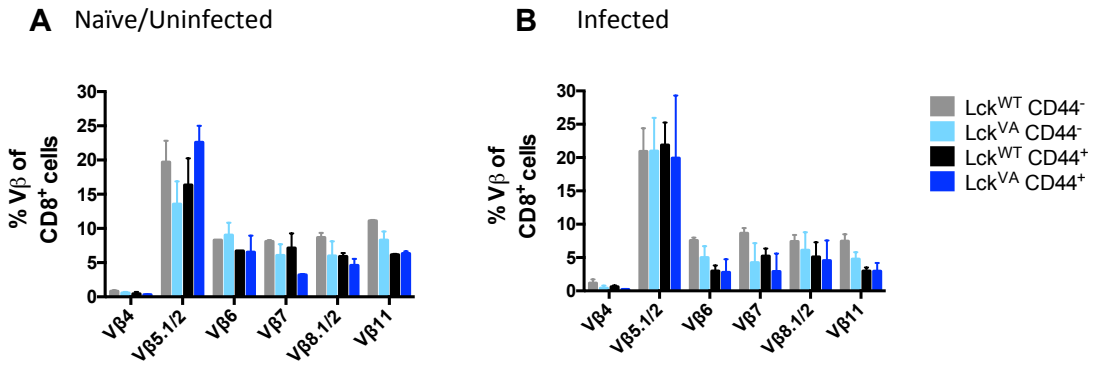

Fig. 5.18 TCRβ chain usage during secondary response to *LmOVA* infection.
CD8- splenocytes from (A) naïve/uninfected Lck^{WT} (n=2), Lck^{VA} (n=2) and (B) infected Lck^{WT} (n=4), Lck^{VA} (n=3) mice were assessed for expression of the indicated Vβ chains 4 days after secondary infection. Shown are proportions of Vβ- of all CD8- CD44 or all CD44- T cells. The bar charts show average proportions ± SD. SD was only calculated for groups where n≥3. Data are representative of one experiment.

5.3 Summary

- Lck^{VA} mice made significantly reduced primary and secondary T cell responses to the immunodominant Ova-peptide as compared to Lck^{WT} mice, shown by reduced numbers of Ova-specific cells (Fig.5.2) and N4 specific effector cytokine production (Fig.5.6 and 5.7).

- Cytokine production by $CD4^+$ T cells $LLO_{190-201}$ was similar in primary response but reduced in secondary *LmOVA* infection in Lck^{VA} mice (Fig. 5.6 and 5.7).

- The overall proliferative response to *Listeria* was similar in primary infection in Lck^{VA} and Lck^{WT} mice as measured by $CD8^+$ T cell numbers (Fig.5.1) and Ki-67 expression (Fig.5.3), however, the secondary response was reduced.

- Total effector cytokine production, in both primary and secondary immune responses to *Listeria* when recalled with HKL, were similar between Lck^{VA} and Lck^{WT}mice (Fig.5.5).

- Lck^{VA} mice had enhanced maintenance of *Listeria* specific $CD8^+CD127^+$ $KLRG1^+BrdU^+$ memory T cells (Fig.5.9 and Fig.5.14) during the contraction phase.

- The TCR Vβ repertoire is similar between Lck^{WT} and Lck^{VA} mice during secondary infection (Fig.5.18).

5.4 Discussion

This chapter has examined the consequences of reduced Lck expression on the response to *in vivo LmOVA* infection. The overall primary proliferative response to *Listeria* was similar in Lck^{VA} and Lck^{WT} mice, yet the secondary $CD8^+$ T cell response was reduced (Fig.5.1 and 5.3), as were both primary and secondary responses to Ova (Fig.5.2). Yet, the *Listeria* specific effector cytokine production, in both primary and secondary immune responses when recalled with HKL, was similar between Lck^{VA} and Lck^{WT} mice (Fig.5.5). The following discussion will address these findings in the context of current literature with regards to the roles of Lck expression levels in effector and memory cell development during infection.

It has previously been shown that low expression of Lck reduced TCR functional avidity (Caserta et al., 2010). In the case of $CD4^+$ T cells with reduced Lck expression responding to tumour antigens, the maintenance of T_{EM} populations was increased and the generation of self-renewing, recirculating, tumour-antigen specific T_{CM} $CD4^+$ T cells was improved. Lck^{ind} $CD4^+$ T cells were also shown to have 3-fold better survival than Lck^{WT} cells in the face of chronic antigen presentation (Caserta et al., 2010). In the present chapter there were no significant differences in proportions of T_{CM} (Fig. 5.12) or MPEC (Fig.5.14) populations between Lck^{WT} and Lck^{VA} mice on day 42. Although in agreement with published reports MPECs did represent the majority of CD8 T cells at this time point with ~60% in Lck^{WT} and ~50%Lck^{VA} mice (Obar et al., 2011).

Interestingly, we showed increased proportions of $CD8^+$ and $CD4^+$ T_{EM} populations (Fig.5.12 and Fig.5.13, respectively) as well as $CD8^+KRLG1^+$ SLEC and DPEC populations (Fig.5.14 and 5.15) during the contraction phase of the immune response to *Listeria* in Lck^{VA} mice. At first sight the persistence of $KLRG1^+$ cells, particularly $KLRG1^+CD127^-$ appears striking because it is in contrast with their definition, as they are expected to be short-lived and not persist 6 weeks post-infection (Kaech and Cui, 2012). It is, however, important to note several things here. Firstly, fewer than 10% of cells in both

Lck^{WT} and Lck^{VA} mice were SLECs at the day 42 time point, and it has been shown that such low levels can appear later than 54 days post-infection (Obar et al., 2011). Additionally, Obar et al. showed that equal proportions of MPECs and DPECs could survive until day 54 of infection and DPECs may represent a memory population with an intermediate capacity for expansion in secondary infections (Obar et al., 2011). However, DPECs were not able to give rise to true memory cells in subsequent expansions (Obar et al., 2011). Considering that only Lck^{VA} mice developed a significant pool of DPECs, their generation may be related to the functional avidity of Lck^{VA} cells. Lck^{VA} $CD8^+$ T cells had decreased TCR sensitivity in cytokine production, which indicated that they required more antigen to be activated to the same extent as Lck^{WT} cells during infection (Fig.5.6 and Fig.5.7). Secondly we used a rather crude method, only two markers, of categorizing these cells into MPECs and SLECs, which may not be the most definitive way of subsetting these cells, as many other markers have been shown to be important for their phenotyping (Kaech and Cui, 2012). Bcl-2 been shown to be important for both effector and memory population survival (Kurtulus et al., 2011). How much increased expression of Bcl-2 expression in Lck^{VA} mice contributed to survival of T_{EM} and $KLRG1^+$ effector cells is unclear (Fig.5.11). Despite Bcl-2 being critical for memory cell development (Dunkle et al., 2013), we did not see increased proportions of MPEC populations in Lck^{VA} mice (Fig.5.12).

Interestingly, our data indicated that the Ova-specific response in Lck^{VA} mice was clearly reduced (Fig.5.2, Fig.5.6 and Fig.5.7), but there were no apparent differences in the overall recall response to *Listeria* as assessed by overnight culture with HKL (Fig.5.5). Although this experiment was only done once, it may be an indication of Lck^{VA} mice are responding to a broader range of *Listeria* peptides. Meaning that, although OVA-specific responses were reduced, other peptides from the pathogen may dominate the response when TCR sensitivity is reduced (Zehn et al., 2009). However, when we assessed the Vβ repertoire, although we found that in an uninfected Lck^{VA} mice the $CD44^{hi}$ cells already expressed high levels of TCR Vβ5.1/5.2 and this did not change during infection, the proportions of other TCR Vβ tested were similar to Lck^{WT} mice (Fig.5.18). In chapter 3, when we analysed the TCR Vβ

repertoire of mature thymocytes we did not notice an inherent bias toward TCR Vβ5.1/5.2 expression in Lck^{VA} mice. It is possible, therefore that such a bias is inherent to the antigens, which may be gut derived, driving expansion of the $CD44^{hi}$ population in uninfected Lck^{VA} mice. Yet, how much the $CD44^{hi}$ cells in uninfected Lck^{VA} mice contribute to the immune response to *Listeria* is unclear. It has been found, however, that 50% of $CD4^{+}$ memory phenotype cells in humans are specific for viral antigens that the person has never encountered before (Su et al., 2013). This suggests memory-phenotype cells may have significant implications for immune responses due to high levels of cross-reactivity amongst T cell specificities (Su et al., 2013). Interestingly, we found a high background in Ki-67 expression in Lck^{VA} $CD8^{+}CD44^{+}$ T cells (Fig.5.3) and when we labelled cells with BrdU, we found that the $CD44^{hi}$ pool of memory-phenotype cells in naïve/uninfected mice diluted BrdU within 42 days of labelling (Fig.5.8). This suggested that the $CD44^{hi}$ memory phenotype pool of cells exhibited high turnover and potentially undergoes constant renewal. The $CD44^{hi}$ cells in Lck^{VA} may have thus been recruited to the *Listeria* response, however, they may also have been dying more. In support of the latter argument we showed that the proportions of $CD8^{+}Ki\text{-}67^{+}CD44^{+}$ cells were higher in Lck^{VA} mice on days 7 and 46, but the numbers of proliferating cells were either similar in primary or reduced in secondary responses compared to Lck^{WT} mice (Fig.5.3).

The balance of SLECs and MPECs resulting from an infection is dictated by the sum of strength and duration of the initial trigger between naïve T cells and p:MHC complexes (signal 1), co-stimulation (signal 2) and inflammatory stimuli (signal 3) (Williams and Bevan, 2007). Changes to any of these three signals would change the biological outcome by ultimately affecting the expression of transcription factors. Low-functional avidity interactions can drive T cell proliferation, effector and memory cell development, however, high avidity interactions are required for more prolonged and substantial T cells expansion (Kaech and Ahmed, 2001; Zehn et al., 2009). Zehn et al. showed that there were very few phenotypic differences between cells responding to low-functional avidity or high-functional avidity interactions, but one the markers was CD25 (Zehn et al., 2009). CD25 is the high-affinity

IL-2 receptor α chain and it is upregulated in response to T cell activation. IL-2 can exert both positive and negative effects on T cells (Malek, 2008), and Kalia et al. showed that in LCMV infection prolonged IL-2 signals promoted terminal-effect differentiation *in vivo* (Kalia et al., 2010). Cells with $CD25^{hi}$ expression underwent greater proliferation, apoptosis and had higher KLRG-1 expression, features in line with a terminal effector phenotype (Kalia et al., 2010). Kalia et al. proposed that the mechanism behind the distinct memory outcomes associated with $CD25^{hi}$ cells is enhanced STAT5 phosphorylation and enhanced Blimp-1 expression (Kalia et al., 2010), the latter of which is known to drive terminal-effector differentiation (Rutishauser et al., 2009). Our results in chapter 4 indicated that CD25 surface expression was comparable to $F5Lck^{WT}$, during *in vitro* peptide stimulation, in Lck^{VA} cells and they also had increased IL-2 production. One could speculate that this would also be the case *in vivo* and may be part of the mechanism driving the development of increased proportions of T_{EM}, DPEC, and SLEC populations. Thus it would be interesting to assess CD25 expression and IL-2 production during *LmOVA* infection in Lck^{VA} cells. Perhaps we would also find enhanced Blimp-1 expression, which could be driving terminal-effector differentiation in Lck^{VA} T cells.

The study by Kalia et al. highlights the role of the transcriptional profile that governs the effector and memory cell populations (Kalia et al., 2010). Indeed, Best et al. recently published an extensive profiling of gene-expression signatures throughout infection grouping different factors into clusters based on their kinetic patterns of expression and the biological processes associated with them (Best et al., 2013). For example, they showed that cells biased toward memory precursor potential had lower expression of genes of cell cycle and division cluster, and of short-lived effector memory cluster, than their short-lived effector memory counterparts (Best et al., 2013). T-bet regulates many genes encoding effector molecules and thus belongs to the effector cell specific cluster (Best et al., 2013). Eomes has cooperative and redundant functions to T-bet in regulating effector gene transcription (Intlekofer et al., 2005). Mice with mutations in both Eomes and T-bet expression ($Eomes^{+/-}Tbet^{+/-}$) were shown to have defects in memory $CD8^{+}$ T

cells development and cytotoxic effector programming (Intlekofer et al., 2005). Given these important roles of T-bet and Eomes in MPEC versus SLEC differentiation its perhaps surprising that we found no striking Lck-dependent differences in T-bet or Eomes expression during *LmOVA* infection (Fig.5.16).

The transcription factors Id2 and Id3 have also been implicated in memory $CD8^+$ T cell subset formation (Yang et al., 2011). A deficiency in both Id2 and Id3 leads to a loss of $CD8^+$ effector and memory populations (Yang et al., 2011). Id3 expression is regulated in response to TCR signals as well as environmental cues, perhaps there is an effect on Id3 expression in Lck^{VA} mice that leads to a deficiency in memory T cell development, as high Id3 expression would be expected to drive CD127 upregulation and memory cell formation (Yang et al., 2011). Interestingly, Blimp-1 has been shown to antagonise Id3 expression (Savitsky et al., 2007). From our data we predict that Lck^{VA} might have enhanced IL-2 expression, which could, lead to enhanced Blimp-1 expression and subsequently diminished Id3 expression, such an axis could be the mechanism behind enhanced effector cell maintenance in Lck^{VA} mice.

The heterogeneity among effector $CD8^+$ T cells is also influenced by the composition of the cytokine milieu, for example IL-12 promotes SLEC formation (Cui et al., 2009). In different sites, blood versus secondary lymphoid organs, different patterns of cytokines are expressed, which differentially regulate expression of chemokine receptors and their ligands, to ensure appropriate $CD8^+$ T cell migration (Hu et al., 2011; Plumlee et al., 2013). For example CCR7 expression ensures naïve $CD8^+$ T cells localise within the T-zone areas of spleen and lymph nodes. However, upon T cell activation by antigen and signals from type I IFNs, CCR7 is downregulated and inflammatory chemokine receptors such as CXCR3, CXCR6 and CCR5 are upregulated, which direct the activated T cell to sites of inflammation (Hu et al., 2011). Whilst studying LCMV infection, Hu et al. showed that CXCR3 deficiency increased memory cell formation and better recall response, because there was less colocalization of effector T cells with

antigen in the spleen (Hu et al., 2011). Although, looking at a completely different infectious model, we showed that Lck^{VA} mice had constitutively enhanced CXCR3 expression in the MPEC population of $CD8^+$ T cells (Fig.5.16) and reduced proportions of MPECs on day 42 (Fig.5.15). Indeed, Zehn et al. showed that OT-1 T cells stimulated by weak ligands could be detected in blood earlier than cells stimulated by stronger signals. They show that there is earlier downgregulation of CCR7, which leads to weakly stimulated cells leaving the splenic periarteriolar lymphocyte sheaths (PALS) sooner (Zehn et al., 2009). It would be interesting to assess CCR7 expression in Lck^{VA} T cells during *LmOVA* infection. Extrapolating from the above studies, it appears possible that we might find during a time course assay, that Lck^{VA} T cells downregulate CCR7 earlier than Lck^{WT} cells.

Several models of memory development have been proposed and were discussed in the introduction to the thesis (Section 1.5.1)(Kaech and Cui, 2012). Overall, this chapter has investigated the role of Lck abundance in effector and memory cell development during *in vivo LmOVA* infection. The data presented here are in line with the view that it is the strength of the TCR trigger that determines the relative memory potential of the effector populations and their proportional distribution. Lck^{VA} mice, potentially due to low-avidity interactions, made a reduced Ova-specific primary response, but had enhanced maintenance of $KLRG1^+$ effector cells, particularly of $CD127^+KLRG1^+$ effectors, which may represent an intermediate quality memory cell population as Lck^{VA} did make an enhanced memory response, above the primary, but it was inferior to the memory response in Lck^{WT} T cells.

Chapter 6: Discussion

The overall aims of this thesis were to determine the influence of Lck abundance on thymocyte development, peripheral T cell activation and memory formation.

Our experiments, conducted *in vitro* showed that <5% of WT levels of Lck were sufficient to restore thymocyte development compared to Lck^{KO} mice, yet the prioritisation of signalling pathways in peripheral activation was altered as compared to $F5Lck^{WT}$ mice. We are not the first to describe augmented signalling downstream of Lck. Methi et al. have shown that Lck knockdown (Lck-kd) with short interfering RNAs (siRNAs) leads to reduced phosphorylation of CD3ζ chains, Zap-70 kinase and Ca^{2+} signalling and a paradoxical prolonged hyperactivity of the ERK1/2 pathway, with enhanced IL-2 production (Methi et al., 2005). They proposed that enhanced activation of ERK1/2 was due to: 1) the decreased Lck-dependent phosphorylation and activation of SHP1, which therefore does not negatively regulate TCR activation; 2) the reduced phosphorylation of CD3ζ chains that can recruit Grb2-SOS and mediate Ras-MAPK signalling, whereas in WT cells total CD3ζ phosphorylation leads to recruitment of Zap-70, which potentially normally displaces Grb2 binding to CD3ζ chains (Methi et al., 2007); and 3) reduction in c-Cbl and Cbl-b activity, which failed to target TCR/CD3 complexes for degradation upon activation induced internalisation, leading to prolonged TCR signalling (Methi et al., 2008).

Although, in this thesis we found a slightly different phenotype upon signalling with reduced Lck expression than reported by Methi et al. (2005), with reduced ERK activation but enhanced Ca^{2+} flux, IL-2 production, and proliferation, it must be noted that they studied acute siRNA Lck-kd in Jurkat and mature human T cells whereas we were looking at constitutively low Lck expression in mouse cells, which may have adapted to the lower levels of Lck during differentiation in the thymus.

Our results for ERK activation and Ca^{2+} flux were obtained with different activation methods. For the ERK study we used NP68 stimulation, whereas for Ca^{2+} flux analysis we used CD8 and TCR crosslinking. It is plausible that some of the difference we see in Lck^{VA} mice between ERK activation and Ca^{2+} flux is explained by the relative proportions of active versus inactive Lck and/or co-receptor bound versus co-receptor free Lck. Conceivably, by crosslinking we are studying the role of co-receptor bound Lck, and perhaps ERK activation is more dependent on free-Lck or requires an additional step of recruiting and/or activating Lck.

Indeed, recently emphasis has been given to the spatiotemporal arrangement of TCR signalosomes, and the involvement of membrane compartmentalisation in TCR signal transduction (Filipp et al., 2012; Rossy et al., 2013; Singleton et al., 2009). The importance of compartmentalisation of Lck, and other signalling molecules, is supported by data from Nika et al. that showed Lck in naïve cells exists in a doubly phosphorylated state and is heavily regulated (Nika et al., 2010). Lck is maintained in a poised state by constant but reciprocal activity of positive and negative regulators. Upon T cell activation the balance has to tip such that the positive regulation overcomes the negative. The plasma membrane is laterally segregated into distinct microdomains, also known as lipid rafts, providing an explanation as to how spatiotemporal arrangement of signalling molecules, particularly of Lck, could regulate TCR signalling (Horejsi, 2003). It was shown that in CD4 T cells a pool of Lck, phosphorylated on Y394 and therefore in an activate state, was associated with high-density detergent-resistant membranes (heavy DRM) that also include CD4 and CD45 (Ballek et al., 2012). Upon TCR/CD4 activation Lck translocated from heavy DRMs to light DRMs that did not contain CD45, which in this context was sufficient for initiating downstream TCR signal transduction as the light DRMs contained the LAT signalosome (Ballek et al., 2012). Additionally, a recent report postulated an Lck-centric view of TCR activation where Lck conformational states were proposed to regulate its clustering, such that active and conformationally open Lck associated with other such Lck molecules leading to Lck hot-spots and enabling frequent TCR-Lck interactions, whereas, closed and inactive

Lck was released from such clusters (Rossy et al., 2013). Perhaps, when the abundance of Lck within a cell is low the arrangement of microdomains and Lck activity is different, such that Lck is less negatively regulated ensuring a rapid response upon TCR engagement. Indeed, the patterning of signalling molecules has been shown to be influenced by the strength and context of TCR signalling with physiologically distinct outcomes (Singleton et al., 2009). Additionally, reduced Lck abundance not only leads to reduced immediate phosphorylation events, as has been published (Methi et al., 2005) and also shown in this thesis (Fig.4.3), but somewhat counter-intuitively, this could prolong signal transduction by reducing the activation of negative regulatory pathways (Methi et al., 2007). This may also influence and contribute to the spatiotemporal arrangement of signalling molecules.

Indeed, spatiotemporal regulation and compartmentalisation of signaling molecules is important for sequestration of negative regulators to the opposite pole of the IS, the distal pole complex (DPC) (Mosenden et al., 2011). Type I protein kinase A (PKA), upon TCR triggering, normally phosphorylates and activates Csk which in turn phosphorylates Lck on the inhibitory Y505 residue reducing TCR signalling, but upon sustained activation, PKA was sequestered to the DPC, thereby enhancing Lck activity and TCR signalling (Mosenden et al., 2011). Perhaps in Lck^{VA} mice we would thus find altered activity of Lck, Csk or localisation of PKA, if indeed there is an absence of negative regulation that leads to sustained TCR signalling. It would be interesting to assess the relative ratios of total Lck and Lck Y505 versus Y394 from which we might infer its activation status in Lck^{VA} mice, and whether there is a complementary change in Csk activity or localisation of PKA.

There cannot, however, be a complete absence of negative regulation in Lck^{VA} mice, as they do not have overt lymphoproliferative disorders as might be expected from the enhanced proliferative capacity (Fig.4.9).

During thymocyte development, T cells are selected based on their avidity for self-peptide MHC complexes. The interaction with self is important for

peripheral T cell survival and lymphopenic expansion (Sprent and Surh, 2011). Studies have shown that interactions with self-peptide MHC can 'prewire' T cells and influence interactions of naïve T cells with foreign antigen-MHC complexes (Gascoigne et al., 2010; Krogsgaard et al., 2007; Persaud et al., 2014). In a recent report, Persaud et al. studied a pair of $CD4^+$ T cells with different avidities for self-peptide, but shared avidity for a foreign immunodominant listeriolysin epitope (LLO) in *Listeria monocytogenes* infection *in vivo* (Persaud et al., 2014). They used CD5 expression as a marker for TCR affinity for self-peptide and found that $CD5^{hi}$LLO56 cells, with stronger affinity for self, induced greater phosphorylation of ERK and IL-2 production but underwent AICD upon secondary infection, whereas $CD5^{lo}$LLO118 cells accumulated more (Persaud et al., 2014). Could higher affinity for self-peptides explain why we were potentially seeing more activation induced cell death in secondary response to *Listeria* in Lck^{VA} mice?

Although, we did not assess CD5 expression in our *Listeria* experiments in Lck^{VA} mice, in chapter 3 we showed that mature $CD4^+$ SP cells had only slightly lower CD5 expression than Lck^{WT} mice and in $CD8^+$ SP thymocytes there was no difference, suggesting that the affinity to self should be similar between the strains (Fig.3.7). Although, our data showed enhanced IL-2 production in F5Lck^{VA} T cells upon *in vitro* stimulation (Fig.4.8), Lck^{VA} T cells did not exhibit an enhanced response to *in vivo* infection as we showed that the primary and secondary Ova-specific responses were reduced in *Listeria* infection (Fig.5.2 and 5.7). Interestingly, however, we found that uninfected Lck^{VA} mice had higher proportions of TCR Vβ 5.1/2 expressing $CD8^+CD44^{hi}$ T cells (Fig.5.18). This is the Vβ chain expressed predominantly by cells that recognise the immunodominant Ova-peptide in *LmOVA* with high affinity. Unlike in Lck^{WT} mice the proportions of TCR Vβ 5.1/2 expressing CD8 T cells did not increase upon infection. Thus, it is possible that the expansion of high proportions of $CD44^+$ memory-phenotype cells in Lck^{VA} mice before infection results in increased proportions of TCR Vβ 5.1/2 expressing $CD8^+$ T cells that are exhausted during *Listeria* infection (Fig.5.18). Indeed, Su et al. have shown that $CD4^+$ memory-phenotype cells can be highly cross-reactive and

provide immunity for pathogens never encountered previously (Su et al., 2013).

At first sight, our results appear to be in contrast to data published by Caserta et al., that reported reduced exhaustion and enhanced memory development of $CD4^+$ T cells with low Lck expression in the face of chronic antigen. However, we showed that both $CD4^+$ and $CD8^+$ T cells in Lck^{VA} mice maintained higher proportions of T_{EM} cells (Fig.5.12 and 5.13) and also more $CD8^+$ $BrdU^+$ memory/effector T cells at day 42 following *Listeria* infection (Fig.5.9 and 5.14). More detailed analysis revealed that Lck^{VA} $CD8^+$ T cells developed a unique effector-memory phenotype, with increased proportions of the $CD127^+KLRG\text{-}1^+$ (DPEC) population, compared to Lck^{WT} mice that was maintained better through the contraction phase (Fig.5.15). Published data have shown that upon recall the DPEC population exhibits weaker proliferation than a true MPEC population, which was also in keeping with our results of reduced proliferation seen in secondary infection (Obar et al., 2011). Other apparent discrepancies with the data of Caserta et al. could be due to the fact that very different antigens were being studied (tumours versus acute bacteria) and/or that they were following $CD4^+$ T cell responses, whereas here the primary emphasis was on $CD8^+$ T cell responses (Caserta et al., 2010).

TCR signalling cascade is traditionally thought of as progressing linearly with one molecule activating the next. Our data, in agreement with published studies (Methi et al., 2005; Methi et al., 2007), suggest that reduced Lck expression, paradoxically, can lead to prolonged hyperactivation of some T cell signalling pathways but not all. Therefore, our results support the view that we are influencing particular branches of T cell signalling but not others (Brownlie and Zamoyska, 2013) and that the cumulative result of spatiotemporal regulation of positive and negative signalling units and the interplay between them determines the biological outcome upon T cell activation (Acuto et al., 2008).

The absence of Lck has severe consequences for the development and function of the immune system (Molina et al., 1992) thus the signalling network has potentially evolved to accommodate for scenarios with reduced Lck expression. Indeed, clinical reports of Lck deficiencies in humans highlight the importance of Lck. A complete Lck deficiency in a child, resulting from a genetic mutation that compromised the kinase function of Lck, led to severe T cell immunodeficiency and death at 30 months (Hauck et al., 2012). The phenotype was similar to Lck^{KO} mice with lymphopenia, reduced $CD4^+$ and $CD8^+$ T cell expression and function (Hauck et al., 2012). However, patients with aberrant splicing and expression of an abnormal splice variant Lck (without exon 7) had combined immunodeficiency (CID) with some T cell functions intact (Goldman et al., 1998; Hubert et al., 2000; Sawabe et al., 2001). Patients with alternative splice variant Lck lived to be adults and had $CD4^+$ T cell lymphopenia, but intact Ca^{2+} flux and MAPK activation. The Lck^{YA} mouse strain is therefore of great value and clinical relevance for furthering our understanding of the branching of TCR signalling networks.

Chapter 7: Appendices

7.1 Appendix 1

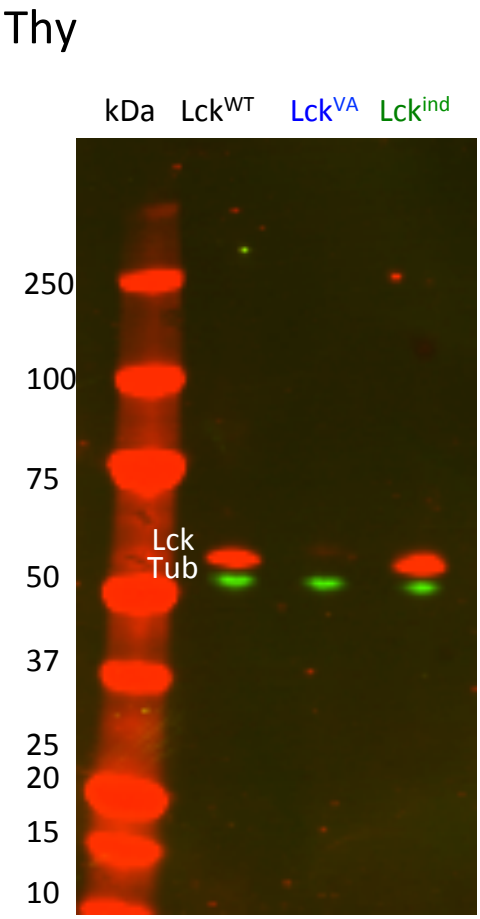

Fig. 7.1 Lck^{VA} and Lck^{ind} mice have reconstituted thymic development (Full Blot). Thymocyte lysates were analysed from age-matched (7-10 weeks) polyclonal Lck^{WT}, Lck^{ind}, and Lck^{VA} mice by western blot (pre-cast gel). The blot was probed with anti-Lck (Upstate) and anti-Tubulin antibodies overnight at 4°C, and then with anti-mouse (for Lck) and anti-rabbit (for Tubulin) fluorescent secondary antibodies for 1 hour. The blot was subsequently scanned using the Li-Cor system. Data are representative of 3 independent experiments.

7.2 Appendix 2

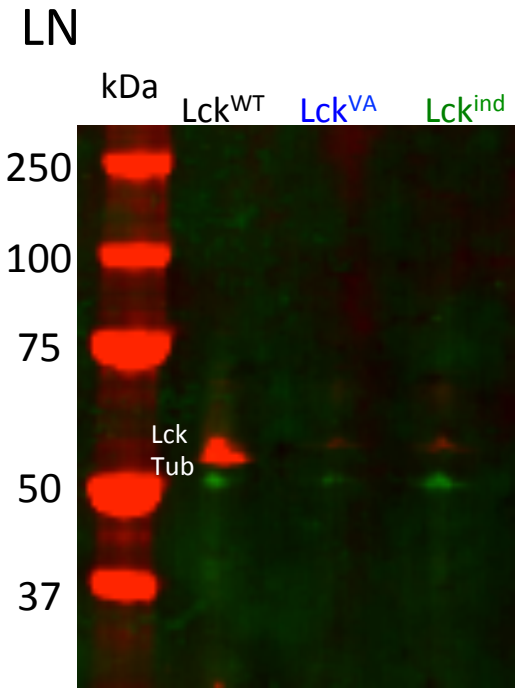

Fig. 7.2 Low Lck expression in peripheral lymphocytes (Full Blot).
Cell lysates from lymph node cells from polyclonal Lck^{WT}, Lck^{ind}, and Lck^{VA} mice were analysed by WB (pre-cast gel). The blot was first probed with anti-Lck (Upstate) and anti-Tubulin antibodies overnight at 4°C, and then with anti-mouse (for Lck) and anti-rabbit (for Tubulin) fluorescent secondary antibodies for 1 hour. The blot was subsequently scanned using the Li-Cor system.

7.3 Appendix 3

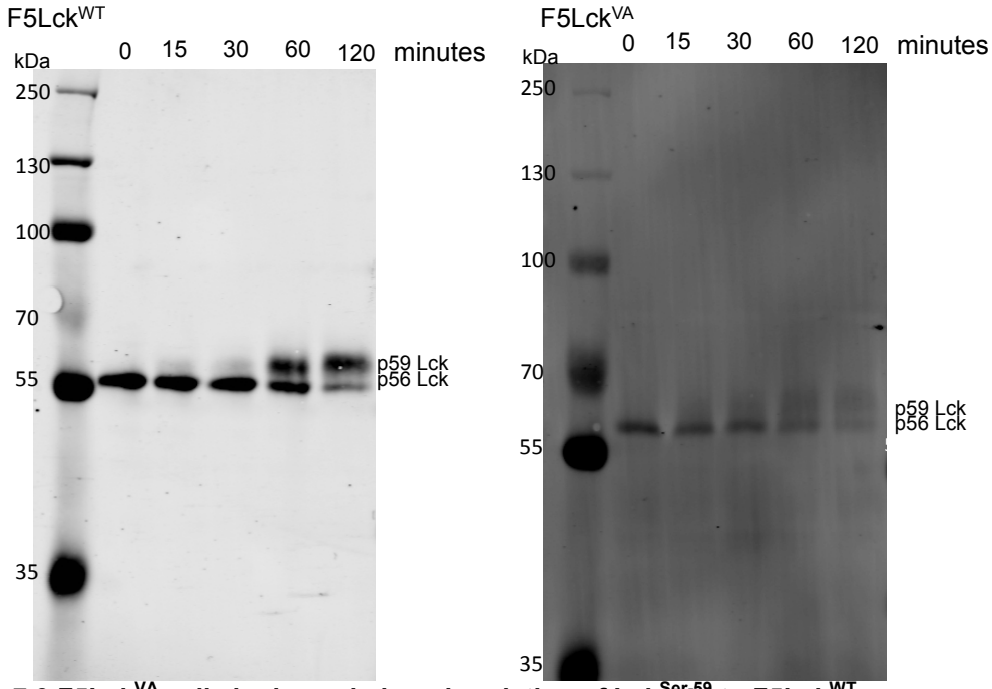

Fig. 7.3 F5Lck^{VA} cells had equal phosphorylation of Lck^{Ser-59} to F5Lck^{WT}.
LN cells were stimulated with 1 μM NP68 for the indicated times. Lysates were resolved by SDS/PAGE on a big gel overnight (Methods 2.11.4). F5Lck^{WT} and F5Lck^{VA} were probed with anti-Lck and anti-V5 tag, respectively, followed by detection with goat anti-mouse AF680. The ladder used was PageRuler Plus Prestained Protein Ladder (Cat. 26619; Thermo Scientific, USA). Blots were analysed using the Li-Cor Odyssey machine. Data are representative of three independent experiments.

7.4 Appendix 4

Table 7.1 Summary of *LmOVA* infection experiments

Exp	Lck^{WT} nr. of mice		Lck^{VA} nr. of mice		Infection Analysis (days)	Age (weeks)
	Naïve	Infected	Naïve	Infected		
1	4	12	3	12	7, 42, 46	10-13
2	3	5	3	5	7	7-8
3	4	8	4	8	42, 46	10-12

Chapter 8: References

Abraham, K.M., Levin, S.D., Marth, J.D., Forbush, K.A., and Perlmutter, R.M. (1991). Thymic tumorigenesis induced by overexpression of p56lck. Proc Natl Acad Sci U S A 88, 3977-3981.

Acuto, O., Di Bartolo, V., and Michel, F. (2008). Tailoring T-cell receptor signals by proximal negative feedback mechanisms. Nat Rev Immunol 8, 699-712.

Ahmed, R., and Gray, D. (1996). Immunological memory and protective immunity: understanding their relation. Science 272, 54-60.

Alarcon, B., and van Santen, H.M. (2010). Two receptors, two kinases, and T cell lineage determination. Sci Signal 3, pe11.

Anderson, G., and Takahama, Y. (2012). Thymic epithelial cells: working class heroes for T cell development and repertoire selection. Trends Immunol 33, 256-263.

Anderson, S.J., Levin, S.D., and Perlmutter, R.M. (1993). Protein tyrosine kinase p56lck controls allelic exclusion of T-cell receptor beta-chain genes. Nature 365, 552-554.

Apostolou, I., and von Boehmer, H. (2004). In vivo instruction of suppressor commitment in naive T cells. J Exp Med 199, 1401-1408.

Appleby, M.W., Gross, J.A., Cooke, M.P., Levin, S.D., Qian, X., and Perlmutter, R.M. (1992). Defective T cell receptor signaling in mice lacking the thymic isoform of p59fyn. Cell 70, 751-763.

Araki, K., Turner, A.P., Shaffer, V.O., Gangappa, S., Keller, S.A., Bachmann, M.F., Larsen, C.P., and Ahmed, R. (2009). mTOR regulates memory CD8 T-cell differentiation. Nature 460, 108-112.

Araki, Y., Fann, M., Wersto, R., and Weng, N.P. (2008). Histone acetylation facilitates rapid and robust memory CD8 T cell response through differential expression of effector molecules (eomesodermin and its targets: perforin and granzyme B). J Immunol 180, 8102-8108.

Artyomov, M.N., Lis, M., Devadas, S., Davis, M.M., and Chakraborty, A.K. (2010). CD4 and CD8 binding to MHC molecules primarily acts to enhance Lck delivery. Proc Natl Acad Sci U S A 107, 16916-16921.

Ashwell, J.D. (2006). The many paths to p38 mitogen-activated protein kinase activation in the immune system. Nat Rev Immunol 6, 532-540.

Azzam, H.S., Grinberg, A., Lui, K., Shen, H., Shores, E.W., and Love, P.E. (1998). CD5 expression is developmentally regulated by T cell receptor (TCR) signals and TCR avidity. J Exp Med 188, 2301-2311.

Bachmann, M.F., Gallimore, A., Linkert, S., Cerundolo, V., Lanzavecchia, A., Kopf, M., and Viola, A. (1999). Developmental regulation of Lck targeting to the CD8 coreceptor controls signaling in naive and memory T cells. J Exp Med 189, 1521-1530.

Badovinac, V.P., Porter, B.B., and Harty, J.T. (2004). CD8+ T cell contraction is controlled by early inflammation. Nat Immunol 5, 809-817.

Ballek, O., Brouckova, A., Manning, J., and Filipp, D. (2012). A specific type of membrane microdomains is involved in the maintenance and translocation of kinase active Lck to lipid rafts. Immunol Lett 142, 64-74.

Barber, E.K., Dasgupta, J.D., Schlossman, S.F., Trevillyan, J.M., and Rudd, C.E. (1989). The CD4 and CD8 antigens are coupled to a protein-tyrosine kinase (p56lck) that phosphorylates the CD3 complex. Proc Natl Acad Sci U S A 86, 3277-3281.

Begovich, A.B., Carlton, V.E., Honigberg, L.A., Schrodi, S.J., Chokkalingam, A.P., Alexander, H.C., Ardlie, K.G., Huang, Q., Smith, A.M., Spoerke, J.M., et al. (2004). A missense single-nucleotide polymorphism in a gene encoding a protein tyrosine phosphatase (PTPN22) is associated with rheumatoid arthritis. Am J Hum Genet 75, 330-337.

Benigni, F., Zimmermann, V.S., Hugues, S., Caserta, S., Basso, V., Rivino, L., Ingulli, E., Malherbe, L., Glaichenhaus, N., and Mondino, A. (2005). Phenotype and homing of CD4 tumor-specific T cells is modulated by tumor bulk. J Immunol 175, 739-748.

Best, J.A., Blair, D.A., Knell, J., Yang, E., Mayya, V., Doedens, A., Dustin, M.L., Goldrath, A.W., Monach, P., Shinton, S.A., et al. (2013). Transcriptional insights into the CD8(+) T cell response to infection and memory T cell formation. Nat Immunol 14, 404-412.

Bommhardt, U., Cole, M.S., Tso, J.Y., and Zamoyska, R. (1997). Signals through CD8 or CD4 can induce commitment to the CD4 lineage in the thymus. Eur J Immunol 27, 1152-1163.

Borger, J.G., Filby, A., and Zamoyska, R. (2013). Differential polarization of C-terminal Src kinase between naive and antigen-experienced CD8+ T cells. J Immunol 190, 3089-3099.

Bosselut, R., Feigenbaum, L., Sharrow, S.O., and Singer, A. (2001). Strength of signaling by CD4 and CD8 coreceptor tails determines the number but not the lineage direction of positively selected thymocytes. Immunity 14, 483-494.

Bottini, N., Vang, T., Cucca, F., and Mustelin, T. (2006). Role of PTPN22 in type 1 diabetes and other autoimmune diseases. Semin Immunol 18, 207-213.

Bramson, H.N., Casnellie, J.E., Nachod, H., Regan, L.M., and Sommers, C. (1991). Synthetic fragments of the CD4 receptor cytoplasmic domain and

large polycations alter the activities of the pp56lck tyrosine protein kinase. J Biol Chem 266, 16219-16225.

Brownlie, R.J., Miosge, L.A., Vassilakos, D., Svensson, L.M., Cope, A., and Zamoyska, R. (2012). Lack of the phosphatase PTPN22 increases adhesion of murine regulatory T cells to improve their immunosuppressive function. Sci Signal 5, ra87.

Brownlie, R.J., and Zamoyska, R. (2013). T cell receptor signalling networks: branched, diversified and bounded. Nat Rev Immunol 13, 257-269.

Brugnera, E., Bhandoola, A., Cibotti, R., Yu, Q., Guinter, T.I., Yamashita, Y., Sharrow, S.O., and Singer, A. (2000). Coreceptor reversal in the thymus: signaled CD4+8+ thymocytes initially terminate CD8 transcription even when differentiating into CD8+ T cells. Immunity 13, 59-71.

Burgering, B.M., and Kops, G.J. (2002). Cell cycle and death control: long live Forkheads. Trends Biochem Sci 27, 352-360.

Byth, K.F., Conroy, L.A., Howlett, S., Smith, A.J., May, J., Alexander, D.R., and Holmes, N. (1996). CD45-null transgenic mice reveal a positive regulatory role for CD45 in early thymocyte development, in the selection of CD4+CD8+ thymocytes, and B cell maturation. J Exp Med 183, 1707-1718.

Cabaniols, J.P., Fazilleau, N., Casrouge, A., Kourilsky, P., and Kanellopoulos, J.M. (2001). Most alpha/beta T cell receptor diversity is due to terminal deoxynucleotidyl transferase. J Exp Med 194, 1385-1390.

Caserta, S., Kleczkowska, J., Mondino, A., and Zamoyska, R. (2010). Reduced functional avidity promotes central and effector memory CD4 T cell responses to tumor-associated antigens. J Immunol 185, 6545-6554.

Chang, J.T., Palanivel, V.R., Kinjyo, I., Schambach, F., Intlekofer, A.M., Banerjee, A., Longworth, S.A., Vinup, K.E., Mrass, P., Oliaro, J., et al. (2007). Asymmetric T lymphocyte division in the initiation of adaptive immune responses. Science 315, 1687-1691.

Charest, A., Wagner, J., Kwan, M., and Tremblay, M.L. (1997). Coupling of the murine protein tyrosine phosphatase PEST to the epidermal growth factor (EGF) receptor through a Src homology 3 (SH3) domain-mediated association with Grb2. Oncogene 14, 1643-1651.

Chung, J., Kuo, C.J., Crabtree, G.R., and Blenis, J. (1992). Rapamycin-FKBP specifically blocks growth-dependent activation of and signaling by the 70 kd S6 protein kinases. Cell 69, 1227-1236.

Cloutier, J.F., and Veillette, A. (1999). Cooperative inhibition of T-cell antigen receptor signaling by a complex between a kinase and a phosphatase. J Exp Med 189, 111-121.

Croft, M. (2003). Costimulation of T cells by OX40, 4-1BB, and CD27. Cytokine Growth Factor Rev 14, 265-273.

Cui, W., Joshi, N.S., Jiang, A., and Kaech, S.M. (2009). Effects of Signal 3 during CD8 T cell priming: Bystander production of IL-12 enhances effector T cell expansion but promotes terminal differentiation. Vaccine 27, 2177-2187.

D'Oro, U., Vacchio, M.S., Weissman, A.M., and Ashwell, J.D. (1997). Activation of the Lck tyrosine kinase targets cell surface T cell antigen receptors for lysosomal degradation. Immunity 7, 619-628.

Daniels, M.A., Teixeiro, E., Gill, J., Hausmann, B., Roubaty, D., Holmberg, K., Werlen, G., Hollander, G.A., Gascoigne, N.R., and Palmer, E. (2006). Thymic selection threshold defined by compartmentalization of Ras/MAPK signalling. Nature 444, 724-729.

Danova, M., Riccardi, A., Giordano, M., Girino, M., Mazzini, G., Dezza, L., and Ascari, E. (1988). Cell cycle-related proteins: a flow cytofluorometric study in human tumors. Biol Cell 64, 23-28.

Davis, C.B., Killeen, N., Crooks, M.E., Raulet, D., and Littman, D.R. (1993). Evidence for a stochastic mechanism in the differentiation of mature subsets of T lymphocytes. Cell 73, 237-247.

Davis, S.J., and van der Merwe, P.A. (2006). The kinetic-segregation model: TCR triggering and beyond. Nat Immunol 7, 803-809.

Deindl, S., Kadlecek, T.A., Brdicka, T., Cao, X., Weiss, A., and Kuriyan, J. (2007). Structural basis for the inhibition of tyrosine kinase activity of ZAP-70. Cell 129, 735-746.

Di Bartolo, V., Montagne, B., Salek, M., Jungwirth, B., Carrette, F., Fourtane, J., Sol-Foulon, N., Michel, F., Schwartz, O., Lehmann, W.D., and Acuto, O. (2007). A novel pathway down-modulating T cell activation involves HPK-1-dependent recruitment of 14-3-3 proteins on SLP-76. J Exp Med 204, 681-691.

Dong, C., Davis, R.J., and Flavell, R.A. (2002). MAP kinases in the immune response. Annu Rev Immunol 20, 55-72.

Dong, S., Corre, B., Foulon, E., Dufour, E., Veillette, A., Acuto, O., and Michel, F. (2006). T cell receptor for antigen induces linker for activation of T cell-dependent activation of a negative signaling complex involving Dok-2, SHIP-1, and Grb-2. J Exp Med 203, 2509-2518.

Dunkle, A., Dzhagalov, I., Gordy, C., and He, Y.W. (2013). Transfer of CD8+ T cell memory using Bcl-2 as a marker. J Immunol 190, 940-947.

Erman, B., Alag, A.S., Dahle, O., van Laethem, F., Sarafova, S.D., Guinter, T.I., Sharrow, S.O., Grinberg, A., Love, P.E., and Singer, A. (2006). Coreceptor signal strength regulates positive selection but does not determine CD4/CD8 lineage choice in a physiologic in vivo model. J Immunol 177, 6613-6625.

Fabre, S., Carrette, F., Chen, J., Lang, V., Semichon, M., Denoyelle, C., Lazar, V., Cagnard, N., Dubart-Kupperschmitt, A., Mangeney, M., et al. (2008). FOXO1 regulates L-Selectin and a network of human T cell homing molecules downstream of phosphatidylinositol 3-kinase. J Immunol 181, 2980-2989.

Farber, D.L., Acuto, O., and Bottomly, K. (1997). Differential T cell receptor-mediated signaling in naive and memory CD4 T cells. Eur J Immunol 27, 2094-2101.

Fearon, D.T., and Locksley, R.M. (1996). The instructive role of innate immunity in the acquired immune response. Science 272, 50-53.

Fehling, H.J., Krotkova, A., Saint-Ruf, C., and von Boehmer, H. (1995). Crucial role of the pre-T-cell receptor alpha gene in development of alpha beta but not gamma delta T cells. Nature 375, 795-798.

Filipp, D., Ballek, O., and Manning, J. (2012). Lck, Membrane Microdomains, and TCR Triggering Machinery: Defining the New Rules of Engagement. Front Immunol 3, 155.

Finlay, D., and Cantrell, D.A. (2011). Metabolism, migration and memory in cytotoxic T cells. Nat Rev Immunol 11, 109-117.

Foulds, K.E., Zenewicz, L.A., Shedlock, D.J., Jiang, J., Troy, A.E., and Shen, H. (2002). Cutting edge: CD4 and CD8 T cells are intrinsically different in their proliferative responses. J Immunol 168, 1528-1532.

Fracchia, K.M., Pai, C.Y., and Walsh, C.M. (2013). Modulation of T Cell Metabolism and Function through Calcium Signaling. Front Immunol 4, 324.

Francisco, L.M., Sage, P.T., and Sharpe, A.H. (2010). The PD-1 pathway in tolerance and autoimmunity. Immunol Rev 236, 219-242.

Freedman, B.D., Liu, Q.H., Somersan, S., Kotlikoff, M.I., and Punt, J.A. (1999). Receptor avidity and costimulation specify the intracellular Ca2+ signaling pattern in CD4(+)CD8(+) thymocytes. J Exp Med 190, 943-952.

Fu, G., Casas, J., Rigaud, S., Rybakin, V., Lambolez, F., Brzostek, J., Hoerter, J.A., Paster, W., Acuto, O., Cheroutre, H., et al. (2013). Themis sets the signal threshold for positive and negative selection in T-cell development. Nature 504, 441-445.

Gambineri, E., Torgerson, T.R., and Ochs, H.D. (2003). Immune dysregulation, polyendocrinopathy, enteropathy, and X-linked inheritance (IPEX), a syndrome of systemic autoimmunity caused by mutations of FOXP3, a critical regulator of T-cell homeostasis. Curr Opin Rheumatol 15, 430-435.

Gascoigne, N.R., and Palmer, E. (2011). Signaling in thymic selection. Curr Opin Immunol 23, 207-212.

Gascoigne, N.R., Zal, T., Yachi, P.P., and Hoerter, J.A. (2010). Co-receptors and recognition of self at the immunological synapse. Curr Top Microbiol Immunol 340, 171-189.

Geginat, G., Schenk, S., Skoberne, M., Goebel, W., and Hof, H. (2001). A novel approach of direct ex vivo epitope mapping identifies dominant and subdominant CD4 and CD8 T cell epitopes from Listeria monocytogenes. J Immunol 166, 1877-1884.

Gerdes, J., Schwab, U., Lemke, H., and Stein, H. (1983). Production of a mouse monoclonal antibody reactive with a human nuclear antigen associated with cell proliferation. Int J Cancer 31, 13-20.

Germain, R.N. (2002). T-cell development and the CD4-CD8 lineage decision. Nat Rev Immunol 2, 309-322.

Gerondakis, S., Fulford, T.S., Messina, N.L., and Grumont, R.J. (2014). NF-kappaB control of T cell development. Nat Immunol 15, 15-25.

Gillis, S., and Smith, K.A. (1977). Long term culture of tumour-specific cytotoxic T cells. Nature 268, 154-156.

Goldman, F.D., Ballas, Z.K., Schutte, B.C., Kemp, J., Hollenback, C., Noraz, N., and Taylor, N. (1998). Defective expression of p56lck in an infant with severe combined immunodeficiency. J Clin Invest 102, 421-429.

Goldrath, A.W., Bogatzki, L.Y., and Bevan, M.J. (2000). Naive T cells transiently acquire a memory-like phenotype during homeostasis-driven proliferation. J Exp Med 192, 557-564.

Gong, Q., Cheng, A.M., Akk, A.M., Alberola-Ila, J., Gong, G., Pawson, T., and Chan, A.C. (2001). Disruption of T cell signaling networks and development by Grb2 haploid insufficiency. Nat Immunol 2, 29-36.

Guy, C.S., Vignali, K.M., Temirov, J., Bettini, M.L., Overacre, A.E., Smeltzer, M., Zhang, H., Huppa, J.B., Tsai, Y.H., Lobry, C., et al. (2013). Distinct TCR signaling pathways drive proliferation and cytokine production in T cells. Nat Immunol 14, 262-270.

Haring, J.S., and Harty, J.T. (2006). Aberrant contraction of antigen-specific CD4 T cells after infection in the absence of gamma interferon or its receptor. Infect Immun 74, 6252-6263.

Harty, J.T., and Bevan, M.J. (1995). Specific immunity to Listeria monocytogenes in the absence of IFN gamma. Immunity 3, 109-117.

Hauck, F., Randriamampita, C., Martin, E., Gerart, S., Lambert, N., Lim, A., Soulier, J., Maciorowski, Z., Touzot, F., Moshous, D., et al. (2012). Primary T-cell immunodeficiency with immunodysregulation caused by autosomal recessive LCK deficiency. J Allergy Clin Immunol 130, 1144-1152 e1111.

Hayashi, K., and Altman, A. (2007). Protein kinase C theta (PKCtheta): a key player in T cell life and death. Pharmacol Res 55, 537-544.

Hedrick, S.M. (2009). The cunning little vixen: Foxo and the cycle of life and death. Nat Immunol 10, 1057-1063.

Hedrick, S.M., Hess Michelini, R., Doedens, A.L., Goldrath, A.W., and Stone, E.L. (2012). FOXO transcription factors throughout T cell biology. Nat Rev Immunol 12, 649-661.

Herbein, G., and O'Brien, W.A. (2000). Tumor necrosis factor (TNF)-alpha and TNF receptors in viral pathogenesis. Proc Soc Exp Biol Med 223, 241-257.

Hermiston, M.L., Xu, Z., and Weiss, A. (2003). CD45: a critical regulator of signaling thresholds in immune cells. Annu Rev Immunol 21, 107-137.

Hernandez-Hoyos, G., Sohn, S.J., Rothenberg, E.V., and Alberola-Ila, J. (2000). Lck activity controls CD4/CD8 T cell lineage commitment. Immunity 12, 313-322.

Hogquist, K.A., Baldwin, T.A., and Jameson, S.C. (2005). Central tolerance: learning self-control in the thymus. Nat Rev Immunol 5, 772-782.

Hogquist, K.A., Jameson, S.C., Heath, W.R., Howard, J.L., Bevan, M.J., and Carbone, F.R. (1994). T cell receptor antagonist peptides induce positive selection. Cell 76, 17-27.

Hong, C., Luckey, M.A., and Park, J.H. (2012). Intrathymic IL-7: the where, when, and why of IL-7 signaling during T cell development. Semin Immunol 24, 151-158.

Horejsi, V. (2003). The roles of membrane microdomains (rafts) in T cell activation. Immunol Rev 191, 148-164.

Houtman, J.C., Houghtling, R.A., Barda-Saad, M., Toda, Y., and Samelson, L.E. (2005). Early phosphorylation kinetics of proteins involved in proximal TCR-mediated signaling pathways. J Immunol 175, 2449-2458.

Hu, J.K., Kagari, T., Clingan, J.M., and Matloubian, M. (2011). Expression of chemokine receptor CXCR3 on T cells affects the balance between effector and memory CD8 T-cell generation. Proc Natl Acad Sci U S A 108, E118-127.

Hubert, P., Bergeron, F., Ferreira, V., Seligmann, M., Oksenhendler, E., Debre, P., and Autran, B. (2000). Defective p56Lck activity in T cells from an adult patient with idiopathic CD4+ lymphocytopenia. Int Immunol 12, 449-457.

Imamoto, A., and Soriano, P. (1993). Disruption of the csk gene, encoding a negative regulator of Src family tyrosine kinases, leads to neural tube defects and embryonic lethality in mice. Cell 73, 1117-1124.

Inder, K., Harding, A., Plowman, S.J., Philips, M.R., Parton, R.G., and Hancock, J.F. (2008). Activation of the MAPK module from different spatial locations generates distinct system outputs. Mol Biol Cell 19, 4776-4784.

Intlekofer, A.M., Takemoto, N., Wherry, E.J., Longworth, S.A., Northrup, J.T., Palanivel, V.R., Mullen, A.C., Gasink, C.R., Kaech, S.M., Miller, J.D., et al. (2005). Effector and memory CD8+ T cell fate coupled by T-bet and eomesodermin. Nat Immunol 6, 1236-1244.

Itano, A., Salmon, P., Kioussis, D., Tolaini, M., Corbella, P., and Robey, E. (1996). The cytoplasmic domain of CD4 promotes the development of CD4 lineage T cells. J Exp Med 183, 731-741.

Jameson, S.C., and Bevan, M.J. (1998). T-cell selection. Curr Opin Immunol 10, 214-219.

Jameson, S.C., and Masopust, D. (2009). Diversity in T cell memory: an embarrassment of riches. Immunity 31, 859-871.

Jenkins, M.R., and Griffiths, G.M. (2010). The synapse and cytolytic machinery of cytotoxic T cells. Curr Opin Immunol 22, 308-313.

Joshi, N.S., Cui, W., Chandele, A., Lee, H.K., Urso, D.R., Hagman, J., Gapin, L., and Kaech, S.M. (2007). Inflammation directs memory precursor and short-lived effector CD8(+) T cell fates via the graded expression of T-bet transcription factor. Immunity 27, 281-295.

Joshi, N.S., and Kaech, S.M. (2008). Effector CD8 T cell development: a balancing act between memory cell potential and terminal differentiation. J Immunol 180, 1309-1315.

Joung, I., Kim, T., Stolz, L.A., Payne, G., Winkler, D.G., Walsh, C.T., Strominger, J.L., and Shin, J. (1995). Modification of Ser59 in the unique N-terminal region of tyrosine kinase p56lck regulates specificity of its Src homology 2 domain. Proc Natl Acad Sci U S A 92, 5778-5782.

Kaech, S.M., and Ahmed, R. (2001). Memory CD8+ T cell differentiation: initial antigen encounter triggers a developmental program in naive cells. Nat Immunol 2, 415-422.

Kaech, S.M., and Cui, W. (2012). Transcriptional control of effector and memory CD8+ T cell differentiation. Nat Rev Immunol 12, 749-761.

Kaech, S.M., Tan, J.T., Wherry, E.J., Konieczny, B.T., Surh, C.D., and Ahmed, R. (2003). Selective expression of the interleukin 7 receptor identifies effector CD8 T cells that give rise to long-lived memory cells. Nat Immunol 4, 1191-1198.

Kalia, V., Sarkar, S., Subramaniam, S., Haining, W.N., Smith, K.A., and Ahmed, R. (2010). Prolonged interleukin-2Ralpha expression on virus-

specific CD8+ T cells favors terminal-effector differentiation in vivo. Immunity 32, 91-103.

Kane, L.P., and Hedrick, S.M. (1996). A role for calcium influx in setting the threshold for CD4+CD8+ thymocyte negative selection. J Immunol 156, 4594-4601.

Kerdiles, Y.M., Beisner, D.R., Tinoco, R., Dejean, A.S., Castrillon, D.H., DePinho, R.A., and Hedrick, S.M. (2009). Foxo1 links homing and survival of naive T cells by regulating L-selectin, CCR7 and interleukin 7 receptor. Nat Immunol 10, 176-184.

Kersh, E.N., Fitzpatrick, D.R., Murali-Krishna, K., Shires, J., Speck, S.H., Boss, J.M., and Ahmed, R. (2006). Rapid demethylation of the IFN-gamma gene occurs in memory but not naive CD8 T cells. J Immunol 176, 4083-4093.

Kersh, E.N., Kaech, S.M., Onami, T.M., Moran, M., Wherry, E.J., Miceli, M.C., and Ahmed, R. (2003). TCR signal transduction in antigen-specific memory CD8 T cells. J Immunol 170, 5455-5463.

Kjer-Nielsen, L., Clements, C.S., Purcell, A.W., Brooks, A.G., Whisstock, J.C., Burrows, S.R., McCluskey, J., and Rossjohn, J. (2003). A structural basis for the selection of dominant alphabeta T cell receptors in antiviral immunity. Immunity 18, 53-64.

Klein, L., and Jovanovic, K. (2011). Regulatory T cell lineage commitment in the thymus. Semin Immunol 23, 401-409.

Koretzky, G.A., Abtahian, F., and Silverman, M.A. (2006). SLP76 and SLP65: complex regulation of signalling in lymphocytes and beyond. Nat Rev Immunol 6, 67-78.

Kramer, S., Mamalaki, C., Horak, I., Schimpl, A., Kioussis, D., and Hung, T. (1994). Thymic selection and peptide-induced activation of T cell receptor-transgenic CD8 T cells in interleukin-2-deficient mice. Eur J Immunol 24, 2317-2322.

Kremer, J.M., Westhovens, R., Leon, M., Di Giorgio, E., Alten, R., Steinfeld, S., Russell, A., Dougados, M., Emery, P., Nuamah, I.F., et al. (2003). Treatment of rheumatoid arthritis by selective inhibition of T-cell activation with fusion protein CTLA4Ig. N Engl J Med 349, 1907-1915.

Krogsgaard, M., Juang, J., and Davis, M.M. (2007). A role for "self" in T-cell activation. Semin Immunol 19, 236-244.

Kurtulus, S., Tripathi, P., Moreno-Fernandez, M.E., Sholl, A., Katz, J.D., Grimes, H.L., and Hildeman, D.A. (2011). Bcl-2 allows effector and memory CD8+ T cells to tolerate higher expression of Bim. J Immunol 186, 5729-5737.

Ladel, C.H., Flesch, I.E., Arnoldi, J., and Kaufmann, S.H. (1994). Studies with MHC-deficient knock-out mice reveal impact of both MHC I- and MHC II-

dependent T cell responses on Listeria monocytogenes infection. J Immunol 153, 3116-3122.

Lanzavecchia, A., and Sallusto, F. (2002). Progressive differentiation and selection of the fittest in the immune response. Nat Rev Immunol 2, 982-987.

Legname, G., Seddon, B., Lovatt, M., Tomlinson, P., Sarner, N., Tolaini, M., Williams, K., Norton, T., Kioussis, D., and Zamoyska, R. (2000). Inducible expression of a p56Lck transgene reveals a central role for Lck in the differentiation of CD4 SP thymocytes. Immunity 12, 537-546.

Leonard, W.J., Gnarra, J.R., and Sharon, M. (1990). The multisubunit interleukin-2 receptor. Ann N Y Acad Sci 594, 200-206.

Levin, S.D., Abraham, K.M., Anderson, S.J., Forbush, K.A., and Perlmutter, R.M. (1993). The protein tyrosine kinase p56lck regulates thymocyte development independently of its interaction with CD4 and CD8 coreceptors [corrected]. J Exp Med 178, 245-255.

Ling, P., Meyer, C.F., Redmond, L.P., Shui, J.W., Davis, B., Rich, R.R., Hu, M.C., Wange, R.L., and Tan, T.H. (2001). Involvement of hematopoietic progenitor kinase 1 in T cell receptor signaling. J Biol Chem 276, 18908-18914.

Liston, A., and Gray, D.H. (2014). Homeostatic control of regulatory T cell diversity. Nat Rev Immunol.

Liu, C., Ueno, T., Kuse, S., Saito, F., Nitta, T., Piali, L., Nakano, H., Kakiuchi, T., Lipp, M., Hollander, G.A., and Takahama, Y. (2005). The role of CCL21 in recruitment of T-precursor cells to fetal thymi. Blood 105, 31-39.

Lord, J.D., McIntosh, B.C., Greenberg, P.D., and Nelson, B.H. (1998). The IL-2 receptor promotes proliferation, bcl-2 and bcl-x induction, but not cell viability through the adapter molecule Shc. J Immunol 161, 4627-4633.

Lorenz, U., Ravichandran, K.S., Burakoff, S.J., and Neel, B.G. (1996). Lack of SHPTP1 results in src-family kinase hyperactivation and thymocyte hyperresponsiveness. Proc Natl Acad Sci U S A 93, 9624-9629.

Lorenz, U., Ravichandran, K.S., Pei, D., Walsh, C.T., Burakoff, S.J., and Neel, B.G. (1994). Lck-dependent tyrosyl phosphorylation of the phosphotyrosine phosphatase SH-PTP1 in murine T cells. Mol Cell Biol 14, 1824-1834.

Lovatt, M., Filby, A., Parravicini, V., Werlen, G., Palmer, E., and Zamoyska, R. (2006). Lck regulates the threshold of activation in primary T cells, while both Lck and Fyn contribute to the magnitude of the extracellular signal-related kinase response. Mol Cell Biol 26, 8655-8665.

Lundberg, K., Heath, W., Kontgen, F., Carbone, F.R., and Shortman, K. (1995). Intermediate steps in positive selection: differentiation of CD4+8int TCRint thymocytes into CD4-8+TCRhi thymocytes. J Exp Med 181, 1643-1651.

Malek, T.R. (2008). The biology of interleukin-2. Annu Rev Immunol 26, 453-479.

Malissen, M., Gillet, A., Ardouin, L., Bouvier, G., Trucy, J., Ferrier, P., Vivier, E., and Malissen, B. (1995). Altered T cell development in mice with a targeted mutation of the CD3-epsilon gene. Embo J 14, 4641-4653.

Mallaun, M., Naeher, D., Daniels, M.A., Yachi, P.P., Hausmann, B., Luescher, I.F., Gascoigne, N.R., and Palmer, E. (2008). The T cell receptor's alpha-chain connecting peptide motif promotes close approximation of the CD8 coreceptor allowing efficient signal initiation. J Immunol 180, 8211-8221.

Mallaun, M., Zenke, G., and Palmer, E. (2010). A discrete affinity-driven elevation of ZAP-70 kinase activity initiates negative selection. J Recept Signal Transduct Res 30, 430-443.

Mamalaki, C., Elliott, J., Norton, T., Yannoutsos, N., Townsend, A.R., Chandler, P., Simpson, E., and Kioussis, D. (1993). Positive and negative selection in transgenic mice expressing a T-cell receptor specific for influenza nucleoprotein and endogenous superantigen. Dev Immunol 3, 159-174.

Mamalaki, C., Norton, T., Tanaka, Y., Townsend, A.R., Chandler, P., Simpson, E., and Kioussis, D. (1992). Thymic depletion and peripheral activation of class I major histocompatibility complex-restricted T cells by soluble peptide in T-cell receptor transgenic mice. Proc Natl Acad Sci U S A 89, 11342-11346.

Mamonkin, M., Puppi, M., and Lacorazza, H.D. (2013). Transcription factor ELF4 promotes development and function of memory CD8 T cells in Listeria monocytogenes infection. Eur J Immunol.

Mandl, J.N., Monteiro, J.P., Vrisekoop, N., and Germain, R.N. (2013). T cell-positive selection uses self-ligand binding strength to optimize repertoire recognition of foreign antigens. Immunity 38, 263-274.

Mannering, S.I., Zhong, J., and Cheers, C. (2002). T-cell activation, proliferation and apoptosis in primary Listeria monocytogenes infection. Immunology 106, 87-95.

Mariathasan, S., Zakarian, A., Bouchard, D., Michie, A.M., Zuniga-Pflucker, J.C., and Ohashi, P.S. (2001). Duration and strength of extracellular signal-regulated kinase signals are altered during positive versus negative thymocyte selection. J Immunol 167, 4966-4973.

Marrack, P., Kappler, J., and Mitchell, T. (1999). Type I interferons keep activated T cells alive. J Exp Med 189, 521-530.

Martins, G., and Calame, K. (2008). Regulation and functions of Blimp-1 in T and B lymphocytes. Annu Rev Immunol 26, 133-169.

Martins, G.A., Cimmino, L., Liao, J., Magnusdottir, E., and Calame, K. (2008). Blimp-1 directly represses Il2 and the Il2 activator Fos, attenuating T cell proliferation and survival. J Exp Med 205, 1959-1965.

Mazzucchelli, R., and Durum, S.K. (2007). Interleukin-7 receptor expression: intelligent design. Nat Rev Immunol 7, 144-154.

McNeill, L., Salmond, R.J., Cooper, J.C., Carret, C.K., Cassady-Cain, R.L., Roche-Molina, M., Tandon, P., Holmes, N., and Alexander, D.R. (2007). The differential regulation of Lck kinase phosphorylation sites by CD45 is critical for T cell receptor signaling responses. Immunity 27, 425-437.

Mercado, R., Vijh, S., Allen, S.E., Kerksiek, K., Pilip, I.M., and Pamer, E.G. (2000). Early programming of T cell populations responding to bacterial infection. J Immunol 165, 6833-6839.

Mescher, M.F., Curtsinger, J.M., Agarwal, P., Casey, K.A., Gerner, M., Hammerbeck, C.D., Popescu, F., and Xiao, Z. (2006). Signals required for programming effector and memory development by CD8+ T cells. Immunol Rev 211, 81-92.

Methi, T., Berge, T., Torgersen, K.M., and Tasken, K. (2008). Reduced Cbl phosphorylation and degradation of the zeta-chain of the T-cell receptor/CD3 complex in T cells with low Lck levels. Eur J Immunol 38, 2557-2563.

Methi, T., Ngai, J., Mahic, M., Amarzguioui, M., Vang, T., and Tasken, K. (2005). Short-interfering RNA-mediated Lck knockdown results in augmented downstream T cell responses. J Immunol 175, 7398-7406.

Methi, T., Ngai, J., Vang, T., Torgersen, K.M., and Tasken, K. (2007). Hypophosphorylated TCR/CD3zeta signals through a Grb2-SOS1-Ras pathway in Lck knockdown cells. Eur J Immunol 37, 2539-2548.

Mills, R.E., and Jameson, J.M. (2009). T cell dependence on mTOR signaling. Cell Cycle 8, 545-548.

Mingueneau, M., Kreslavsky, T., Gray, D., Heng, T., Cruse, R., Ericson, J., Bendall, S., Spitzer, M.H., Nolan, G.P., Kobayashi, K., et al. (2013). The transcriptional landscape of alphabeta T cell differentiation. Nat Immunol 14, 619-632.

Minguet, S., Swamy, M., Alarcon, B., Luescher, I.F., and Schamel, W.W. (2007). Full activation of the T cell receptor requires both clustering and conformational changes at CD3. Immunity 26, 43-54.

Mittelstadt, P.R., Salvador, J.M., Fornace, A.J., Jr., and Ashwell, J.D. (2005). Activating p38 MAPK: new tricks for an old kinase. Cell Cycle 4, 1189-1192.

Molina, T.J., Kishihara, K., Siderovski, D.P., van Ewijk, W., Narendran, A., Timms, E., Wakeham, A., Paige, C.J., Hartmann, K.U., Veillette, A., and et al.

(1992). Profound block in thymocyte development in mice lacking p56lck. Nature 357, 161-164.

Mombaerts, P., Clarke, A.R., Rudnicki, M.A., Iacomini, J., Itohara, S., Lafaille, J.J., Wang, L., Ichikawa, Y., Jaenisch, R., Hooper, M.L., and et al. (1992). Mutations in T-cell antigen receptor genes alpha and beta block thymocyte development at different stages. Nature 360, 225-231.

Morgan, D.A., Ruscetti, F.W., and Gallo, R. (1976). Selective in vitro growth of T lymphocytes from normal human bone marrows. Science 193, 1007-1008.

Morris, G.P., and Allen, P.M. (2012). How the TCR balances sensitivity and specificity for the recognition of self and pathogens. Nat Immunol 13, 121-128.

Mosenden, R., Moltu, K., Ruppelt, A., Berge, T., and Tasken, K. (2011). Effects of type I protein kinase A modulation on the T cell distal pole complex. Scand J Immunol 74, 568-573.

Murphy, K.P., Travers, P., Walport, M., and Janeway, C. (2008). Janeway's immunobiology, Seventh edition / edn (New York: Garland Science).

Naeher, D., Daniels, M.A., Hausmann, B., Guillaume, P., Luescher, I., and Palmer, E. (2007). A constant affinity threshold for T cell tolerance. J Exp Med 204, 2553-2559.

Nagaleekar, V.K., Diehl, S.A., Juncadella, I., Charland, C., Muthusamy, N., Eaton, S., Haynes, L., Garrett-Sinha, L.A., Anguita, J., and Rincon, M. (2008). IP3 receptor-mediated Ca2+ release in naive CD4 T cells dictates their cytokine program. J Immunol 181, 8315-8322.

Nakayama, T., Singer, A., Hsi, E.D., and Samelson, L.E. (1989). Intrathymic signalling in immature CD4+CD8+ thymocytes results in tyrosine phosphorylation of the T-cell receptor zeta chain. Nature 341, 651-654.

Nicholson, D.W., and Thornberry, N.A. (1997). Caspases: killer proteases. Trends Biochem Sci 22, 299-306.

Niederberger, N., Holmberg, K., Alam, S.M., Sakati, W., Naramura, M., Gu, H., and Gascoigne, N.R. (2003). Allelic exclusion of the TCR alpha-chain is an active process requiring TCR-mediated signaling and c-Cbl. J Immunol 170, 4557-4563.

Nika, K., Soldani, C., Salek, M., Paster, W., Gray, A., Etzensperger, R., Fugger, L., Polzella, P., Cerundolo, V., Dushek, O., et al. (2010). Constitutively active Lck kinase in T cells drives antigen receptor signal transduction. Immunity 32, 766-777.

Nishimura, H., Okazaki, T., Tanaka, Y., Nakatani, K., Hara, M., Matsumori, A., Sasayama, S., Mizoguchi, A., Hiai, H., Minato, N., and Honjo, T. (2001).

Autoimmune dilated cardiomyopathy in PD-1 receptor-deficient mice. Science 291, 319-322.

Obar, J.J., Jellison, E.R., Sheridan, B.S., Blair, D.A., Pham, Q.M., Zickovich, J.M., and Lefrancois, L. (2011). Pathogen-induced inflammatory environment controls effector and memory CD8+ T cell differentiation. J Immunol 187, 4967-4978.

Odake, S., Kam, C.M., Narasimhan, L., Poe, M., Blake, J.T., Krahenbuhl, O., Tschopp, J., and Powers, J.C. (1991). Human and murine cytotoxic T lymphocyte serine proteases: subsite mapping with peptide thioester substrates and inhibition of enzyme activity and cytolysis by isocoumarins. Biochemistry 30, 2217-2227.

Oehen, S., and Brduscha-Riem, K. (1998). Differentiation of naive CTL to effector and memory CTL: correlation of effector function with phenotype and cell division. J Immunol 161, 5338-5346.

Oh-hora, M., and Rao, A. (2008). Calcium signaling in lymphocytes. Curr Opin Immunol 20, 250-258.

Olson, J.A., McDonald-Hyman, C., Jameson, S.C., and Hamilton, S.E. (2013). Effector-like CD8(+) T cells in the memory population mediate potent protective immunity. Immunity 38, 1250-1260.

Olszowy, M.W., Leuchtmann, P.L., Veillette, A., and Shaw, A.S. (1995). Comparison of p56lck and p59fyn protein expression in thymocyte subsets, peripheral T cells, NK cells, and lymphoid cell lines. J Immunol 155, 4236-4240.

Palacios, E.H., and Weiss, A. (2004). Function of the Src-family kinases, Lck and Fyn, in T-cell development and activation. Oncogene 23, 7990-8000.

Palacios, E.H., and Weiss, A. (2007). Distinct roles for Syk and ZAP-70 during early thymocyte development. J Exp Med 204, 1703-1715.

Palmer, E., and Naeher, D. (2009). Affinity threshold for thymic selection through a T-cell receptor-co-receptor zipper. Nat Rev Immunol 9, 207-213.

Pamer, E.G. (2004). Immune responses to Listeria monocytogenes. Nat Rev Immunol 4, 812-823.

Pani, G., Fischer, K.D., Mlinaric-Rascan, I., and Siminovitch, K.A. (1996). Signaling capacity of the T cell antigen receptor is negatively regulated by the PTP1C tyrosine phosphatase. J Exp Med 184, 839-852.

Pape, K.A., Khoruts, A., Mondino, A., and Jenkins, M.K. (1997). Inflammatory cytokines enhance the in vivo clonal expansion and differentiation of antigen-activated CD4+ T cells. J Immunol 159, 591-598.

Papiernik, M., de Moraes, M.L., Pontoux, C., Vasseur, F., and Penit, C. (1998). Regulatory CD4 T cells: expression of IL-2R alpha chain, resistance to clonal deletion and IL-2 dependency. Int Immunol 10, 371-378.

Parasrampuria, D.A., de Boer, P., Desai-Krieger, D., Chow, A.T., and Jones, C.R. (2003). Single-dose pharmacokinetics and pharmacodynamics of RWJ 67657, a specific p38 mitogen-activated protein kinase inhibitor: a first-in-human study. J Clin Pharmacol 43, 406-413.

Patel, R.K., and Mohan, C. (2005). PI3K/AKT signaling and systemic autoimmunity. Immunol Res 31, 47-55.

Persaud, S.P., Parker, C.R., Lo, W.L., Weber, K.S., and Allen, P.M. (2014). Intrinsic CD4 T cell sensitivity and response to a pathogen are set and sustained by avidity for thymic and peripheral complexes of self peptide and MHC. Nat Immunol.

Peterson, E.J., Woods, M.L., Dmowski, S.A., Derimanov, G., Jordan, M.S., Wu, J.N., Myung, P.S., Liu, Q.H., Pribila, J.T., Freedman, B.D., et al. (2001). Coupling of the TCR to integrin activation by Slap-130/Fyb. Science 293, 2263-2265.

Petrie, H.T., and Zuniga-Pflucker, J.C. (2007). Zoned out: functional mapping of stromal signaling microenvironments in the thymus. Annu Rev Immunol 25, 649-679.

Pieper, K., Grimbacher, B., and Eibel, H. (2013). B-cell biology and development. J Allergy Clin Immunol 131, 959-971.

Pihlgren, M., Dubois, P.M., Tomkowiak, M., Sjogren, T., and Marvel, J. (1996). Resting memory CD8+ T cells are hyperreactive to antigenic challenge in vitro. J Exp Med 184, 2141-2151.

Plumlee, C.R., Sheridan, B.S., Cicek, B.B., and Lefrancois, L. (2013). Environmental cues dictate the fate of individual CD8+ T cells responding to infection. Immunity 39, 347-356.

Poe, M., Blake, J.T., Boulton, D.A., Gammon, M., Sigal, N.H., Wu, J.K., and Zweerink, H.J. (1991). Human cytotoxic lymphocyte granzyme B. Its purification from granules and the characterization of substrate and inhibitor specificity. J Biol Chem 266, 98-103.

Prohaska, S.S., Scherer, D.C., Weissman, I.L., and Kondo, M. (2002). Developmental plasticity of lymphoid progenitors. Semin Immunol 14, 377-384.

Rao, R.R., Li, Q., Gubbels Bupp, M.R., and Shrikant, P.A. (2012). Transcription factor Foxo1 represses T-bet-mediated effector functions and promotes memory CD8(+) T cell differentiation. Immunity 36, 374-387.

Rao, R.R., Li, Q., Odunsi, K., and Shrikant, P.A. (2010). The mTOR kinase determines effector versus memory CD8+ T cell fate by regulating the expression of transcription factors T-bet and Eomesodermin. Immunity 32, 67-78.

Rossi, F.M., Corbel, S.Y., Merzaban, J.S., Carlow, D.A., Gossens, K., Duenas, J., So, L., Yi, L., and Ziltener, H.J. (2005). Recruitment of adult thymic progenitors is regulated by P-selectin and its ligand PSGL-1. Nat Immunol 6, 626-634.

Rossy, J., Owen, D.M., Williamson, D.J., Yang, Z., and Gaus, K. (2013). Conformational states of the kinase Lck regulate clustering in early T cell signaling. Nat Immunol 14, 82-89.

Rothenberg, E.V., Moore, J.E., and Yui, M.A. (2008). Launching the T-cell-lineage developmental programme. Nat Rev Immunol 8, 9-21.

Round, J.L., Humphries, L.A., Tomassian, T., Mittelstadt, P., Zhang, M., and Miceli, M.C. (2007). Scaffold protein Dlgh1 coordinates alternative p38 kinase activation, directing T cell receptor signals toward NFAT but not NF-kappaB transcription factors. Nat Immunol 8, 154-161.

Rudd, C.E., Trevillyan, J.M., Dasgupta, J.D., Wong, L.L., and Schlossman, S.F. (1988). The CD4 receptor is complexed in detergent lysates to a protein-tyrosine kinase (pp58) from human T lymphocytes. Proc Natl Acad Sci U S A 85, 5190-5194.

Rudolph, M.G., Stanfield, R.L., and Wilson, I.A. (2006). How TCRs bind MHCs, peptides, and coreceptors. Annu Rev Immunol 24, 419-466.

Russell, J.H., and Ley, T.J. (2002). Lymphocyte-mediated cytotoxicity. Annu Rev Immunol 20, 323-370.

Rutishauser, R.L., Martins, G.A., Kalachikov, S., Chandele, A., Parish, I.A., Meffre, E., Jacob, J., Calame, K., and Kaech, S.M. (2009). Transcriptional repressor Blimp-1 promotes CD8(+) T cell terminal differentiation and represses the acquisition of central memory T cell properties. Immunity 31, 296-308.

Saini, M., Sinclair, C., Marshall, D., Tolaini, M., Sakaguchi, S., and Seddon, B. (2010). Regulation of Zap70 expression during thymocyte development enables temporal separation of CD4 and CD8 repertoire selection at different signaling thresholds. Sci Signal 3, ra23.

Sakaguchi, N., Takahashi, T., Hata, H., Nomura, T., Tagami, T., Yamazaki, S., Sakihama, T., Matsutani, T., Negishi, I., Nakatsuru, S., and Sakaguchi, S. (2003). Altered thymic T-cell selection due to a mutation of the ZAP-70 gene causes autoimmune arthritis in mice. Nature 426, 454-460.

Sallusto, F., Lenig, D., Forster, R., Lipp, M., and Lanzavecchia, A. (1999). Two subsets of memory T lymphocytes with distinct homing potentials and effector functions. Nature 401, 708-712.

Salmond, R.J., Emery, J., Okkenhaug, K., and Zamoyska, R. (2009a). MAPK, phosphatidylinositol 3-kinase, and mammalian target of rapamycin pathways converge at the level of ribosomal protein S6 phosphorylation to control metabolic signaling in CD8 T cells. J Immunol 183, 7388-7397.

Salmond, R.J., Filby, A., Pirinen, N., Magee, A.I., and Zamoyska, R. (2011). Mislocalization of Lck impairs thymocyte differentiation and can promote development of thymomas. Blood 117, 108-117.

Salmond, R.J., Filby, A., Qureshi, I., Caserta, S., and Zamoyska, R. (2009b). T-cell receptor proximal signaling via the Src-family kinases, Lck and Fyn, influences T-cell activation, differentiation, and tolerance. Immunol Rev 228, 9-22.

Salvador, J.M., Mittelstadt, P.R., Belova, G.I., Fornace, A.J., Jr., and Ashwell, J.D. (2005). The autoimmune suppressor Gadd45alpha inhibits the T cell alternative p38 activation pathway. Nat Immunol 6, 396-402.

Sarkar, S., Kalia, V., Haining, W.N., Konieczny, B.T., Subramaniam, S., and Ahmed, R. (2008). Functional and genomic profiling of effector CD8 T cell subsets with distinct memory fates. J Exp Med 205, 625-640.

Savitsky, D., Cimmino, L., Kuo, T., Martins, G.A., and Calame, K. (2007). Multiple roles for Blimp-1 in B and T lymphocytes. Adv Exp Med Biol 596, 9-30.

Sawabe, T., Horiuchi, T., Nakamura, M., Tsukamoto, H., Nakahara, K., Harashima, S.I., Tsuchiya, T., and Nakano, S. (2001). Defect of lck in a patient with common variable immunodeficiency. Int J Mol Med 7, 609-614.

Schepers, K., Swart, E., van Heijst, J.W., Gerlach, C., Castrucci, M., Sie, D., Heimerikx, M., Velds, A., Kerkhoven, R.M., Arens, R., and Schumacher, T.N. (2008). Dissecting T cell lineage relationships by cellular barcoding. J Exp Med 205, 2309-2318.

Schluns, K.S., Kieper, W.C., Jameson, S.C., and Lefrancois, L. (2000). Interleukin-7 mediates the homeostasis of naive and memory CD8 T cells in vivo. Nat Immunol 1, 426-432.

Schmedt, C., Saijo, K., Niidome, T., Kuhn, R., Aizawa, S., and Tarakhovsky, A. (1998). Csk controls antigen receptor-mediated development and selection of T-lineage cells. Nature 394, 901-904.

Schmitt, T.M., and Zuniga-Pflucker, J.C. (2002). Induction of T cell development from hematopoietic progenitor cells by delta-like-1 in vitro. Immunity 17, 749-756.

Schoenborn, J.R., Tan, Y.X., Zhang, C., Shokat, K.M., and Weiss, A. (2011). Feedback circuits monitor and adjust basal Lck-dependent events in T cell receptor signaling. Sci Signal 4, ra59.

Schroder, K., Hertzog, P.J., Ravasi, T., and Hume, D.A. (2004). Interferon-gamma: an overview of signals, mechanisms and functions. J Leukoc Biol 75, 163-189.

Schwartz, R.H. (2003). T cell anergy. Annu Rev Immunol 21, 305-334.

Seddon, B., Legname, G., Tomlinson, P., and Zamoyska, R. (2000). Long-term survival but impaired homeostatic proliferation of Naive T cells in the absence of p56lck. Science 290, 127-131.

Seddon, B., and Zamoyska, R. (2002). TCR signals mediated by Src family kinases are essential for the survival of naive T cells. J Immunol 169, 2997-3005.

Setoguchi, R., Hori, S., Takahashi, T., and Sakaguchi, S. (2005). Homeostatic maintenance of natural Foxp3(+) CD25(+) CD4(+) regulatory T cells by interleukin (IL)-2 and induction of autoimmune disease by IL-2 neutralization. J Exp Med 201, 723-735.

Sharpe, A.H., and Freeman, G.J. (2002). The B7-CD28 superfamily. Nat Rev Immunol 2, 116-126.

Shinkai, Y., Rathbun, G., Lam, K.P., Oltz, E.M., Stewart, V., Mendelsohn, M., Charron, J., Datta, M., Young, F., Stall, A.M., and et al. (1992). RAG-2-deficient mice lack mature lymphocytes owing to inability to initiate V(D)J rearrangement. Cell 68, 855-867.

Shui, J.W., Boomer, J.S., Han, J., Xu, J., Dement, G.A., Zhou, G., and Tan, T.H. (2007). Hematopoietic progenitor kinase 1 negatively regulates T cell receptor signaling and T cell-mediated immune responses. Nat Immunol 8, 84-91.

Sinclair, C., Bains, I., Yates, A.J., and Seddon, B. (2013). Asymmetric thymocyte death underlies the CD4:CD8 T-cell ratio in the adaptive immune system. Proc Natl Acad Sci U S A 110, E2905-2914.

Sinclair, L.V., Finlay, D., Feijoo, C., Cornish, G.H., Gray, A., Ager, A., Okkenhaug, K., Hagenbeek, T.J., Spits, H., and Cantrell, D.A. (2008). Phosphatidylinositol-3-OH kinase and nutrient-sensing mTOR pathways control T lymphocyte trafficking. Nat Immunol 9, 513-521.

Singer, A., Adoro, S., and Park, J.H. (2008). Lineage fate and intense debate: myths, models and mechanisms of CD4- versus CD8-lineage choice. Nat Rev Immunol 8, 788-801.

Singleton, K.L., Roybal, K.T., Sun, Y., Fu, G., Gascoigne, N.R., van Oers, N.S., and Wulfing, C. (2009). Spatiotemporal patterning during T cell activation is highly diverse. Sci Signal 2, ra15.

Sloan-Lancaster, J., Evavold, B.D., and Allen, P.M. (1993). Induction of T-cell anergy by altered T-cell-receptor ligand on live antigen-presenting cells. Nature 363, 156-159.

Smida, M., Posevitz-Fejfar, A., Horejsi, V., Schraven, B., and Lindquist, J.A. (2007). A novel negative regulatory function of the phosphoprotein associated with glycosphingolipid-enriched microdomains: blocking Ras activation. Blood 110, 596-615.

Smith-Garvin, J.E., Koretzky, G.A., and Jordan, M.S. (2009). T cell activation. Annu Rev Immunol 27, 591-619.

Smyth, L.A., Williams, O., Huby, R.D., Norton, T., Acuto, O., Ley, S.C., and Kioussis, D. (1998). Altered peptide ligands induce quantitatively but not qualitatively different intracellular signals in primary thymocytes. Proc Natl Acad Sci U S A 95, 8193-8198.

Soares, A., Govender, L., Hughes, J., Mavakla, W., de Kock, M., Barnard, C., Pienaar, B., Janse van Rensburg, E., Jacobs, G., Khomba, G., et al. (2010). Novel application of Ki67 to quantify antigen-specific in vitro lymphoproliferation. J Immunol Methods 362, 43-50.

Sprent, J., and Surh, C.D. (2011). Normal T cell homeostasis: the conversion of naive cells into memory-phenotype cells. Nat Immunol 12, 478-484.

Springer, T.A. (1990). Adhesion receptors of the immune system. Nature 346, 425-434.

Starborg, M., Gell, K., Brundell, E., and Hoog, C. (1996). The murine Ki-67 cell proliferation antigen accumulates in the nucleolar and heterochromatic regions of interphase cells and at the periphery of the mitotic chromosomes in a process essential for cell cycle progression. J Cell Sci 109 (Pt 1), 143-153.

Stefanova, I., Dorfman, J.R., and Germain, R.N. (2002). Self-recognition promotes the foreign antigen sensitivity of naive T lymphocytes. Nature 420, 429-434.

Stefanova, I., Hemmer, B., Vergelli, M., Martin, R., Biddison, W.E., and Germain, R.N. (2003). TCR ligand discrimination is enforced by competing ERK positive and SHP-1 negative feedback pathways. Nat Immunol 4, 248-254.

Stein, P.L., Lee, H.M., Rich, S., and Soriano, P. (1992). pp59fyn mutant mice display differential signaling in thymocytes and peripheral T cells. Cell 70, 741-750.

Stemberger, C., Huster, K.M., Koffler, M., Anderl, F., Schiemann, M., Wagner, H., and Busch, D.H. (2007). A single naive CD8+ T cell precursor can develop into diverse effector and memory subsets. Immunity 27, 985-997.

Straus, D.B., and Weiss, A. (1992). Genetic evidence for the involvement of the lck tyrosine kinase in signal transduction through the T cell antigen receptor. Cell 70, 585-593.

Su, L.F., Kidd, B.A., Han, A., Kotzin, J.J., and Davis, M.M. (2013). Virus-specific CD4(+) memory-phenotype T cells are abundant in unexposed adults. Immunity 38, 373-383.

Sudo, T., Nishikawa, S., Ohno, N., Akiyama, N., Tamakoshi, M., and Yoshida, H. (1993). Expression and function of the interleukin 7 receptor in murine lymphocytes. Proc Natl Acad Sci U S A 90, 9125-9129.

Sulic, S., Panic, L., Barkic, M., Mercep, M., Uzelac, M., and Volarevic, S. (2005). Inactivation of S6 ribosomal protein gene in T lymphocytes activates a p53-dependent checkpoint response. Genes Dev 19, 3070-3082.

Sullivan, B.M., Juedes, A., Szabo, S.J., von Herrath, M., and Glimcher, L.H. (2003). Antigen-driven effector CD8 T cell function regulated by T-bet. Proc Natl Acad Sci U S A 100, 15818-15823.

Sun, J.C., Williams, M.A., and Bevan, M.J. (2004). CD4+ T cells are required for the maintenance, not programming, of memory CD8+ T cells after acute infection. Nat Immunol 5, 927-933.

Tan, J.T., Dudl, E., LeRoy, E., Murray, R., Sprent, J., Weinberg, K.I., and Surh, C.D. (2001). IL-7 is critical for homeostatic proliferation and survival of naive T cells. Proc Natl Acad Sci U S A 98, 8732-8737.

Tanaka, S., Maeda, S., Hashimoto, M., Fujimori, C., Ito, Y., Teradaira, S., Hirota, K., Yoshitomi, H., Katakai, T., Shimizu, A., et al. (2010). Graded attenuation of TCR signaling elicits distinct autoimmune diseases by altering thymic T cell selection and regulatory T cell function. J Immunol 185, 2295-2305.

Taniguchi, T., Matsui, H., Fujita, T., Takaoka, C., Kashima, N., Yoshimoto, R., and Hamuro, J. (1983). Structure and expression of a cloned cDNA for human interleukin-2. Nature 302, 305-310.

Tarakhovsky, A., Kanner, S.B., Hombach, J., Ledbetter, J.A., Muller, W., Killeen, N., and Rajewsky, K. (1995). A role for CD5 in TCR-mediated signal transduction and thymocyte selection. Science 269, 535-537.

Tewari, K., Walent, J., Svaren, J., Zamoyska, R., and Suresh, M. (2006). Differential requirement for Lck during primary and memory CD8+ T cell responses. Proc Natl Acad Sci U S A 103, 16388-16393.

Tough, D.F., and Sprent, J. (1994). Turnover of naive- and memory-phenotype T cells. J Exp Med 179, 1127-1135.

Townsend, A.R., Rothbard, J., Gotch, F.M., Bahadur, G., Wraith, D., and McMichael, A.J. (1986). The epitopes of influenza nucleoprotein recognized

by cytotoxic T lymphocytes can be defined with short synthetic peptides. Cell 44, 959-968.

Trobridge, P.A., and Levin, S.D. (2001). Lck plays a critical role in Ca(2+) mobilization and CD28 costimulation in mature primary T cells. Eur J Immunol 31, 3567-3579.

van der Merwe, P.A., and Dushek, O. (2011). Mechanisms for T cell receptor triggering. Nat Rev Immunol 11, 47-55.

van Oers, N.S., Killeen, N., and Weiss, A. (1994). ZAP-70 is constitutively associated with tyrosine-phosphorylated TCR zeta in murine thymocytes and lymph node T cells. Immunity 1, 675-685.

van Oers, N.S., Killeen, N., and Weiss, A. (1996a). Lck regulates the tyrosine phosphorylation of the T cell receptor subunits and ZAP-70 in murine thymocytes. J Exp Med 183, 1053-1062.

van Oers, N.S., Lowin-Kropf, B., Finlay, D., Connolly, K., and Weiss, A. (1996b). alpha beta T cell development is abolished in mice lacking both Lck and Fyn protein tyrosine kinases. Immunity 5, 429-436.

van Oers, N.S., Tohlen, B., Malissen, B., Moomaw, C.R., Afendis, S., and Slaughter, C.A. (2000). The 21- and 23-kD forms of TCR zeta are generated by specific ITAM phosphorylations. Nat Immunol 1, 322-328.

Veillette, A., Bookman, M.A., Horak, E.M., and Bolen, J.B. (1988). The CD4 and CD8 T cell surface antigens are associated with the internal membrane tyrosine-protein kinase p56lck. Cell 55, 301-308.

Wade, T., Bill, J., Marrack, P.C., Palmer, E., and Kappler, J.W. (1988). Molecular basis for the nonexpression of V beta 17 in some strains of mice. J Immunol 141, 2165-2167.

Walk, S.F., March, M.E., and Ravichandran, K.S. (1998). Roles of Lck, Syk and ZAP-70 tyrosine kinases in TCR-mediated phosphorylation of the adapter protein Shc. Eur J Immunol 28, 2265-2275.

Wang, H., Kadlecek, T.A., Au-Yeung, B.B., Goodfellow, H.E., Hsu, L.Y., Freedman, T.S., and Weiss, A. (2010). ZAP-70: an essential kinase in T-cell signaling. Cold Spring Harb Perspect Biol 2, a002279.

Wang, R., and Green, D.R. (2012). Metabolic checkpoints in activated T cells. Nat Immunol 13, 907-915.

Waterhouse, P., Penninger, J.M., Timms, E., Wakeham, A., Shahinian, A., Lee, K.P., Thompson, C.B., Griesser, H., and Mak, T.W. (1995). Lymphoproliferative disorders with early lethality in mice deficient in Ctla-4. Science 270, 985-988.

Watts, J.D., Sanghera, J.S., Pelech, S.L., and Aebersold, R. (1993). Phosphorylation of serine 59 of p56lck in activated T cells. J Biol Chem 268, 23275-23282.

Waugh, C., Sinclair, L., Finlay, D., Bayascas, J.R., and Cantrell, D. (2009). Phosphoinositide (3,4,5)-triphosphate binding to phosphoinositide-dependent kinase 1 regulates a protein kinase B/Akt signaling threshold that dictates T-cell migration, not proliferation. Mol Cell Biol 29, 5952-5962.

Wei, S.H., Safrina, O., Yu, Y., Garrod, K.R., Cahalan, M.D., and Parker, I. (2007). Ca2+ signals in CD4+ T cells during early contacts with antigen-bearing dendritic cells in lymph node. J Immunol 179, 1586-1594.

Wenger, R.H., Rochelle, J.M., Seldin, M.F., Kohler, G., and Nielsen, P.J. (1993). The heat stable antigen (mouse CD24) gene is differentially regulated but has a housekeeping promoter. J Biol Chem 268, 23345-23352.

Werlen, G., Hausmann, B., Naeher, D., and Palmer, E. (2003). Signaling life and death in the thymus: timing is everything. Science 299, 1859-1863.

Williams, L.M., and Rudensky, A.Y. (2007). Maintenance of the Foxp3-dependent developmental program in mature regulatory T cells requires continued expression of Foxp3. Nat Immunol 8, 277-284.

Williams, M.A., and Bevan, M.J. (2007). Effector and memory CTL differentiation. Annu Rev Immunol 25, 171-192.

Wilson, A., Day, L.M., Scollay, R., and Shortman, K. (1988). Subpopulations of mature murine thymocytes: properties of CD4-CD8+ and CD4+CD8-thymocytes lacking the heat-stable antigen. Cell Immunol 117, 312-326.

Winkler, D.G., Park, I., Kim, T., Payne, N.S., Walsh, C.T., Strominger, J.L., and Shin, J. (1993). Phosphorylation of Ser-42 and Ser-59 in the N-terminal region of the tyrosine kinase p56lck. Proc Natl Acad Sci U S A 90, 5176-5180.

Winslow, M.M., Neilson, J.R., and Crabtree, G.R. (2003). Calcium signalling in lymphocytes. Curr Opin Immunol 15, 299-307.

Woolf, E., Xiao, C., Fainaru, O., Lotem, J., Rosen, D., Negreanu, V., Bernstein, Y., Goldenberg, D., Brenner, O., Berke, G., et al. (2003). Runx3 and Runx1 are required for CD8 T cell development during thymopoiesis. Proc Natl Acad Sci U S A 100, 7731-7736.

Wyllie, A.H. (2010). "Where, O death, is thy sting?" A brief review of apoptosis biology. Mol Neurobiol 42, 4-9.

Xiong, J., Armato, M.A., and Yankee, T.M. (2011). Immature single-positive CD8+ thymocytes represent the transition from Notch-dependent to Notch-independent T-cell development. Int Immunol 23, 55-64.

Xiong, N., and Raulet, D.H. (2007). Development and selection of gammadelta T cells. Immunol Rev 215, 15-31.

Xiong, Y., and Bosselut, R. (2012). CD4-CD8 differentiation in the thymus: connecting circuits and building memories. Curr Opin Immunol 24, 139-145.

Yamasaki, S., and Saito, T. (2007). Molecular basis for pre-TCR-mediated autonomous signaling. Trends Immunol 28, 39-43.

Yamashita, I., Nagata, T., Tada, T., and Nakayama, T. (1993). CD69 cell surface expression identifies developing thymocytes which audition for T cell antigen receptor-mediated positive selection. Int Immunol 5, 1139-1150.

Yang, C.Y., Best, J.A., Knell, J., Yang, E., Sheridan, A.D., Jesionek, A.K., Li, H.S., Rivera, R.R., Lind, K.C., D'Cruz, L.M., et al. (2011). The transcriptional regulators Id2 and Id3 control the formation of distinct memory CD8+ T cell subsets. Nat Immunol 12, 1221-1229.

Yasuda, T., Bundo, K., Hino, A., Honda, K., Inoue, A., Shirakata, M., Osawa, M., Tamura, T., Nariuchi, H., Oda, H., et al. (2007). Dok-1 and Dok-2 are negative regulators of T cell receptor signaling. Int Immunol 19, 487-495.

Youle, R.J., and Strasser, A. (2008). The BCL-2 protein family: opposing activities that mediate cell death. Nat Rev Mol Cell Biol 9, 47-59.

Youngblood, B., Hale, J.S., and Ahmed, R. (2013). T-cell memory differentiation: insights from transcriptional signatures and epigenetics. Immunology 139, 277-284.

Youngblood, B., Oestreich, K.J., Ha, S.J., Duraiswamy, J., Akondy, R.S., West, E.E., Wei, Z., Lu, P., Austin, J.W., Riley, J.L., et al. (2011). Chronic virus infection enforces demethylation of the locus that encodes PD-1 in antigen-specific CD8(+) T cells. Immunity 35, 400-412.

Yu, Q., Park, J.H., Doan, L.L., Erman, B., Feigenbaum, L., and Singer, A. (2006). Cytokine signal transduction is suppressed in preselection double-positive thymocytes and restored by positive selection. J Exp Med 203, 165-175.

Zamoyska, R., Basson, A., Filby, A., Legname, G., Lovatt, M., and Seddon, B. (2003). The influence of the src-family kinases, Lck and Fyn, on T cell differentiation, survival and activation. Immunol Rev 191, 107-118.

Zehn, D., King, C., Bevan, M.J., and Palmer, E. (2012). TCR signaling requirements for activating T cells and for generating memory. Cell Mol Life Sci 69, 1565-1575.

Zehn, D., Lee, S.Y., and Bevan, M.J. (2009). Complete but curtailed T-cell response to very low-affinity antigen. Nature 458, 211-214.

Zhang, J., Zahir, N., Jiang, Q., Miliotis, H., Heyraud, S., Meng, X., Dong, B., Xie, G., Qiu, F., Hao, Z., et al. (2011). The autoimmune disease-associated PTPN22 variant promotes calpain-mediated Lyp/Pep degradation associated with lymphocyte and dendritic cell hyperresponsiveness. Nat Genet 43, 902-907.

zur Hausen, J.D., Burn, P., and Amrein, K.E. (1997). Co-localization of Fyn with CD3 complex, CD45 or CD28 depends on different mechanisms. Eur J Immunol 27, 2643-2649.